Role of Grafting on Particle Morphology and Film Properties of Polyurethane-Polyacrylate Hybrid Dispersions

Samane Mehravar

Chemical Engineering Group
University of the Basque Country
Donostia-San Sebastián
(2018)

POLYMAT

Content

Acknowledgements

I would like to express my sincere gratitude to my supervisors Prof. José M. Asua, Prof. Radmila Tomovska and Dr.Nicholas Ballard for their valuable guidance, support, encouragement and patience. It was a precious opportunity for me to work under their supervision.

I would like to extent my gratitude to the professors of the Chemical Engineering Group, Professors Jose R. Leiza, María Paulis, Maria J. Barandiaran, Jose C. de la Cal, Alejandro Müller and David Mecerreyes, and for their insightful comments and encouragement in the seminars. I would like to show my gratitude to Inés Plaza for her endless help and support in every aspect.

I would like to thank the former and current members of our research group in Polymat for creating a nice research environment full of joy, learning and scientific discussions.

I would like to gratefully thank Dr. Bernd Reck and Dr. Konrad Roschmann who provided me an opportunity to join their team as intern and for their support during the three months stay in BASF. I would like to thank other members of BASF company specially Dr. Paola Uribe Arocha and Dr. Dirk Wulff for technical support. Ms. Christina Weigert, Ms. Antonietta Meliset-Lisanti, Ms.Tanja Becker and Mr. Rolf Mayer for their assistance in the laboratory.

I would like to acknowledge the financial support of Industrial Liaison Program in Polymerization in Dispersed Media.

Special thanks to Sgiker Services of University of the Basque Country. To Dr. Mariano Barrado and Dr. Maite for TEM analysis and. Dr. Loli Martin for AFM analysis. I would like to thank Dr. Mercedes Fernandes for technical support and discussions in DMTA analysis. To Dr. Jose I. Mirando and Dr. Iñaki Santos for their kind help with the NMR analysis and Dr. Veloso for MALDI analysis.

I would like to thank my family. I owe a lot to my parents, who encouraged and helped me at every stage of my personal and academic life, and longed to see this achievement come true. And of course my siblings for their encouragements.

And the last but not the least, my beloved husband. Ehsan, thank you for your endless love, encouragement and positive energy. Without your emotional and scientific supports I would never been able to make it.

Chapter 1. Introduction and Objectives

1.1. Introduction

Polyurethanes (PUs) are used in a wide variety of applications, including insulating materials, adhesives, coatings, elastomers and fillers due to their superior properties such as chemical resistance, toughness and flexibility [1–4]. PU chemistry was launched by Dr. Otto Bayer and coworkers in 1937 [5] in response to the polyesters being developed by Carothers at DuPont. The unique properties of PUs brought about their rapid development and subsequently led to PUs becoming an important part of the worldwide production of polymers [6]. Later, in order to minimize the use of volatile organic compounds (VOCs) for environmental reasons, waterborne polyurethanes or polyurethane dispersions (PUDs) were developed [7–9]. Nowadays PUDs are important industrial products and the global PUD market size exceeded 290 kilo tons in 2014 and it is projected to be worth USD 2.04 billion by 2020, registering a compound annual growth rate (CAGR) of 6.8% between 2015 and 2020 [10].

PUDs are usually prepared in two steps, first an NCO terminated PU prepolymer is synthesized by the polyaddition reaction of a diisocyanate and a polyol (long chain diol) together with a diol containing ionic or non-ionic moieties for water dispersability. Subsequently, the prepolymer is dispersed in water followed by extension of the polymer chains using diol or diamine. Although waterborne PUs often exhibit excellent physical

properties, they suffer from a poor water and alkali resistance [11]. On the other hand, the use of isocyanates leads to a relatively high cost of PUDs compared to alternative polymers such as acrylics [7,12,13]. A potential way of overcoming these issues is through the combination of PU and acrylic polymers, yielding a hybrid product with lower price and superior properties over those of individual components [14–19]. In order to ensure that such hybrid materials offer a true synergy between the PU and acrylic components, control of the polymer microstructure is of great importance.

There are numerous reviews published on both PUDs [9,12,20–22] and PU/acrylic hybrids [23–25]. Regarding PUDs, besides a brief overview on synthesis procedures, these works provide discussions on the influence of the structural engineering of PU molecules on the properties of the aqueous dispersions and the final polymer. In the case of PU/acrylic hybrids, these works are mainly an overview of the synthesis methods, presenting insights in the chemistry and the properties of the hybrid dispersions and films. However, no attempts have been made to summarize and critically compared the works dedicated to understand the relationship between the composition and properties of the hybrids with their final performance, which will be discussed in this chapter.

The aim here is to provide a comprehensive state-of-the-art study covering the various synthetic pathways and the structure-property relationships of both PUD and PU/(meth)acrylic hybrid dispersions and their films. In the first part of this chapter, the basic chemistry of PUs and the effect of the choice of the major components for their synthesis on the polymer characteristics and final properties are discussed in detail. In the second part, the various techniques for preparing PU/(meth)acrylic hybrids including chemically bonded

hybrids are presented comparing the performance of grafted and non-grafted hybrids. Some examples on the tuning the adhesive properties in the PU/(meth)acrylic hybrids are given.

1.2. PUD synthesis and its chemistry

1.2.1. The basic chemistry

Polyurethane dispersions (PUDs) are a broad class of polymers produced by the polyaddition of a diisocyanate or a polymeric isocyanate and a mixture of a polyol, and a diol containing ionic or non-ionic hydrophilic groups to introduce water dispersability. The reaction is carried out with an excess of isocyanate groups in the presence of suitable catalysts and afterwards dispersed in water. Finally the isocyanate terminated polymer chains are extended with diamines or diols (chain extender). As both the characteristics and concentration of each of the components involved in polyaddition reaction may be varied, a virtually unlimited portfolio of different products can be obtained. The resulting polymer is a random copolymer containing low glass transition temperature (T_g) soft segments (SS) rich in polyol and high T_g hard segments (HS) rich in the isocyanate, chain extender and the ionic monomer [2]. Because of the basic thermodynamic incompatibility of these two segments, localized microphase separation occurs, contributing to the unique properties of PUs. The urethane groups (which are in the hard segment) link the rigid hard and the flexible soft segments together by means of intramolecular covalent bonds and intermolecular hydrogen bonds (Figure 1.1). Hydrogen bonds are largely responsible for the strength of PU materials relative to many other polymers. Schematic representations of a well phase segregated PU and a phase mixed PU are shown in Figures 1.2(a) and 1.2(b),

respectively. The degree of phase separation and phase mixing depends on three main parameters: the length of each segment, the incompatibility between two segments and the composition of the hard and soft segments in the PU [26–29]. PU composition and structure can be varied within wide ranges resulting in a highly diverse range of materials with some PUs being soft and highly elastic whereas, others are hard and rigid materials [7].

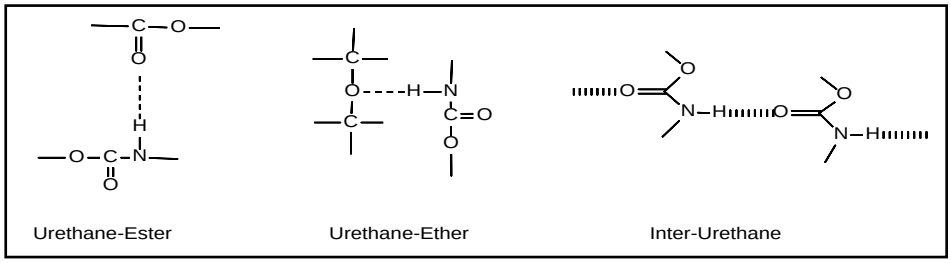

Figure 1.1. Hydrogen bonding interaction in polyurethanes [2]

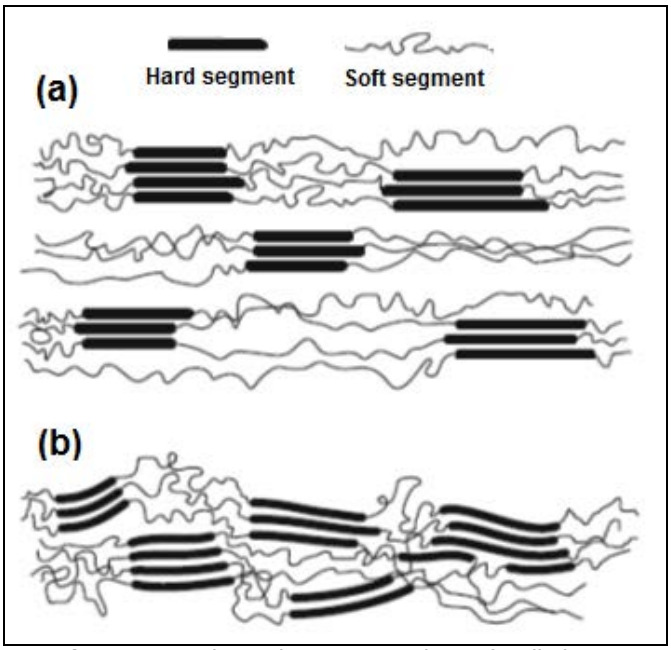

Figure 1.2. Schematic representations of well phase segregated PU (a) and phase mixed PU (b) [2]

Commercial production of isocyanates involves the reaction of toxic phosgene gas with amines. As phosgene is very toxic, many attempts to obtain non-isocyanate PUs (NIPUs) can be found in the academic literature [3,30–43]. As it is shown in Figure 1.3, at least four methods are considered for NIPU synthesis: (i) step-growth polyaddition of cyclic dicarbonates and diamines [32,44–46],(ii) step-growth polycondensation of linear activated dicarbonates and diamines [30,47] ,(iii) step-growth polycondensation of linear activated carbamates and diols [48] and (iv) ring-opening polymerization of cyclic carbamates [49,50]. The reaction between a cyclic carbonate and an amine which is traditionally known to produce poly(hydroxyurethane)s (PHUs) is nowadays seen as the best possible alternative for PU synthesis [32,44–46]. However, in spite of these efforts, commercial PUs and PUDs are still mainly based on the reaction of isocyanate compounds with nucleophiles, mainly due to the higher reaction rate and lower cost of the polymerization process combined with the superior mechanical properties and better chemical resistance that the synthesized materials offer [3]. The resonance structures of the isocyanate group and the scheme of isocyanate reaction with hydroxyl groups are shown in Figures 1.4(a) and 1.4(b), respectively. In the isocyanate group, the electron density is smaller in the carbon atom, average in nitrogen and larger in oxygen [51]. Isocyanate reactions mainly occur through addition to C=N double bond, so an active hydrogen atom-containing nucleophilic center attacks the electrophilic carbon atom in the isocyanate group with an active hydrogen added to the nitrogen atom (Figure 1.4b). The reactivity of isocyanates towards nucleophiles is thus directly based on their polarization; the higher the polarization, the higher the carbon´s electron attraction and hence the higher the reactivity [2].

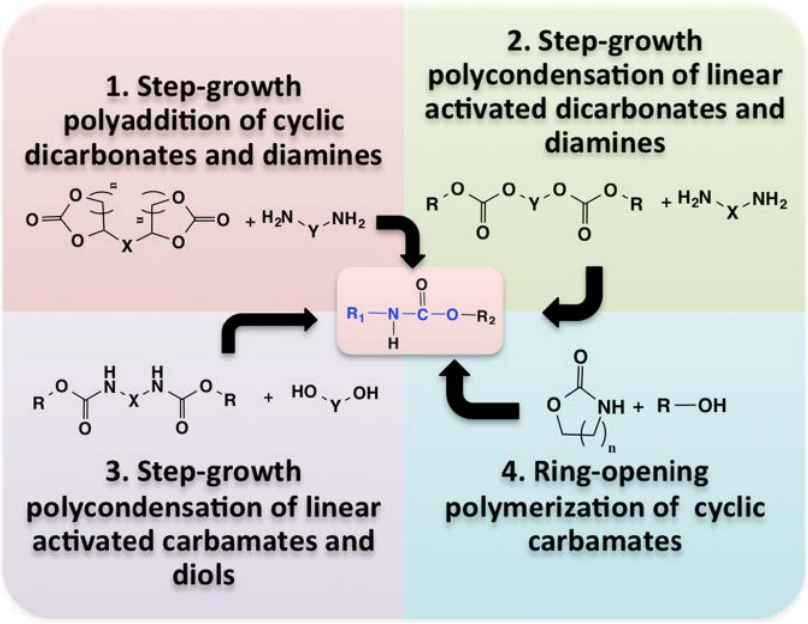

Figure 1.3. Most employed isocyanate-free approached for synthesizing PUs [52]

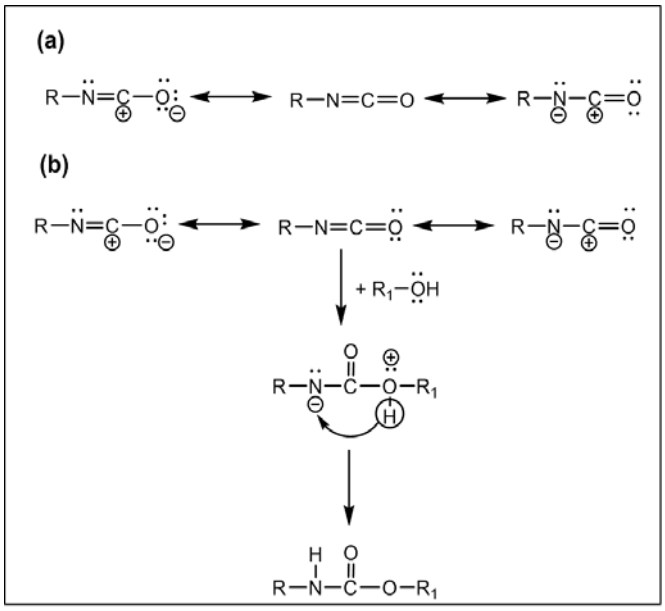

Figure 1.4. Resonance structures of the isocyanate group (a) and the reaction scheme of isocyanate with hydroxyl group (b)[51,53]

Isocyanates can react readily with many nucleophilic compounds including amines, alcohols, acids or water (primary reactions, Figure 1.5) and to a lesser extent with urethanes, urea and amide (secondary reactions, Figure 1.6). In general, the reactivity of isocyanates with alcohols is much lower than that of amines, which is similar to that of water and higher than that of acids (Table 1.1) [51]. Furthermore, the reactivity of secondary hydroxyl groups is lower than the primary groups due to neighboring methyl group steric hindrance in the secondary hydroxyl group [51]. Among amines, the aliphatic ones react more quickly than aromatics, since the electronegativity of the aromatic ring substituent is larger and there is less positive load on the carbon of isocyanate group in this case [53]. Moreover, isocyanates can homopolymerize (Figure 1.7) depending upon the reaction conditions such as the temperature and the presence of catalyst [54–58]. For example the formation of carbodiimide usually begins above 150 ºC and it accelerates in the presence of phosphine, tin and basic catalysts [55]. The dimerization of isocyanate to form uretdiones is usually conducted at low temperatures using organic phosphine catalysts [56]. Isocyanate trimerization is of commercial importance since its product (isocyanurate) has excellent thermal stability [59]. This reaction is usually carried out in the presence of catalysts such as quaternary hydroxides of nitrogen, phosphorus and especially tertiary amines.

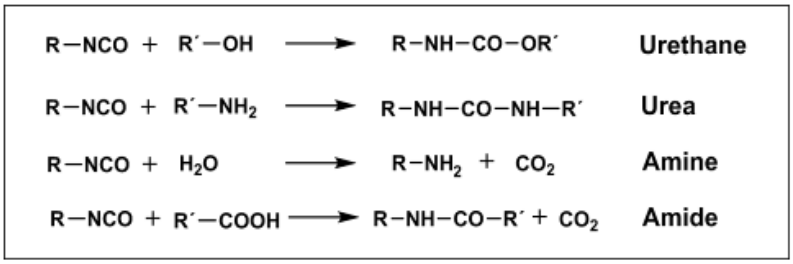

Figure 1.5. Primary isocyanate reactions

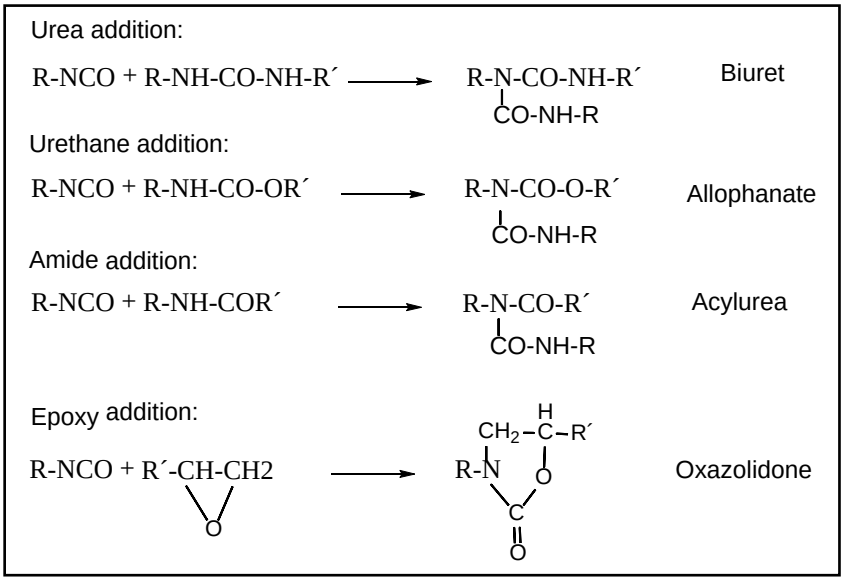

Figure 1.6. Secondary isocyanate reactions

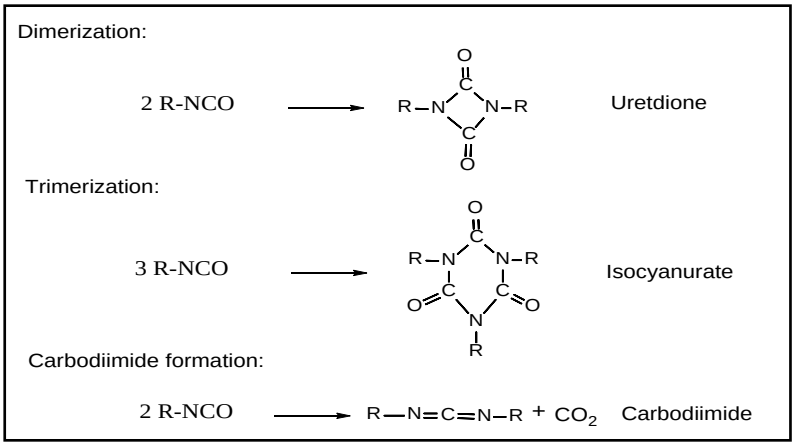

Figure 1.7. Isocyanate self condensation reactions

Table 1.1. Relative reactivity of isocyanates with active hydrogen compounds [51]

Active hydrogen compound	Typical structure	Relative reaction rate*
Primary aliphatic amine	$R\text{-}NH_2$	100,000
Secondary aliphatic amine	RR´NH	20,000-50,000
Primary aromatic amine	$R\text{-}NH_2$ (R: Aromatic)	200-300
Primary hydroxyl	$RCH_2\text{-}OH$	100
Water	H_2O	100
Carboxylic acid	R-COOH	40
Secondary hydroxyl	RR´CH-OH	30
Urea	R-NH-CO-NH-R´	15
Tertiary hydroxyl	RR´R´´C-OH	0.5
Urethane	R-NH-CO-O-R	0.3
Amide	$RCO\text{-}NH_2$	0.1

* uncatalyzed at 25 ºC

1.2.2. Raw materials

The versatility of PUs can be directly correlated to the high variety of raw materials used in their synthesis, which determines the final properties of the products. In this section an overview of the most common materials utilized in synthesis of PUDs is provided and the influence of the molecular structure of each of them on the synthesis of PU and final polymer properties is highlighted.

1.2.2.1. Isocyanates

Isocyanates are essential components in the PU synthesis. They can have two or more NCO groups per molecule; however di-functional isocyanates are more common in PU synthesis. Diisocyanates can be either aromatic or aliphatic. Figure 1.8 shows examples of the most common diisocyanates [2]. Table 1.2 presents the relative rate constants for the

reaction of isocyanate with an alcohol [60]. Aromatic diisocyanates are substantially more reactive than aliphatic ones [2,7,9,23,61] as the aromatic rings on the nitrogen atom of the isocyanate group increases the carbon's electrophilicity through electron attraction (Figure 1.4) [53]. The reactivity of an isocyanate group may also vary even within aromatic diisocyanates (Table 1.2). For example, toluene diisocyanate (TDI) is more reactive than diphenyl methane diisocyanate (MDI). NCO groups in diisocyanates exhibit different reactivities depending on the location in the molecule. For example in 2,4-TDI, the isocyanate group in para position to the methyl group is 25 times more reactive than the NCO group at the ortho position [2]. Similarly the reactivity of the two NCO groups in isophorone diisocyanate (IPDI) is different with higher reactivity of secondary NCO. However, which one is more reactive NCO group can depend on the catalyst (see Section 1.2.2.4). Furthermore, the reactivity of the second NCO group in IPDI can change as a result of the reaction of the first NCO group due to the change in the electron attraction upon formation of urethane group [2]. For example, it has been observed that in diisocyanates with both NCO groups in the same aromatic ring (like TDI), the reactivity falls significantly when the NCO conversion reaches 50% [51]. In addition, the reactivity of NCO depends on the type of solvent, diol and the catalyst used [62].

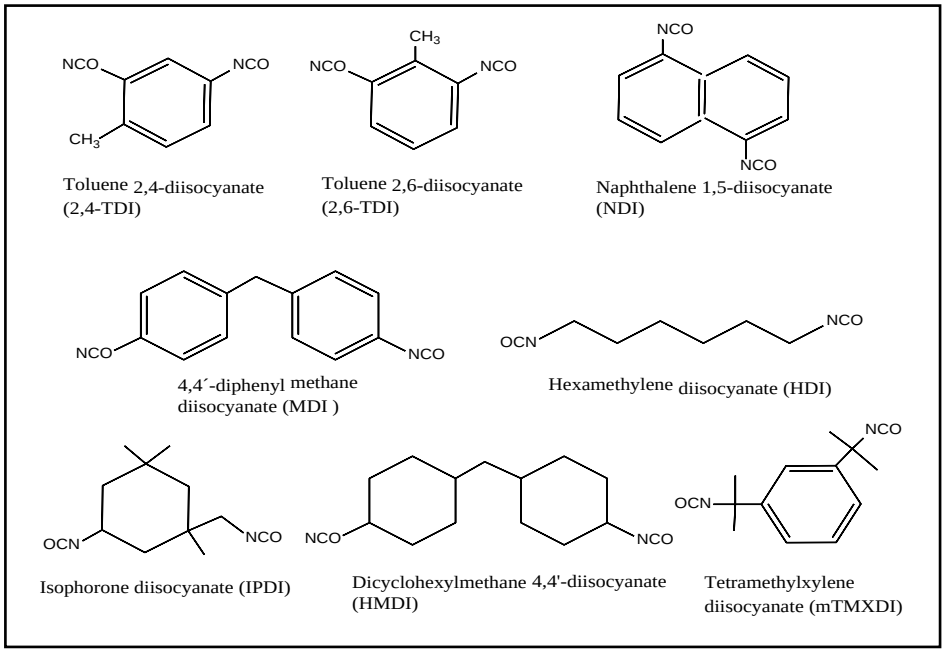

Figure 1.8. Common diisocyanates in PU synthesis

Table 1.2. Relative reactivity of the first (K_1) and second (K_2) NCO groups in reaction with alcohol in different diisocyanates [60]

Diisocyanate	K_1*	K_2**
TDI	400	33
MDI	320	110
HDI	1	0.5
HMDI	0.57	0.4
IPDI	0.62	0.23

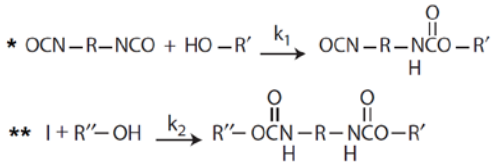

The choice of the diisocyanate is governed by the required properties for end-use applications. Aliphatic diisocyanates offer ultraviolet stability and resistance to hydrolytic degradation, while materials made from aromatic isocyanates are more rigid but they

undergo photo-degradation which leads to coloring of the polymer with time making them inappropriate for many coatings applications [2,7,63]. Furthermore, in the case of the highly reactive aromatic diisocyanates the side reaction of NCO with water during dispersion seems to be inevitable. For this reason, the majority of commercial PUDs are based on aliphatic types, which display low reactivity toward water [23,64,65]. However, because of the high price of aliphatic diisocyanates, the use of aromatic diisocyanates provides cost benefits for the products in which oxidative discoloration is not an application issue [61,66,67]. Furthermore, by the use of mixed diisocyanates favorable properties for lower price can be obtained [66,68].

The effect of diisocyanate type on the synthesis and properties of PUD have been studied and reported in the literature [66,69–71]. The type of diisocyanate determines the properties of the hard segments of the PU chains, the extent of hydrogen bonding between the chains, and subsequently, the mechanical and thermal performance. Cheong *et al.* [66] synthesized PUD nanoparticles with mixture of MDI/IPDI (MDI from 0 to 50 mol%) at fixed NCO/OH ratio of 1.2. It was observed that by increasing the MDI content both the particle size and the average molecular weight increased. The author claimed that when the MDI content increased, the molecular weight of the prepolymer increased as a result of higher conversion of NCO groups leading to a higher viscosity of the prepolymer, which in turn was more difficult to disperse, and hence higher particle size was obtained. It is worth pointing out that no information regarding the viscosity of the prepolymer and the NCO conversion is given by the author. Similarly, Król *et al.* [69] found that the highest values of molecular weights were offered by aromatic-based PUDs (using TDI or MDI diisocyanate) while the

much lower molecular weight PUDs were obtained in the case of cycloaliphatic ones (using IPDI or HMDI diisocyanate). The reasons for the higher molecular weight of PU prepolymer were not given but the observation was likely due to the higher NCO conversion in the case of aromatic diisocyanates. Different aliphatic diisocyanates (IPDI, TXMDI, HMDI and HDI) were used by Hourston *et al.* [70] in the preparation of ionic PUDs. It was demonstrated that the IPDI systems possessed superior mechanical properties due to its chemical structure. TMXDI-derived PU prepolymers had low viscosity due to low reactivity of NCO group in TMXDI and the corresponding PU films showed highly elastomeric behavior. However, no information regarding the polymer molecular weight was given by the authors that could offer additional insight on the presented tensile behavior.

The degradation profiles of PU, PU-urea films casted from the aqueous dispersions containing different diisocyanates (TDI, HDI, HMDI and IPDI) was studied by Coutinho *et al.* [71]. It was shown that the type of hard segment influenced the degradation profile. HMDI, with a more symmetrical structure, improved the interactions between chains leading to polymers with higher thermal stability and HDI which contains a relative large flexible portion, $–(CH_2)_6$, seems to facilitate the thermal degradation. On the other hand, the aromatic rings in TDI formed more rigid chains but also more asymmetrical, which seems to make the interactions between the hard segments difficult, leading a reduction of the thermal resistance.

1.2.2.2. Polyol (Macrodiol)

Long-chain diols or macrodiols, which make up the soft segment in PUs, are typically polyester, polyether or polycarbonate polyols, with molecular weights between 500 and

5000 g/mol. In practice, molecular weights of 1000 and 2000 g/mol are mainly used. Short chain diols, such as 1,4-butane diol or 1,6-hexane diol can also be used to control the hard segment content [9,23]. Figure 1.9 presents some examples of common polyols. The type of the polyol influences significantly the PU performance mainly through the control of the supramolecular bonding and subsequently through the phase separation behavior. Namely, the ether (C–O) bond in the polyether and the ester (CO–O) bond in the polyester are capable of hydrogen bonding with the urethane linkages (NH–CO) in the hard domain, influencing the degree of microphase segregation between hard and soft phases [9]. Soft segments from polyesters and polycarbonates having sufficiently high molecular weight (> 1500) can crystallize when the soft segment fraction is high enough [72].

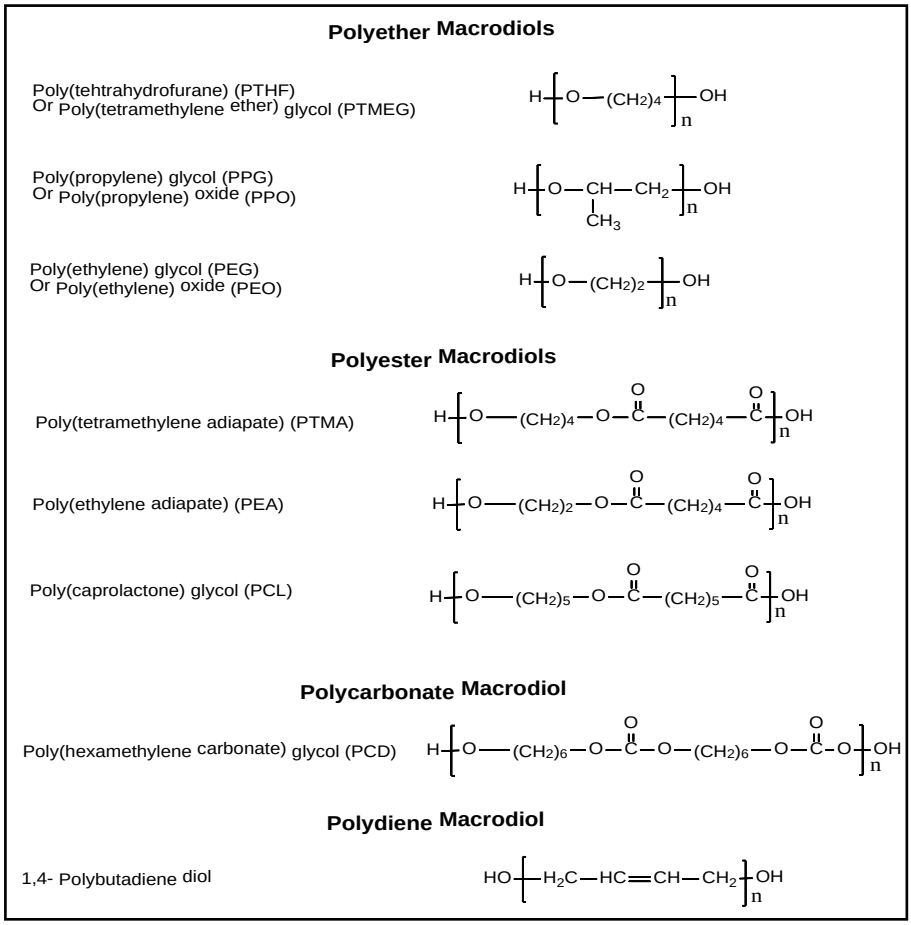

Figure 1.9. Examples of commonly used polyols in PU synthesis

Given the importance of the polyol on polymer properties, the influence of the type (polyether, polycarbonates or polyester) and molar mass of the polyol on the characteristics of PUDs have been studied extensively [70,72–83]. The choice of the type of polyol depends on the physical requirements of the polymer for the potential application and the final product cost. Polyether polyols have the advantage of imparting flexibility [73,76], hydrolytic stability and low cost. However, they are susceptible to light and oxygen under heat, and the films tend to have poor exterior durability and poor solvent resistance. Due to

the presence of the methyl side groups in polypropylene glycol (PPG) (which hinder the polymer chains aligning for hydrogen-bond formation), PPG polyols are more compatible with the hard segment than polytetrahydrofurane (PTHF) [70]. The better phase-separation structure of the PTHF-based PUD resulted in a strong, tough material, while maintaining a high degree of elasticity and an improved solvent resistance. The increased polarity of the ester carbonyl group in polyesters leads to stronger hydrogen bond acceptors than polyethers [2,9]. Thus, polyesters have the advantages of toughness, abrasion resistance, exterior durability, outstanding resistance to light and aging. Although they can be designed to give a wide variety of PU chains with different mechanical properties, they suffer from limited hydrolytic stability [84]. Polycarbonates combine properties of both polyethers and polyesters offering good mechanical properties as well as providing good resistance to hydrolysis, oil, weathering and fungi [82,85–87], but at higher cost. They have been often selected as starting materials for commercially available PUD applied for wood lacquers and steel [88,89]. Martín-Martínez and coworkers [89] have studied the use of polycarbonate diols for PUDs synthesis for coating applications. In comparison to PUDs based on polyether and polyester diols, polycarbonates produced PUs with higher soft segment content and imparted lower degree of phase separation, better adhesion (on stainless steel) under shear stresses, higher chemical resistance, higher gloss and lower yellowish. Adhesive properties of waterborne PUs as a function of polyol type were studied, too [73]. Rahman and Kim [73] showed that polyester-polyol based PUs have higher adhesive strength than polyether-polyol. Polyester PUs have highly polar nature which result in better interactions not only between the chains within the film but as well with the nylon fabric substrates.

The polyol molecular weight also affects the PUD characteristics and properties. Lee *et al.* [72] reported that with increasing the number average molecular weight (M_n) of the polyol, the particle size of the aqueous dispersion decreased. As the change in the hydrophilicity of the chains with increased M_n is negligible, the decrease in the particle size was explained by the increase in chain flexibility of PU that led to a low viscosity, which in turn allowed easier dispersion and smaller particle size. With respect to mechanical properties of the PUs, their elongation at break was higher using longer diol, because of the higher flexibility of PU and the improved phase separation. In addition, the stress at break of the PU films changed in the following order with the diol chain lengths: polyol 2000 > 1500 > 600 > 1000 [72]. The observed results were explained by simultaneous action of phase separation (which increases as the polyol M_n increase) and of soft segment crystallization (which occurred for polyol with M_n higher than or equal to 1500). The total mass of PU and the NCO/OH ratio were kept constant in the formulation. As the M_n of the polyol increased from 600 to 1000, the PU chains became more flexible resulting in decreased strength. When the M_n of polyol increased further, the soft segments crystallized and as a result the tensile strength increased. Somehow conflicting results were reported in a similar investigation performed by Hourston *et al.* [70]. They reported that the increase of M_n of the polyol reduced the tensile strength, Young´s modulus, and elongation at break. No evidence of crystallininty was reported in this study even when the M_n of the polyol was 2000. It is worth pointing out that in order to fix NCO/OH ratio and hard segment content (the ratio of diisocyanate + DMPA + chain extender to polyol) in the formulation, the amount of diisocyanate and chain extender was varied. The influence of the molecular weight of the PPG diol on the adhesive properties has been investigated [74]. It was reported that the

work of adhesion and the fibrillation plateau increased with increasing PPG molecular weight because of the higher number of chain entanglements of the soft segment.

In order to attain better and specific physical properties, mixtures of different types (as blend or block copolymer) of polyols were used as soft segment [90,91]. Yen and Kuo [90] used PCL–PEG–PCL triblock ester–ether polyol for preparation of PUDs. The final polymers had improved mechanical properties, but higher water vapor permeability when compared to the blend of the same polyols. It was claimed that this was due to better phase separation in the case of block co-polymers. Similar findings were reported by Kwak *et al*. [91] in the case of polyester and polyether polyols, their blend and their tri-block copolymers. It was reported that the coating synthesized with triblock glycol is a good candidate to prepare waterborne polyurethanes for water-vapor-permeable coating materials.

In addition to the conventional polyols presented above, poly(dimethylsiloxane) diols (PDMS) and their mixture with other polyols have been used in order to introduce polysiloxane segment in to the polymer chain and to obtain tough films for coatings [92,93]. Kozakiewicz reported synthesis of aqueous dispersions of polysiloxane urethanes [92]. Fluorinated siloxane units were used by Su et al [93] for synthesis of PUDs. Fei et al. [94] used mixture of PU and PDMS for PUDs preparation. In all of the cases, water repellant polymer films, transparent coatings with good adhesion to steel, good low temperature flexibility [92] and improved mechanical properties [93] were obtained.

Because of sustainability and environmental concerns, the use of polyols originating from renewable resources has received special attention [95–97]. For instance, for PUD synthesis, triglyceride polyols from sunflower seeds and castor oil have been used [98–101]. In general, rigid and flexible foams and coatings have been prepared from renewable polyols with properties comparable to those of their petroleum-based analogs [102–104]. Fully biobased WPU dispersions from castor oil were prepared by Fu et al. [96]. An improvement in water sensitivity was achieved due to the hydrophobic character of castor oil. Similarly, waterborne PU coatings synthesized from dimer fatty acid-based polyester polyols exhibited improved water resistance [105]. Moreover, the thermal stability of the PU coatings enhanced due to the presence of cyclic structure of dimer fatty acid. The functionality of the polyol affected the properties of the final product. Namely, the higher the hydroxyl number and functionality of the polyol, the higher the crosslinking density, the T_g, and the tensile strength of the PUs [106,107]. It is worth pointing out that high functionality can lead to highly crosslinked PUs, which would be an issue during the synthesis of prepolymer. This could induce a gelation and high viscosity preventing the dispersion process [108]. In spite of their promise, vegetable oils and their derivatives still face challenges due to their high cost. In this regard, efforts have been done to produce low cost bio-based polyols [104]

1.2.2.3. Stabilizer

Due to agitation and Brownian motion, colloidal particles in a dispersion medium frequently collide with each other. The stability of colloids is thus determined by the interaction between the particles during collisions. There are two basic interactions: one

being attractive and the other repulsive [109]. Van der Waals forces are the primary source of attraction between colloidal particles. Therefore, a colloidal dispersion is stable only when a sufficiently strong repulsive force counteracts the van der Waals attraction [109]. Colloidal stability can be provided by: i) electrical charges (electrostatic or charge stabilization, Figure 1.10a), ii) adsorbed or chemically attached amphiphilic polymeric molecules (steric stabilization, Figure 1.10b). The combination of these two stabilization mechanisms leads to electrosteric stabilization (Figure 1.10c).

Conventional PUs, are hydrophobic materials immiscible with water. One approach to prepare PUDs is the used of an external surfactant under high shear mixing. The obtained dispersion by this method had large particle size with poor colloidal stability [9]. Modification of the PU structure by using either ionic groups (ionic or electrostatic stabilization) [12,110–112] or non-ionic hydrophilic segments (non-ionic steric stabilization) [113–115] leads to the formation of a self-emulsifiable PU that has shown to be a much better approach for the preparation of PUDs with controlled particle size and properties. The self-emulsification has several advantages, such as lower water sensitivity of the obtained film and higher resistance to non-polar agents [9].

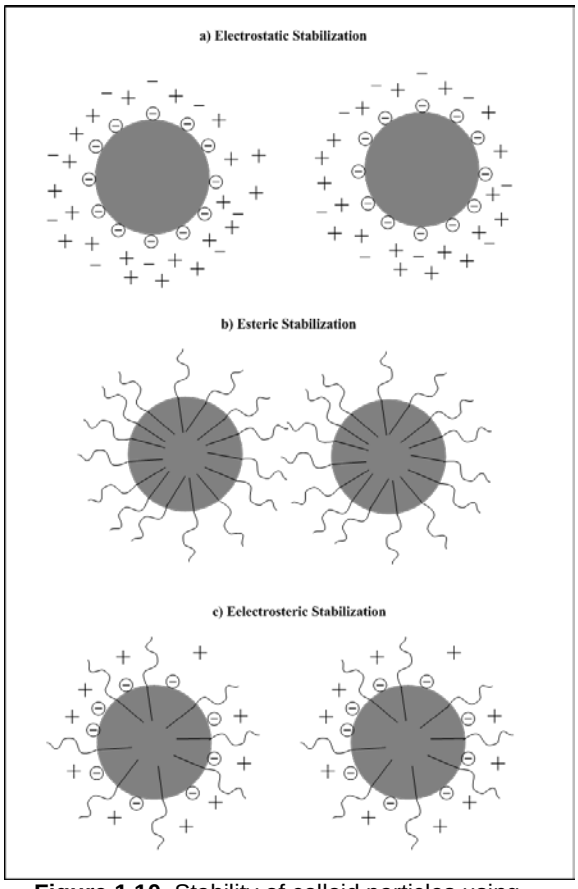

Figure 1.10. Stability of colloid particles using electrostatic stabilization (a), steric stabilization (b) and electrosteric stabilization (c)

1.2.2.3.1 Ionic diols (Ionomers)

If a diol containing suitable ionic group is added during the reaction between diisocyanates and polyols, the ionic group is incorporated within the PU chains which provide the PUs with water dispersible properties [12,110]. The ionic groups enable the PU to be dispersed in the water under mild conditions without using any external emulsifier [7,9,110]. Figure 1.11 presents some examples of ionomers.

There are three types of PU ionomers [116]: anionomer [117–119], cationomer [120–123], and zwitterionomer [124,125], which incorporate anionic, cationic or zwitterionic groups in the polymer chains, respectively. Typical functionalities are pendant acid (in anionomers), quaternary nitrogen (in cationomers) and tertiary nitrogen groups (in zwitterionomers), which are neutralized or quaternized to form salts. Cationic PUDs provide good adhesion to various substrates and they have been proven to be useful in applications such as adhesives, coagulants and also in membranes and synthetic leathers with micropores [120], but anionic PUDs are of greater commercial importance. Sulfonic [126,127] phosphoric [128] or carboxylic acids [129,130] are the most used functions and they allow the production of high solids content PUDs by preparing dispersions with broad or multimodal particle size distribution [127,131–133]. Apart from the role of ionic group in the stability of PUDs, the ionic pendant groups influence the physical properties of the films due to the formation of intermolecular coulombic forces between ionic centers [134,135]. These ionic groups form aggregates, act as physical crosslinkers and increase the modulus of the polymer films [87]. Different studies confirmed that the type and concentration of ionic groups affect the particle size [136–139], the viscosity [140,141], the glass transition temperature (T_g) [87,142,143], and the thermal, mechanical [87,90,143] and adhesive [141,142,144] properties of the polymer films.

Among diols with anionic groups, dimethylol propionic acid (DMPA) has received widespread attention in the literature [145–148]. Beside the steric hindrance of the COOH group that prevents the side reaction with isocyanate groups, DMPA is cheap, non-toxic and easy to use and works with all types of isocyanates providing excellent water dispersability

[149]. The influence of the DMPA content on the properties of the aqueous dispersion and final films have been widely investigated [87,131,136,138,141–143].

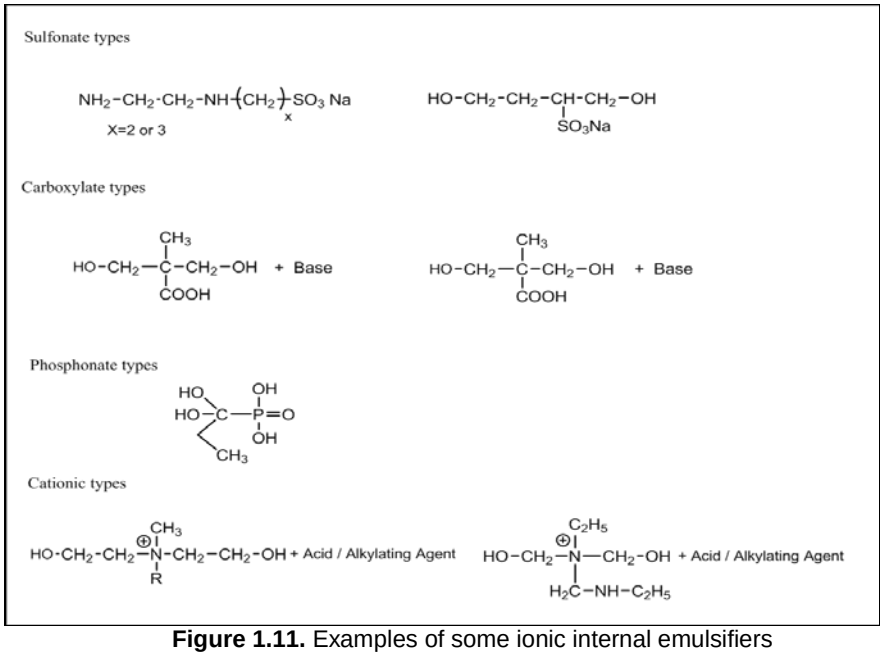

Figure 1.11. Examples of some ionic internal emulsifiers

It was demonstrated that in general the particle size decreases as the DMPA content increases up to a certain concentration (different depending on the other components of PU and the process), but then, the particle size decreased slowly or remained constant upon further increase of DMPA content [141,143]. The viscosity of PUDs increased with DMPA content and remained constant at higher amounts. This is due to the fact that by increasing the DMPA content, the particle size decreased and the number of particles increased. Therefore the distance between the particles became smaller, which resulted in more

interaction among particles and higher viscosity. As in the case of conventional latexes [150,151], control of the particle size and distribution has been used to increase significantly the solids content, maintaining the dispersion viscosity. For example Peng *et al.* [131] implemented two-step emulsification process in order to have the strict control of particle size distribution. In the first step, a polyester-based PUD with relatively large particle size (using low amout of DMPA) was synthesized and in the second step, a polyether-based prepolymer with high DMPA content was emulsified in the PUD of the first step forming a population of small particle size. The final PUD showed low viscosity (under 1000 mPa s^{-1}) with 55% solid content. It is worth poiting out that the viscosity of the PUD is generally higher than the regular latexes [150]due to the presence of strong H-bonding.

The amount of DMPA added in the synthesis of PUDs has shown to influence the final polymer properties. It is reported that by increasing the DMPA content and hence increasing the hard segment content, the glass transition temperature increased [87,143] and the soft segment crystallinity decreased [142] due to the restriction of the soft segment motions caused by the hard segments. The thermal stability also decreased due to higher hard segment content [87,142]. Moreover, polymer films containing more DMPA showed higher modulus and lower elongation at break [87,141,143]. Finally, with increasing the DMPA content, the water uptake of the PUD films increased due to the higher hydrophilicity of PU chains [141]. Regarding the application properties, it has been shown that in coating applications a high DMPA content led to an increase in König hardness and a decrease in gloss [87]. In adhesives applications, the adhesive strength increased as the DMPA content

decreased, because the adhesion was mainly governed by the soft segment content in the PU [141,142].

1.2.2.3.2. Non-ionic stabilizing diols

PUDs can also be stabilized by non-ionic hydrophilic pendant groups (predominantly polyethylene oxide) [113,152–154]. The non-ionic dispersing diol is prepared by reacting polyethylene oxide units with diisocyanate at 35-50 ºC, followed by reaction with a dialkanolamine (such as diethanol amine) (Figure 1.12). The non-ionic dispersing diol is added to the polyol and diisocyanate to react at high temperature (50-80 ºC) and to obtain a NCO terminated prepolymer. Then, the prepolymer is cooled down to 10ºC and the deionized water is added to emulsify the prepolymer and finally the PU chains are extended using a diamine. Figure 1.13 presents the preparation process for non-ionic PUDs.

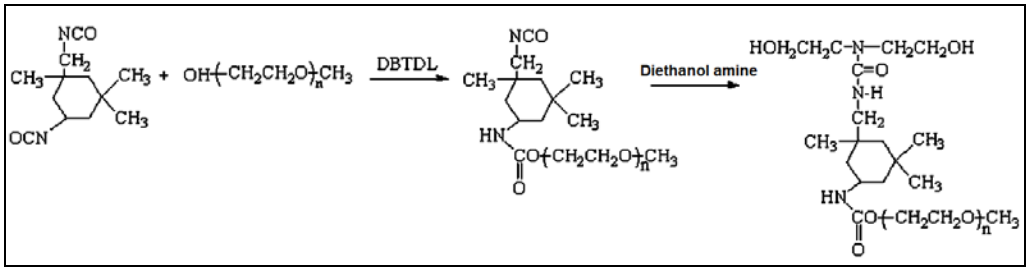

Figure 1.12. Preparation process for nonionic dispersing center [155]

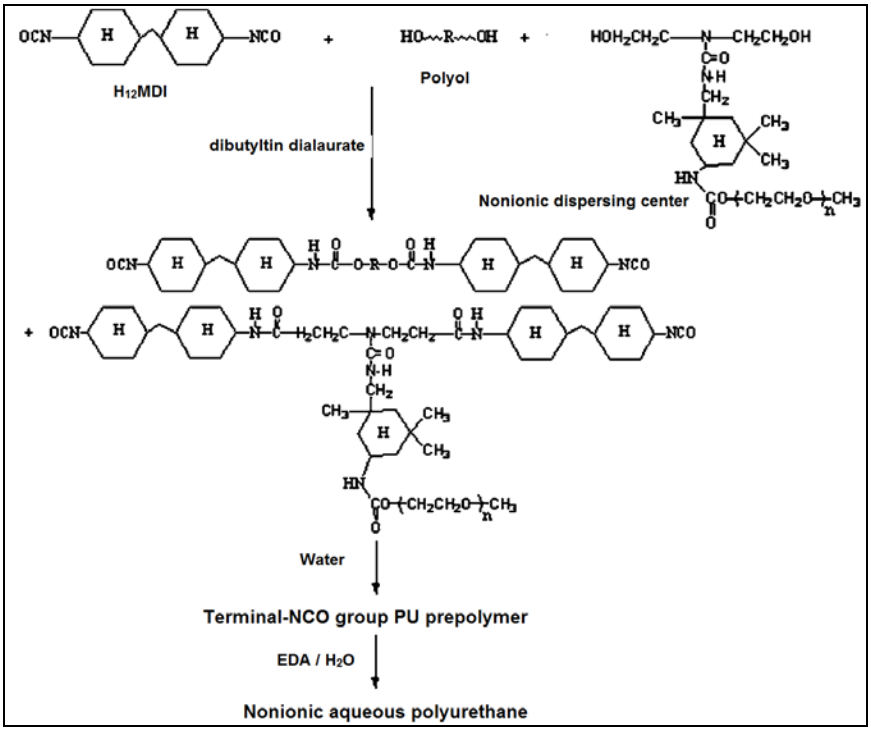

Figure 1.13. Preparation process of nonionic aqueous polyurethane dispersion [155]

In order to obtain an efficient stabilization, it is necessary to have enough number of dispersing diol containing polyether segments with sufficient length in the structure of PU chains [9,113,156]. However, these hydrophilic segments may have a negative effect on the polymer film water sensitivity. Li *et al.* used a synthetic long chain diol called MPEG-$(OH)_2$ (monomethoxypolyethylene glycol, M_w=2000 g/mol) to prepare non-ionic PUDs, finding that increasing the amount of MPEG-$(OH)_2$, the tensile strength decreased and the elongation at break increased due to the increase in the soft segment content. However, the water resistance of the final polymer film decreased.

Similar to regular non-ionically stabilized latexes, PU dispersions stabilized by non-ionic moieties are stable against freeze-thaw cycles, pH change, electrolytes, and strong shear forces (Table 1.3) [64]. The stability against the electrolytes is important in some applications in which pigments, fillers, thickener, and other additives are included in the formulations. On the other hand, since the solubility of polyether in water decreases with increasing temperature, the coagulation of non-ionic PUDs at high temperature is possible [9,155,157].

Table 1.3. Stability of ionic and non-ionic PUDs [64]

	Dispersion Type	
	Ionic	**Non-ionic**
Freezing	Unstable	Stable
High Temperatures	Stable	Unstable
Addition of electrolytes	Unstable	Stable
Strong shear forces	Partly stable	Stable
PH variation	Unstable	Stable

1.2.2.3.3. Combination of ionic groups and hydrophilic segments

As mentioned before, both ionic and non-ionic PUDs have their own advantages and disadvantages. Ionic PUDs are characterized by relatively small particle size, film-forming properties as well as displaying good mechanical and adhesion properties, but are sensitive to pH value and electrolytes. On the other hand, non-ionic PUDs are stable against freezing, pH change and electrolytes [7] but they are unstable at high temperature. Therefore, they have complementary characteristics and PUDs with ionic and non-ionic emulsifiers built into the same polymer chain yield stable dispersions of small particle size and satisfactory

resistance to freezing and electrolytes [156–158]. Usually, during the PU synthesis the combination of DMPA (ionic diol) and some different type of oxyethyl segments containing polyols are used. At constant DMPA content, Kim *et al.* reported that by replacing the polyol (polytetramethylene adipate glycol) with nonionic hydrophilic PEG, the particle size of the emulsion and the tensile strength of the emulsion-cast film decreased due to the weaker interchain forces caused by the incorporation of ether polyol, while the emulsion viscosity, water uptake and elongation at break increased [158]. Lijie *et al.*[156] showed that by incorporating 1 wt% PEG (based on weight of prepolymer), the amount of DMPA needed to stabilize the PUD decreased from 2.4 wt% to 2.0 wt% (based on weight of prepolymer), and the solids content increased from 42 wt% (using DMPA alone) to 52 wt%. Also a better water resistance was obtained due to the lower ionic content. Moreover, it was observed that when M_n of PEG was increased from 200 Da to ≥ 400 Da the stability of the dispersion improved.

1.2.2.4. Catalyst

Catalysis plays an important role in the reactions of isocyanates [58]. Usually during PU synthesis, catalysts are added to increase the rate of the addition reaction, especially when aliphatic diisocyanates are employed in the formulation. Aromatic and aliphatic amines (e.g., diaminobicyclooctane), organomethalic compounds (e.g., dibutyltin dialaurate), and alkali metal salts of carboxylic acids and phenols (e.g., calcium, magnesium) are commonly used as catalyst [58,159]. The reactivity of the NCO groups of the IPDI is catalyst dependent, the primary NCO being more reactive when the catalyst is a tertiary amine, and the secondary NCO when a tin catalyst and/or no catalyst is used [62].

Moreover, it has been demonstrated that tin catalysts are specific in catalyzing the isocyanate-alcohol reaction with respect to the isocyanate-water reaction [58]. Tertiary amines show a strong catalytic effect on both PU formation and reaction with water in the presence of CO_2 as blowing molecule (urea formation). This is very important in PU foam technology where organometalic compounds are commonly used to catalyze PU formation, while tertiary amines are employed to catalyze the blowing reaction [51].

Table 1.4. Rate constants of the different reactions using various catalysts[3]

Catalyst	Urethane formation *k* (L^2/(g.mol.h))	Urea formation* *k* (L^2/(g.mol.h))
Triethylamine (TEA)	11	6.0
2-2′-diazabicyclooctane (DABCO)	109	14.5
trimethylamino-ethyl-ethanolamine	28.9	43.3
Dibutyltin dilaurate (DBTDL)	144	4.8

* reaction of amine (formed from isocyanate-water reaction) and isocyanate

It is worth mentioning that the catalyst removal from PUs is often exceedingly difficult, and its cost is prohibitive, which is an important drawback for most applications, especially in the biomedical field [52,160]. Attempts have been made in order to replace them with less toxic catalysts such as bismuth, aluminum or zirconium compounds [161–163]. As an environmental friendly alternative, organocatalysis, i.e. the use of small organic molecules to catalyze chemical reactions, has gained increased attention [164–166]. The development of organocatalyzed PU syntheses provides greater accessibility, faster kinetics, convenience, and most importantly, functional group tolerance [160,167,168]. Organocatalysts can be classified as either nucleophilic and electrophilic activators or organic bases and acids, respectively [52]. The efficient performance of bicyclic alkylated

guanidines [39,40] and organic acids in the polyurethane formation even under mild polymerization conditions and low catalyst loadings has been reported [169].

1.2.2.5. Neutralization of the ionic groups in the PU chains

In the case of ionomer PUs, after the step of synthesis of PU chains, the preparation of PUDs involves the neutralization of ionic groups before dispersing the PU prepolymer in water. In anionomers, the acid group is neutralized with a base, typically triethylamine. As this process strongly influences the stability and properties of the PUDs it has been widely investigated. The effect of neutralization degree on the particle size was studied in different works [138,170,171]. It was found that the smallest particle sizes were achieved at 100% neutralization. Nanda *et al.*[136] used different strategies in the neutralization of carboxylic acid groups in the PU-DMPA chains. In this study, the acid groups were first partly neutralized with triethylamine (called pre-neutralization) and after dispersion in water, the remaining portion of neutralizing amine was added (called post-neutralization). Surprisingly, it was observed that the particle size increases after post-neutralization, according to the authors likely due to the water absorption inside the particle by the carboxylic acid group converted into ionic group during post-neutralization. Jang et al. [170] reported that neutralization process influenced the molar mass of PUs and mechanical properties of the films. The highest molar masses and better mechanical properties were obtained for 100% neutralization. The observed results was explained with the fact that smaller particle size was obtained at 100% neutralization and therefore the efficiency of chain extension (which is diffusion-controlled) was higher leading to achieve higher molar masses at 100% neutralization (see Section 1.2.2.6). The effect of countercations of different bases

(ammonia, trimethylamine, triethylamine, lithium hydroxide, sodium hydroxide and potassium hydroxide) on the neutralization step of carboxylic acid groups was also studied [172]. Using alkali metal cations (lithium, sodium and potassium) the particle size was smaller than using ammonium cations (ammonia, trimethylamine and triethylamine). It is suggested that the alkali metal cation was hydrated in the aqueous phase easier than ammonia and resulted in smaller particle size (Hofmeister effect [173]).

1.2.2.6. Chain Extender

PU prepolymers are chain extended with different types of hydrogen active compounds. Typical chain extenders are low molecular weight (M_w < 400 g/mol) difunctional intermediates designed to react with the isocyanate groups to become part of the hard segment, increase polymer molecular weight and improve the mechanical properties [2]. Diamines [87,136,144,170,174] or diols [68,75,77,79,80,175–178] are suitable examples of chain extenders leading to produce urea and urethane segments respectively. Figure 1.14 shows some examples of diamines and diols used as chain extenders. In the case of diols, they react with NCO at roughly the same rate as water and it is usually recommended that the chain extension step is done before emulsifying of the prepolymer in water. However this makes the dispersion more difficult due to the increase in the viscosity of the PU prepolymer. Diamines typically react with the isocyanate groups several orders of magnitude faster than water does (see Table 1.1). Therefore, using diamine it is possible to extend the NCO-terminated prepolymer in dispersed form [9].

The effect of the required amount of chain extender for optimum chain extension was studied by Jhon *et al.* [179]. It was observed by increasing the amount of chain extender the

molar mass of PU increased up to a point (optimum value) and by further increase in chain extender amount, the molar mass became constant. It was shown that the particle size had a great influence on the required amounts of chain extender for optimal chain extension; the smaller the particle size the higher was the optimum amount of chain extender. This was explained by the fact that the process of chain extension was driven by diffusion of diamine into the prepolymer-ionomer micelles, which is easier for smaller particles. Moreover, it was verified that the excess of amines can act as impurity and had an unfavorable influence on the adhesive strength.

The chain extension has been performed through different approaches in the work of El-Aasser and coworkers [18]. In the first way, no chain extender was added to the PU/acrylic dispersion; therefore the free NCO of prepolymer was reacted with water eventually. It was observed that the particle size increased from the initial 50 nm to 70-80 nm after several days at room temperature. In the second approach, a water-soluble diamine was used as chain extender and it resulted in an increase in particle size followed by coagulation. Finally by using a hydrophobic chain extender, bisphenol A, the latex particles maintained at their original size. The authors claimed that in the case of hydrophobic chain extender, the reaction of free NCO group and chain extender occurred inside the particles, whereas by using a hydrophilic chain extender, the reaction with the NCO groups occurred at the interface between the particles and aqueous phase. This would increase the likelihood that the latex particles aggregated by bridging flocculation, resulting in coagulation. However it is not clear how the reaction at the particle surface may induce bridging flocculation.

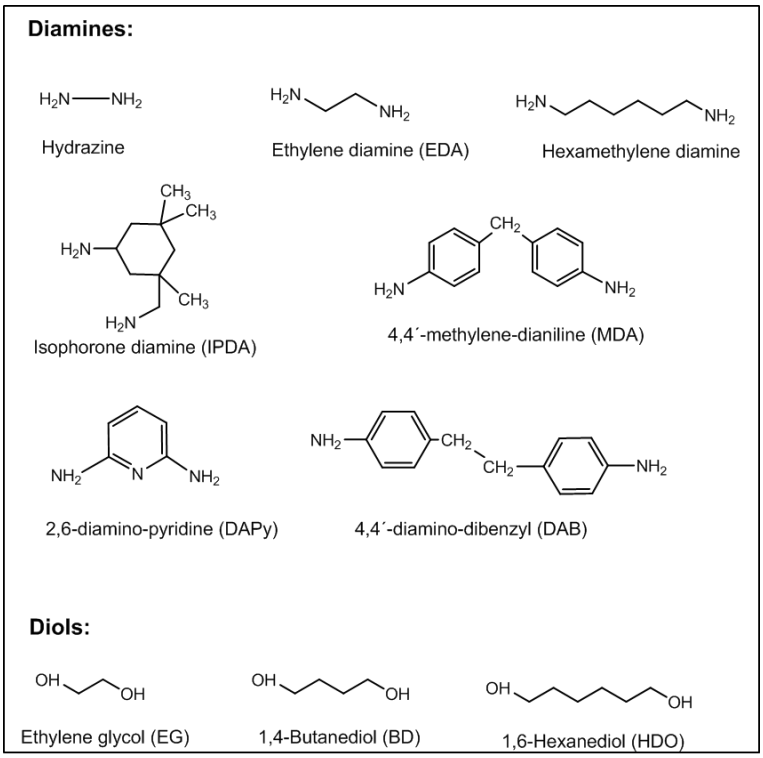

Figure 1.14. Examples of commonly used diol and diamine extenders

The type of chain extender strongly influences the mechanical performance of the PUs [180,181]. When a diamine is used as a chain extender, better physical properties than with diols are obtained, due to stronger hydrogen bonds arising from the urea linkage. Coutinho *et al.* [71,182] studied the thermal degradation profile of films cast from aqueous PUDs. They observed that the type of chain extender affects the whole process of thermal degradation and the presence of urea groups formed when diamines were used improved the thermal resistance of the chains. Moreover it was found that the PU properties depend on whether the chain extender has an even or odd number of methylene (CH_2) groups [2,180,183–185]. The PU with even number of carbon atoms in the chain extender adopts the lowest energy fully extended conformations that allow hydrogen bonding in both

directions perpendicular to the chain axis which is not possible with odd number of carbon atoms. This led to polymer films with higher tensile strength in the case of even number of carbon atoms in the chain extender [185]. The chemical and structural characteristics of the chain extension being linear or non-linear [186] or, being aromatic or aliphatic with different compositions [181] influence the properties of the PUs. This is because PU chains with different hard domain structure, cohesion and chain length, yield different degrees of phase separation and hydrogen bonding. In general, fine tuning of the PU final properties may be achieved by adjusting a balance between the phase separation and mixing and connectivity by hydrogen bonding either between hard segments (promoted microphase separation) or between hard and soft segments (promoted phase mixing) [181,187]. The microphase separation of hard and soft segment leads to the unique properties of the PU elastomers:high tensile strength and high elongation at break.

In addition to diols and diamines, low molecular weight multi-functional polyols and polyamines can also be used as chain extender. The PU produced with polyamines such as diethylene triamine (DETA) and triethylene tetramine (TETA) leads to internal crosslinking and results in an increase in modulus, strength and thermal stability as well as the water and solvent resistance of the dispersion cast films [188].

1.2.3 Preparation methods

There are number of approaches to manufacture the PUDs. Most of them have one preparation process in common, which is the first phase of production, synthesis of a low molecular weight "NCO-terminated prepolymer". The step that is different in the various

processes is the chain extension which is a build-up of the PU prepolymer into a high molecular weight PU [189].

1.2.3.1. Solvent process

In the solvent process, in order to control the viscosity, the prepolymer is synthesized in a water miscible polar solvent such as acetone, tetrahydrofuran (THF) or methyl ethyl ketone (MEK). However as the acetone is the most used solvent in this process, it is often called acetone process. The PU prepolymer is then reacted with chain extender followed by dispersion in water (Figure 1.15). The dispersion process of PU/solvent in water follows three consecutive steps with the slow addition of water to the PU solution [140,190]. Initially, water is soluble in the PU/solvent solution and therefore the viscosity slightly decreased. Later, the generation of water droplets makes the viscosity rise sharply. After reaching a maximum point, which is known as phase inversion point [140], PU particles are formed in the water phase and the viscosity drops again because the effect of adding more water is just to dilute the dispersion. The solvent is then removed by evaporation. In this method, the polymer formation is done in a homogenous solution, yielding a product that usually has high quality and the synthesis is reproducible. However, production of branched and crosslinked PUDs is virtually impossible because they cannot be dispersed in water and hence mostly linear PUs are produced by this method. A disadvantage of acetone process is the use of high amount of organic solvent, which is economically unfavorable due to the solvent cost, the distillation process and the low reactor volume yield [9].

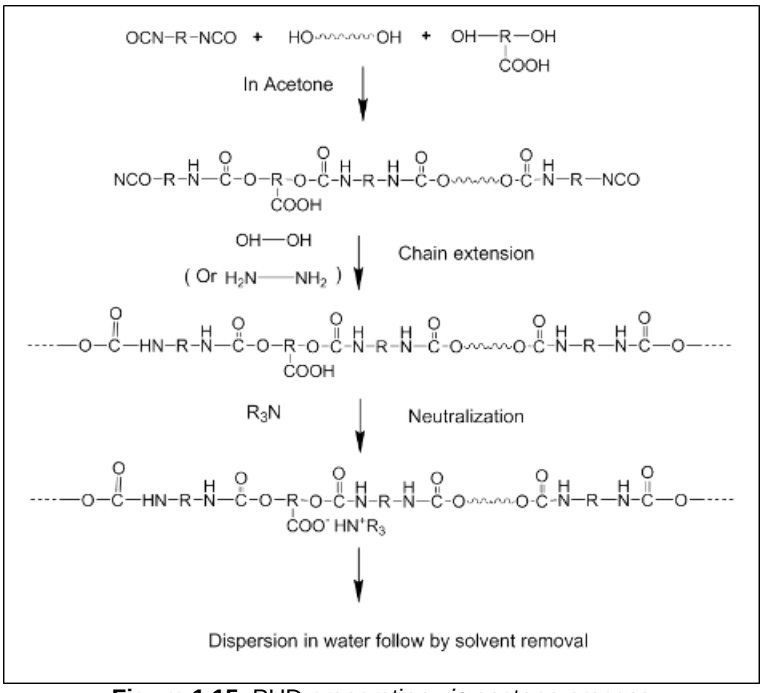

Figure 1.15. PUD preparation *via* acetone process

1.2.3.2. Prepolymer mixing process

The prepolymer mixing method avoids using the high amounts of solvents that are required in the acetone process. In this method, the NCO-terminated PU prepolymers containing ionic groups are synthesized in bulk and afterwards dispersed in water, followed by addition of suitable chain extender to avoid the side reaction of NCO group with water (Figure 1.16). Usually the dispersion is carried out at low temperature to avoid this side reaction and aliphatic diisocyanates are more suitable for this method due to their lower reactivity [9,189]. The prepolymer viscosity is an important factor in this method and it needs to be controlled in order to obtain a good dispersion. A small amount of solvent (around 15 wt%), often N-methylpyrollidone (NMP), is frequently added to the prepolymer in order to

reduce the viscosity before the dispersion. In this method, the chain extension reaction is performed in the dispersion and the polymer is heterogeneous in structure [9]. There are some examples in the literature comparing the acetone and prepolymer mixing processes [136,138,191–193]. It was observed that the minimum amount of DMPA needed to obtain a stable dispersion was 2 wt% and 4 wt% for acetone and prepolymer mixing processes, respectively [138,193]. Two reasons were proposed by author to explain this difference: i) a decrease in surface activity of the carboxylate group on the surface of PU particles caused by the NMP, and ii) a decrease in the stability of the particles resulting from the low molecular weight prepolymers during dispersion.

The prepolymer mixing process is an easy method suitable for low viscosity PU prepolymers. On the other hand, crosslinked products can be made by starting with branched prepolymers and this may be important for some applications that need cross-linking [189]. By tuning the type and the amount of chain extender or using multifunctional polyamines, PUD with internal crosslinking can be obtained with superior mechanical properties for high performance coatings.

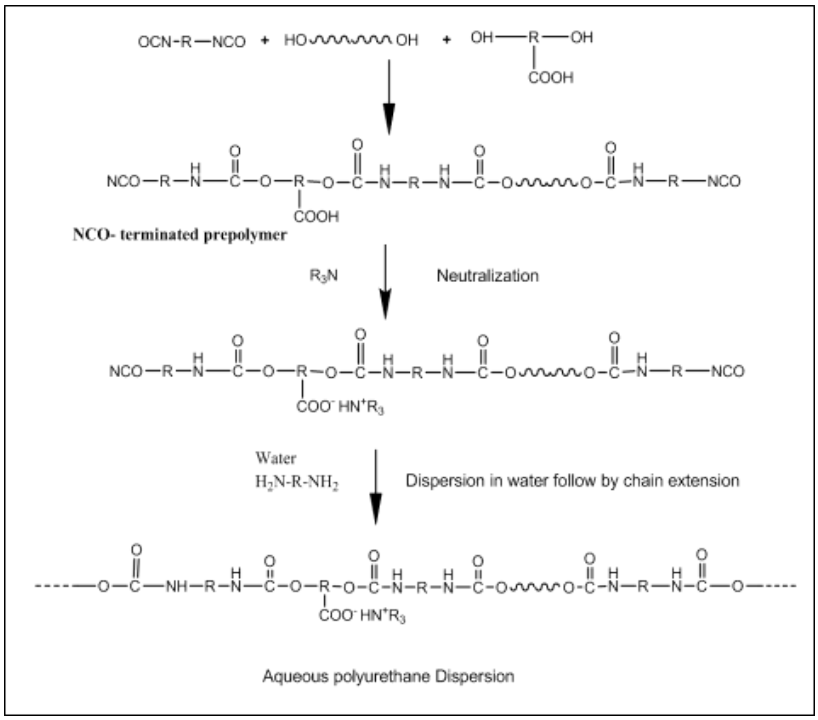

Figure 1.16. PUD preparation *via* prepolymer mixing process

1.2.3.3. Melt dispersion process

Figure 1.17 presents the PUD preparation *via* melt dispersion process. In this method, the NCO-terminated prepolymer is reacted with an excess of urea and/or ammonia (at temperature > 130 °C) resulting in prepolymer terminated with biuret or urea groups. This capped oligomer can be dispersed in water (at temperature > 100 °C) to reduce the viscosity of the system. The biuret group is methyllated with formaldehyde by lowering the pH to acidic condition and the chain extension is performed within the dispersed phase. This process is not practical and cost-effective due to the high reaction temperature and the toxicity of formaldehyde.

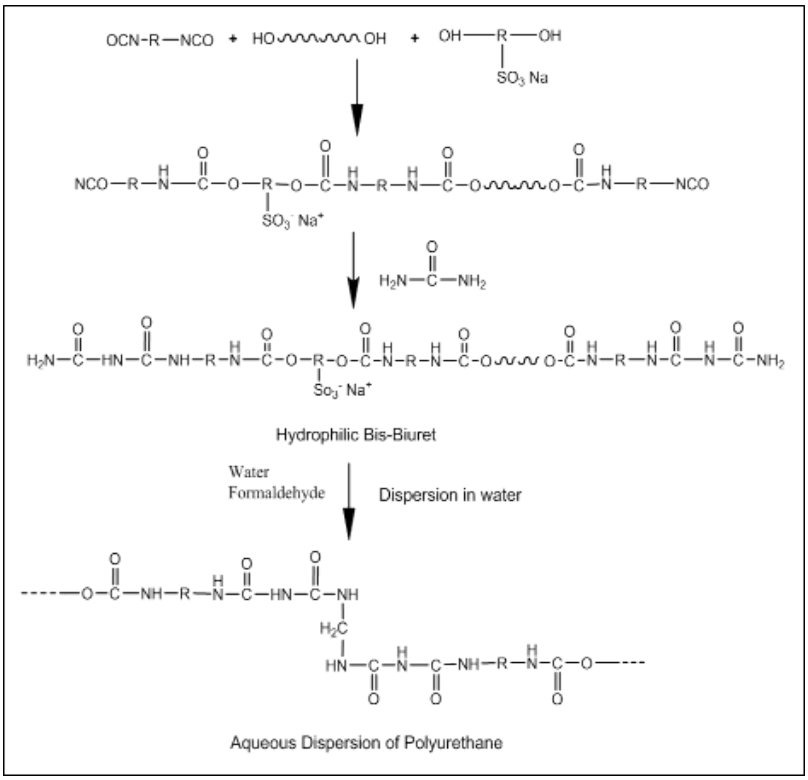

Figure 1.17. PUD preparation *via* melt dispersion process

1.2.3.4. Ketamine/ketazine process

The ketamine/ketazine process can be regarded as a variant of the prepolymer mixing process. The only difference is that in this method, the chain-extending agent is a ketone-blocked diamine (ketamine) or ketone-blocked hydrazine (ketazine) that are inert towards isocyanate groups. These compounds are mixed directly with the isocyanate terminated PU prepolymer [194]. During the subsequent water dispersion step, the ketamine or ketazine is hydrolyzed to generate free diamine or hydrazine, respectively (Figure 1.18). As this process is faster than water - isocyanate reaction, quantitative chain extension can efficiently take place. The advantage of the ketamine process over the

prepolymer mixing process is that it is better suited for preparing aqueous urethanes based on the more reactive aromatic isocyanates. However as the chain extension and the dispersion step occur simultaneously, the viscosity increases steadily until a phase inversion takes place. For this reason powerful agitation and/or some co-solvent is often required.

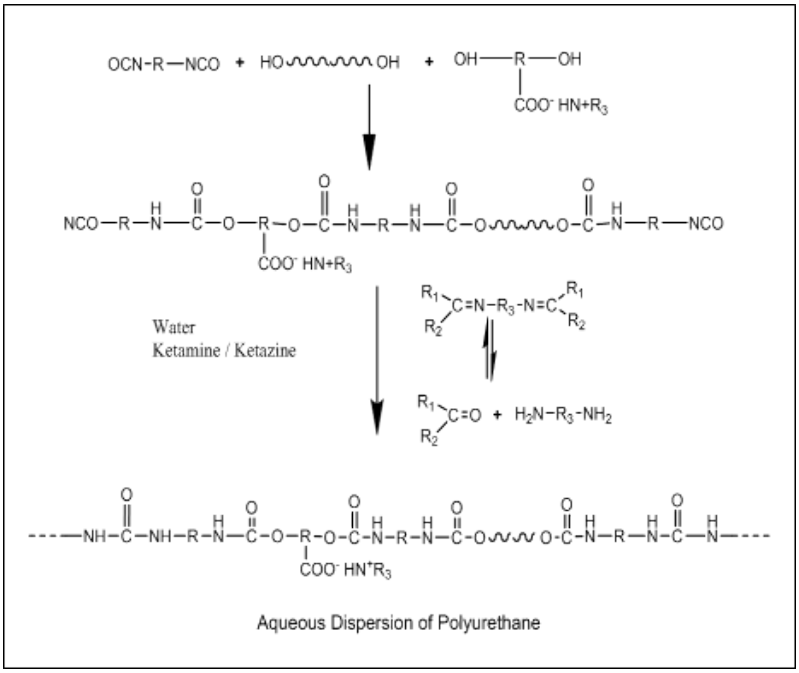

Figure 1.18. PUD preparation *via* Ketamine/ketazine process

1.2.3.5. Miniemulsion polyaddition process

In the methods presented up to this point, PUDs are synthesized *via* two-step procedures. The main disadvantage of these processes is the strong dependence of the polymer and colloidal dispersion characteristics, and polymer performance on the type and amount of dispersing unit added (mostly by use of DMPA). To eliminate this disadvantage

an alternative approach to synthesize PUD has been proposed, through one-step procedure, in which the polyaddition reaction is performed in pre-formed aqueous miniemulsion [17,195,196]. A miniemulsion is formed by emulsification of the organic reactants (hydrophobic diol and diisocyanate) in water using surfactants and co-stabilizers and afterward applying high shear to break the droplets. The emulsifier ensures stability against droplet coalescence and the co-stabilizer against diffusional droplet degradation (Ostwald ripening) [197]. In this way, the small droplets (~200 nm) containing the reactants serve as reactors. It has been shown that the polyaddition reactions of diisocyanate with the diol is the main reaction, whereas the reaction of diisocyanate with water is negligible [195]. Polymerization of these stable monomeric droplets leads to particles, which ideally maintain the same size distribution as the initial miniemulsion. The procedure is schematically presented in Figure 1.19. To further decrease the possibility of reaction of isocyanate groups with water and to obtain high molecular weight PUs using the miniemulsion technique, the following requirements have to be fulfilled: (1) reactants should have low water solubility, (2) the reaction between diisocyanate and diol has to be slow to allow enough time for the miniemulsification, and (3) the reaction of the diisocyanate with water in the dispersed state has to be slower than the reaction with the diol. Various approaches have been developed towards the control of the side reactions and production of high molecular weight PUs [17], such as increasing the particle size, increasing the amount of hydrophobic diol, or, the use of organo-tin compounds as catalyst [17,196]. It is worth mentioning that the choice of polyol is very important in this method and highly reactive polyols are better options [196].

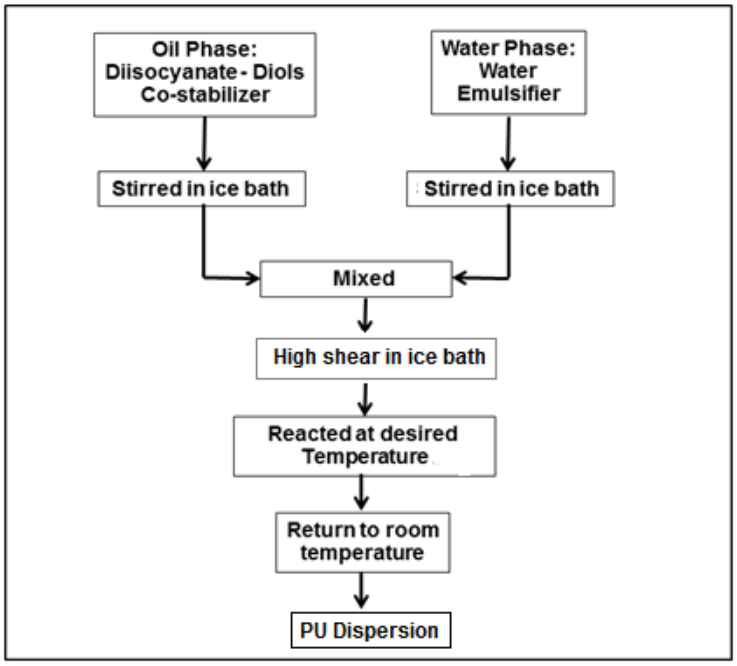

Figure 1.19. PUD preparation *via* Miniemulsion polyaddition process

Polyols from renewable sources have been used in miniemulsion. Castor oil was used as polyol [198–200] and vegetable oils such as olive oil and açaí oil were considered in the formulation as costabilizers to prepare PUDs via one step miniemulsion polymerization. Cramail and coworkers [201] synthesized bio-based hydrophobe-free PU-urea latexes with high solids content (up to 50%) through miniemulsion polymerization. They used hydrophobic vegetable-based diol in PU synthesis which acted as hydrophobe and allowed stabilizing the droplets against Ostwald ripening.

However, miniemulsification adds complexity and cost of the process and increases the energy consumption for industrial applications [202].

The most implemented methods of PUD preparation are solvent process and prepolymer mixing process.

1.3. PU/poly(meth)acrylic hybrid dispersions

Although researchers have successfully developed PUDs into practical systems, their high cost and low water and alkali resistance can be a drawback for some applications. In order to optimize the cost/performance ratio, PUs are often used in hybrid systems with polyesters [203], alkyds and poly(meth)acrylics [11,203], of which the combination of PU/ poly(meth)acrylic is the most common. (Meth)acrylics bring the outdoor and alkali resistance, good compatibility with pigment and low cost; while PU enhances the toughness, flexibility and film forming performance [11,23,204]. In the following section, the different synthetic methods to produce PU/poly(meth)acrylic hybrid dispersions are outlined.

1.3.1. Blending

Blending of PUDs and (meth)acrylic dispersions is a simple and tempting approach to combine the beneficial properties of both polymers [205]. However, in many cases the performance of these products is compromised because of the incompatibility between the two polymers and the fact that both polymers are present in separated particles [15,206–209], which induces significant undesired phase separation [206,209]. To overcome this drawback, the acrylic and/or the PU particles have been functionalized with crosslinkable functionalities [11,210–212]. Mostly OH-NCO reactions were used for this aim [210–212]. A different approach was used by Okamoto *et al.* [11] who blended an acrylic emulsion

polymer containing keto or aldo groups and a PUD incorporating a hydrazine group. Aldo or keto carbonyl groups (from diacetone acrylamide in acrylics) reacted with the hydrazine in the PU (See Figure 1.20). The cross-linking of PU and acrylic phases was determined by the decrease in the intensity of the signal arising from the keto group in Fourier-transform infrared spectroscopy (FTIR) even at room temperature. The authors reported that the crosslinked blends exhibited synergistic effects in film properties, such as good solvent resistance, flexibility at low temperature, toughness at high temperature and good abrasion resistance.

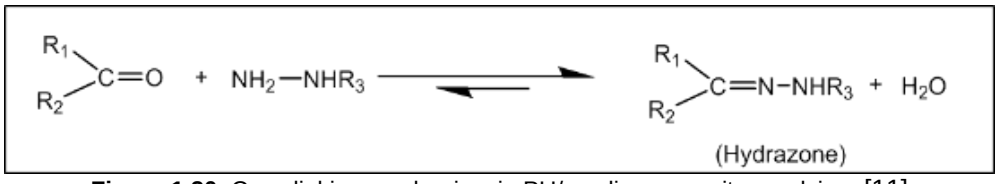

Figure 1.20. Crosslinking mechanism in PU/acrylic composite emulsion [11]

Although in this synthetic method, the phase separation between the PU and the acrylic polymer decreased, the control of the final film nanostructure is not guaranteed and other approaches are necessary to avoid phase separation in many cases.

1.3.2 Hybrids

An alternative to physical mixing of dispersions of acrylic polymers and PUDs is the polymerization of acrylic monomers in a PUD. This is usually performed by miniemulsion polymerization [209,213,214] or by seeded emulsion polymerization process [14,19,207,208,215–217]. In order to avoid possible phase separation between PU and (meth)acrylic polymers, covalent bonds between PU and acrylic polymers can be formed by

means of grafting or crosslinking mechanisms. For that purpose, difunctional monomers containing hydroxyl and (meth)acrylic functional groups, such as hydroxyethyl methacrylate (HEMA) [18,218–220], 2-hydroxypropyl acrylate (HPA)[221] or hydroxyethyl acrylate (HEA) [222] have been utilized in the PU synthesis. Moreover, functional monomers having two hydroxyl groups and one vinyl group such as 3-allyloxy-1,2-propanediol glycerol allyl ether (GAE) [223], allyl polyoxyethylene ether [224] and bisphenol A bis(2-hydroxy-3-methacryloxypropyl) ether (Bis- GMA) [225] have been used to functionalize PUs. Renewable materials such as castor oil and linseed oil were also used in order to provide vinyl functionality to PUs [226–228]. The functionalized PUs reacted with acrylic monomers in emulsion [14,16,218,219,221] or miniemulsion polymerization [18,229–231] in order to prepare the chemically-bounded PU/(meth)acrylic hybrid dispersions [202].

The literature on the PU/(meth)acrylic hybrids and also covalently bonded hybrids obtained from emulsion and miniemulsion is discussed in this section.

1.3.2.1. Miniemulsion polymerization

A miniemulsion is prepared by dissolving the preformed PU in a mixture of monomers and eventually a costabilizer mixing the solution with an aqueous solution of emulsifier and the resulting coarse dispersion is emulsified into small droplets by a high energy dispersion device. Then the monomers are polymerized through a free radical polymerization process. In some cases [213], PU acts as a hydrophobe and stabilizes the miniemulsion against Ostwald ripening, avoiding use of costabilizer. PU/(meth)acrylic hybrid dispersions have been prepared in different ways: i) dissolving PU in (meth)acrylic monomers followed by miniemulsification and polymerization (no chemical bond between PU and (meth)acrylic)

[209], ii) dissolving PU containing double bonds in (meth)acrylic monomers followed by miniemulsification and polymerization (grafted PU/(meth)acrylic hybrid) [229,230,232] and iii) dissolving the NCO-terminated PU in a mixture of (meth)acrylic monomers in which at least one monomer contains an OH group followed by miniemulsification and polymerization (grafted PU/(meth)acrylic hybrid) [233–241].

1.3.2.1.1. No grafting

Hybrid polymer latexes containing PU and acrylic copolymer of MMA/BA have been synthesized *via* miniemulsion polymerization by Wang et al. [209]. The composition of the hybrids was varied (MMA/BA ratio and PU/Ac ratio). These hybrid latexes were compared with blends of acrylic emulsions and PUDs, showing that the hybrids had better mechanical properties. The effect was attributed to the more homogeneous morphology achieved in the hybrids. However, this effect depends on the hybrid composition and was significantly lower at higher PU content in the hybrid.

1.3.2.1.2. Free radical polymerization in the presence of vinyl functionalized PU

Miniemulsion polymerization was employed to synthesize hybrids by free radical polymerization of (meth)acrylics in presence of a vinyl terminated PU prepolymer [232]. The prepolymer was prepared by adding hydroxyl-terminated polybutadiene (HTPB) to the reaction mixture used to synthesize the PU. Various vinyl monomers (styrene, MMA and BA) were used and the polymerization was initiated by ɣ-ray radiation at room temperature (Figure 1.21) [232]. The TEM images of hybrids obtaining from different vinyl monomers

(Figure 1.22) showed that the PU- polystyrene (PS) particles were more homogenous than the PU-PMMA and PU-PBA. The author claimed that the morphology and the grafting efficiency were influenced by the hydrophilicity of the monomer and its compatibility with PU. The hydrophobic monomer, which had good miscibility with the PU, resulted in a more homogeneous morphology and higher grafting efficiency. The grafting efficiency of PU with polystyrene (PS) was calculated from ^{1}H NMR spectroscopy of the samples before and after extraction with methanol as polystyrene is not soluble in methanol. It is worth pointing out the degree of grafting for hybrids containing (meth)acrylic polymers was not calculated and the conclusion of higher grafting efficiency in the case of PU-PS based on TEM images is not precise.

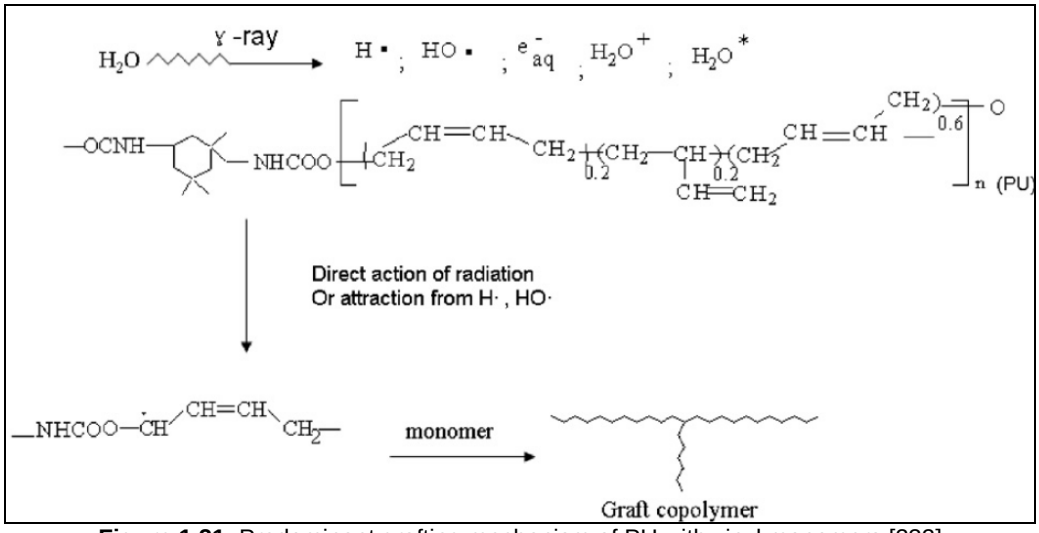

Figure 1.21. Predominant grafting mechanism of PU with vinyl monomers [232]

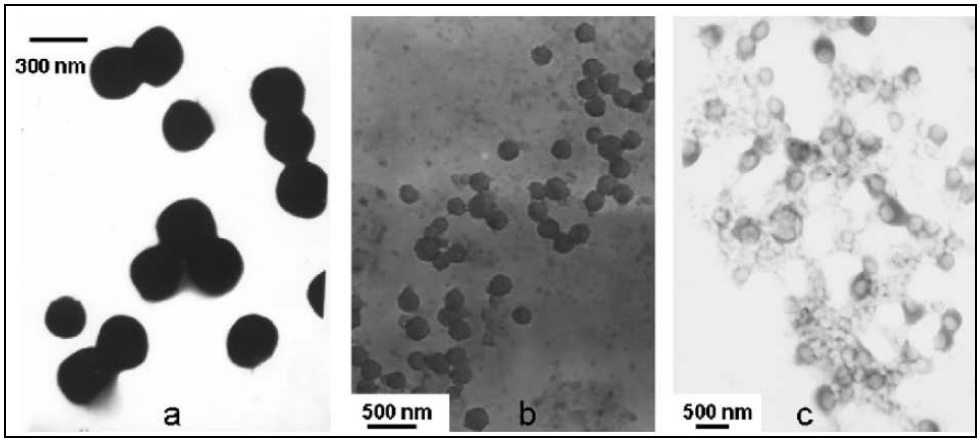

Figure 1.22. TEM images of samples using different vinyl monomers: (a) Styrene, (b) BA, (c) MMA [232]

Commercially available isocyanate terminated PU prepolymer (Incorez 701) was reacted with HEMA and the modified PUs were reacted with acrylic monomers by free radical polymerization in miniemulsion to obtain pressure sensitive adhesives (PSAs) [229,230]. The effect of PU weight fraction (5-50 wt% relative to acrylic monomers) and the degree of grafting of the PU prepolymer on the acrylic backbone (controlled by the ratio between HEMA and the chain extender, Bisphenol A) on the mechanical and adhesive properties were studied. It was observed that PSAs with PU fractions lower than 25 wt% had low fibrillation stress and a high maximum strain (strain at debonding) which is characteristic of PSAs with a low level of elasticity due to the low level of crosslinking. On the other hand, for PSAs with more than 35 wt% PU fraction, probe-tack curves showed almost no fibrillation plateau and the maximum strain was low. The PSA with 25 wt% of PU showed the best adhesive properties as it formed a fibrillar structure and debonded at a maximum strain. On the other hand, at fixed PU fraction (25 wt%) with increasing the degree of grafting (ratio of HEMA/BPA) the maximum strain decreased markedly and the

fibrillation stress and the shear resistance increased. It is worth mentioning that the degree of grafting was not reported quantitatively and no information regarding the molar mass of the soluble part was given. In this investigation, a homogeneous incorporation of PUs was assumed, which was consistent with the transparent and crack-free film at macroscopic level [230]. In a further study, the same group [231] showed that the hypothesis of fully homogeneous particle morphology was insufficient to explain the mechanical test results satisfactorily. Whereas the films were considered to be homogeneous at the scale of the polymer network in their previous studies [230], the TEM images clearly indicated a significant degree of phase separation at high PU contents [231]. Thus, while at 5 wt% and 25 wt% PU, the particles were predominantly homogeneous, at 50 wt% PU the chemical grafting was not sufficient and particles with core–shell morphology were observed, with PU-rich domains preferentially located in the outer shell (Figure 1.23). It was observed that the core–shell morphology persisted in the adhesive films, resulting in a percolating network of stiffer PU-rich shells. The reduced miscibility between the two phases limited the particle interpenetration leading to dramatic changes in the film properties. Therefore, the observed unexpected adhesive properties can only be explained in terms of the mentioned morphological changes.

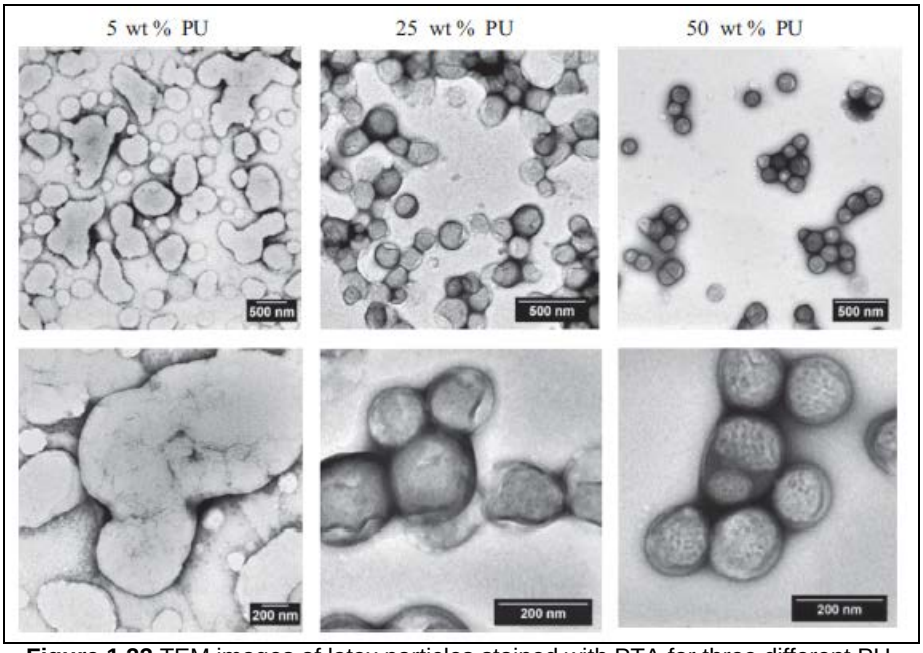

Figure 1.23.TEM images of latex particles stained with PTA for three different PU weight fractions [231]

1.3.2.1.3. Simultaneous addition and Free radical polymerization

Incorez 701 was added to the mixture of (meth)acrylic monomers and HEMA and the polyaddition reaction of PU prepolymer with HEMA and the free radical polymerization of (meth)acrylics were performed simultaneously [233–236] *via* semicontinuous miniemulsion polymerization. Figure 1.24 presents the reaction scheme of the process of synthesis.

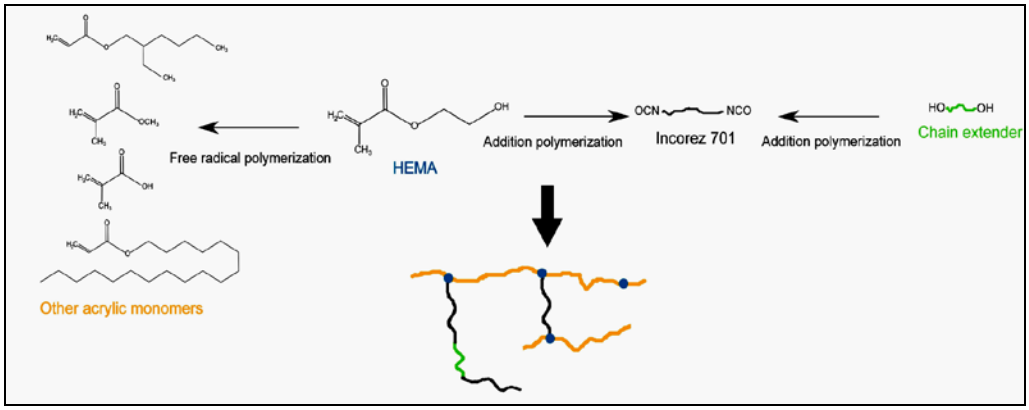

Figure 1.24. Reaction scheme: reaction between Incorez701 (PU prepolymer), HEMA and (meth)acrylic monomers for giving crosslinking of PU and reaction between prepolymer and chain extender [233–235]

Different ways of modifying the polymer microstructure, and hence the adhesive properties of PU/(meth)acrylic hybrids were studied: i) varying the PU chains (changing the chain extender and its concentration) [234], ii) altering the acrylic chains (varying concentrations of chain transfer agent) [235] and iii) altering the number of crosslinking points between the PU and the acrylic chains (by changing the concentrations of HEMA and chain extending diol – Bisphenol A) [236]. Using different diols as chain extenders, it was observed that the polymerization rate was different, as the diols are efficient chain transfer agents [234]. Although similar gel content was observed in all the cases, important differences were noticed in the type of network due to variation of the acrylic chain length and the number of PU/acrylic linking points, which strongly affected the adhesive properties of a PSA. Moreover, it was found that with increasing CTA concentration the gel content decreased, which led to a decrease in cohesive strength and to an initial increase in the tackiness and peel resistance of adhesives [235]. However, at higher CTA concentration, due to the very low cohesion of the polymer, both tack and peel resistance decreased. On

the other hand, the effect of HEMA concentration depends on the OH/NCO ratio, controlled by using different diol (Bisphenol A) contents. At OH/NCO=1, the gel content and the crosslinking density increased with the HEMA content leading to a decrease of both work of adhesion and peel resistance. The shear resistance and shear adhesion failure temperature (SAFT) were already high at low HEMA concentration and they were not affected by increasing its concentration. At OH/NCO=2, as the diol content was increased it induced changes only in acrylic chain lengths and not in the PU-acrylics connections [236]. It is worth mentioning that in this system, no evidence of phase separation between PU and acrylic polymer was observed, perhaps due to the low (10 %wt) PU content, and the polymer particles presented a homogeneous morphology [234]. For the same system, it has been reported [237] that using redox initiator the polymerization temperature strongly affects the polymer architecture and subsequently the adhesive properties. The optimum temperature range to obtained appropriate microstructure of the hybrid for balanced adhesive properties was proposed to be 40-60ºC. At higher temperatures, the acrylic chain length decreased due to a higher radical flux that led to faster termination and to a decrease in the gel content. On the other hand, at lower temperature the conversion of isocyanate groups was very low. Therefore, the optimum adhesive properties were obtained where the sol molecular weight of the polymer was within appropriate limits such that high entanglement was achieved allowing for sufficient fibril formation during debonding, whilst maintaining a reasonable degree of viscous flow giving good tack and peel properties and gel content was high enough to give good shear strength.

In the PU/acrylic PSAs discussed above [229,230,233–237], usually the increase of shear strength that gives cohesiveness to the PSA was accompanied with a decrease in the tack adhesion. In order to design a balanced PSA, a compromise should be found between these two properties. The flexibility of photopolymerization process provided the opportunity to synthesize a wide variety of PSAs, some having desired and unusual combination of high work of adhesion and maximum shear resistance at high temperature [238–241].

Daniloska *et al.* [238,239] employed miniemulsion photopolymerization at room temperature in a continuous tubular reactor in order to prepare PU/acrylic hybrid. The miniemulsion droplets contained an isocyanate terminated PU prepolymer (Incorez 701) dissolved in a mixture of (meth)acrylic monomers containing HEMA. The hybrid was formed by free radical polymerization and accomplished by some addition polymerization, leading to a complex polymer architecture. However, due to the low reaction temperature, most of the NCO of the PU prepolymer did not react during the photopolymerization reaction. Thus, PU/acrylic latexes undergo spontaneous formation of nanogels within the latex particles during storage at room temperature, firstly due to NCO reactions (with the OH groups of both HEMA and water) and afterwards due to supramolecular interactions and H-bonding [240,241]. Therefore the polymer microstructure and hence the adhesive properties evolved during storage and the final configuration was reached over a period of time as long as 7 months. By variation of photoinitiator type and concentration, incident light irradiation and residence time, excellent control over the polymer microstructure (MWD, gel fraction and sol molecular weight) was obtained. This allowed the synthesis of a wide range of polymers with different microstructure and performance as PSAs using the same formulation of

PU/acrylics, some of them with well balanced adhesive properties (simultaneous good cohesion and adhesion) [239].

In most of these studies, commercial PU prepolymers were used, probably synthesized using solvents. In addition, the miniemulsification step adds complexity and cost to the process and increases the investment and energy consumption for industry [202]. Moreover, in the miniemulsification, an external surfactant is usually used in order to stabilize the dispersion which can migrate during film formation and influence negatively the final properties. Therefore, the seeded emulsion polymerization using PUD as a seed appears as a better option, especially for commercial aims.

1.3.2.2. Seeded emulsion polymerization

In seeded emulsion polymerization, core(acrylic)/shell(PU) type particles are synthesized by using PUDs as seeds. These PUDs are usually prepared by introducing ionic groups (most often carboxylic acid groups) in the PU chains, which allow performing of emulsifier-free emulsion polymerization. Figure 1.25 shows the schematic representation of the process. There are several examples in both open [14,207–209,217,242] and patent [243,244] literature for this seeded emulsion polymerization.

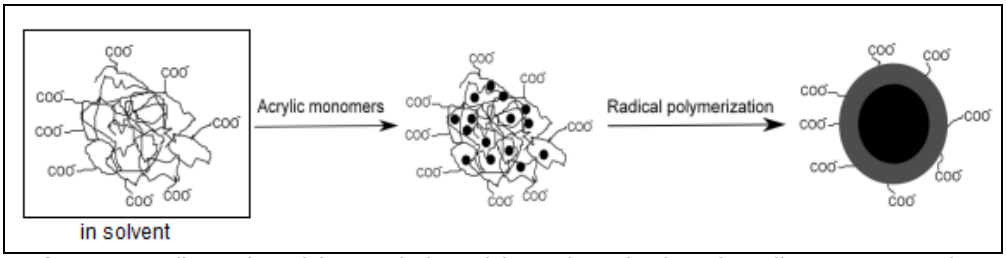

Figure 1.25. Illustration of the seeded emulsion polymerization of acrylic monomers using PUD as a seed

As it was discussed in detail in Section 1.2.3, the PUD can be synthesized *via* different methods. Generally the process involves preparing the PU prepolymer containing DMPA moiety in a solvent followed by neutralization of carboxylic acid group. After dispersing in water and chain extension, the (meth)acrylic monomers are added to the PUD and polymerized in batch [14,215] or semibatch [15] mode. Hybrid particles usually present core/shell morphology (with the acrylic in the core and the PU in the shell), however hemispherical and sandwich-like morphologies have been also reported for PU/(meth)acrylic hybrid particles [15] probably due to the high interfacial tension between PU and acrylics. The comparison of hybrids and corresponding physical blends showed that the hybrids had higher Koenig hardness, tensile strength, elongation at break and water sensitivity because of the improved compatibility and phase-mixing between the (meth)acrylic and the PU component [15,207].

With the aim of finding the optimum properties, the effect of different weight ratio of PU/(meth)acrylics was studied by different authors [19,216]. Son *et al.* [216] observed that the yield point of stress–strain curve, hardness and water resistance of hybrid films increased with the acrylic monomer content, whereas the abrasion resistance and elongation at break decreased. They concluded that the optimum (meth)acrylic monomer content to have a balance of good mechanical properties and abrasion resistance as well as an acceptable water sensitivity was about 30 wt%. However, the optimum proportion could be different depending on the desired application. In another study [19] it was observed that by increasing the acrylic content to 50 wt%, the hardness, alkali resistance and solvent resistance increased. However by further increase in the acrylic content, all the mentioned

properties decreased. They claimed that this was due to the incompatibility of PU and acrylic phases that at higher acrylic content resulted in phase separation during film formation. Therefore, it was concluded that the optimum performance properties for coating applications were provided by a hybrid synthesized with a 50:50 wt ratio of PU and polyacrylic components. Moreover, the effect of different ratios of methyl methacrylate (MMA) and butylacrylate (BA) was studied by Šebenik *et al.* [217]. PU/acrylic (50/50 wt/wt) hybrids were prepared using semibatch emulsion polymerization of MMA and BA. The results revealed that the hybrid prepared with a MMA/BA weight ratio of 65/35 showed the best properties for the production of a coating for hard substrates.

In order to increase the compatibility of PU and (meth)acrylic polymers, grafted PU/acrylic hybrids were prepared by polymerizing vinyl monomers in the presence of a vinyl terminated PU. The formation of the graft copolymers gave transparent films [16] due to higher compatibility between two polymers. Grafting of the PU and (meth)acrylics influenced he morphology of the particles (core-shell) and the adhesion to various substrates [16]. It is reported that with grafting the particle size of the aqueous dispersions decreased [16]. However, in this process as the PU droplets (swollen with acrylic monomers) are formed before the polymerization of acrylics, the final particle size is supposed to be similar to the value before radical polymerization. Therefore, the observed change in the particle size might be attributed to particle coalescence during free radical polymerization. The effect of the DMPA, acrylic content (MMA) and crosslinking monomer (hydroxypropyl acrylate, HPA) of the PU/MMA hybrids on the dispersion and film properties has been investigated by Zhang *et al.* [221]. It was shown that by increasing the content of DMPA, MMA and HPA,

the particle size decreased, mainly with DMPA. The tensile strength of the film increased, while the elongation at break decreased with increasing HPA (increasing crosslinking), with increasing DMPA (according to the authors due to smaller particles that form better film) and with increasing MMA (higher T_g) [221].

Wang *et al*. [245] compared PU/acrylic hybrids synthesized *via* miniemulsion polymerization and seeded emulsion polymerization. In the miniemulsion polymerization an external emulsifier was used while in the seeded emulsion polymerization method, stabilization was provided by the DMPA contained in the PU. There was no significant difference in polymerization kinetics. However, the comparison was not straightforward as the initiator was different; benzoyl peroxide (BPO) in the miniemulsion polymerization and azobisisobutyronitrile (AIBN) for seeded emulsion polymerization. In the case of miniemulsion, the size of the polymer particles was always close to those of the initial droplets (around 200 nm), whereas the sizes of the seeded polymerizations increased during polymerization (from 70 to 250 nm) and it was different depending on the amount of DMPA in the formulation. It is worth pointing out that the increase in the particle size during batch polymerization is not expected as all the monomers were added before polymerization and they swelled into the PU particles. Moreover, it was observed DMPA has a reinforcement effect on the mechanical properties of the polymer film synthesized in seeded emulsion polymerization. However no information regarding water sensitivity is given and it would be interesting to compare the effect of hydrophilic PU containing DMPA units on the water resistance with that of the conventional surfactant.

In all of the presented studies the PUDs were synthesized in procedures using solvents. An alternative that is discussed in the next section is to use (meth)acrylic monomers as diluents during the synthesis of the PU .

1.3.2.3. Solvent-free processes

Due to the environmental issues and for economical reasons, solvent-free PU/(meth)acrylic hybrids have attracted an increasing attention from academia and industry [246,247]. Solvent-free processes for preparing PU/Poly(meth)acrylic hybrids using (meth)acrylic monomers as diluents have been reported in patent [247–255] and open literature [222,224,246,256,257]. For example, Zhang *et al.* synthesized solvent-free polysiloxane modified PU/acrylics using BA and BA/BMA (butyl methacrylate) as diluents [246]. The effect of DMPA content (varied in the range of 1.7 wt% to 2.5 wt%) on the stability and water sensitivity of the polymer film was studied. The optimal range for colloidal stability was 1.9-2.1%. Further increase of the DMPA concentration affected negatively the water resistance of the films. However, no attempts were done to improve the water sensitivity of the polymer films at higher DMPA contents and the stability of the dispersion was not studied at high DMPA content. The same group studied the synthesis of TDI-based PU/acrylic composites using different proportions of MMA/BA (from 0/100 to 100/0 wt/wt) as diluents for application as binders for coatings [222]. The emulsification in water of the PU prepolymer/monomer mixture was done at 85 ºC in order to reduce the viscosity of the organic phase and to make easier the dispersion in water. The mechanical properties of the hybrids were studied as a function on (meth)acrylic formulation. As the

ratio MMA/(BA+MMA) increased, the tensile strength and the pendulum hardness of the hybrids increased due to the high T_g of PMMA.

Ryu *et al.* used a mixture of monomers (MMA / BA / glycidyl methacrylate-GMA and acrylonitrile-AN) as solvent to obtain PU/acrylic hybrids for binders [256]. The influence of the GMA/AN ratio on dispersion and polymer properties was studied. By increasing this ratio polymer films with better modulus and higher hardness were obtained, but the elongation at break and water uptake decreased. Yi *et al.* [224] used allyl polyoxyethylene glycol ether as functional monomer in order to graft PU and acrylics and also to increase the self-emulsifying ability (due to hydrophilicity of allyl polyoxyethylen ether). It was observed that the PU/acrylic hybrid was composed of linear polymers, but not cross-linked as the polymer was soluble in THF during soxhlet extraction. This was attributed to two possible reasons: i) high amount of acrylic monomers and small amount of PU containing double bonds (acrylic/PU from 55/45 to 75/25) and ii) low polymerization rate of allyl group compared to that of acrylic monomers that resulted in no (or low) reaction of ally groups with acrylic monomers during radical polymerization. However, no information regarding the degree of grafting is given and hybrids were not compared with the similar ones with no ally ether in order to see the effect of grafting on the synthesis and properties of solvent-free PU/(meth)acrylic dispersion. Moreover, the comparison of the degree of grafting and performance of grafted hybrids with functional monomers having different vinyl functionalities (allyl ether, methacrylic or acrylic) would be interesting.

In the solvent-free PU/(meth)acrylic hybrid dispersions, several factors may affect the application properties: the type of PU (that can be varied by varying the raw materials

discussed in Section 1.2.2), the type of (meth)acrylic copolymer (that can be different in terms of composition and monomer sequence distribution), the PU/(meth)acrylic ratio, the DMPA content, the molecular weight distribution, the compatibility of PU vs. (meth)acrylate and grafting (that can be achieved using different type of functional monomers). In the works discussed above, the effect of PU/(meth)acrylic ratio and the (meth)acrylic monomer composition have been studied [222,246,256]. However, the polymer microstructure was only scarcely studied and consequently very limited information on the effect of the polymer microstructure on the final properties is available. Moreover, the effect of the type of PU and grafting is not reported in the solvent-free PU/(meth)acrylic hybrid system.

1.4. Conclusions

In the first part of Chapter 1, the effect of PU composition on the characteristic of PUDs and film properties was discussed. It was shown that the properties of the PU films can be tuned through selection of raw material. But in general, PUDs have the disadvantage of high cost and low water and alkali resistance. Therefore the combination of PU and (meth)acrylic polymers has attracted attention as (meth)acrylics have low cost and high water and alkali resistance.

Among many methods for the synthesis of PU/(meth)acrylic hybrid dispersions, seeded emulsion polymerization seems to be a promising method for production of surfactant-free waterborne PU/(meth)acrylic hybrids. However, in most of the reported studies, the PU prepolymer was synthesized in solvents. Due to environmental reasons, protection of the health of workers and in order to decrease the production costs, there has

been a shift of interest towards solvent-free procedures, in which PU prepolymers are synthesized using (meth)acrylic monomer mixture as reaction diluents to control the viscosity. In the reported work on solvent-free PU/(meth)acrylic hybrids mostly the mechanical properties of the hybrids was studied and no details of dispersion properties and attempts to control them were presented. No further studies on PU composition and its effect on the final properties of the polymer film were found (polyol type or chain extender type). Moreover there is a lack of information regarding the effect of grafting and type of the functional monomer on the polymer microstructure, particle and film morphology and polymer final properties.

1.5. Objectives of the thesis

The objective of this thesis is to study the emulsion polymerization of solvent-free and emulsifier-free polyurethane/(meth)acrylic hybrid dispersions, in which the PU chains will be grafted onto acrylic chains during the polymerization. In this method, the use of volatile organic compound (VOC) in the synthesis of PU is avoided and therefore the solvent removal step is eliminated, which is a big advantage In terms of technical advances. In addition, a fundamental study on the effect of each component of the hybrid on the polymer microstructure and final properties is carried out with the aim of understanding the structure-property relationship of the hybrids.

The complexity of this thesis is drawn by the fact that the main process involves various sub-process, such as solvent free synthesis of PU, preparation of aqueous PU/(meth)acrylic hybrid dispersions, and seeded emulsion polymerization of

(meth)acrylates. In each of them, the process parameters influenced the final results, that all together simultaneously determine the properties and the performance of the hybrid PU/(meth)acrylic polymers.

The main challenges thus are to produce colloidally stable hybrid aqueous dispersions with controlled particle size and polymer microstructure, in which the stability will be provided by COOH containing PU chains. In order to have a fundamental knowledge about the effect of each parameter on the microstructure and final properties of such a complex polymeric system, the composition of the water dispersible PU is varied by means of use of different types of polyols and chain extenders and different amounts of DMPA diol, which on one hand allows control of colloidal properties of the hybrid dispersions and on the other the properties of the hybrid polymer. Grafting is introduced in the system by means of use of different functional monomers in the formulations. The degree of grafting is quantified and the effect of type of functional monomer on the polymer microstructure, the particle and film morphology and the final properties of the polymer film is studied. Finally, the performance of the synthesized PU/(meth)acrylic hybrids in coating applications will be investigated for non-grafted and grafted hybrids using different functional monomers.

1.6. Outline of the Thesis

In **Chapter 1**, the state-of-the-art in production of waterborne PU/(meth)acrylic hybrids is critically reviewed. As the synthesis of water dispersible PUs is an important task toward the hybrids synthesis, in the first part of Chapter 1 the basic chemistry of PUs,

including the main chemical components and methods for the synthesis is discussed. Moreover, the main objectives of the thesis are described.

Chapter 2 is devoted to achieve control of particle size and colloidal stability of the hybrid PU/(meth)acrylic dispersions by means of variation of amount of COOH containing diol (DMPA) and type of chain extender used (different hydrophylicity/phobicity) during PU synthesis. In the second part of this chapter, the polymer characteristics and final properties of the corresponding films from the hybrids are evaluated in terms of mechanical properties and water sensitivity.

In the present thesis, the properties of the polyurethane/(meth)acrylic are varied by modifying the polymer microstructure through i) grafting polyurethane into (meth)acrylics ii) altering the polyurethane chains and iii) modifying the (meth)acrylic chains. The results are in Chapters 3,4 and 5.

Chapter 3 describes the modification of polymer microstructure *via* grafting polyurethanes into (meth)acrylics. The effect of grafting and type of functional monomer on polymer microstructure, morphology and film properties of the hybrids is investigated.

In **Chapter 4**, the modification of polymer microstructure *via* modifying polyurethane chains is presented. The chemical structure of polyurethanes is modified by using different polyol types. The effect of polyol type on the properties of PU/(meth)acrylic final films was studied. Grafting was introduced in the system and the grafted and nongrafted hybrids were compared in mechanical properties and water sensitivity.

Chapter 5 reports on the modification of the polymer microstructure by varying the (meth)acrylic chains. The effect of different proportion of MMA/BA as (meth)acrylic monomers on the film properties is discussed in grafted and non grafted hybrids.

In **Chapter 6**, polyurethane/(meth)acrylic hybrid dispersions are used for wood floor coatings. Three different functional monomers (with two hydroxyl groups in their structures but different vinyl functionalities) are used in order to graft PU and (meth)acrylics. The effect of the type of functional monomer on polymer microstructure, degree of grafting and final coating properties are discussed.

Chapter 7 summarizes the most relevant conclusions of this thesis.

In order to avoid repetition of the experimental and characterization techniques, a detailed description of the materials, characterization method and coating performance is given in **Appendixes I** and **II**, respectively. Finally the **Abbreviations** used in the thesis is listed.

1.7. References

[1] P. Król, Synthesis methods, chemical structures and phase structures of linear polyurethanes. Properties and applications of linear polyurethanes in polyurethane elastomers, copolymers and ionomers, Prog. Mater. Sci. 52 (2007) 915–1015.

[2] C. Prisacariu, Polyurethane Elastomers, Springer Vienna, Vienna, 2011.

[3] E. Delebecq, J. Pascault, B. Boutevin, On the Versatility of Urethane: Urea Bonds/Reversibility , Blocked Isocyanate and Non-isocyanate Polyurethane, Chem. Rev. 113 (2013) 80–118.

[4] I. Yilgör, E. Yilgör, G.L. Wilkes, Critical parameters in designing segmented polyurethanes and their effect on morphology and properties: A comprehensive review, Polymer (Guildf). 58 (2015) A1–A36.

[5] O. Bayer, W. Siefken, H. Rinke, L. Orthner, H. Schild, A process for the production of polyurethanes and polyureas, DRP 728981, 1937.

[6] O. Bayer, Das Di-Isocyanat-Polyadditionsverfahren (Polyurethane), Angew. Chemie. 59 (1947) 257–272.

[7] D. Dieterich, Aqueous emulsions, dispersions and solutions of polyurethanes; synthesis and properties, Prog. Org. Coatings. 9 (1981) 281–340.

[8] H. Xiao, H.X. Xiao, K.C. Frisch, N. Malwitz, Polyurethane–urea anionomer dispersions. I, J. Appl. Polym. Sci. 54 (1994) 1643–1650.

[9] B.K. Kim, Aqueous polyurethane dispersions, Colloid Polym. Sci. 274 (1996) 599–611.

[10] Polyurethane Dispersions Market by Type, End-Use Industry and Region - Global Forecast to 2021, (2017). www.marketsandmarkets.com.

[11] Y. Okamoto, Y. Hasegawa, F. Yoshino, Urethane/acrylic composite polymer emulsions, Prog. Org. Coatings. 29 (1996) 175–182.

[12] S. Ramesh, K. Tharanikkarasu, G.N. Mahesh, G. Radhakrishnan, Synthesis, Physicochemical Characterization, and Applications of Polyurethane Ionomers: A Review, J. Macromol. Sci. Part C Polym. Rev. 38 (1998) 481–509.

[13] S.W. Lee, Y.H. Lee, H. Park, H. Do Kim, Effect of total acrylic/fluorinated acrylic monomer contents on the properties of waterborne polyurethane/acrylic hybrid emulsions, Macromol. Res. 21 (2013) 709–718.

[14] M. Hirose, F. Kadowaki, J. Zhou, The structure and properties of core-shell type acrylic-polyurethane hybrid aqueous emulsions, Prog. Org. Coatings. 31 (1997) 157–169.

[15] D. Kukanja, J. Golob, A. Zupancic-valant, M. Krajnc, The structure and properties of acrylic-polyurethane hybrid emulsions and comparison with physical blends, J. Appl. Polym. Sci. 78 (2000) 67–80.

[16] M. Hirose, J. Zhou, K. Nagai, Structure and properties of acrylic-polyurethane hybrid emulsions, Prog. Org. Coatings. 38 (2000) 27–34.

[17] M. Barrère, K. Landfester, High molecular weight polyurethane and polymer hybrid

particles in aqueous miniemulsion, Macromolecules. 36 (2003) 5119–5125.

[18] M. Li, E.S. Daniels, V. Dimonie, E.D. Sudol, M.S. El-Aasser, Preparation of Polyurethane/Acrylic Hybrid Nanoparticles via a Miniemulsion Polymerization Process, Macromolecules. 38 (2005) 4183–4192.

[19] V.D. Athawale, M.A. Kulkarni, Preparation and properties of urethane/acrylate composite by emulsion polymerization technique, Prog. Org. Coatings. 65 (2009) 392–400.

[20] J. Kozakiewicz, Developments in aqueous polyurethane and polyurethane-acrylic dispersion technology. Part I. Polyurethane dispersions, Polimery. 60 (2015) 525–535.

[21] A. Noreen, K.M. Zia, M. Zuber, S. Tabasum, M.J. Saif, Recent trends in environmentally friendly water-borne polyurethane coatings: A review, Korean J. Chem. Eng. 33 (2016) 388–400.

[22] X. Zhou, Y. Li, C. Fang, S. Li, Y. Cheng, W. Lei, X. Meng, Recent Advances in Synthesis of Waterborne Polyurethane and Their Application in Water-based Ink: A Review, J. Mater. Sci. Technol. 31 (2015) 708–722.

[23] H.L. Manock, New developments in polyurethane and PU/acrylic dispersions, Pigment Resin Technol. 29 (2000) 143–151.

[24] V.D. Athawale, M.A. Kulkarni, A review on recent developments in polyurethane/acrylate hybrid dispersions, Paintindia. 59 (2009) 67.

[25] J. Kozakiewicz, Developments in aqueous polyurethane and polyurethane-acrylic dispersion technology Part II. Polyurethane-acrylic dispersions and modification of polyurethane and polyurethane-acrylic dispersions, Polimery/Polymers. 61 (2016) 81–91.

[26] K. Nakamae, T. Nishino, S. Asaoka, Microphase separation and surface properties of segmented polyurethane m Effect of hard segment content, Int. J. Adhes. Adhes. 16 (1996) 233–239.

[27] S. Velankar, S.L. Cooper, Microphase Separation and Rheological Properties of Polyurethane Melts . 1 . Effect of Block Length, Macromolecules. 31 (1998) 9181–9192.

[28] S. Velankar, S.L. Cooper, Microphase Separation and Rheological Properties of Polyurethane Melts . 2 . Effect of Block Incompatibility on the Microstructure, Macromolecules. 33 (2000) 382–394.

[29] S. Velankar, S.L. Cooper, Microphase Separation and Rheological Properties of Polyurethane Melts . 3 . Effect of Block Incompatibility on the Viscoelastic Properties, Macromolecules. 33 (2000) 395–403.

[30] H. Sardon, A.C. Engler, J.M.W. Chan, D.J. Coady, J.M. O'Brien, D. Mecerreyes, Y.Y. Yang, J.L. Hedrick, Homogeneous isocyanate- and catalyst-free synthesis of polyurethanes in aqueous media, Green Chem. 15 (2013) 1121.

[31] O. Figovsky, L. Shapovalov, A. Leykin, O. Birukova, R. Potashnikova, Progress in Elaboration of Nonisocyanate Polyurethanes Based on Cyclic Carbonates, Int. Lett. Chem. Phys. Astron. 3 (2013) 52–66.

[32] L. Maisonneuve, A.S. More, S. Foltran, C. Alfos, F. Robert, Y. Landais, T. Tassaing, E. Grau, H. Cramail, Novel green fatty acid-based bis-cyclic carbonates for the synthesis of isocyanate-free poly(hydroxyurethane amide)s, RSC Adv. 4 (2014) 25795.

[33] A. Lee, Y. Deng, Green polyurethane from lignin and soybean oil through non-isocyanate reactions, Eur. Polym. J. 63 (2015) 67–73.

[34] B. Lebedev, V. Veridusova, H. Höcker, H. Keul, Thermodynamics of Aliphatic Cyclic Urethanes, of Their Ring-Opening Polymerization, and of Corresponding Polyurethanes, Macromol. Chem. Phys. 203 (2002) 1114.

[35] B. Nohra, L. Candy, J.-F. Blanco, C. Guerin, Y. Raoul, Z. Mouloungui, From Petrochemical Polyurethanes to Biobased Polyhydroxyurethanes, Macromolecules. 46 (2013) 3771–3792.

[36] O. Kreye, H. Mutlu, M.A.R. Meier, Sustainable routes to polyurethane precursors, Green Chem. 15 (2013) 1431.

[37] G. Rokicki, P.G. Parzuchowski, M. Mazurek, Non-isocyanate polyurethanes: synthesis, properties, and applications, Polym. Adv. Technol. 26 (2015) 707–761.

[38] A. Yuen, A. Bossion, E. Gómez-Bengoa, F. Ruipérez, M. Isik, J.L. Hedrick, D. Mecerreyes, Y.Y. Yang, H. Sardon, Room temperature synthesis of non-isocyanate polyurethanes (NIPUs) using highly reactive N-substituted 8-membered cyclic carbonates, Polym. Chem. 7 (2016) 2105–2111.

[39] J. Alsarraf, Y.A. Ammar, F. Robert, E. Cloutet, H. Cramail, Y. Landais, Cyclic guanidines as efficient organocatalysts for the synthesis of polyurethanes, Macromolecules. 45 (2012) 2249–2256.

[40] J. Alsarraf, F. Robert, H. Cramail, Y. Landais, Latent catalysts based on guanidine templates for polyurethane synthesis, Polym. Chem. 4 (2013) 904.

[41] C.A. Smith, H. Cramail, T. Tassaing, Insights into the organocatalyzed synthesis of urethanes in supercritical carbon dioxide: An in Situ FTIR spectroscopic kinetic study, ChemCatChem. 6 (2014) 1380–1391.

[42] L. Maisonneuve, O. Lamarzelle, E. Rix, E. Grau, H. Cramail, Isocyanate-Free Routes to Polyurethanes and Poly(hydroxy Urethane)s, Chem. Rev. 115 (2015) 12407–12439.

[43] M.S. Kathalewar, P.B. Joshi, A.S. Sabnis, V.C. Malshe, Non-isocyanate polyurethanes: from chemistry to applications, RSC Adv. 3 (2013) 4110.

[44] C. Carré, L. Bonnet, L. Avérous, Original biobased nonisocyanate polyurethanes: solvent- and catalyst-free synthesis, thermal properties and rheological behaviour, RSC Adv. 4 (2014) 54018–54025.

[45] L. Maisonneuve, A.-L. Wirotius, C. Alfos, E. Grau, H. Cramail, Fatty acid-based (bis) 6-membered cyclic carbonates as efficient isocyanate free poly(hydroxyurethane) precursors, Polym. Chem. 5 (2014) 6142–6147.

[46] O. Lamarzelle, P.-L. Durand, A.-L. Wirotius, G. Chollet, E. Grau, H. Cramail, Activated lipidic cyclic carbonates for non-isocyanate polyurethane synthesis, Polym. Chem. 7 (2016) 1439–1451.

[47] W.C. Pan, C.H. Lin, S.A. Dai, High-performance segmented polyurea by transesterification of diphenyl carbonates with aliphatic diamines, J. Polym. Sci. Part A Polym. Chem. 52 (2014) 2781–2790.

[48] M. Unverferth, O. Kreye, A. Prohammer, M.A.R. Meier, Renewable non-isocyanate based thermoplastic polyurethanes via polycondensation of dimethyl carbamate monomers with diols, Macromol. Rapid Commun. 34 (2013) 1569–1574.

[49] S. Neffgen, H. Keul, H. Höcker, Ring-opening polymerization of cyclic urethanes and ring-closing depolymerization of the respective polyurethanes, Macromol. Rapid Commun. 17 (1996) 373–382.

[50] J. Kušan, H. Keul, H. Höcker, Cationic ring-opening polymerization of tetramethylene urethane, Macromolecules. 34 (2001) 389–395.

[51] W.D. Vilar, Chemistry and Technology of Polyurethanes, Vilar Consultoria Ltda., Rio de Janeiro, 2002.

[52] H. Sardon, A. Pascual, D. Mecerreyes, D. Taton, H. Cramail, J.L. Hedrick, Synthesis of polyurethanes using organocatalysis: A perspective, Macromolecules. 48 (2015) 3153–3165.

[53] A. Goldschmidt, H.-J. Streitberger, BASF handbook on Basics of coating technology, Second, Vincentz Network, Hannover, 2007.

[54] J.-P. Pascault, H. Sautereau, V. Jacques, R.J. Williams, Thermosetting Polymers, Vol. 64, CRC Press, 2002.

[55] W. Neumann, P. Fisher, The Preparation of Carbodiimides from Isocyantes, Angew. Chemie Int. Ed. English. 1 (1962) 621–625.

[56] W. Dell, W. Kubitza, D. Liebsch, Process for the preparation of polyisocyanates containing uretdione and isocyanurate groups, the polyisocyanates obtained by this process and their use in two-component polyurethane coatings, US4994541 A, 1991.

[57] A. Lapprand, F. Boisson, F. Delolme, F. Méchin, J.P. Pascault, Reactivity of isocyanates with urethanes: Conditions for allophanate formation, Polym. Degrad. Stab. 90 (2005) 363–373.

[58] K.C. Frisch, L.P. Rumao, Catalysis in Isocyanate Reactions, J. Macromol. Sci. Part C Polym. Rev. 5 (1970) 103–149.

[59] J.H. Fabris, M.E. Maxey, H. Uelzmann, Trimerization of aromatic isocyanates catalyzed by certain ammonium salts, US3980594 A, 1976.

[60] Michael Szycher, Szycher's Handbook of Polyurethanes, second edi, CRC Press, 2013.

[61] S. Sugano, C. Chinwanitcharoen, S. Kanoh, T. Yamada, S. Hayashi, K. Tada, Preparation of aqueous polyurethane dispersions using aromatic diisocyanate, Macromol. Symp. 239 (2006) 51–57.

[62] H.-K. Ono, F.N. Jones, S.P. Pappas, Relative reactivity of isocyanate groups of isophorone diisocyanate. Unexpected high reactivity of the secondary isocyanate group, J. Polym. Sci. Polym. Lett. Ed. 23 (1985) 509–515.

[63] S.A. Madbouly, J.U. Otaigbe, Recent advances in synthesis, characterization and rheological properties of polyurethanes and POSS/polyurethane nanocomposites dispersions and films, Prog. Polym. Sci. 34 (2009) 1283–1332.

[64] K.-L. Noble, Waterborne Polyurethanes, Prog. Org. Coatings. 32 (1997) 131–136.

[65] Z.W. Wicks, D.A. Wicks, J.W. Rosthauser, Two package waterborne urethane systems, Prog. Org. Coatings. 44 (2002) 161–183.

[66] I.W. Cheong, H.C. Kong, J.H. An, J.H. Kim, Synthesis and characterization of

polyurethane-urea nanoparticles containing methylenedi-p-phenyl diisocyanate and isophorone diisocyanate, J. Polym. Sci. Part A Polym. Chem. 42 (2004) 4353–4369.

[67] N. Williams, Aqueos dispersions of polyurethane-addition polymer hybrid particles especially for use in coating applications, US 2005/0256252 A1, 2005.

[68] C. Prisacariu, R.H. Olley, A.A. Caraculacu, D.C. Bassett, C. Martin, The effect of hard segment ordering in copolyurethane elastomers obtained by using simultaneously two types of diisocyanates, Polymer (Guildf). 44 (2003) 5407–5421.

[69] P. Król, B. Król, L. Subocz, P. Andruszkiewicz, Polyurethane anionomers synthesised with aromatic, aliphatic or cycloaliphatic diisocyanates, polyoxyethylene glycol and 2,2-bis-(hydroxymethyl)propionic acid. Part 3. Electrical properties of polyurethane coatings, Colloid Polym. Sci. 285 (2006) 177–183.

[70] D.J. Hourston, G. Williams, R. Satguru, J.D. Padget, D. Pears, Structure-property study of polyurethane anionomers based on various polyols and diisocyanates, J. Appl. Polym. Sci. 66 (1997) 2035–2044.

[71] F.M.B. Coutinho, M.C. Delpech, T.L. Alves, A.A. Ferreira, Degradation profiles of cast films of polyurethane and poly(urethane-urea) aqueous dispersions based on hydroxy-terminated polybutadiene and different diisocyanates, Polym. Degrad. Stab. 81 (2003) 19–27.

[72] Y.M. Lee, J.C. Lee, B.K. Kim, Effect of soft segment length on the properties of polyurethane anionomer dispersion, Polymer (Guildf). 35 (1994) 1095–1099.

[73] M.M. Rahman, H.-D. Kim, Characterization of waterborne polyurethane adhesives containing different soft segments, J. Adhes. Sci. Technol. 21 (2007) 81–96.

[74] N. Akram, R.S. Gurney, M. Zuber, M. Ishaq, J.L. Keddie, Influence of Polyol Molecular Weight and Type on the Tack and Peel Properties of Waterborne Polyurethane Pressure-Sensitive Adhesives, Macromol. React. Eng. 7 (2013) 493–503.

[75] F. Mumtaz, M. Zuber, K.M. Zia, T. Jamil, R. Hussain, Synthesis and properties of aqueous polyurethane dispersions: Influence of molecular weight of polyethylene glycol, Korean J. Chem. Eng. 30 (2013) 2259–2263.

[76] G. Gündüz, R.R. Kısakürek, Structure–Property Study of Waterborne Polyurethane Coatings with Different Hydrophilic Contents and Polyols, J. Dispers. Sci. Technol. 25 (2004) 217–228.

[77] A. Eceiza, M.D. Martin, K. De La Caba, G. Kortaberria, N. Gabilondo, M.A. Corcuera, I. Mondragon, Thermoplastic polyurethane elastomers based on

polycarbonate diols with different soft segment molecular weight and chemical structure: Mechanical and thermal properties, Polym. Eng. Sci. 48 (2008) 297–306.

[78] V. García-Pacios, J.A. Jofre-Reche, V. Costa, M. Colera, J.M. Martín-Martínez, Coatings prepared from waterborne polyurethane dispersions obtained with polycarbonates of 1,6-hexanediol of different molecular weights, Prog. Org. Coatings. 76 (2013) 1484–1493.

[79] J. Kloss, M. Munaro, G.P. De Souza, J.V. Gulmine, S.H. Wang, S. Zawadzki, L. Akcelrud, Poly(ester urethane)s with polycaprolactone soft segments: A morphological study, J. Polym. Sci. Part A Polym. Chem. 40 (2002) 4117–4130.

[80] M. Rogulska, A. Kultys, S. Pikus, Studies on thermoplastic polyurethanes based on new diphenylethane-derivative diols. III. The effect of molecular weight and structure of soft segment on some properties of segmented polyurethanes, J. Appl. Polym. Sci. 110 (2008) 1677–1689.

[81] K. Gisselfält, B. Helgee, Effect of soft segment length and chain extender structure on phase separation and morphology in poly(urethane urea)s, Macromol. Mater. Eng. 288 (2003) 265–271.

[82] D.-K. Lee, H.-B. Tsai, R.-S. Tsai, Effect of composition on aqueous polyurethane dispersions derived from polycarbonatediols, J. Appl. Polym. Sci. 102 (2006) 4419–4424.

[83] F. Li, R. Tuinier, I. van Casteren, R. Tennebroek, A. Overbeek, F. A. M. Leermakers, Self-Organization of Polyurethane Pre-Polymers as Studied by Self-Consistent Field Theory, Macromol. Theory Simulations. 25 (2016) 16–27.

[84] Z.W. Wicks, F.N. Jones, S.P. Pappas, D.A. Wicks, Organic Coatings: Science and Technology, 3rd editio, Wiley, Hoboken, NJ, USA, 2007.

[85] T. Chen, H. Li, Y. Gao, M. Zhang, Study on epoxy resins modified by polycarbonate polyurethanes, J. Appl. Polym. Sci. 69 (1998) 887–893.

[86] D. Lee, H. Tsai, W. Yu, R. Tsai, Polyurethane Dispersions Derived from Polycarbonatediols and a Carboxylic Polycaprolactonediol, J. Macromol. Sci. Part A. 42 (2005) 85–93.

[87] S.M. Cakić, M. Spírková, I.S. Ristić, J.K. B-Simendić, M. M-Cincović, R. Poreba, The waterborne polyurethane dispersions based on polycarbonate diol: Effect of ionic content, Mater. Chem. Phys. 138 (2013) 277–285.

[88] V. Garcia-Pacios, V. Costa, M. Colera, J.M. Martin-Martinez, Waterborne polyurethane dispersions obtained with polycarbonate of hexanediol intended for use

as coatings, Prog. Org. Coatings. 71 (2011) 136–146.

[89] V. García-Pacios, M. Colera, Y. Iwata, J.M. Martín-Martínez, Incidence of the polyol nature in waterborne polyurethane dispersions on their performance as coatings on stainless steel, Prog. Org. Coatings. 76 (2013) 1726–1729.

[90] M. Yen, S. Kuo, PCL – PEG – PCL Triblock Ester – Ether Copolydiol-Based Waterborne Polyurethane . II . Effect of NCO / OH Mole Ratio and DMPA Content on the Physical Properties, J. Appl. Polym. Sci. 67 (1997) 1301–1311.

[91] Y.-S. Kwak, S.-W. Park, Y.-H. Lee, H.-D. Kim, Preparation and properties of waterborne polyurethanes for water-vapor-permeable coating materials, J. Appl. Polym. Sci. 89 (2003) 123–129.

[92] J. Kozakiewicz, Polysiloxaneurethanes: New polymers for potential coating applications, Prog. Org. Coatings. 27 (1996) 123–131.

[93] T. Su, G.Y. Wang, X.D. Xu, C.P. Hu, Preparation and properties of waterborne polyurethaneurea consisting of fluorinated siloxane units, J. Polym. Sci. Part A Polym. Chem. 44 (2006) 3365–3373.

[94] G. Fei, Y. Shen, H. Wang, Y. Shen, Effects of polydimethylsiloxane concentration on properties of polyurethane/polydimethylsiloxane hybrid dispersions, J. Appl. Polym. Sci. 102 (2006) 5538–5544.

[95] D. V. Palaskar, A. Boyer, E. Cloutet, J. Le Meins, B. Gadenne, C. Alfos, C. Farcet, H. Carmail, Original Diols from Sunflower and Ricin Oils:Synthesis, Characterization, and Use as Polyurethane Building Block, Polym. Chem. 50 (2012) 1766–1782.

[96] C. Fu, Z. Zheng, Z. Yang, Y. Chen, L. Shen, A fully bio-based waterborne polyurethane dispersion from vegetable oils: From synthesis of precursors by thiol-ene reaction to study of final material, Prog. Org. Coatings. 77 (2014) 53–60.

[97] C. Vilela, A.F. Sousa, A.C. Fonseca, A.C. Serra, J.F.J. Coelho, C.S.R. Freirea, A.J.D. Silvestrea, The quest for sustainable polyesters–insights into the future, Polym. Chem. 5 (2014) 3119–3141.

[98] E. Hablot, D. Zheng, M. Bouquey, L. Avérous, Polyurethanes based on castor oil: Kinetics, chemical, mechanical and thermal properties, Macromol. Mater. Eng. 293 (2008) 922–929.

[99] V. Athawale, S. Kolekar, Interpenetrating polymer networks based on polyol modified castor oil polyurethane and polymethyl methacrylate, Eur. Polym. J. 34 (1998) 1447–1451.

[100] S.A. Madbouly, Y. Xia, M.R. Kessler, Rheological behavior of environmentally friendly castor oil-based waterborne polyurethane dispersions, Macromolecules. 46 (2013) 4606–4616.

[101] L. Poussard, J. Lazko, J. Mariage, J.M. Raquez, P. Dubois, Biobased waterborne polyurethanes for coating applications: How fully biobased polyols may improve the coating properties, Prog. Org. Coatings. 97 (2016) 175–183.

[102] Y.H. Hu, Y. Gao, N. De Wang, C.P. Hu, S. Zu, L. Vanoverloop, D. Randall, Rigid polyurethane foam prepared from a rape seed oil based polyol, J. Appl. Polym. Sci. 84 (2002) 591–597.

[103] H. Yeganeh, M.R. Mehdizadeh, Synthesis and properties of isocyanate curable millable polyurethane elastomers based on castor oil as a renewable resource polyol, Eur. Polym. J. 40 (2004) 1233–1238.

[104] H.P. Benecke, B.R. Vijayendran, D.B. Garbark, K.P. Mitchell, Low cost and highly reactive biobased polyols: A co-product of the emerging biorefinery economy, Clean - Soil, Air, Water. 36 (2008) 694–699.

[105] X. Liu, K. Xu, H. Liu, H. Cai, J. Su, Z. Fu, Y. Guo, M. Chen, Preparation and properties of waterborne polyurethanes with natural dimer fatty acids based polyester polyol as soft segment, Prog. Org. Coatings. 72 (2011) 612–620.

[106] A. Zlatanic, C. Lava, W. Zhang, Z.S. Petrovic, Effect of structure on properties of polyols and polyurethanes based on different vegetable oils, J. Polym. Sci. Part B Polym. Phys. 42 (2004) 809–819.

[107] C.-S. Wang, L.-T. Yang, B.-L. Ni, G. Shi, Polyurethane networks from different soy-based polyols by the ring opening of epoxidized soybean oil with methanol, glycol, and 1,2-propanediol, J. Appl. Polym. Sci. 114 (2009) 125–131.

[108] Z.S. Petrović, M.J. Cevallos, I. Javni, D.W. Schaefer, R. Justice, Soy-oil-based segmented polyurethanes, J. Polym. Sci. Part B Polym. Phys. 43 (2005) 3178–3190.

[109] T. Cosgrove, Colloid Science Principles, Methods and Applications, Blackwell Publishing, 2005.

[110] O. Jaudouin, J.-J. Robin, J.-M. Lopez-Cuesta, D. Perrin, C. Imbert, Ionomer-based polyurethanes: a comparative study of properties and applications, Polym. Int. 61 (2012) 495–510.

[111] H. Chen, D. Chen, Q. Fan, X. Yu, Synthesis and properties of polyurethane ionomers based on carboxylated polycaprolactone, J. Appl. Polym. Sci. 76 (2000) 2049–2056.

[112] W.-C. Chan, S.-A. Chen, Polyurethane ionomers: effects of emulsification on properties of hexamethylene diisocyanate-based polyether polyurethane cationomers, Polymer (Guildf). 29 (1988) 1995–2001.

[113] B. Li, D. Peng, N. Zhao, Q. Mu, J. Li, The physical properties of nonionic waterborne polyurethane with a polyether as side chain, J. Appl. Polym. Sci. 127 (2013) 1848–1852.

[114] M.S. Yen, P.Y. Chen, H.C. Tsai, Synthesis, properties, and dyeing application of nonionic waterborne polyurethanes with different chain length of ethyldiamines as the chain extender, J. Appl. Polym. Sci. 90 (2003) 2824–2833.

[115] R.G. Coogan, R. Vartan-Boghossian, Aqueous dispersions of a nonionic, water dispersible polyurethane having pendent polyoxyethylene chains, US patent 5043381, 1991.

[116] H. Honarkar, M. Barmar, M. Barikani, Synthesis, characterization and properties of waterborne polyurethanes based on two different ionic centers, Fibers Polym. 16 (2015) 718–725.

[117] V. Durrieu, A. Gandini, M.N. Belgacem, A. Blayo, G. Eiselé, J.L. Putaux, Preparation of aqueous anionic poly-(urethane-urea) dispersions: Influence of the nature and proportion of the urethane groups on the dispersion and polymer properties, J. Appl. Polym. Sci. 94 (2004) 700–710.

[118] M.G. Lu, J.Y. Lee, M.J. Shim, S.W. Kim, Synthesis and properties of anionic aqueous polyurethane dispersions, J. Appl. Polym. Sci. 86 (2002) 3461–3465.

[119] M.C. Delpech, F.M.. Coutinho, Waterborne anionic polyurethanes and poly(urethane-urea)s: influence of the chain extender on mechanical and adhesive properties, Polym. Test. 19 (2000) 939–952.

[120] H.-C. Tsai, P.-D. Hong, M.-S. Yen, Preparation and physical properties of MDEA-based polyurethane cationomers and their application to textile coatings, Text. Res. J. 77 (2007) 710–720.

[121] E.C. Buruiana, T. Buruiana, G. Strat, M. Strat, Synthesis and optical properties of new polyurethane cationomers with anchored stilbene chromophores, J. Polym. Sci. Part A Polym. Chem. 40 (2002) 1918–1928.

[122] H.A. Al-Salah, H.X. Xiao, J.A. McLean Jr., K.C. Frisch, Polyurethane cationomers. I. Structure–properties relationships, J. Polym. Sci. Part A Polym. Chem. 26 (1988) 1609–1620.

[123] S. Mohanty, N. Krishnamurti, Synthesis and characterization of aqueous

cationomeric polyurethanes and their use as adhesives, J. Appl. Polym. Sci. 62 (1996) 1993–2003.

[124] K.K.S. Hwang, C.-Z. Yang, S.L. Cooper, Properties of polyether-polyurethane zwitterionomers, Polym. Eng. Sci. 21 (1981) 1027–1036.

[125] C.-Z. Yang, K.K.S. Hwang, S.L. Cooper, Morphology and properties of polybutadiene- and polyether-polyurethane zwitterionomers, Die Makromol. Chemie. 184 (1983) 651–668.

[126] P.K.H. Lam, M.H. George, J.A. Barrie, Sulphonated polyurethane ionomers with new ionic diols, Polymer (Guildf). 30 (1989) 2320–2323.

[127] L. He, D. Sun, Synthesis of high-solid content sulfonate-type polyurethane dispersion by pellet process, J. Appl. Polym. Sci. 127 (2013) 2823–2831.

[128] D.K. Kakati, R. Gosain, M.H. George, New polyurethane ionomers containing phosphonate groups, Polymer (Guildf). 35 (1994) 398–402.

[129] S. Ramesh, G. Radhakrishnan, Polyurethane anionomers using phenolphthalins: 1. Synthesis and characterization, Polymer (Guildf). 35 (1994) 3107–3112.

[130] C.-Z. Yang, T.G. Grasel, J.L. Bell, R.A. Register, S.L. Cooper, Carboxylate-containing chain-extended polyurethanes, J. Polym. Sci. Part B Polym. Phys. 29 (1991) 581–588.

[131] S.J. Peng, Y. Jin, X.F. Cheng, T.B. Sun, R. Qi, B.Z. Fan, A new method to synthesize high solid content waterborne polyurethanes by strict control of bimodal particle size distribution, Prog. Org. Coatings. 86 (2015) 1–10.

[132] S.K. Lee, B.K. Kim, High solid and high stability waterborne polyurethanes via ionic groups in soft segments and chain termini, J. Colloid Interface Sci. 336 (2009) 208–214.

[133] F. Zhang, X. Wei, Z. Xiao, Study on high-solid content Si/PU polyurethane dispersion with PES/PPG composite soft segment, J. Appl. Polym. Sci. 127 (2013) 1730–1736.

[134] Y. Zhu, J.L. Hu, K.W. Yeung, Y.Q. Liu, H.M. Liem, Influence of ionic groups on the crystallization and melting behavior of segmented polyurethane ionomers, J. Appl. Polym. Sci. 100 (2006) 4603–4613.

[135] H.M. Jeong, B.K. Ahn, S.M. Cho, B.K. Kim, Water vapor permeability of shape memory polyurethane with amorphous reversible phase, J. Polym. Sci. Part B Polym. Phys. 38 (2000) 3009–3017.

[136] A.K. Nanda, D.A. Wicks, S.A. Madbouly, J.U. Otaigbe, Effect of ionic content, solid content, degree of neutralization, and chain extension on aqueous polyurethane dispersions prepared by prepolymer method, J. Appl. Polym. Sci. 98 (2005) 2514–2520.

[137] T. Tawa, S. Ito, The Role of Hard Segments of Aqueous Polyurethane-urea Dispersion in Determining the Colloidal Characteristics and Physical Properties, Polym. J. 38 (2006) 686–693.

[138] A.K. Nanda, D.A. Wicks, The influence of the ionic concentration, concentration of the polymer, degree of neutralization and chain extension on aqueous polyurethane dispersions prepared by the acetone process, Polymer (Guildf). 47 (2006) 1805–1811.

[139] J. Bullermann, S. Friebel, T. Salthammer, R. Spohnholz, Novel polyurethane dispersions based on renewable raw materials - Stability studies by variations of DMPA content and degree of neutralisation, Prog. Org. Coatings. 76 (2013) 609–615.

[140] H. Sardon, L. Irusta, M.J. Fernández-Berridi, J. Luna, M. Lansalot, E. Bourgeat-Lami, Waterborne polyurethane dispersions obtained by the acetone process: A study of colloidal features, J. Appl. Polym. Sci. 120 (2011) 2054–2062.

[141] M.M. Rahman, H. Do Kim, Synthesis and characterization of waterborne polyurethane adhesives containing different amount of ionic groups (I), J. Appl. Polym. Sci. 102 (2006) 5684–5691.

[142] M.A. Pérez-Limiñana, F. Arán-Aís, A.M. Torró-Palau, A.C. Orgilés-Barceló, J.M. Martín-Martínez, Characterization of waterborne polyurethane adhesives containing different amounts of ionic groups, Int. J. Adhes. Adhes. 25 (2005) 507–517.

[143] M. Barikani, M. Valipour Ebrahimi, S.M. Seyed Mohaghegh, Preparation and characterization of aqueous polyurethane dispersions containing ionic centers, J. Appl. Polym. Sci. 104 (2007) 3931–3937.

[144] M.M. Rahman, H.-D. Kim, Effect of polyisocyanate hardener on waterborne polyurethane adhesive containing different amounts of ionic groups, Macromol. Res. 14 (2006) 634–639.

[145] C. Mao, L.C. Jiang, W.P. Luo, H.K. Liu, J.C. Bao, X.H. Huang, J. Shen, Novel blood-compatible polyurethane ionomer nanoparticles, Macromolecules. 42 (2009) 9366–9368.

[146] S. Zhang, H. Lv, H. Zhang, B. Wang, Y. Xu, Waterborne polyurethanes: Spectroscopy and stability of emulsions, J. Appl. Polym. Sci. 101 (2006) 597–602.

[147] B. Kim, J. Yang, S. Yoo, J. Lee, Waterborne polyurethanes containing ionic groups in soft segments, Colloid Polym. Sci. 281 (2003) 461–468.

[148] L.K. Saw, B.W. Brooks, K.J. Carpenter, D. V. Keight, Catastrophic phase inversion in region II of an ionomeric polymer-water system, J. Colloid Interface Sci. 279 (2004) 235–243.

[149] Dimethylolpropionic Acid in Waterborne PUDs for Coating Applications, (2017). http://www.geosc.com/.

[150] I. de F.A. Mariz, J.C. de la Cal, J.R. Leiza, Control of particle size distribution for the synthesis of small particle size high solids content latexes, Polymer (Guildf). 51 (2010) 4044–4052.

[151] I. de F.A. Mariz, J.R. Leiza, J.C. de la Cal, Competitive particle growth: A tool to control the particle size distribution for the synthesis of high solids content low viscosity latexes, Chem. Eng. J. 168 (2011) 938–946.

[152] G. Pramod, L. Jurgen, N. Roland, R. Helmut, W. Harro, Non-ionic polyurethane dispersions having side chains of polyoxyethylene, US 3920598, 1975.

[153] T.G. Savino, T.C. Balch, A.L. Steinmetz, S.E. Balatin, N. Caiozzo, Novel non-ionic polyurethane resins having polyether backbones in water-dilutable basecoats, US 4946910 A, 1990.

[154] K. Noll, Aqueous dispersions of polyurethane having side chain polyoxyethylene units, US3905929 A, 1975.

[155] H.-C. Tsai, P.-D. Hong, M.-S. Yen, Preparation and physical properties of nonionic aqueous polyurethane coatings containing different side chain PEGME length, J. Appl. Polym. Sci. 108 (2008) 2266–2273.

[156] H. Lijie, D. Yongtao, Z. Zhiliang, S. Zhongsheng, S. Zhihua, Synergistic effect of anionic and nonionic monomers on the synthesis of high solid content waterborne polyurethane, Colloids Surfaces A Physicochem. Eng. Asp. 467 (2015) 46–56.

[157] M.S. Yen, H.C. Tsai, P. Da Hong, The physical properties of aqueous cationic-nonionic polyurethane with poly(ethylene glycol methyl ether) side chain and its blend with aqueous cationic polyurethane, J. Appl. Polym. Sci. 100 (2006) 2963–2974.

[158] B.K. Kim, Y.M. Lee, Aqueous dispersion of polyurethanes containing ionic and nonionic hydrophilic segments, J. Appl. Polym. Sci. 54 (1994) 1809–1815.

[159] R. Lomölder, F. Plogmann, P. Speier, Selectivity of isophorone diisocyanate in the

urethane reaction influence of temperature, catalysis, and reaction partners, J. Coatings Technol. 69 (1997) 51–57.

[160] M.K. Kiesewetter, E.J. Shin, J.L. Hedrick, R.M. Waymouth, Organocatalysis: Opportunities and challenges for polymer synthesis, Macromolecules. 43 (2010) 2093–2107.

[161] W.J. Blank, New developments in catalysis, Macromol. Symp. 187 (2002) 261–270.

[162] W.J. Blank, Z.A. He, E.T. Hessell, Catalysis of the isocyanate-hydroxyl reaction by no n- tin catalysts, 35 (1999) 19–29.

[163] H. Sardon, L. Irusta, M.J. Fernández-Berridi, Synthesis of isophorone diisocyanate (IPDI) based waterborne polyurethanes: Comparison between zirconium and tin catalysts in the polymerization process, Prog. Org. Coatings. 66 (2009) 291–295.

[164] D.W.C. MacMillan, The advent and development of organocatalysis, Nature. 455 (2008) 304–308.

[165] W.N. Ottou, H. Sardon, D. Mecerreyes, J. Vignolle, D. Taton, Update and challenges in organo-mediated polymerization reactions, Prog. Polym. Sci. 56 (2016) 64–115.

[166] H. Sardon, A.P. Dove, D. Taton, O. Coulembier, A.J. Müller, Special Issue in: Organocatalyzed polymerizations, Eur. Polym. J. 95 (2017) 625–627.

[167] N.E. Kamber, W. Jeong, R.M. Waymouth, R.C. Pratt, B.G.G. Lohmeijer, J.L. Hedrick, Organocatalytic ring-opening polymerization, Chem. Rev. 107 (2007) 5813–5840.

[168] H. Sardon, J.M.W. Chan, R.J. Ono, D. Mecerreyes, J.L. Hedrick, Highly tunable polyurethanes: organocatalyzed polyaddition and subsequent post-polymerization modification of pentafluorophenyl ester sidechains, Polym. Chem. 5 (2014) 3547–3550.

[169] H. Sardon, A.C. Engler, J.M.W. Chan, J.M. García, D.J. Coady, A. Pascual, D. Mecerreyes, G.O. Jones, J.E. Rice, H.W. Horn, J.L. Hedrick, Organic acid-catalyzed polyurethane formation via a dual-activated mechanism: Unexpected preference of n-activation over o-activation of isocyanates, J. Am. Chem. Soc. 135 (2013) 16235–16241.

[170] J. Yoon Jang, Y. Kuk Jhon, I. Woo Cheong, J. Hyun Kim, Effect of process variables on molecular weight and mechanical properties of water-based polyurethane dispersion, Colloids Surfaces A Physicochem. Eng. Asp. 196 (2002) 135–143.

[171] S.-H. Son, H.-J. Lee, J. Kim, Effects of carboxyl groups dissociation and dielectric

constant on particle size of polyurethane dispersions, Colloids Surfaces A Physicochem. Eng. Asp. 133 (1998) 295–301.

[172] Y. Chen, Y.-L. Chen, Aqueous dispersions of polyurethane anionomers: Effects of countercation, J. Appl. Polym. Sci. 46 (1992) 435–443.

[173] A.M. Hyde, S.L. Zultanski, J.H. Waldman, Y.-L. Zhong, M. Shevlin, F. Peng, General Principles and Strategies for Salting-Out Informed by the Hofmeister Series, Org. Process Res. Dev. 21 (2017) 1355–1370.

[174] Y.S. Kwak, S.W. Park, H. Do Kim, Preparation and properties of waterborne polyurethane-urea anionomers - Influences of the type of neutralizing agent and chain extender, Colloid Polym. Sci. 281 (2003) 957–963.

[175] C.-Y. Li, W.-Y. Chiu, T.-M. Don, Preparation of polyurethane dispersions by miniemulsion polymerization, J. Polym. Sci. Part A Polym. Chem. 43 (2005) 4870–4881.

[176] S. Asaoka, Relation Between the Phase Structure and Surface Structure of Films Made From Polyurethane Dispersions, J. Appl. Polym. Sci. 73 (1999) 741–748.

[177] B. Fernández d'Arlas, L. Rueda, K. de la Caba, I. Mondragon, A. Eceiza, Microdomain composition and properties differences of biodegradable polyurethanes based on MDI and HDI, Polym. Eng. Sci. 48 (2008) 519–529.

[178] C. Prisacariu, C.P. Buckley, A.A. Caraculacu, Mechanical response of dibenzyl-based polyurethanes with diol chain extension, Polymer (Guildf). 46 (2005) 3884–3894.

[179] Y.K. Jhon, I.W. Cheong, J.H. Kim, Chain extension study of aqueous polyurethane dispersions, Colloids Surfaces A Physicochem. Eng. Asp. 179 (2001) 71–78.

[180] C. Hepburn, Polyurethane Elastomers, Springer Netherlands, Dordrecht, 1992.

[181] D.K. Chattopadhyay, B. Sreedhar, K.V.S.N. Raju, Effect of chain extender on phase mixing and coating properties of polyurethane ureas, Ind. Eng. Chem. Res. 44 (2005) 1772–1779.

[182] F.M.B. Coutinho, M.C. Delpech, Degradation profile of films cast from aqueous polyurethane dispersions, Polym. Degrad. Stab. 70 (2000) 49–57.

[183] J. Blackwell, M.R. Nagarajan, T.B. Hoitink, Structure of polyurethane elastomers: effect of chain extender length on the structure of MDI/diol hard segments, Polymer (Guildf). 23 (1982) 950–956.

[184] A. Takahara, J. Tashita, T. Kajiyama, M. Takayanagi, W.J. MacKnight, Microphase separated structure and blood compatibility of segmented poly(urethaneureas) with different diamines in the hard segment, Polymer (Guildf). 26 (1985) 978–986.

[185] C. Prisacariu, E. Scortanu, Influence of the type of chain extender and urethane group content on the mechanical properties of polyurethane elastomers with flexible hard segments, High Perform. Polym. 23 (2011) 308–313.

[186] J.Y. Bae, D.J. Chung, J.H. An, D.H. Shin, Effect of the structure of chain extenders on the dynamic mechanical behaviour of polyurethane, J. Mater. Sci. 34 (1999) 2523–2527.

[187] S. Oprea, Structure and properties of cross-linked polyurethane copolymers, Adv. Polym. Technol. 28 (2009) 165–172.

[188] B.K. Kim, J.C. Lee, Polyurethane ionomer dispersions from poly(neopentylene phthalate) glycol and isophorone diisocyanate, Polymer (Guildf). 37 (1996) 469–475.

[189] H. Reiff, D. Dieterich, Urethane-based dispersions, in: Ionomers, Springer Netherlands, Dordrecht, 1997: pp. 444–476.

[190] L.K. Saw, B.W. Brooks, K.J. Carpenter, D. V. Keight, Different dispersion regions during the phase inversion of an ionomeric polymer-water system, J. Colloid Interface Sci. 257 (2003) 163–172.

[191] A. Barni, M. Levi, Aqueous polyurethane dispersions: A comparative study of polymerization processes, J. Appl. Polym. Sci. 88 (2003) 716–723.

[192] M.Á. Pérez-Limiñana, F. Arán-Aís, A.M. Torró-Palau, C. Orgilés-Barceló, J.M. Martín-Martínez, Structure and properties of waterborne polyurethane adhesives obtained by different methods, J. Adhes. Sci. Technol. 20 (2006) 519–536.

[193] S.A. Madbouly, J.U. Otaigbe, A.K. Nanda, D.A. Wicks, Rheological behavior of aqueous polyurethane dispersions: Effects of solid content, degree of neutralization, chain extension, and temperature, Macromolecules. 38 (2005) 4014–4023.

[194] K. Nachtkamp, J. Pedain, J. Grammel, Process for the preparation of aqueous polyurethane dispersions and solutions, US4269748, 1981.

[195] F. Tiarks, K. Landfester, M. Antonietti, One-step preparation of polyurethane dispersions by miniemulsion polyaddition, J. Polym. Sci. Part A Polym. Chem. 39 (2001) 2520–2524.

[196] C.-Y. Li, Y.-H. Li, K.-H. Hsieh, W.-Y. Chiu, High-molecular-weight polyurethanes prepared by one-step miniemulsion polymerization, J. Appl. Polym. Sci. 107 (2008)

840–845.

[197] J.M. Asua, Miniemulsion polymerization, Prog. Polym. Sci. 27 (2002) 1283–1346.

[198] B.G. Zanetti-Ramos, E. Lemos-Senna, V. Soldi, R. Borsali, E. Cloutet, H. Cramail, Polyurethane nanoparticles from a natural polyol via miniemulsion technique, Polymer (Guildf). 47 (2006) 8080–8087.

[199] B.G. Zanetti-Ramos, E. Lemos-Senna, H. Cramail, E. Cloutet, R. Borsali, V. Soldi, The role of surfactant in the miniemulsion polymerization of biodegradable polyurethane nanoparticles, Mater. Sci. Eng. C. 28 (2008) 526–531.

[200] A. Valério, S.R.P. da Rocha, P.H.H. Araújo, C. Sayer, Degradable polyurethane nanoparticles containing vegetable oils, Eur. J. Lipid Sci. Technol. 116 (2014) 24–30.

[201] E. Rix, G. Ceglia, J. Bajt, G. Chollet, V. Heroguez, E. Grau, H. Cramail, Hydrophobe-free miniemulsion polymerization: towards high solid content of fatty acid-based poly(urethane-urea) latexes, Polym. Chem. 6 (2015) 213–217.

[202] J.M. Asua, Challenges for industrialization of miniemulsion polymerization, Prog. Polym. Sci. 39 (2014) 1797–1826.

[203] M.F. Schick, W.C. Hickman, G.T. Clark, R.R. Stockl, Aqueous dispersion blends of polyesters and polyurethane materials and printing inks therefrom, US4847316, 1989.

[204] B.K. Kim, J.C. Lee, Modification of waterborne polyurethanes by acrylate incorporations, J. Appl. Polym. Sci. 58 (1995) 1117–1124.

[205] M. Linnenbrink, P. Kuehnemund, J. Mueller, One-Component Aqueous Dispersion Adhesive, US 20080262131, 2008.

[206] L. Wu, B. You, D. Li, Synthesis and characterization of urethane/acrylate composite latex, J. Appl. Polym. Sci. 84 (2002) 1620–1628.

[207] S. Chen, L. Chen, Structure and properties of polyurethane/polyacrylate latex interpenetrating networks hybrid emulsions, Colloid Polym. Sci. 282 (2003) 14–20.

[208] R.A. Brown, R.G. Coogan, D.G. Fortier, M.S. Reeve, J.D. Rega, Comparing and contrasting the properties of urethane/acrylic hybrids with those of corresponding blends of urethane dispersions and acrylic emulsions, Prog. Org. Coatings. 52 (2005) 73–84.

[209] C. Wang, F. Chu, C. Graillat, A. Guyot, C. Gauthier, J.P. Chapel, Hybrid polymer latexes: Acrylics-polyurethane from miniemulsion polymerization: Properties of

hybrid latexes versus blends, Polymer (Guildf). 46 (2005) 1113–1124.

[210] E. Nienhaus, B. Mayer, U. Meisenburg, Aqueous two-component polyurethane coating composition, process for its preparation, and its use in processes for the production of a multicoat finish, US 5670600, 1997.

[211] M. Brunnemann, U. Meisenburg, E. Nienhaus, H.-P. Rink, Aqueous two-component polyurethane coating composition, process for its preparation, and its use in methods of producing a multicoat paint system, US 5876802, 1999.

[212] A. Maier, S. Ingrisch, N. Steidl, F. Weinelt, Polyurethane-polymer hybrid-dispersion with enhanced surface properties, method for the production and utilization thereof, US7265178, 2007.

[213] C. Wang, F. Chu, C. Graillat, A. Guyot, C. Gauthier, C.L.F.V.F. Cpe Lyon, N.P.R.C. Inst Chem Ind Forestry Prod, G.L.F. Insa, Hybrid polymer latexes-acrylics-polyurethane: II. Mechanical properties, Polym. Adv. Technol. 16 (2005) 139–145.

[214] C.-Y. Li, W.-Y. Chiu, T.-M. Don, Morphology of PU/PMMA hybrid particles from miniemulsion polymerization: Thermodynamic considerations, J. Polym. Sci. Part A Polym. Chem. 45 (2007) 3359–3369.

[215] A.J. Dong, Y.L. An, S.Y. Feng, D.X. Sun, Preparation and morphology studies of core-shell type waterborne polyacrylate-polyurethane microspheres, J. Colloid Interface Sci. 214 (1999) 118–122.

[216] S.-J. Son, K.-B. Kim, Y.-H. Lee, D.-J. Lee, H.-D. Kim, Effect of acrylic monomer content on the properties of waterborne poly(urethane-urea)/acrylic hybrid materials, J. Appl. Polym. Sci. 124 (2012) 5113–5121.

[217] U. Šebenik, M. Krajnc, Properties of acrylic-polyurethane hybrid emulsions synthesized by the semibatch emulsion copolymerization of acrylates using different polyurethane particles, J. Polym. Sci. Part A Polym. Chem. 43 (2005) 4050–4069.

[218] J.I. Amalvy, A kinetic study in emulsion polymerization of polyurethane-acrylate hybrids, Pigment Resin Technol. 31 (2002) 275–283.

[219] A.C. Aznar, O.R. Pardini, J.I. Amalvy, Glossy topcoat exterior paint formulations using water-based polyurethane/acrylic hybrid binders, Prog. Org. Coatings. 55 (2006) 43–49.

[220] O.R. Pardini, J.I. Amalvy, FTIR,1H-NMR spectra, and thermal characterization of water-based polyurethane/acrylic hybrids, J. Appl. Polym. Sci. 107 (2008) 1207–1214.

[221] H.T. Zhang, R. Guan, Z.H. Yin, L.L. Lin, Soap-free seeded emulsion copolymerization of MMA onto PU-A and their properties, J. Appl. Polym. Sci. 82 (2001) 941–947.

[222] R. Shi, X. Zhang, J. Dai, Synthesis of TDI-Polyurethane/Polyacrylate Composite Emulsion by Solvent-free Method and Performances of the Latex Film, J. Macromol. Sci. Part A. 50 (2013) 350–357.

[223] L. Zhao, S.N. Sauca, C. Berges, Aqueous polyurethane acrylate hybrid dispersions, EP 3067399 A1, 2016.

[224] T. Yi, G. Ma, C. Hou, S. Li, R. Zhang, J. Wu, X. Hao, H. Zhang, Polyurethane-acrylic hybrid emulsions with high acrylic/polyurethane ratios: Synthesis, characterization, and properties, J. Appl. Polym. Sci. 44488 (2016) 1–9.

[225] R. Ballestero, B.M. Sundaram, H. V. Tippur, M.L. Auad, Sequential graft-interpenetrating polymer networks based on polyurethane and acrylic/ester copolymers, Express Polym. Lett. 10 (2016) 204–215.

[226] Y. Lu, R.C. Larock, New hybrid latexes from a soybean oil-based waterborne polyurethane and acrylics via emulsion polymerization, Biomacromolecules. 8 (2007) 3108–3114.

[227] Y.S. Hu, Y. Tao, C.P. Hu, Polyurethaneurea / Vinyl Polymer Hybrid Aqueous Dispersions Based on Renewable Material, (2001) 80–84.

[228] J.W. Gooch, H. Dong, F.J. Schork, Waterborne oil-modified polyurethane coatings via hybrid miniemulsion polymerization, J. Appl. Polym. Sci. 76 (2000) 105–114.

[229] R. Udagama, E. Degrandi-Contraires, C. Creton, C. Graillat, T.F.L. McKenna, E. Bourgeat-Lami, Synthesis of acrylic-polyurethane hybrid latexes by miniemulsion polymerization and their pressure-sensitive adhesive applications, Macromolecules. 44 (2011) 2632–2642.

[230] E. Degrandi-Contraires, R. Udagama, E. Bourgeat-Lami, T. McKenna, K. Ouzineb, C. Creton, Mechanical properties of adhesive films obtained from PU-acrylic hybrid particles, Macromolecules. 44 (2011) 2643–2652.

[231] E. Degrandi-Contraires, R. Udagama, T. McKenna, E. Bourgeat-Lami, C.J.G. Plummer, C. Creton, Influence of composition on the morphology of polyurethane/acrylic latex particles and adhesive films, Int. J. Adhes. Adhes. 50 (2014) 176–182.

[232] H. Wang, M. Wang, X. Ge, Graft copolymers of polyurethane with various vinyl monomers via radiation-induced miniemulsion polymerization: Influential factors to

grafting efficiency and particle morphology, Radiat. Phys. Chem. 78 (2009) 112–118.

[233] A. Lopez, E. Degrandi-contraires, E. Canetta, C. Creton, J.L. Keddie, M. Asua, Waterborne Polyurethane - Acrylic Hybrid Nanoparticles by Miniemulsion Polymerization : Applications in Pressure-Sensitive Adhesives, Langmuir. 27 (2011) 3878–3888.

[234] A. Lopez, E. Degrandi, E. Canetta, J.L. Keddie, C. Creton, J.M. Asua, Simultaneous free radical and addition miniemulsion polymerization: Effect of the diol on the microstructure of polyurethane-acrylic pressure-sensitive adhesives, Polymer (Guildf). 52 (2011) 3021–3030.

[235] A. Lopez, Y. Reyes, E. Degrandi-Contraires, E. Canetta, C. Creton, J.L. Keddie, J.M. Asua, Simultaneous free-radical and addition miniemulsion polymerization: Effect of the chain transfer agent on the microstructure of polyurethane-acrylic pressure-sensitive adhesives, Macromol. Mater. Eng. 298 (2013) 53–66.

[236] E. Degrandi-Contraires, A. Lopez, Y. Reyes, J.M. Asua, C. Creton, High-shear-strength waterborne polyurethane/acrylic soft adhesives, Macromol. Mater. Eng. 298 (2013) 612–623.

[237] N. Ballard, P. Carretero, J.M. Asua, Effect of Reaction Temperature on Adhesive Properties of Waterborne Polyurethane/Acrylic Hybrids Synthesized by Semicontinuous Miniemulsion Polymerization, Macromol. React. Eng. 7 (2013) 504–514.

[238] V. Daniloska, R. Tomovska, J.M. Asua, Hybrid miniemulsion photopolymerization in a continuous tubular reactor-A way to expand the characteristics of polyurethane/acrylics, Chem. Eng. J. 184 (2012) 308–314.

[239] V. Daniloska, P. Carretero, R. Tomovska, J.M. Asua, High performance pressure sensitive adhesives by miniemulsion photopolymerization in a continuous tubular reactor, Polymer (Guildf). 55 (2014) 5050–5056.

[240] V. Daniloska, P. Carretero, R. Tomovska, M. Paulis, J.M. Asua, High-performance adhesives resulting from spontaneous formation of nanogels within miniemulsion particles, ACS Appl. Mater. Interfaces. 6 (2014) 3559–3567.

[241] S. Mehravar, N. Ballard, A. Agirre, R. Tomovska, J.M. Asua, Relating polymer microstructure to adhesive performance in blends of hybrid polyurethane/acrylic latexes, Eur. Polym. J. 87 (2017) 300–307.

[242] L. Wu, H. Yu, J. Yan, B. You, Structure and composition of the surface of urethane/acrylic composite latex films, Polym. Int. 50 (2001) 1288–1293.

[243] R.O. Carlsen, J. Kawa, D. Krawczak, T.H.-H. Lee, S.C. Piette, Water - dispersable polyurethane / acrylic polymer compositions, WO 1989010380, 1989.

[244] S. Swarup, A. Natesh, N.E. Fortuna, K.G. Olson, Aqueous urethane/acrylic resins with branched chain extension and coating compositions made therefrom, US 5854332, 1998.

[245] C. Wang, F. Chu, A. Guyot, C. Gauthier, F. Boisson, Hybrid acrylic-polyurethane latexes: Emulsion versus miniemulsion polymerization, J. Appl. Polym. Sci. 101 (2006) 3927–3941.

[246] C. Zhang, X. Zhang, J. Dai, C. Bai, Synthesis and properties of PDMS modified waterborne polyurethane-acrylic hybrid emulsion by solvent-free method, Prog. Org. Coatings. 63 (2008) 238–244.

[247] D. Chen, Water dispersible polyurethane and process for preparation thereof, US 5306764, 1994.

[248] D. Mestach, A. van der Zand, A crosslinkable polymer binder, WO2010066902 A1, 2010.

[249] P. Loewrigkeit, K.A. Van Dyk, Aqueous polyurethane-polyolefin compositions, US 4644030, 1987.

[250] A.B. Gruber, R. Dervy, Processes for producing organic solvent free urethane/acrylic polymer laminating adhesive for flexible packaging, US 5571857, 1996.

[251] H. Stanley, Process for preparing urethane/acrylic-or-vinyl latexes, US5371133, 1994.

[252] C. Yuan, G. Chen, X. Zhang, Z. Li, Z. Liu, Method for preparing aqueous polyacrylate modified polyurethane dispersions, US9234068 B2, 2016.

[253] T.H. Killilea, Water-dispersible polyurethane-vinyl polymer compositions, US7968641 B2, 2011.

[254] A. Maier, S. Ingrisch, H. Winkelmann, F. Wolfertstetter, A. Kern, W. Temme, R. Bergs, Solvent-free polyrethane-polymer-hybrid-dispersion and use thereof, US6787596 B1, 2004.

[255] R. Gertzmann, J. Petzoldt, H. Muller, Polyurethane-polyacrylate hybrid coating compositions, US 20040034146 A1, 2004.

[256] Y.-S. Ryu, Y.-H. Lee, J.-S. Kim, C.-C. Park, H.-D. Kim, Preparation and properties of emulsifier-/solvent-free polyurethane-acrylic hybrid emulsions for binder materials:

Effect of the glycidyl methacrylate/acrylonitrile content, J. Appl. Polym. Sci. 44497 (2016) 1–9.

[257] R. Shi, X. Zhang, J. Dai, C. Zhang, Synthesis of Fluorinated Polyurethane/Polyacrylate Hybrid Emulsion Initiated by ^{60}Co γ-Ray and Properties of the Latex Film, J. Macromol. Sci. Part A. 47 (2010) 1104–1110.

Chapter 2. Control of the particle size and stability in solvent-free waterborne Polyurethanes / (meth)acrylic hybrid dispersions

2.1. Introduction

As pointed out in Section 1.3.2.3 of Chapter 1, solvent-free PU/(meth)acrylic hybrids produced by emulsifier-free emulsion polymerization have attracted increasing attention from academia and industry due to both environmental issues and economic reasons. Since colloidal stability is provided by the incorporation of ionic groups into the PU chains, the ionic content in the PU composition is an important parameter that influences the emulsification process and properties of the dispersion [1–5] as well as the final properties of the PU films [5–16] (Chapter 1, Section 1.2.2.3). In PUD systems, the particle size is controlled by varying the ionic content in the PU chains (dimethylol propionic acid, DMPA) [3,17] and it was reported that with increasing the DMPA content the particle size decreased up to a point and then it became constant. However, no attention has been paid to the control of particle size in solvent-free PU/(meth)acrylic hybrid emulsions. Perhaps because it was thought that there is a simple relationship between particle size and ionic group (DMPA), which usually is the case for PUDs synthesized in solvent [1–5].

On the other hand, the type of chain extender that determines the hydrophilicity/phobicity of the PU chains may be additional parameter that will influence the

colloidal properties of the dispersions, and only limited data is available on this issue. Li *et al.* [5] showed that hydrophobic/hydrophilic nature of different chain extenders influences the stability of PU/acrylic hybrids synthesized in miniemulsion polymerization. It was reported that the hybrids containing hydrophobic chain extenders were more stable during storage, while hydrophilic chain extenders can lead to coagulation upon long term storage.

In addition, different studies have confirmed that the ionic content affects the mechanical [7–9] and adhesive [6,10,11] properties of the polymer films. It has been demonstrated that the ionic groups interact by Coulombic forces and hydrogen bonds between the polymer chains [7]. These ionic groups cause interaction between the polymer chains and act as physical crosslinkers and increase the storage modulus in the polymer films [7,8,11]. On the other hand, the nature of the chain extender also significantly affects the final properties [12–16,18,19]. Diamine chain extenders ,which lead to formation of urea groups, are more commonly used than diols as they typically react with the isocyanate groups several orders of magnitude faster than water [20].

This chapter presents the effect of the ionic content (controlled by the DMPA content) and PU hydrophilicity (controlled by the type of chain extender) on the particle size and colloidal stability of emulsifier-free and solvent-free PU/(meth)acrylic aqueous dispersions. The composition of the low molar mass chains was determined using Matrix-assisted laser desorption/ionization time-of-flight (MALDI - TOF) mass spectrometer. A Monte Carlo-based model simulation was performed in order to predict the compositions of the PU chains and the result was compared with the MALDI-TOF mass spectrometer analysis. Finally the

influence of the DMPA content and chain extender type on the properties of the PU/(meth)acrylic hybrid films was studied.

2.2. Experimental

2.2.1. Materials

The materials are given in Appendix I.

2.2.2. Synthesis procedures

Scheme 2.1 summarizes the synthesis of the PU-Urea (PUU) dispersion. The synthesis of the PU prepolymer was performed in a 250 mL glass reactor fitted with a reflux condenser, a sampling device (and feeding inlet), a nitrogen inlet, a thermometer and a flat blade turbine stirrer. Reaction temperature was controlled by an automatic control system, Camile TG (Biotage). The formulations are presented in Table 2.1. To synthesize the prepolymer, DMPA, polypropylene glycol (PPG), isophorone diisocyanate (IPDI) (7.73 g), dibutyltin dilaurate (DBTDL) (0.05 g) and 60% of the (meth)acrylic monomers (mixture of methyl methacrylate (MMA)/ and butyl acrylate (BA), 1/1 by weight) were charged into the reactor. The reaction mixture was brought to 70°C under agitation (250 rpm) and held for 4-5 hours. The free NCO at the end of the reaction was checked with amine-back titration [16] and FTIR (see Figure III.1 ,Appendix III). The mixture was cooled to 25°C and additional (meth)acrylic monomers (20 wt% of the MMA/BA 1/1 wt/wt) was added to reduce the viscosity. Then, triethylamine (TEA) dissolved in (meth)acrylic monomers (20 wt% of the

MMA/BA 1/1 wt/wt) was added and kept at 25°C for 45 min in order to neutralize the carboxylic groups of DMPA.

It is well known that the dispersion process strongly depends on the agitation system. As discussed in Chapter 1, in the solvent process to prepare the PUD water is added to the PU prepolymer. In our work, in addition to the above mentioned method, another method was implemented in order to prepare PUD. In this method the mixture of PU prepolymer and (meth)acrylic monomers was added to the water. It was observed that more homogeneous and more stable PUDs were obtained by the former method. This is most probably due to the effect of agitation system used in our work. Therefore, to prepare the aqueous dispersions, the reactor was charged with double deionized water under nitrogen at 25°C and the prepolymer-monomer mixture was added in 15 min under high agitation (750 rpm). Then, the chain extender (0.92 g ethylene diamine (EDA)) dissolved in water (2 g) was added to the reactor and left to react one hour at 70°C. The theoretical molar ratio of NCO/OH (defined as the ratio of the moles of IPDI and sum of the moles of PPG, DMPA and chain extender) was 1.8 before chain extension and 1.0 after chain extension.

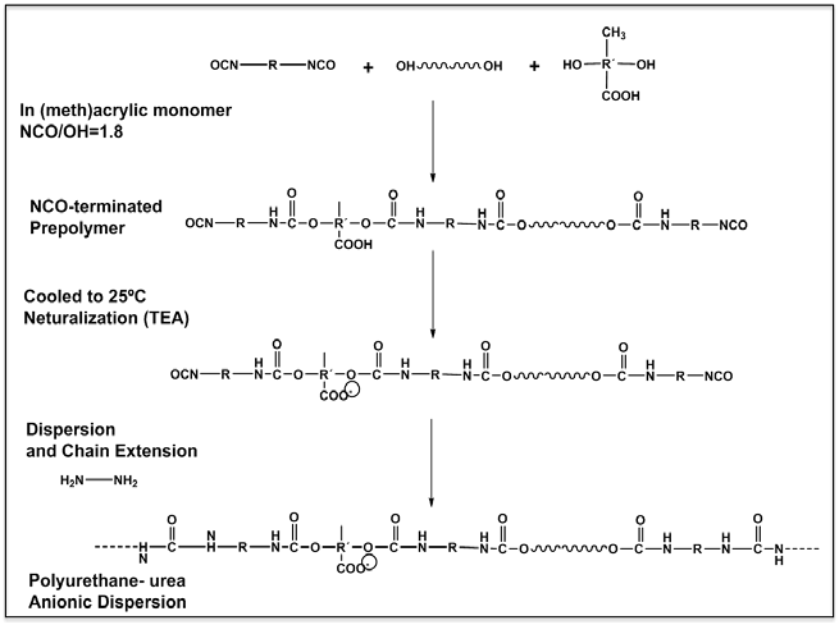

Scheme 2.1. Preparation process for PU-Urea dispersion

Table 2.1. Recipes for the synthesis of 40% solids content PU/(meth)acrylic hybrids with constant amount of IPDI (7.73 g) and DBTDL (0.05 g)

Chain extender	Experiment	PPG	DMPA	Chain extender	TEA[a]	HS[b] (wt%)	MMA/BA (1/1 wt/wt) (g)	Water (g)	KPS[c] (g)
		(mols per 1 mol of IPDI)							
EDA	2%DMPA	0.28	0.27	0.44	0.28	38	15.4	93	0.15
	2.9%DMPA	0.22	0.34	0.44	0.36	40	13.1	80	0.13
	3.5%DMPA	0.19	0.37	0.44	0.39	45	12	71	0.12
	4%DMPA	0.16	0.39	0.44	0.42	49	11.2	66	0.11
	5%DMPA	0.12	0.44	0.44	0.46	57	9.8	58	0.098
1,6-DAH	5%DMPA	0.12	0.44	0.44	0.46	59	9.8	58	0.098
1,8-DAO	5%DMPA	0.12	0.44	0.44	0.46	60	9.8	58	0.098
1,12-DAD	2.9%DMPA	0.22	0.34	0.44	0.36	45	13.1	80	0.13
	3.5%DMPA	0.19	0.37	0.44	0.39	49	12	71	0.12
	4%DMPA	0.16	0.39	0.44	0.42	53	11.2	66	0.11
	5%DMPA	0.12	0.44	0.44	0.46	62	9.8	58	0.098

a) 1.05*mol of DMPA

b) Hard Segment content $= \frac{(\text{IPDI+DMPA+chain extender})\ (g)}{(\text{IPDI+PPG+DMPA+chain extender})\ (g)} * 100$

c) 0.5% based on (meth)acrylic monomer

Then, the free radical polymerization of (meth)acrylic monomers was performed at 70°C by adding potassium persulfate (KPS) dissolved in water (3 g) as a single shot. The polymerization was performed in batch for 2 hours and the final conversion of (meth)acrylic monomers was higher than 95% in all the cases. The resulting hybrid latexes consist of PU-Urea/(meth)acrylics (50/50 wt/wt) with 40% solids content. The pH of the PU prepolymer was 9.5 indicating that the carboxylic acid groups were neutralized completely. After the dispersion (before chain extension), the pH was 7.7 and it increased to 10 after addition of the chain extender. The final value of pH was 8.5 after adding the initiator.

For comparison, PUD synthesis was performed in methyl ethyl ketone (MEK) solvent and the formulation of this reaction is presented in Table 2.2.

Table 2.2. Recipe for solvent-based synthesis of PUD in MEK with EDA chain extender

Experiment	PPG	DMPA	EDA	TEA	HS (wt%)	MEK (g)	Water (g)
	(Mols per 1 mol IPDI)						
5%DMPA	0.12	0.44	0.44	0.46	60	19.6	58

Moreover, for comparison purposes a latex of (meth)acrylics with MMA/BA 50/50 (wt/wt) with solid content of 40% using Dowfax 2A (2 wt% based on monomer) as surfactant and KPS (0.5 wt% based on monomer) as initiator was prepared in batch polymerization for 2 hours.

2.2.3. Characterization

The final particle size of the latexes was measured by dynamic light scattering (DLS). The unreacted NCO groups were determined by titration and FTIR. The conversion of (meth)acrylic monomers was measured gravimetrically. The gel fraction and swelling degree were measured by Soxhlet extraction, using tetrahydrofuran (THF) as the solvent. The molar mass distribution of the soluble fraction of polymers was determined by size exclusion chromatography (SEC/RI/UV). The thermal characterization of the hybrids was carried out by differential scanning calorimetry (DSC). The mechanical properties of the polymer films were measured by tensile tests. The morphology of latex particles and films was studied by means of transmission electron microscopy (TEM) and the water sensitivity of polymer films was analyzed in terms of static contact angle measurement and water uptake test. The detailed description of the characterization methods is provided in Appendix I.

2.3. Results and Discussion

2.3.1. Control of particle size and stability

The amount of DMPA in the formulation was varied (2 to 5 wt % based on organic phase) in order to control the particle size. The droplet size of the PUD swollen with (meth)acrylic monomers, final average particle size and the observation with respect to the colloidal stability of the final hybrid PU/(meth)acrylics latexes are presented in Table 2.3.

Table 2.3. Average particle size and stability of PU/(meth)acrylic hybrids at different DMPA content using EDA as chain extender

DMPA in PU/(meth)acrylic formulation (wt%)*	Colloidal stability	Droplet size (nm)**	Final Particle size (nm)
2	Coagulated	-	-
2.9	Stable	90	129
3.5	Stable	68	110
4	Stable	52	100
5	Coagulated after chain extension	46	-

* Based on the organic phase
** Before polymerization of (meth)acrylics

As it can be seen from Table 2.3, stable PU/(meth)acrylic dispersions were achieved with DMPA concentrations in a range of 2.9 – 4 wt%. In this range, with increasing the amount of DMPA in the system, the particle size decreased due to the higher amount of ionic species available to stabilize the particles. It was observed that by decreasing the DMPA content to 2 wt%, the amount of carboxylic acid groups was not enough to obtain stable dispersions. On the other hand, at 5 wt% DMPA, although the solution of PU prepolymer/(meth)acrylics formed a stable aqueous dispersion, after the chain extension step carried out using the hydrophilic EDA and before the addition of the initiator, the system coagulated. This result was surprising, because the DMPA is expected to enhance the colloidal stability in the system. It was speculated that the possible reason was that the PU chains containing many carboxylic acid groups, reacted with the hydrophilic EDA yielding water soluble polymer chains that do not contribute to the stability of the dispersion and furthermore are often deleterious for colloidal stability.

In order to check this hypothesis, beside the completely water soluble EDA, diamines with different water solubility were employed for the extension of the PU prepolymer chains:

hydrophobic diamine diaminododecane (DAD), and partially water soluble diamines diaminohexane (DAH) and diaminooctane (DAO). The octanol/water partitioning coefficients (defined as the ratio of concentration of a compound in organic and aqueous phase) of these chain extenders and the stability of the dispersion obtained with them are shown in Table 2.4 [21]. As can be seen when DAD and DAO were used, stable PU/(meth)acrylic hybrids were obtained even at high DMPA amount (5%). This is likely due to the increased hydrophobicity of the PU chains extended with hydrophobic chain extenders, which prevented the migration of the DMPA rich PU chains toward the aqueous phase. Therefore, the use of hydrophobic chain extenders permitted working with higher amount of DMPA, which gives a space for better control of the final particle size. As it can be seen in Table 2.5, increasing amount of the DMPA led to decrease in the final average particle size in both cases.

Table 2.4. Octanol/water partitioning coefficient [21]

Chain extender	Log P_{oct}/P_{wat} * @ 25 °C	Stable Dispersion at 5% DMPA
Ethylene diamine (EDA)	-1.2	×
1,6-Diaminohexane (DAH)	0.02	×
1,8-Diaminooctane (DAO)	1.2	✓
1,12-Diaminododecane (DAD)	2.8	✓

* Octanol / water partitioning coefficient: log ($[solute]_{octanol}/[solute]_{water}$)

Table 2.5. Particle size evolution of PU/acrylic hybrid using 1,8-DAO and 1,12-DAD as chain extender

DMPA in PU/acrylic formulation (wt%)*	Final Particle size (nm)	
	DAO as chain extender	DAD as chain extender
2.9	135	152
3.5	129	135
4	128	125
5	118	121

*Based on organic phase

With the aim of the comparison of the amount of polymer chains in the aqueous phase of the hybrids with different chain extenders, the final latexes containing both PU and acrylics were centrifuged for 2 h at 30000 rpm and the transparent serum was separated and analyzed. As representative, the ^{1}H NMR spectra of the separated serum from the hybrids containing 2.9 wt% DMPA with EDA (the most hydrophilic) and DAD (the most hydrophobic) chain extender are presented in Figure 2.1. From the spectra, the concentrations of the IPDI and PPG in the aqueous phase of the latexes ($[IPDI]_{aq}$ and $[PPG]_{aq}$) were determined according to Equations 2.1 and 2.2 using a known amount of Dimethylformamide (DMF) as external standard. More detail is given in Appendix III.

$$[IPDI] = [DMF]\frac{I_{0.75-1}}{I_{7.9}*9} \qquad (2.1)$$

$$[PPG] = [DMF]\frac{I_{1.1}}{I_{7.9}*3*DP_{PPG}} \qquad (2.2)$$

Due to the low number of hydrogen atoms in the DMPA unit and in the chain extenders, and due to the overlap of these peaks with other signals in the NMR spectra it was not possible to determine the concentrations of these components. Although the signals from TEA are strong, since it is not covalently bonded to the polymer, it does not provide a direct measure of the concentration of polymer in the aqueous phase.

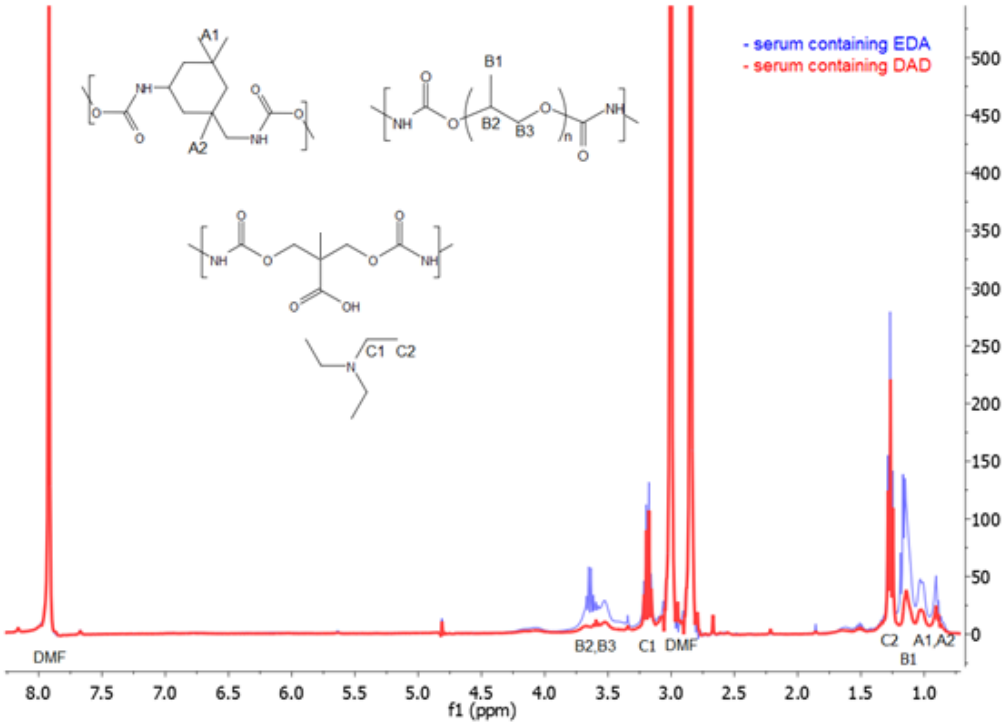

Figure 2.1. ^{1}H NMR spectra of the serum of hybrids containing EDA and DAD as chain extender (2.9% DMPA). The signal intensity is normalized to the reference DMF peak in both cases. The assignment of the spectra is based on reference [22]

Table 2.6 presents the concentrations of IPDI and PPG in the aqueous phase of the latex which gives an indication about the amount of polymer in the aqueous phase, as well as, its composition. In both cases (EDA and DAD), the concentration of IPDI is much higher than the concentration of PPG, and the IPDI:PPG ratio is significantly higher than the initial concentrations in the formulation (1:0.22). As water solubility comes mainly from DMPA units incorporated, this suggests that the polymer in the aqueous phase is richer in the more hydrophilic groups containing DMPA. This is confirmed by the high concentrations of TEA (Figure 2.1, peaks C1 and C2), which may be expected to be primarily present as a counter-ion to the DMPA units in the polymer in the aqueous phase. It can also be observed from

Table 2.6 that the total concentration of IPDI in the aqueous phase is significantly higher in the case of using EDA as chain extender. Based on this information the fraction of IPDI in the initial formulation that ends up incorporated into water soluble polymer is around 7 % in the case of EDA as chain extender but only 3 % when using DAD as chain extender.

Table 2.6. Concentration of IPDI and PPG in the serum of hybrids containing EDA and DAD as chain extender (2.9% DMPA)

Chain extender	$[IPDI]_{aq}$ (mM)	$[PPG]_{aq}$ (mM)[a]
EDA	30	4
DAD	14	1

a) Calculated with $DP_{PPG} = 35$

For comparison, PU was synthesized with 5% DMPA using MEK as a solvent (the formulation is presented in Table 2.2). A stable aqueous dispersion of PU/MEK with average particle size of around 70 nm was obtained using EDA as chain extender likely due to the contribution of MEK to the better incorporation of EDA into the polymer particles.

To get more detailed information on the structure of the short PU chains, the PU prepolymer obtained when monomers were used as solvents was analyzed by MALDI-TOF mass spectrometry [23,24] . To prevent the reaction of the isocyanate groups of PU prepolymer during sample preparation, the isocyanate groups were terminated with a secondary mono amine di-butylamine (DBA).

Figure 2.2 compares the number distributions obtained by MALDI-TOF calculated from equation 2.3 [25,26] and size exclusion chromatography (SEC/RI/UV). It can be seen that MALDI-TOF was able to detect well the molar masses below 2000 g/mol, but failed to detect

the high molar masses. Therefore, the mass distributions obtained from MALDI-TOF are only accurate for molar mass < 2000 g/mol. The reason for that maybe attributed to the mass discrimination of MALDI for higher molar mass chains specially in polymers with broad molar mass distribution [27–29]. Nevertheless, the part of the spectrum around 3000 g/mol may contain useful information about the composition of these chains.

$$n\,(m) = \frac{\mathbf{I\,(m)}}{\mathbf{m^{1/2}}} \qquad (2.3)$$

where the n(m) is the number distribution, I(m) is the Intensity and m is the molar mass [26].

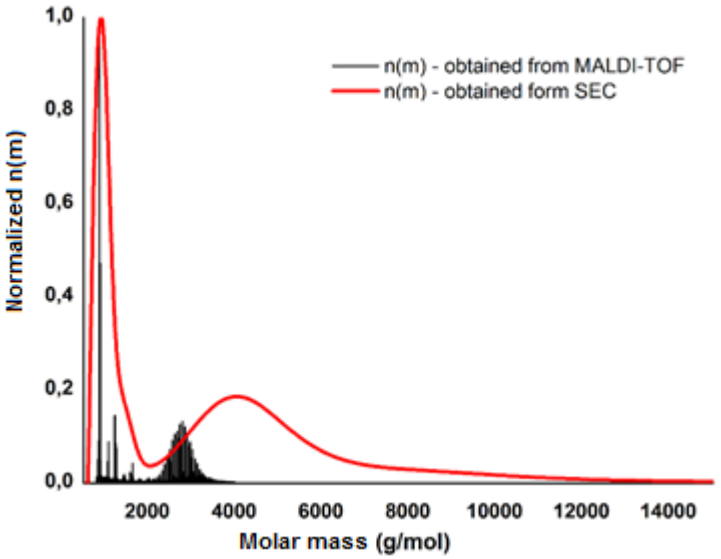

Figure 2.2. MALDI-TOF number distribution of PU prepolymer with 3.5 wt% DMPA, n(m) from equation 2.1 and number distribution n(M) determined from the SEC

Figure 2.3 (a) presents the whole MALDI-TOF mass spectrum of the PU prepolymer obtained with 3.5 wt% DMPA in linear detection mode, where three different regions with

distinct molar masses were identified. Two of them are in the regions of relatively low molar masses (<1600 Da, Figures 2.3 b-1 and b-2) and one of them at higher molar masses (>2500 Da, Figure 2.3 b-3). Each of these regions has been analyzed in reflector mode in order to improve the resolution of the peaks, to obtain good isotopic distribution and assign the different species correctly and they are shown Figure 2.3 (b). The PPG diol was also analyzed and the result is presented in Figure 2.4, where it is shown that the average molar mass of the original PPG is 2000 Da. The peaks are equally spaced at *m/z* = 58 Da, which represents the molar mass of the repeating units C_3H_6O in PPG. The peaks of MALDI-TOF distribution of the prepolymer in the region of 2500-3000 Da (Figure 2.3a) are also spaced at m/z=58 Da. This distribution is attributed to the PU chains containing two units of IPDI reacted with one PPG unit, terminated with two units of DBA and cationized with sodium ion $[M+Na]^+$ (M being polymer). This structure, denoted as S1 in Scheme 2.2. Comparison of Figures 2.3 and 2.4 shows that the PPG was fully incorporated in the prepolymer.

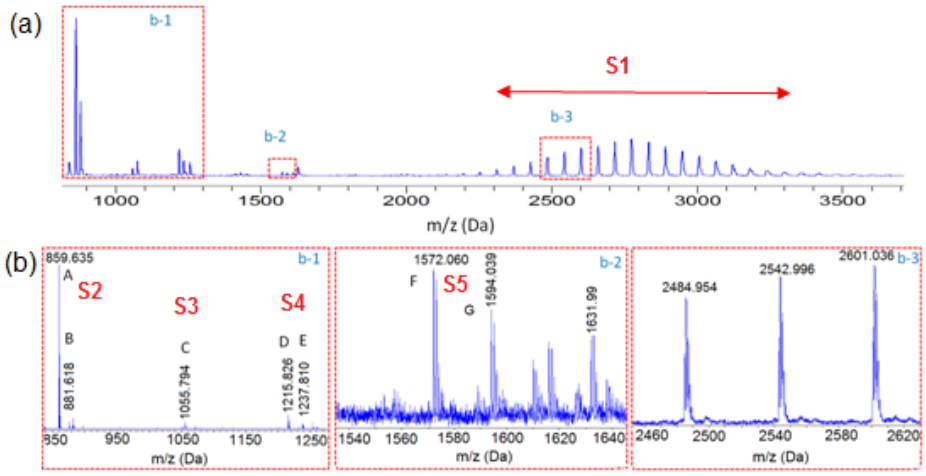

Figure 2.3. (a) Whole MALDI-TOF mass spectrum of PU prepolymer with 3.5 wt% DMPA obtained in linear mode; and (b) MALDI-TOF mass spectra of PU prepolymer with 3.5 wt% DMPA obtained in reflector mode.

The structures with lower molar masses, present in regions b-1 and b-2, apparently do not contain any PPG unit (the molar masses are lower than 1650 Da). In the region b-1 in Figure 2.3 (b), the multiple peaks are assigned as follows. The lowest molar mass peaks (A and B) are attributed to PU chains containing two IPDI units and one DMPA unit terminated with 2 DBA units, cationized with $[M+Na]^+$ and $[M+2Na-H]^+$, respectively (structure S2 in Scheme 2.2). The peak C at 1055 Da corresponds to the structure from trimerization (homopolyaddition) of NCO groups (reaction of three NCO and termination with three DBA, Scheme 2.2) cationized with hydrogen [30,31]. The peaks D and E (Figure 2.3 (b), b-1 region) correspond to specie made of three IPDI and two DMPA, terminated with 2 DBA units, ionized by $[M+Na]^+$ and $[M+2Na-H]^+$, respectively (see structure S4 in Scheme 2.2).

The peaks F and G in region b-2 (Figure 2.3 b) are assigned to the PU prepolymer chains with four IPDI, three DMPA, terminated with two DBA units and cationized with sodium forming two different adducts, $[M+Na]^+$ and $[M+2Na-H]^+$, respectively. Its chemical composition is presented in Scheme 2.2, denoted as structure S5.

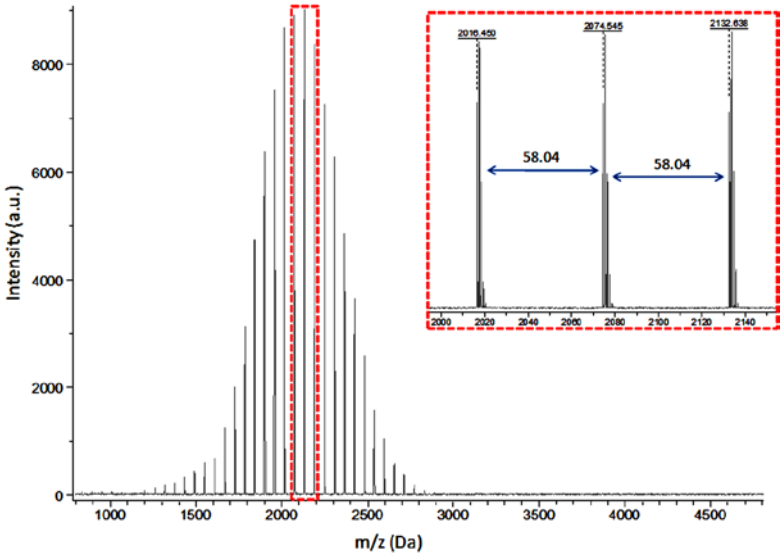

Figure 2.4. MALDI-TOF mass spectrum (reflector mode) of PPG

These structures were present in the other PU prepolymers (with 2.9 wt% and 5 wt% DMPA) and are presented in Figure III.2, Appendix III (in reflector mode).

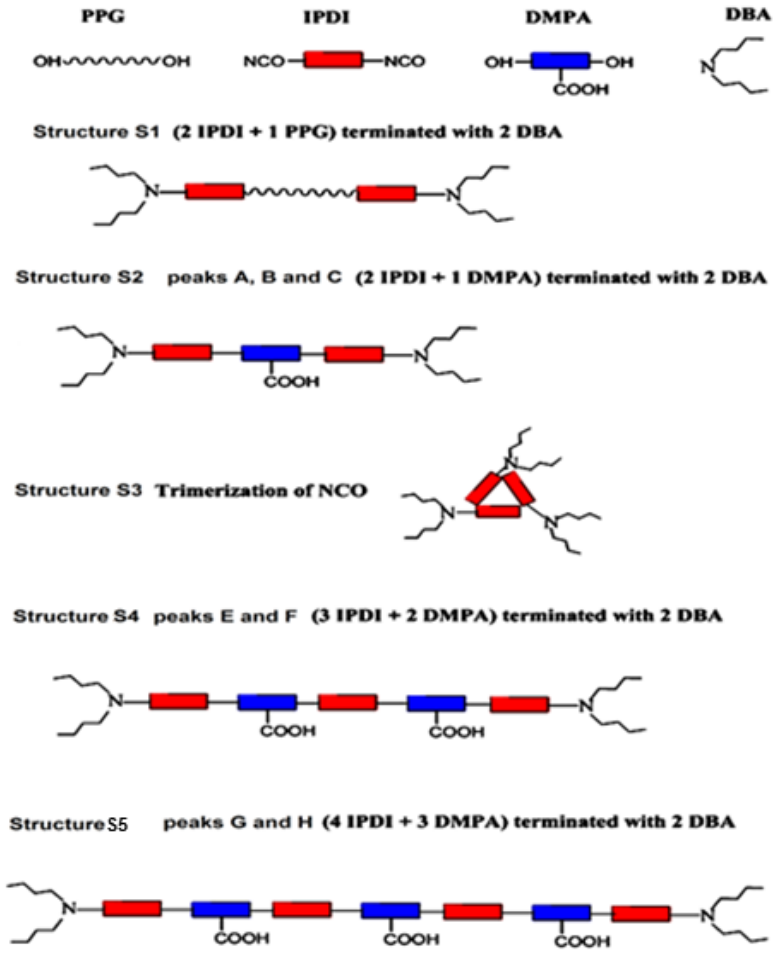

Scheme 2.2. Possible structures derived from the reaction of IPDI and diols, terminated with DBA

It is worth pointing out that the mass spectrum of PU prepolymer synthesized in MEK solvent (Figure III.3, Appendix III) shows similar composition as the ones synthesized in (meth)acrylic monomers under similar conditions (Figure III.2, Appendix III).

MALDI-TOF mass spectrometry analysis demonstrated that during the synthesis of prepolymer, the fraction of relatively low molar mass PU chains contains wide variety of chains with different chemical structures. To further analyze these findings, a Monte Carlo simulation of the polyaddition reaction between hydroxyl groups of two diols (PPG and DMPA) with NCO groups of IPDI was performed. The model is based on the work of Johnson and O'Driscoll [32] and Po' *et al.* [33] The model gives an opportunity to determine the molar mass and the compositional distribution of PU chains.

The kinetic scheme used in the simulation is given in Scheme 2.3. The simulation were carried out using algorithm provided by Gillespie [34].

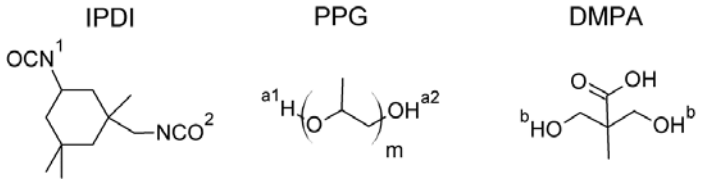

$$\sim NCO^1 + \sim PPG^{a1} \xrightarrow{k_{1a1}} \sim NCO^1 - PPG^{a1} \sim$$

$$\sim NCO^1 + \sim PPG^{a2} \xrightarrow{k_{1a2}} \sim NCO^1 - PPG^{a2} \sim$$

$$\sim NCO^2 + \sim PPG^{a1} \xrightarrow{k_{2a1}} \sim NCO^2 - PPG^{a1} \sim$$

$$\sim NCO^2 + \sim PPG^{a2} \xrightarrow{k_{2a2}} \sim NCO^2 - PPG^{a2} \sim$$

$$\sim NCO^1 + \sim DMPA^{b} \xrightarrow{k_{1b}} \sim NCO^1 - DMPA^{b} \sim$$

$$\sim NCO^2 + \sim DMPA^{b} \xrightarrow{k_{2b}} \sim NCO^2 - DMPA^{b} \sim$$

Scheme 2.3. Kinetic scheme for step-growth copolymerization between IPDI, DPMA and PPG

The rate coefficient of addition of the more reactive secondary NCO group of IPDI to both the primary alcohols of PPG and DMPA was taken from literature values [35]. The reactivity of the less reactive primary NCO group of IPDI was estimated to be a factor of 2.5 times less than that of the secondary NCO based on experimental observations on the relative reactivity of the two sites [36,37]. The reactivity of the primary alcohol of PPG was estimated to be 3 times that of secondary alcohol [38]. The values used in simulations are summarized in Table 2.7.

Table 2.7. Rate coefficients used in simulations

Rate Coefficient	Rate coefficient × 10^3 ($M^{-1}s^{-1}$)
k_{1a1}	2.50
k_{1a2}	0.83
k_{2a1}	1.00
k_{2a2}	0.33
k_{1b}	2.50
k_{2b}	1.00

More details on the simulation process and rate coefficients used are given in Appendix IV. Figure 2.5 presents distributions of the prepolymers with different chemical structures for the four concentrations of DMPA used. The X-axis shows the number of PPG units and the DMPA units are presented in different colors. As can be seen, the PPG units are distributed randomly in the PU chains in all the cases.

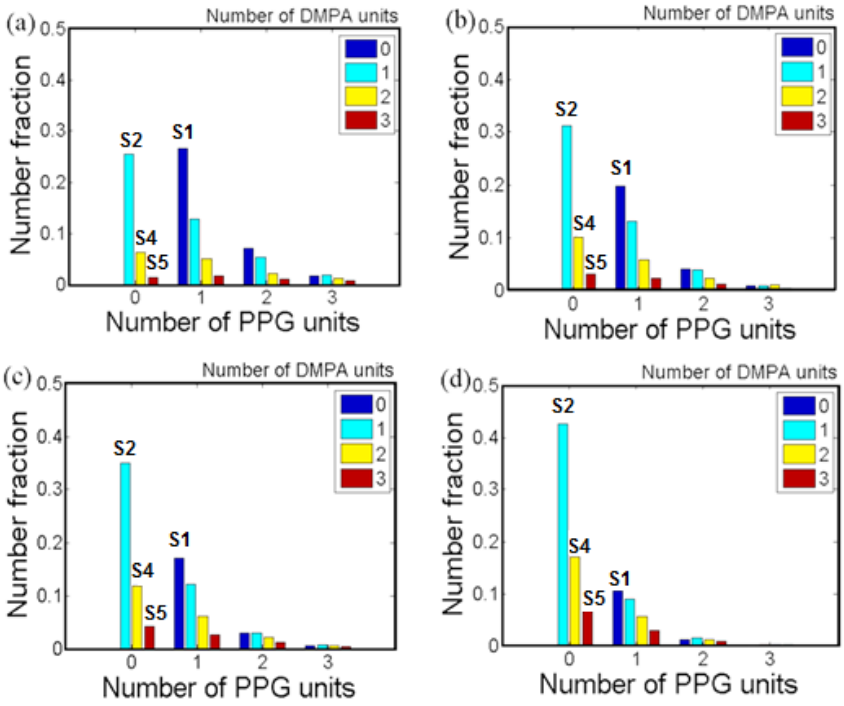

Figure 2.5. Prepolymer compositional distributions with varying the amount of DMPA in the formulation; (a) 2 wt%, (b) 2.9 wt%, (c) 3.5 wt%, (d) 5 wt%.

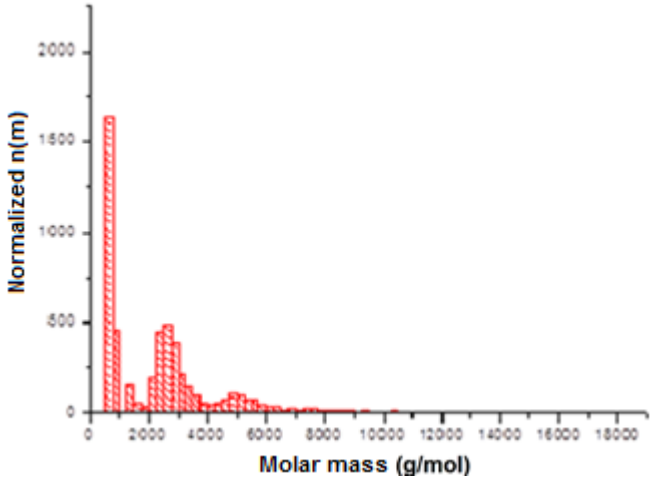

Figure 2.6. Number distribution of PU prepolymer with 3.5 wt% DMPA obtained from Monte Carlo simulation

Similar to the obtained results from MALDI-TOF and SEC (Figure 2.2), the chains with low molar mass (<1500 g/mol) had the highest intensity. Two populations of polymer chains were obtained from the Monte-Carlo simulation. One from 2000 to 4000, which was detected by both MALDI-TOF and SEC analysis, and the second one above 4000 which was not detected by MALDI-TOF. Based on the simulation data, these chains are those that contain two PPG units.

The good agreement between the simulated (Monte Carlo) and experimental (MALDI-TOF and SEC) values in the region of low molar masses (<4000 Da) allows using the simulated values to analyze the effect of the chain extender on the stability of the dispersions. Focusing on the chains containing either no or one PPG unit (corresponding to structures S2, S4 and S5, Scheme 2.2), it can be seen that increasing the DMPA content, the number fraction of the chains with no PPG unit and with more than one DMPA becomes more important, which means the hydrophilicity of the chains increased significantly (Figure 2.5). A great part of the hydrophilic chains will be dissolved in aqueous phase after extending with water soluble chain extender (EDA). This effect is stronger at higher DMPA content (5%) that presented stability problems.

Using the data in Figure 2.5 and assuming that the chains with no PPG unit can migrate to the aqueous phase upon chain extension with water soluble diamine and by taking into account the chains containing one, two and three DMPA units, the number of units of DMPA remaining on the particles was calculated and is shown in Figure 2.7. Knowing that the stable dispersions were produced at the DMPA content of 2.9 wt% and 3.5 wt%, the data in Figure 2.7 indicate that the minimum necessary units of DMPA on the particle to obtain stable

dispersion was around 48 and below this limit the DMPA units remaining on the particles was not enough to stabilize the system.

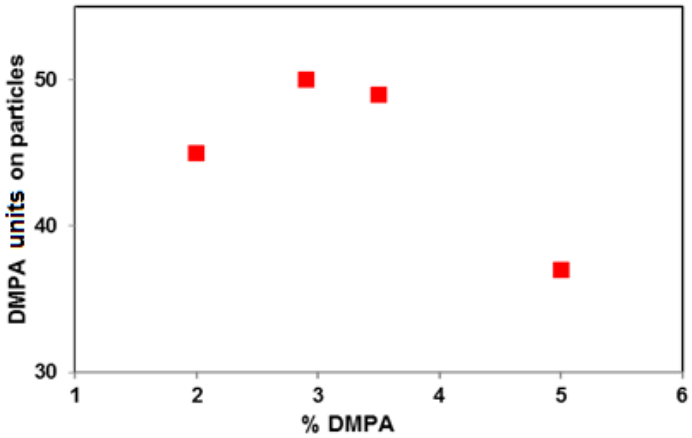

Figure 2.7. DMPA units on the particles as a function on DMPA % in the formulation

It is worth mentioning that the results indicated that, due to the large excess of isocyanate, the rate coefficients do not influence the simulation results and the polymer chemical structure, as it is shown in Appendix III (Figure III.4 and Table III.1). In fact the PU prepolymer structure was mainly affected by the stoichiometry of the components in the reaction rather than their inherent reactivity, thus the results presented herein should be general for most diisocyanate and polyol combinations used in this work.

2.3.2. Characteristics and properties of PU/acrylic hybrids

2.3.2.1. Polymer characteristics

In this section, the effect of chain extender type and DMPA content on the properties of PU/acrylic hybrids is studied. For that purpose, three hybrids were synthesized with fixed amount of DMPA (2.9 wt%) using different chain extender type (EDA, DAO and DAD representing runs 1, 2 and 3, respectively) and three hybrids were synthesized with DAD using various DMPA content (2.9 wt%, 3.5 wt% and 5 wt% representing runs 3, 4 and 5, respectively) were considered (see Table 2.8). The conversion of (meth)acrylic monomers in the batch polymerization system is shown in Figure 2.8. Very fast free radical polymerization of (meth)acrylic monomers was observed and more than 90% conversion was obtained within 15 min. The final conversion of the (meth)acrylic monomers was >95% in all the cases.

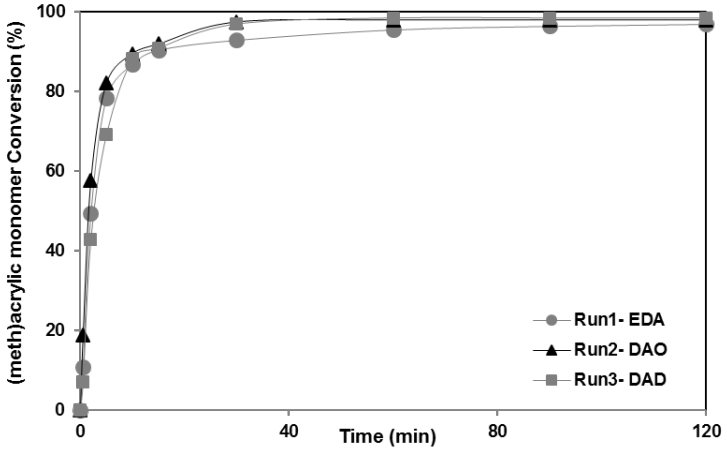

Figure 2.8. The conversion of(meth)acrylic monomers in PU/(meth)acrylic hybrid dispersion with different chain extender type

The polymer characteristics of the synthesized PU/(meth)acrylic hybrids are given in Table 2.8. At constant DMPA content of 2.9 wt%, by increasing the hydrophobicity of the chain extender the final particle size increased, most probably because higher ionic content was needed to provide stability to more hydrophobic particles. By increasing the amount of DMPA in the case of the most hydrophobic chain extender DAD, the particle size decreased, as the amount of ionic groups was higher. No gel content was observed in agreement with what is known in the batch polymerization of MMA/BA, namely that no gel is formed for MMA contents higher than 25 wt% [39]. Figure 2.9 presents the SEC molar mass distribution of the hybrid polymers. They showed bimodal molar mass distribution; one population of polymer chains at low molar mass, which mainly corresponds to the PU chains and the other population of polymer chains at higher molar mass mainly corresponds to the (meth)acrylics (Table 2.8).

At fixed DMPA content (Runs 1-3), the molar mass of high molar mass chains increased with increasing the hydrophobicity of chain extender. With increasing the DMPA content (Runs 3-5), the average of the high molar mass fraction decreased. Higher molar masses were obtained in larger particles. This is puzzling because typically higher molar masses are observed for smaller particles due to the lower rates of termination. The only explanation for observing this opposite behavior can be the difference in the growing time of radicals in the large and small particles. If we consider the growing time of the first and second chains in the particle as t_1 and t_2, respectively. Then in the case of small particles, the t_2 is substantially smaller than t_1 due to lower radical entry rate for small particles and the summation of t_1 and t_2 (which is the growing time of polymer chains) can be considered as t_1.

The (t_1+t_2) in large particle was probably higher than the t_1 in small particles and this may lead to obtain higher molar masses in the larger particles. However, this implies termination by combination, but MMA terminates mainly by disproportionation. It is worth mentioning that similar behavior has been noticed and reported in the case of miniemulsion polymerization of vinyl acetate using polymeric surfactant Brij-35 [40]. It was shown that with increasing surfactant amount, both the particle size and the average molar mass decreased.

Another explanation is the compartmentalization of the entering radicals anchored at the surface of the particle and located in the PU shell. Under these conditions one may imagine that the radicals in the different parts of the shell do not see each other, i.e., they cannot terminate and this will increase the growing time

Table 2.8. The characteristic of synthesized PU/acrylic hybrids

Run	DMPA (wt%)	chain extender	Final Particle Size (nm)	Gel Content (%)	Sol $\overline{Mw}$ **(Kg/mol)		T_g	
					Low M_w	High M_w	T_{g1} (ºC)	T_{g2} (ºC)
Run 1	2.9	EDA	129	0	26	822	-53	+28
Run 2	2.9	1,8-DAO	135	0	25	997	-54	+27
Run 3	2.9	1,12-DAD	152	0	25	1073	-55	+29
Run 4	3.5	1,12-DAD	135	0	24	902	-55	+27
Run 5	5	1,12-DAD	121	0	23	663	-55	+29

* bimodal molar mass distrubution contain both low molar mass non grafted PU chains and high molar mass (meth)acrylic chains

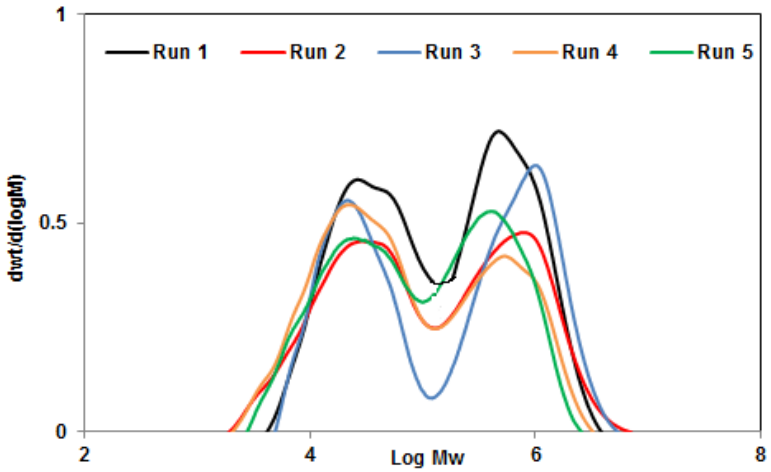

Figure 2.9. Molar mass distribution of soluble fraction in PU/(meth)acrylic hybrids obtained by SEC

The thermal properties of the PU (before polymerization of acrylics), the (meth)acrylic polymer and PU/(meth)acrylic hybrid films dried at standard condition (25 ºC and 55% humidity) determined by DSC are presented in Figure 2.10 for Run 1, as heat flow derivatives vs. temperature for the first and second heating cycles. As can be seen, the PU/(meth)acrylic hybrid film showed three transitions in the first cycle; one at -53 ºC (which corresponds to the soft phase of the PU), one broad transition around +28 ºC (corresponds to the copolymer of MMA/BA in batch system) and the third one between 50 ºC and 70 ºC. However, in the second heating cycle only the first two transitions were observed. It seems that an additional phase or chemical reaction exists that leads to a transition at temperature in the range of 50-70ºC in the first cycle and it disappears in the second heating cycle. This peak also appears in the neat PU film in Figure 2.10, whereas it is not present in the neat (meth)acrylic polymer. This strongly suggests the existence of physical crosslinking in PU chains due to hydrogen bonding between their hard segments, as shown in Figure 2.11. It has been demonstrated

that during thermal treatment, the hydrogen bonding may be destroyed [41]. In order to check if this is the case, the analyzed PU sample left for two days at room temperature in order to give time for hydrogen bonding to be restored and it was analyzed with DSC again. As can be seen in Figure III.5 (Appendix III), the transition peak reappeared with lower intensity, confirming that it is most likely due to the reversible hydrogen bonding between PU chains. It is worth mentioning that this difference for the first and second heating cycle was observed for all the hybrid films. As can be seen in Table 2.8, considering the second heating cycle of the DSC scans, all the PU/acrylic hybrids showed two glass transition temperatures (T_g). The first one at about -53 to -55 °C corresponding to PU (neither the amount of DMPA nor the type of chain extender has changed it) and the second T_g around +27 to +29°C for the copolymer containing MMA/BA polymerized in batch.

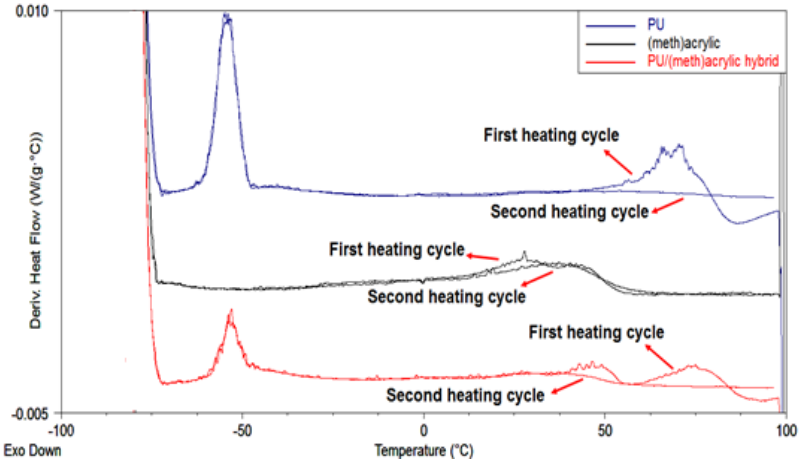

Figure 2.10. DSC derivative curves of PU, (meth)acrylics and PU/(meth)acrylic hybrid films for Run 1

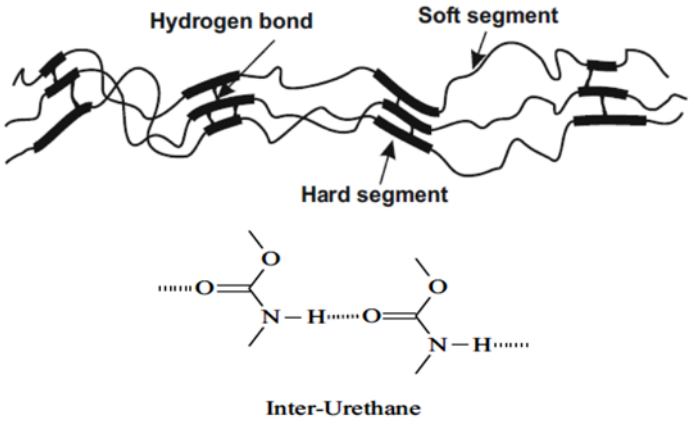

Figure 2.11. Hydrogen bonding interaction between hard segments of PU chains [41]

2.3.2.2. Particle and Film Morphology

The TEM micrographs of PU/Poly(meth)acrylic hybrid for Run 1 and the cross-section surface of the final film are shown in Figure 2.12 (a) and (b), respectively. As can be seen in Figure 2.12 (a), a core-shell like particle morphology was observed. In order to find out if the dark core in the TEM micrographs arose from the PU or (meth)acrylic phase, a PU/PMMA hybrid was synthesized. In this case, if PMMA is in the shell it would not be possible to cast a homogeneous film at ambient temperature due to its high Tg. On the contrary, if the PU is in the shell a homogeneous film would be expected. It was observed that a homogenous film was obtained at ambient temperature from PU/PMMA hybrid. The TEM micrograph of the cross section of the film is shown in Figure 2.13. The dark domains are dispersed in the bright matrix which must belong to the PU domain. Therefore, in the TEM of the particles, acrylics (dark) are in the core and PUs (bright) are in the shell.

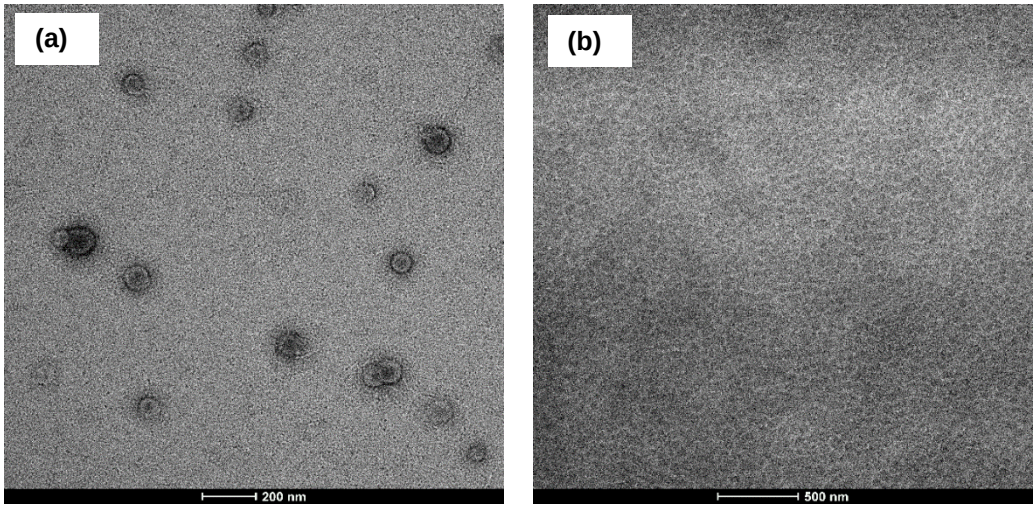

Figure 2.12. The TEM micrographs of PU/ Poly(meth)acrylic hybrid dispersion (left-a) and film cross-section (right-b)- For sample Run 1 with EDA

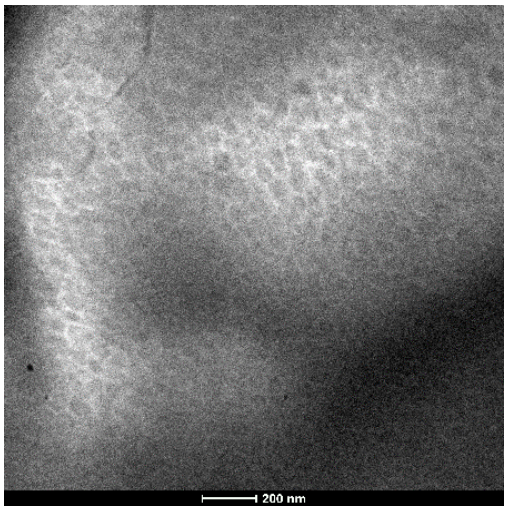

Figure 2.13. Film cross-section (right) of PU/PMMA hybrid

2.3.2.3. Mechanical properties

The stress-strain behavior of the films cast from the hybrid latexes at ambient temperature is shown in Figure 2.14 and the mechanical properties are summarized in Table 2.9. As can be seen, at 2.9 wt% of DMPA, the polymer film obtained using EDA as chain extender had higher toughness and ultimate strength than those obtained with DAO and DAD. This is probably because the PU hard segment (HS) becomes softer (due to the longer alkyl chain) for DAO and DAD compared to EDA and therefore, this leads to lower toughness and ultimate stress. However, the elongation at break was not affected. Figure 2.15 shows that by increasing the amount of DMPA in the PU formulation, the Young´s modulus and yield stress increased, however the elongation at break and ultimate strength decreased. This is due to the fact that by increasing the amount of DMPA in the formulation form 2.9% to 5% and decreasing the amount of PPG the hard segment content of PU was increased from 45% to 62% (Table 2.1), hence the polymer film had higher toughness and lower elongation at break. The hard segment content in the PU chains has a significant effect on the mechanical properties, acting as a reinforcing component in the hybrid structures chains [7,8,11]. This effect was not obvious when DMPA content increased from 2.9% to 3.5% (as the difference in hard segment content was not that high) and just the elongation at break decreased.

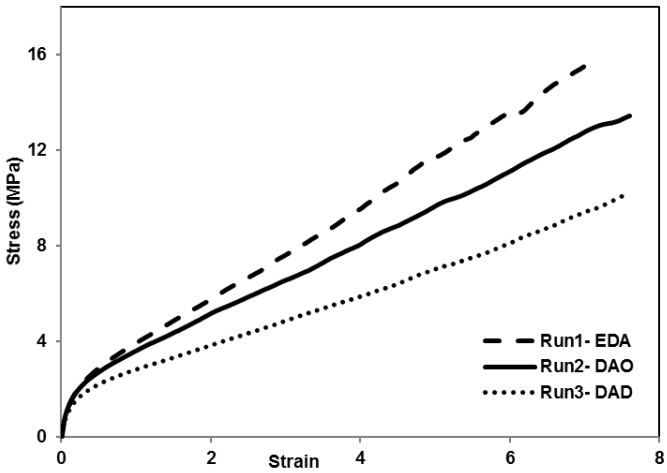

Figure 2.14. The stress-strain behavior of PU/Poly(meth)acylate hybrid films obtained with different chain extenders (2.9% DMPA as internal emulsifier)

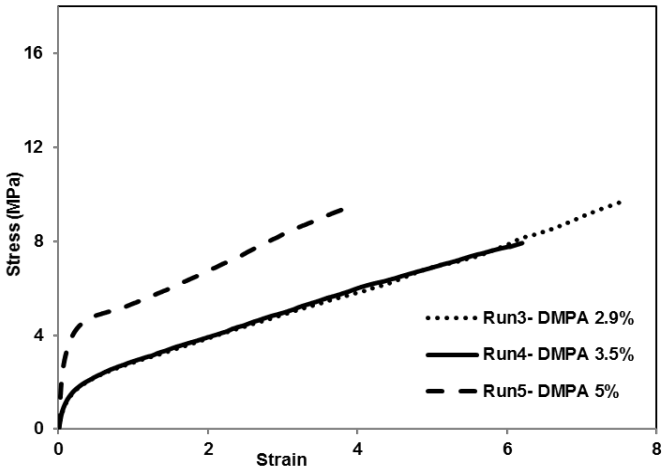

Figure 2.15. The stress-strain behavior of PU/Poly(meth)acylate hybrid films obtained with different DMPA content (DAD as chain extender)

Table 2.9. The mechanical properties of the PU/Poly(meth)acrylic hybrid films

Run	DMPA (wt%)	Type of chain extender	Young´s Modulus MPa/100	Yield Stress (MPa)	Elongation at break	Ultimate Strength (MPa)	Toughness (MPa)
Run 1	2.9	EDA	0.13 ± 0.01	2.4 ± 0.2	7.5 ± 0.2	16.1 ± 0.2	63.8 ± 3.2
Run 2	2.9	1,8-DAO	0.11 ± 0.01	2.3 ± 0.1	7.6 ± 0.1	13.4 ± 0.2	59.2 ± 2.7
Run 3	2.9	1,12-DAD	0.10 ± 0.01	2.2 ± 0.1	7.5 ± 0.1	9.7 ± 0.1	42.8 ± 2.1
Run 4	3.5	1,12-DAD	0.17 ± 0.01	1.8 ± 0.1	6.2 ± 0.2	7.4 ± 0.2	28.8 ± 1.3
Run 5	5	1,12-DAD	0.57 ± 0.03	4.5 ± 0.2	3.9 ± 0.1	9.2 ± 0.1	26.0 ± 1.5

2.3.2.4. Water Sensitivity

The water sensitivity of the polymer films cast at ambient temperature was studied by determination of the static contact angle and liquid-water uptake test in order to check the sensitivity of the film surface and the film bulk respectively.

Static contact angle measurement

The water static contact angles of the film-air interfaces before and after rinsing with water are given in Table 2.10. The films displayed very similar contact angles, around 70°, and rinsing with water did not change these values, indicating that there was no significant migration of additional stabilizing chains to the air-film interface, as it is in the case of conventional surfactants [42]. This is because most of the chains containing DMPA were strongly attached to the polymer and some carboxylic acid groups were already at the surface and they did not move because they were chemically bonded.

Table 2.10. Static contact angle of air-film interface

Run	DMPA (wt%)	Type of chain extender	Contact angle	Contact angle of rinsed film
Run 1	2.9	EDA	68 ± 2	68 ± 3
Run 2	2.9	1,8-DAO	70 ± 3	72 ± 3
Run 3	2.9	1,12-DAD	73 ± 4	73 ± 2
Run 4	3.5	1,12-DAD	71 ± 2	72 ± 2
Run 5	5	1,12-DAD	69 ± 1	70 ± 2

Liquid water uptake measurements

Figures 2.16 and 2.17 present the results of the liquid water uptake measurements. At fixed content of DMPA, in the initial period up to 5 days the liquid water uptake of polymer film with EDA was higher than those with DAO and DAD (Figure 2.16). This is due to the higher hydrophilicity of incorporated EDA segments, which gives more hydrophilic nature to the PU chains. The water uptake of the film containing EDA passed through a maximum and decreased after several days, probably because this film contained higher amount of water soluble oligomers that were dissolved in water. The water uptake behavior of the films is determined by the interplay between the water absorption and solubilization of water soluble species. The water uptake of the films with DAO achieved more gradually the maximum values and reached a plateau, and after 20 days, a slight decrease of the water uptake amount was noticed. This behavior is similar to that of EDA, and indicates the presence of a lower amount of soluble species. On the other hand, the water uptake value of the polymer film containing DAD increases with time and did not reach a plateau within the investigated period. This behavior indicates a very small amount of soluble chains, as the DAD based PU

is more hydrophobic than the other two and therefore the amount of water-soluble polymer is negligible. However, the chains containing DMPA in this hybrid were distributed around the particles and formed a hydrophilic network within the films, which leads toward this continuous water absorption. These ideas are confirmed by the data in Table 2.11, where the weight of water soluble species (as difference in weight before and after water uptake experiments) in each sample is presented. It was observed that 6.3% of the film containing EDA and 4.6% of the film containing DAO was dissolved in the water, confirming the presence of water soluble polymer chains. In contrast, only 2.5% of the film with 1,12-DAD was dissolved in water. The lower amount of hydrophilic polymer led to a slower rate of water uptake, but to a higher long term water uptake.

Figure 2.17 presents the liquid water uptake for the films containing different content of DMPA obtained and DAD as chain extender. With increasing the DMPA content in the chains, the water uptake slightly increased due to the increased amount of carboxylic functional groups in the PU chains. The effect of the increased hydrophilicity in this case was compensated by: i) the increase in the hard segment content of PU which decrease the water absorption and ii) the increase of hydrogen bonding with increasing DMPA content, which decrease the clustering tendency of absorbed water molecules [43]. As can be seen in Table 2.11, the amount of polymer film dissolved in water during the test was in the same range being slightly higher for the film with higher DMPA content.

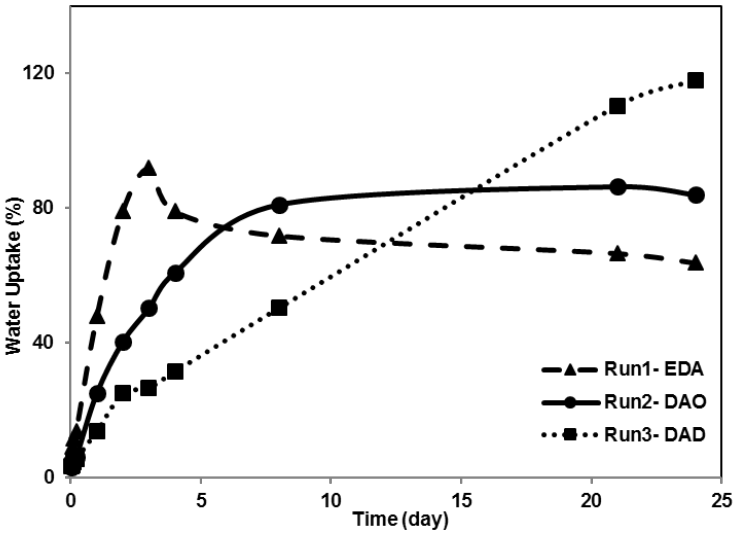

Figure 2.16. Liquid water uptake measurement of the films obtained with different chain extenders (2.9% DMPA as internal emulsifier)

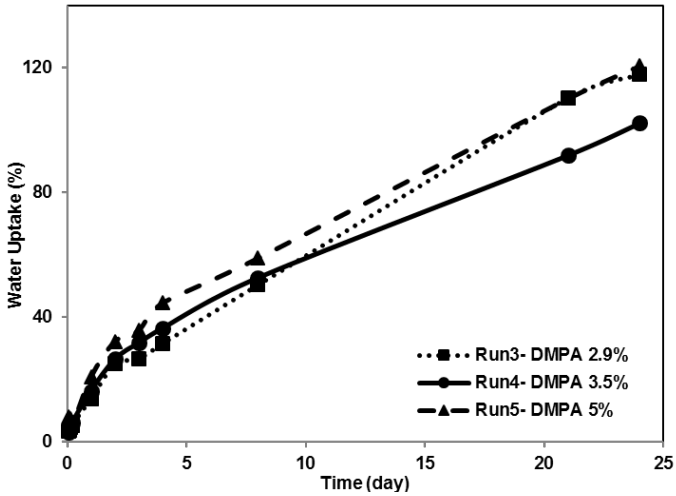

Figure 2.17. Liquid water uptake measurement of the films obtained with different DMPA content (DAD as chain extender)

Table 2.11. Amount of polymer dissolved in the water during the water uptake test

	Polymer weight loss after drying (%)
Run1 – EDA	6.3
Run2 – 1,8-DAO	4.6
Run3 – 1,12-DAD (2.9% DMPA)	2.5
Run4 – 1,12-DAD (3.5% DMPA)	3.4
Run5 –1,12- DAD (5% DMPA)	3.8

After the water uptake test, the water was analyzed by FTIR (Figure 2.18) and by surface tension measurements (Table 2.12). In Figure 2.18, where the FTIR spectra of soluble species in the case of EDA based PU are depicted, it is shown that the soluble polymer contained mainly PU chains as the observed peaks of the dissolved polymer were similar to the one of PU (the peaks at 3400 cm^{-1}, 1600 cm^{-1} and 1150 cm^{-1}). Moreover, as it is shown in Table 2.12, the surface tension of the water containing polymer film with EDA was the lowest, confirming the presence of more polymer chains in the water, while it was higher for the case of DAD.

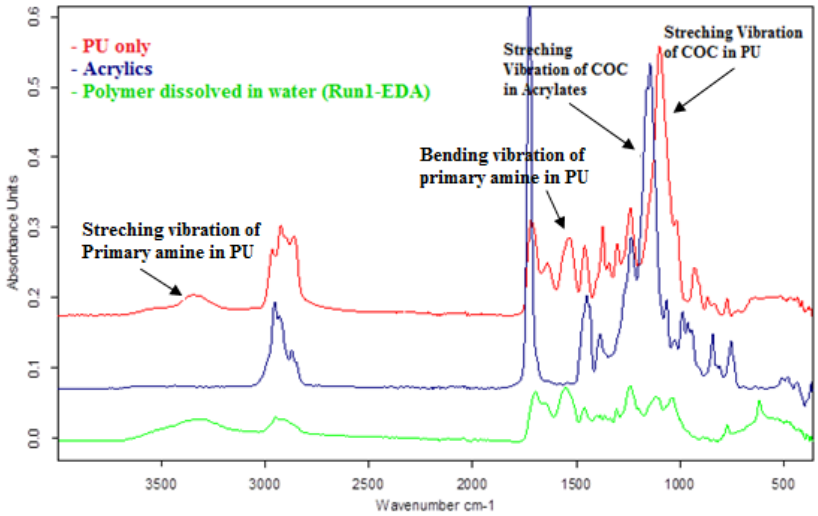

Figure 2.18. FTIR analysis of PU (before polymerization of acrylics), the acrylic polymers and the liquid after the water uptake test

Table 2.12. Surface tension measurement of the liquid after the water uptake test

Run	σ of liquid after test (mN/m)
Run 1 - EDA	48 ± 1
Run 2 – 1,8-DAO	52 ± 2
Run 3 – 1,12-DAD (2.9% DMPA)	62 ± 1
Run 4 – DAD (3.5% DMPA)	64 ± 2
Run 5 – DAD (5% DMPA)	58 ± 2

2.4. Conclusions

Emulsifier-free PU/(meth)acrylic hybrid dispersions were synthesized by emulsion polymerization, where PU prepolymer containing ionic groups (COOH) was used as a colloidal stabilizer. PUs were synthesized by solvent-free method using (meth)acrylic monomers as diluent. The effects of the content of DMPA and type of chain extenders (highly

hydrophilic EDA, less hydrophilic DAO and the hydrophobic DAD) on the colloidal properties of the hybrid dispersions and final properties of the hybrid films were investigated.

It was found that when using a hydrophilic chain extender, the DMPA content and the average particle size do not have a simple linear relationship as is the case for the PU synthesized in solvent. The hydrophilic chain extender (EDA) leads to the formation of high amounts of water soluble oligomers that are not favorable for stabilization as they migrate to the water phase and therefore are not available for particle stabilization. This was more pronounced at higher DMPA content, for which colloidal stability of the hybrid dispersions was not achieved after the chain extension step. By increasing the hydrophobicity of the chain extenders (DAO and DAD) the systems became more stable and the DMPA content (and the particle size) could be varied in wider range. Thus, combination of ionic content and type of chain extender could be a useful tool for control of particle size and colloidal stability of the solvent-free PU/(meth)acrylic hybrid dispersions.

The chemical structure of the short chains in the PU prepolymer was analyzed by MALDI-TOF mass spectrometer and it was observed that the short chain in the PU prepolymer chains were not homogeneous in composition. The presence of hydrophilic polymer chains containing one or more DMPA units with no unit of macrodiol (PPG) was confirmed. As the DMPA content increased, the fraction of these hydrophilic chains increased. Moreover, Monte Carlo based simulation also confirmed the heterogeneity of PU prepolymer composition and it was shown that the heterogeneity was mainly resulted from the stoichiometry than different reactivity of PPG and DMPA towards IPDI.

The properties of the films cast from the hybrid dispersions were studied by means of tensile tests and water sensitivity measurements. It was observed that the Young´s modulus and yield stress of the polymer films decrease with the length of the chain extender, likely because the hard segment of PU becomes softer for longer chain extenders. On the other hand, by increasing the DMPA content and decreasing PPG, the PU became harder as the hard segment content increased and hence the Young´s modulus and yield stress increased, however the elongation at break decreased. The water static contact angle on the air-film interface after rinsing with water did not changed, confirming that there was no migration of the stabilizing units toward air-film film interface as it is in the case of conventional surfactant or that there were already some carboxylic acid groups at the surface. Furthermore, it was observed that the chain extender type influenced significantly the amount of water soluble species and the water uptake behavior of the hybrid polymer films. The films containing EDA as chain extender were highly water sensitive and some chains were dissolved in the water during the test. On the other hand, in the case of more hydrophobic chain extenders (DAO and DAD), lower amount of polymer film was dissolved in the water during the test. Therefore, election of chain extender influences the mechanical properties and may be crucial in determining the water sensitivity characteristics of the final films.

2.5. References

[1] A.K. Nanda, D.A. Wicks, S.A. Madbouly, J.U. Otaigbe, Effect of ionic content, solid content, degree of neutralization, and chain extension on aqueous polyurethane dispersions prepared by prepolymer method, J. Appl. Polym. Sci. 98 (2005) 2514–2520.

[2] T. Tawa, S. Ito, The Role of Hard Segments of Aqueous Polyurethane-urea Dispersion in Determining the Colloidal Characteristics and Physical Properties, Polym. J. 38

(2006) 686–693.

[3] A.K. Nanda, D.A. Wicks, The influence of the ionic concentration, concentration of the polymer, degree of neutralization and chain extension on aqueous polyurethane dispersions prepared by the acetone process, Polymer (Guildf). 47 (2006) 1805–1811.

[4] J. Bullermann, S. Friebel, T. Salthammer, R. Spohnholz, Novel polyurethane dispersions based on renewable raw materials - Stability studies by variations of DMPA content and degree of neutralisation, Prog. Org. Coatings. 76 (2013) 609–615.

[5] M. Li, E.S. Daniels, V. Dimonie, E.D. Sudol, M.S. El-Aasser, Preparation of Polyurethane/Acrylic Hybrid Nanoparticles via a Miniemulsion Polymerization Process, Macromolecules. 38 (2005) 4183–4192.

[6] M.M. Rahman, H.-D. Kim, Effect of polyisocyanate hardener on waterborne polyurethane adhesive containing different amounts of ionic groups, Macromol. Res. 14 (2006) 634–639.

[7] S.M. Cakić, M. Spírková, I.S. Ristić, J.K. B-Simendić, M. M-Cincović, R. Poreba, The waterborne polyurethane dispersions based on polycarbonate diol: Effect of ionic content, Mater. Chem. Phys. 138 (2013) 277–285.

[8] M. Barikani, M. Valipour Ebrahimi, S.M. Seyed Mohaghegh, Preparation and characterization of aqueous polyurethane dispersions containing ionic centers, J. Appl. Polym. Sci. 104 (2007) 3931–3937.

[9] M. Yen, S. Kuo, PCL – PEG – PCL Triblock Ester – Ether Copolydiol-Based Waterborne Polyurethane . II . Effect of NCO / OH Mole Ratio and DMPA Content on the Physical Properties, J. Appl. Polym. Sci. 67 (1997) 1301–1311.

[10] M.A. Pérez-Limiñana, F. Arán-Aís, A.M. Torró-Palau, A.C. Orgilés-Barceló, J.M. Martín-Martínez, Characterization of waterborne polyurethane adhesives containing different amounts of ionic groups, Int. J. Adhes. Adhes. 25 (2005) 507–517.

[11] M.M. Rahman, H. Do Kim, Synthesis and characterization of waterborne polyurethane adhesives containing different amount of ionic groups (I), J. Appl. Polym. Sci. 102 (2006) 5684–5691.

[12] J.Y. Bae, D.J. Chung, J.H. An, D.H. Shin, Effect of the structure of chain extenders on the dynamic mechanical behaviour of polyurethane, J. Mater. Sci. 34 (1999) 2523–2527.

[13] K. Gisselfält, B. Helgee, Effect of soft segment length and chain extender structure on

phase separation and morphology in poly(urethane urea)s, Macromol. Mater. Eng. 288 (2003) 265–271.

[14] D.K. Chattopadhyay, B. Sreedhar, K.V.S.N. Raju, Effect of chain extender on phase mixing and coating properties of polyurethane ureas, Ind. Eng. Chem. Res. 44 (2005) 1772–1779.

[15] A. Takahara, J. Tashita, T. Kajiyama, M. Takayanagi, W.J. MacKnight, Microphase separated structure and blood compatibility of segmented poly(urethaneureas) with different diamines in the hard segment, Polymer (Guildf). 26 (1985) 978–986.

[16] C. Hepburn, Polyurethane Elastomers, Springer Netherlands, Dordrecht, 1992.

[17] S.A. Madbouly, J.U. Otaigbe, A.K. Nanda, D.A. Wicks, Rheological behavior of aqueous polyurethane dispersions: Effects of solid content, degree of neutralization, chain extension, and temperature, Macromolecules. 38 (2005) 4014–4023.

[18] M.C. Delpech, F.M.. Coutinho, Waterborne anionic polyurethanes and poly(urethane-urea)s: influence of the chain extender on mechanical and adhesive properties, Polym. Test. 19 (2000) 939–952.

[19] B. Helgee, K. Gisselfa, S. Chemistry, Effect of Soft Segment Length and Chain Extender Structure on Phase Separation and Morphology in Poly (urethane urea) s, (2003) 265–271.

[20] W.D. Vilar, Chemistry and Technology of Polyurethanes, Vilar Consultoria Ltda., Rio de Janeiro, 2002.

[21] J. Sangster, Octanol-Water Partition Coefficients: Fundamentals and Physical Chemistry, Wiley, 1997.

[22] S. Zhang, L. Cheng, J. Hu, NMR studies of water-borne polyurethanes, J. Appl. Polym. Sci. 90 (2003) 257–260.

[23] S. Lee, M.A. Winnik, R.M. Whittal, L. Li, Synthesis of symmetric fluorescently labeled poly(ethylene glycols) using phosphoramidites of pyrenebutanol and their characterization by MALDI mass spectrometry, Macromolecules. 29 (1996) 3060–3072.

[24] A.T. Jackson, H.T. Yates, J.H. Scrivens, G. Critchley, J. Brown, M.R. Green, R.H. Bateman, The Application of Matrix-assisted Laser Desorption/Ionization Combined with Collision-induced Dissociation to the Analysis of Synthetic Polymers, Rapid Commun. Mass Spectrom. 10 (1996) 1668–1674.

[25] P.M. Lloyd, K.G. Suddaby, J.E. Varney, E. Scrivener, P.J. Derrick, D.M. Haddleton, A comparison between matrix-assisted laser desorption / ionisation time-of-flight mass spectrometry and size exclusion chromatography in the mass characterisation of synthetic polymers with narrow molecular-mass distributions : Poly (methyl methacrylate), Eur. Mass Spectrom. 1 (1995) 293–300.

[26] I. Schnöll-Bitai, T. Hrebicek, A. Rizzi, Towards a quantitative interpretation of polymer distributions from MALDI-TOF spectra, Macromol. Chem. Phys. 208 (2007) 485–495.

[27] S.F. Macha, P. a Limbach, M atrix-assisted laser desorption / ionization (MALDI) mass spectrometry of polymers, Solid State Mater. Sci. 6 (2002) 213–220.

[28] H.C.M. Byrd, C.N. McEwen, The limitations of MALDI-TOF mass spectrometry in the analysis of wide polydisperse polymers, Anal. Chem. 72 (2000) 4568–4576.

[29] K. Shimada, M.A. Lusenkova, K. Sato, T. Saito, H. Nakahara, S. Kinugasa, Evaluation of mass discrimination effects in the quantitative analysis of polydisperse polymers by matrix- assisted laser desorption / ionization time-of- ¯ ight mass spectrometry using uniform oligostyrenes, (2001).

[30] G. Odian, Principles of Polymerization, John Wiley & Sons, Inc., Hoboken, NJ, USA, 2004.

[31] G. Wang, K. Li, W. Zou, A. Hu, C. Hu, Y. Zhu, C. Chen, G. Guo, A. Yang, R. Drumright, J. Argyropoulos, Synthesis of HDI/IPDI hybrid isocyanurate and its application in polyurethane coating, Prog. Org. Coatings. 78 (2015) 225–233.

[32] A.F. Johnson, K.F. O'Driscoll, Monte Carlo simulation of sequence distributions in step growth copolymerization, Eur. Polym. J. 20 (1984) 979–983.

[33] R. Po', E. Occhiello, F. Garbassi, Computer simulation of non-equilibrium step-growth copolymerization processes, Eur. Polym. J. 28 (1992) 79–84.

[34] D.T. Gillespie, Exact stochastic simulation of coupled chemical reactions, J. Phys. Chem. 81 (1977) 2340–2361.

[35] S.R. Liao, Y. Wei, S.L. An, Research on the Reaction of IPDI and PPG with Organo-Tin Mixed Catalyst, in: Front. Adv. Mater. Eng. Technol., Trans Tech Publications, 2012: pp. 399–403.

[36] H.-K. Ono, F.N. Jones, S.P. Pappas, Relative reactivity of isocyanate groups of isophorone diisocyanate. Unexpected high reactivity of the secondary isocyanate group, J. Polym. Sci. Polym. Lett. Ed. 23 (1985) 509–515.

[37] K. Hatada, K. Ute, K.-I. Oka, S.P. Pappas, Unambiguous 13C-NMR assignments for isocyanate carbons of isophorone diisocyanate and reactivity of isocyanate groups in Z - and E-stereoisomers, J. Polym. Sci. Part A Polym. Chem. 28 (1990) 3019–3027.

[38] S. Wang, X. Yang, Q. Bai, T. Li, In Situ Monitoring of Selective Catalysts on Urethane Formation by FT-IR Spectroscopy, Int. J. Polym. Anal. Charact. 18 (2013) 146–153.

[39] I. González, J.M. Asua, J.R. Leiza, The role of methyl methacrylate on branching and gel formation in the emulsion copolymerization of BA/MMA, Polymer (Guildf). 48 (2007) 2542–2547.

[40] X.Q. Wu, F.J. Schork, Kinetics of Miniemulsion Polymerization of Vinyl Acetate with Nonionic and Anionic Surfactants, (2001) 1691–1699.

[41] C. Prisacariu, Polyurethane Elastomers, Springer Vienna, Vienna, 2011.

[42] S. Bilgin, R. Tomovska, J.M. Asua, Effect of ionic monomer concentration on latex and film properties for surfactant-free high solids content polymer dispersions, Eur. Polym. J. 93 (2017) 480–494.

[43] M. Chang, A.S. Myerson, T.K. Kwei, The Effect of Hydrogen Bonding on Vapor Diffusion in Water-Soluble Polymers, J. Appl. Polym. Sci. 66 (1997) 279–291.

Chapter 3: Grafted PU/(meth)acrylic hybrids by incorporation of different functional monomers

3.1. Introduction

PU/(meth)acrylic hybrids are two phase polymer systems whose performance depends significantly on the compatibility between the phases. As was discussed in Chapter 1 (section 1.3.2), different methods have been utilized to improve this compatibility. The use of a functional monomer that can introduce double bonds to PU chains and subsequently integrate them during the free-radical polymerization of (meth)acrylics is an attractive way to produce grafted hybrids and improve the compatibility between PU and (meth)acrylics. These functional monomers often contain both hydroxyl and (meth)acrylic groups [1–10]. This dual functionality allows the monomers to react with the isocyanate groups during the formation of the polyurethane and with radicals during the formation of the poly(meth)acrylic chains.

The grafting of PU and acrylic chains can result in a huge variety of macromolecular structures, depending on the type of the functional monomer and the nature of both PU and (meth)acrylic monomers in the formulation. For example, when the number of double bonds introduced into the PU chain is less than two, the most likely outcome is a linear (meth)acrylic polymer chain with PU branches. If the number of double bonds is two or more, there is higher possibility of crosslinked network formation (as shown in Scheme 3.1), where the PU will

serve to crosslink the (meth)acrylic chains. Furthermore, the reactivity of the double bond can be different depending on the nature of the double bond, which leads to incorporation at different moments in the reaction and can generate a heterogeneous mixture of grafted and non-grafted PU chains [11,12].

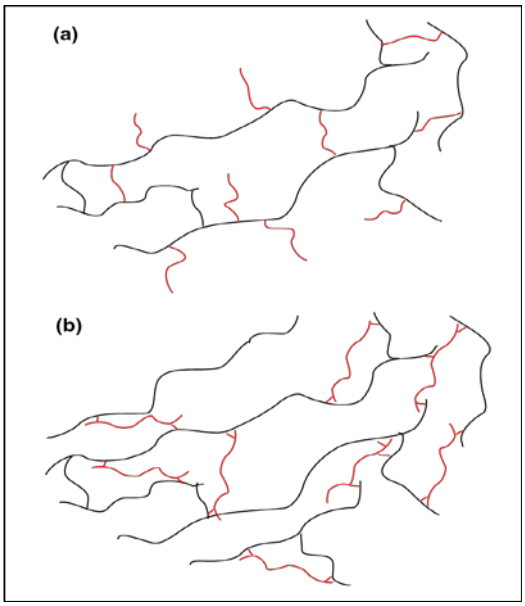

Scheme 3.1. Structure of grafted PU/acrylic hybrid having one or two double bound per PU chain (a), and having two or more double bound per PU chain (b) (PUs= red , Acrylics=black)

Given the extent to which the structure of the hybrid is controlled by the nature of grafting it can also be expected that the material properties differ strongly when grafting is introduced. Thus, it has been demonstrated that the formation of the graft copolymers led to the polymer films with improved tensile strength (the stress at break) [13] and formation of transparent films [3,14], however the elongation at break decreased with grafting [13]. It is also reported that in pressure sensitive adhesives, the cohesive strength can be improved with grafting [7]. Nevertheless, there are no data published that relates the type of functional

monomer with the grafting extent, the morphology of the hybrids, their microstructure and the final properties.

The selection of the functional monomer is crucial in the microstructure of the hybrids and subsequently in the properties. Therefore, this chapter studies the effect of type of functional monomer on the grafting, polymer microstructure, particle and film morphologies and film properties of the PU/acrylic hybrids. Solvent and emulsifier-free grafted hybrid dispersions are synthesized using two different functional monomers with different concentrations; glycerol mono-methacrylate (GMMA) and hydroxyethyl methacrylate (HEMA) (Scheme 3.2). GMMA has two hydroxyl groups and a methacrylic functionality and upon incorporating in the PU chain, the methacrylic groups are located in the side of the PU chains. This creates the possibility of having several grafting points per PU chain. Whereas in the case of HEMA that blocks the PU chains, the methacrylic functionality is located at the end of the chain and a maximum of two grafting points per chain can be obtained.

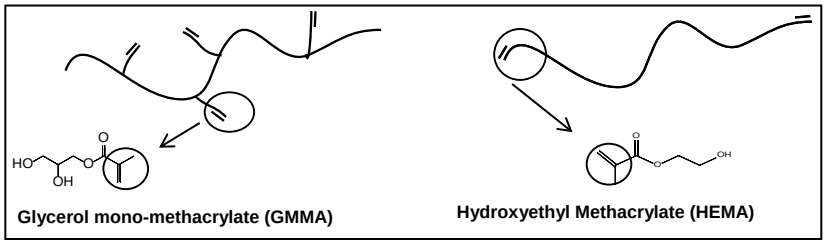

Scheme 3.2. Structure of functional monomers(FM) as grafting point - GMMA (left) and HEMA (right)

3.2. Experimental

3.2.1. Materials

The materials are given in Appendix I.

3.2.2. Synthesis procedures

The synthesis of the PU prepolymer was performed in a 250 mL glass reactor fitted with a reflux condenser, a sampling device (and feeding inlet), a nitrogen inlet, a thermometer and a flat blade turbine stirrer. Reaction temperature was controlled by an automatic control system, Camile TG (Biotage). The formulation of the synthesized PU/Poly(meth)acrylic (50/50 wt/wt) hybrid dispersions using the two functional monomers (GMMA and HEMA) at different concentrations is presented in Table 3.1. In order to gain an insight into the effect of grafting on the macromolecular structure, additional reactions were carried out in the absence of the functional monomers using either butanediol or pentanol to replace GMMA and HEMA respectively. The synthesis of the PU-Urea dispersion using butanediol, GMMA, pentanol and HEMA are shown in Schemes 3.3 to 3.6, respectively.

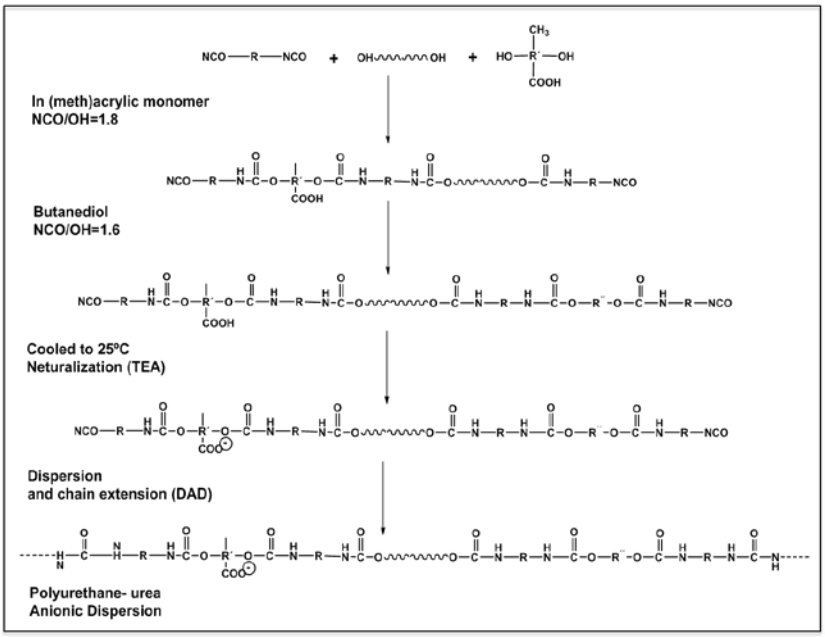

Scheme 3.3. Preparation process for PU-urea dispersion using butanediol

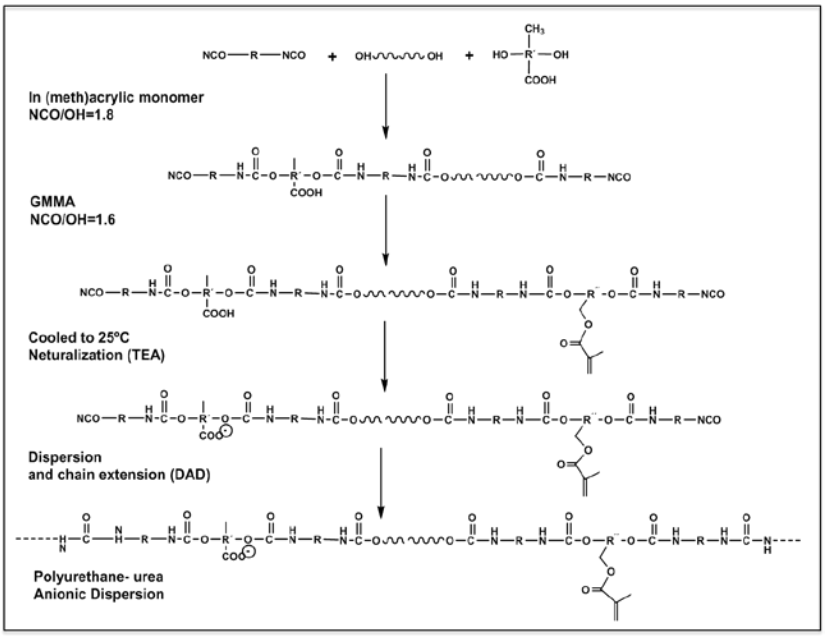

Scheme 3.4. Preparation process for Functionalized PU-urea dispersion using GMMA

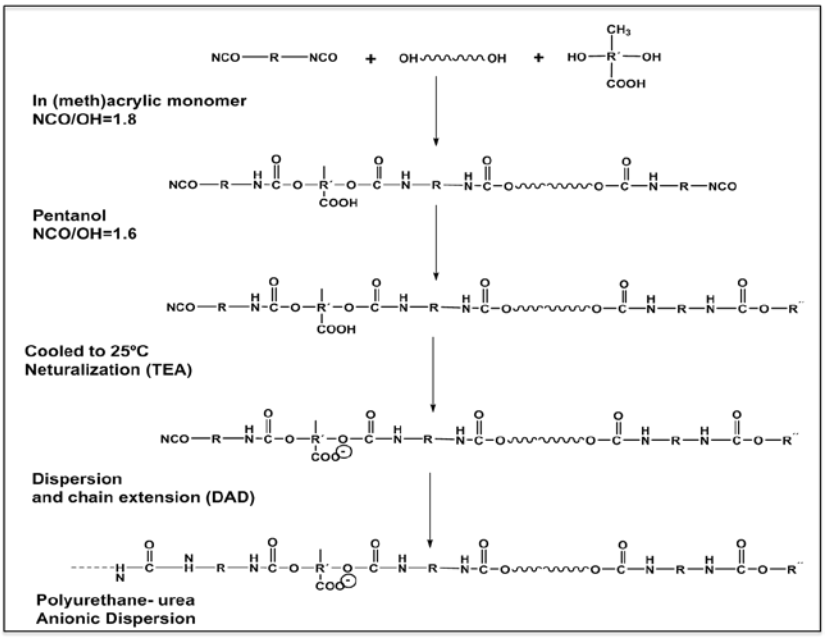

Scheme 3.5. Preparation process for PU-urea dispersion using pentanol

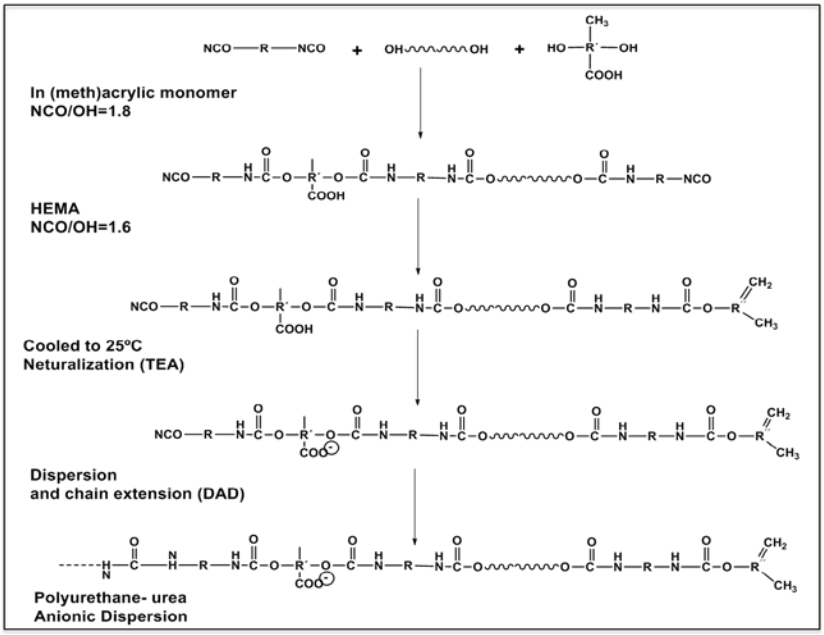

Scheme 3.6. Preparation process for Functionalized PU-urea dispersion using HEMA

To synthesize the PU prepolymer, dimethylol propionic acid (DMPA), polypropylene glycol (PPG), isophorone diisocyanate (IPDI) (7.73 g), dibutyltin dilaurate (DBTDL) (0.05 g) and 50 wt% of the (meth)acrylic monomers (mixture of methyl methacrylate (MMA)/ and butyl acrylate (BA), 1/1 by weight) were charged into the reactor. The reaction mixture was brought to 70°C under agitation (250 rpm) and held for 4-5 hours. The free NCO at the end of the reaction was checked with amine-back titration [15]. Then, the mixture of butanediol/GMMA or pentanol/HEMA dissolved in 20 wt% of (meth)acrylic monomers (mixture of MMA/BA 1/1 wt/wt) were added to the prepolymer to functionalize the PU chains. Butanediol (in the case of GMMA) and pentanol (in the case of HEMA) as short chain diol/alcohol were added with the functional monomer in order to keep a similar NCO/OH value and hence to use fix amount of chain extender in the case of grafted and non grafted hybrids. After 2 hours, the mixture was cooled to 25°C and additional 20 wt% of (meth)acrylic monomers (mixture of MMA/BA 1/1 wt/wt) was added to reduce the viscosity. After that, TEA dissolved in 10 wt% of (meth)acrylic monomers (mixture of MMA/BA 1/1 wt/wt) was added and kept at 25°C for 45 min in order to neutralize the carboxylic groups of DMPA.

Then, the PU/(meth)acrylic solution was dispersed in water. To prepare the aqueous dispersions, the reactor was charged with double deionized water under nitrogen at 25°C and the prepolymer-monomer mixture was added in 15 min under high agitation (750 rpm). After that, the chain extender (DAD) dissolved in 10 wt% of the (meth)acrylic monomers (mixture of MMA/BA 1/1 wt/wt) was added into reactor and left to react one hour at 70°C. The theoretical molar ratio of NCO/OH (defined as a molar ratio of IPDI and sum of molar ratio of

PPG, DMPA, short chain diol/alcohol, functional monomer and DAD) was 1.8 before chain extension, 1.6 for the functionalized prepolymer and 1.0 after chain extension.

The free radical polymerization of (meth)acrylic monomers was performed at 70°C by adding KPS (0.5 wt% based on monomer) dissolved in water as a single shot. The polymerization was performed in batch for 2 hours and a final conversion of (meth)acrylic monomers higher than 98% was achieved in all the cases. The resulting hybrid latexes consist of PU/acrylic with 40% solids content.

Table 3.1. Recipe used to synthesize PU/(meth)acrylic (50/50 wt/wt) hybrids with constant amount of IPDI (7.73 g), DBTDL catalyst (0.05 g), water (71 g) and KPS (0.12 g)

Experiment	PPG	DMPA[b]	Butanediol	GMMA	Pentanol	HEMA	TEA[c]	DAD	MMA/*n*BA (g/g)
	(mols per 1 mol of IPDI)								
No FM-Butanediol	0.19	0.37	0.07	0	-	-	0.39	0.37	12/12
GMMA 2.5%[a]	0.19	0.37	0.045	0.025	-	-	0.39	0.37	12/12
GMMA 5%[a]	0.19	0.37	0.02	0.05	-	-	0.39	0.37	12/12
No FM-Pentanol	0.19	0.37	-	-	0.14[d]	0	0.39	0.37	12/12
HEMA 2.5%[a]	0.19	0.37	-	-	0.115[d]	0.025[d]	0.39	0.37	12/12
HEMA 5%[a]	0.19	0.37	-	-	0.09[d]	0.05[d]	0.39	0.37	12/12

a) Mol FM/Mol IPDI (%)
b) 3.5 wt% based on organic phase
c) 1.05 mol of DMPA
d) mono-alcohol – The NCO/OH value was fixed with pentanol content

3.2.3. Characterization

The final particle sizes of the latexes were measured by dynamic light scattering (DLS); the unreacted NCO groups were determined by titration; the conversion of (meth)acrylic monomers was measured gravimetrically; the gel fraction was measured by Soxhlet

extraction, using THF as the solvent; the molar mass distribution of the soluble fraction of polymers was determined by size exclusion chromatography (SEC/RI/UV); the molar mass distribution of the whole polymer was determined by asymmetric-flow field-flow fractionation (AF_4) using multi angle light scattering and refractive index detectors (MALS/RI); the thermal characterization of the hybrids was carried out by differential scanning calorimetry (DSC); the morphologies of latex particles and films were studied by means of transmission electron microscopy (TEM); the mechanical properties of the polymer films from synthesized latexes were determined by tensile test measurements; the water sensitivity of the polymer films was analyzed by water uptake test. A detailed description of the characterization methods is provided in Appendix I.

3.3. Results and Discussion

3.3.1. Polymer Microstructure

Table 3.2 summarizes the characteristics of the synthesized PU/Poly(meth)acrylic hybrid dispersions. The final particle sizes of the hybrids were in the range of 80-150 nm. The observed trend when using GMMA was different than that for HEMA, although the reason is not clear. The DSC analysis showed two glass transition temperatures (T_g) for all the hybrid films, one at low temperature (around -55 ºC), which corresponds to the PU chains, and another at higher temperature (around 30 ºC), which corresponds to the copolymer of MMA/BA obtained in a batch system. It is worth pointing out that in batch polymerization due to the difference in the reactivity ratios of MMA and BA, some PMMA rich chains with higher T_g are expected to be formed at the beginning of the process. The two T_gs slightly shifted

towards each other in the case of the grafted hybrids, showing more compatibility between PU and (meth)acrylic polymer phases.

A detailed characterization of the effect of the functional monomers on the molecular weight distribution (MWD) was carried out by measuring the gel fraction (fraction of polymer insoluble in THF, Table 3.2), the MWD of the soluble part determined by SEC (Figures 3.1 and 3.2) and the whole MWD determined by AF_4/MALS/RI (Figure 3.3) . This technique provides information on absolute molar mass distribution (MMD) of the whole polymer (gel + sol) [16–19]. The corresponding refractive index (RI) chromatograms vs. elution time for the PU/(meth)acrylic hybrids with GMMA and HEMA are presented in Figures 3.4(a) and 3.4(b), respectively.

Table 3.2. The characteristics of PU/(meth)acrylic hybrids with different functional monomers

Experiment	Particle size (nm)	T_g		Gel content	Sol $\overline{Mw}$ ** (Kg/mol)	
		T_{g1} (ºC)	T_{g2} (ºC)	(%)	Low M_w	High M_w
No FM- Butanediol	145	-56	32	0	36	1019
GMMA 2.5%*	135	-54	27	67 ± 2	30	-
GMMA 5%*	87	-50	27	74 ± 2	32	-
No FM- Pentanol	96	-54	32	0	18	711
HEMA 2.5%*	123	-54	24	0	16	1280
HEMA 5%*	136	-51	23	48 ± 1	16	-

* Mol FM*100/Mol IPDI

** measured by SEC, bimodal molar mass distrubution contain both low molar mass non grafted PU chains and high molar mass (meth)acrylic chains

Table 3.2 shows that no gel was formed in the absence of functional monomer. In this case, one would expect to obtain the same MWD by SEC and by AF_4. However, comparison between Figures 3.1, 3.2 and 3.3 shows that although there are some similarities (e.g., the distributions are bimodal) this is not the case. There are two reasons for this result. First, that

SEC MWD was calculated using the universal calibration with poly(styrene) standards and without knowing for sure the values of the Mark-Houwink parameters for the hybrid polymer. Second, and likely more important, that the samples were filtered before injecting them to the SEC and the high molecular weight chains might be retained by the filter. Therefore, the high molecular weights of the SEC chromatograms should be taken with precaution.

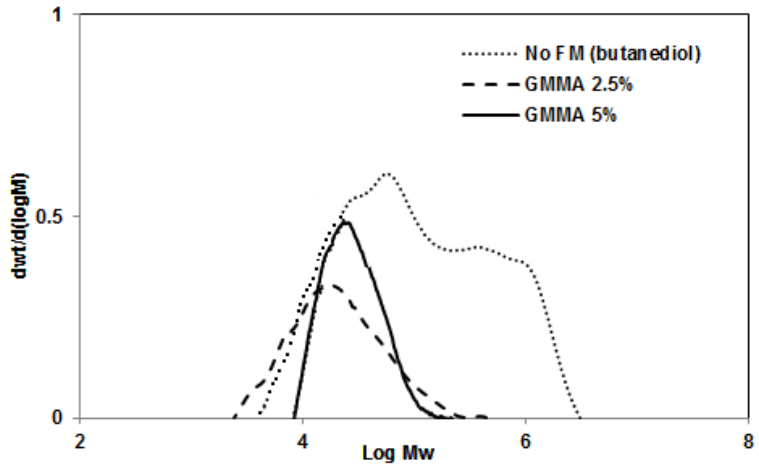

Figure 3.1. Molar mass distribution of soluble fraction of the non-grafted and grafted PU/(meth)acrylic hybrids using GMMA obtained by SEC (the curves are normalized based on the soluble fraction)

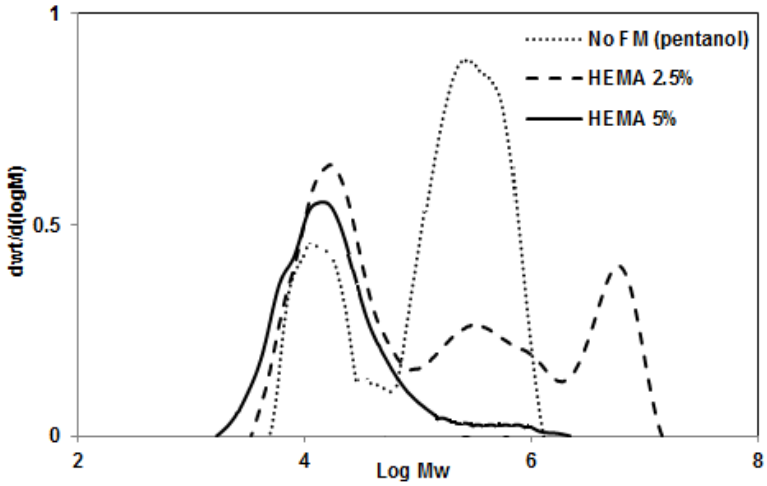

Figure 3.2. Molar mass distribution of soluble fraction of the non-grafted and grafted PU/(meth)acrylic hybrids using HEMA obtained by SEC (the curves are normalized based on the soluble fraction)

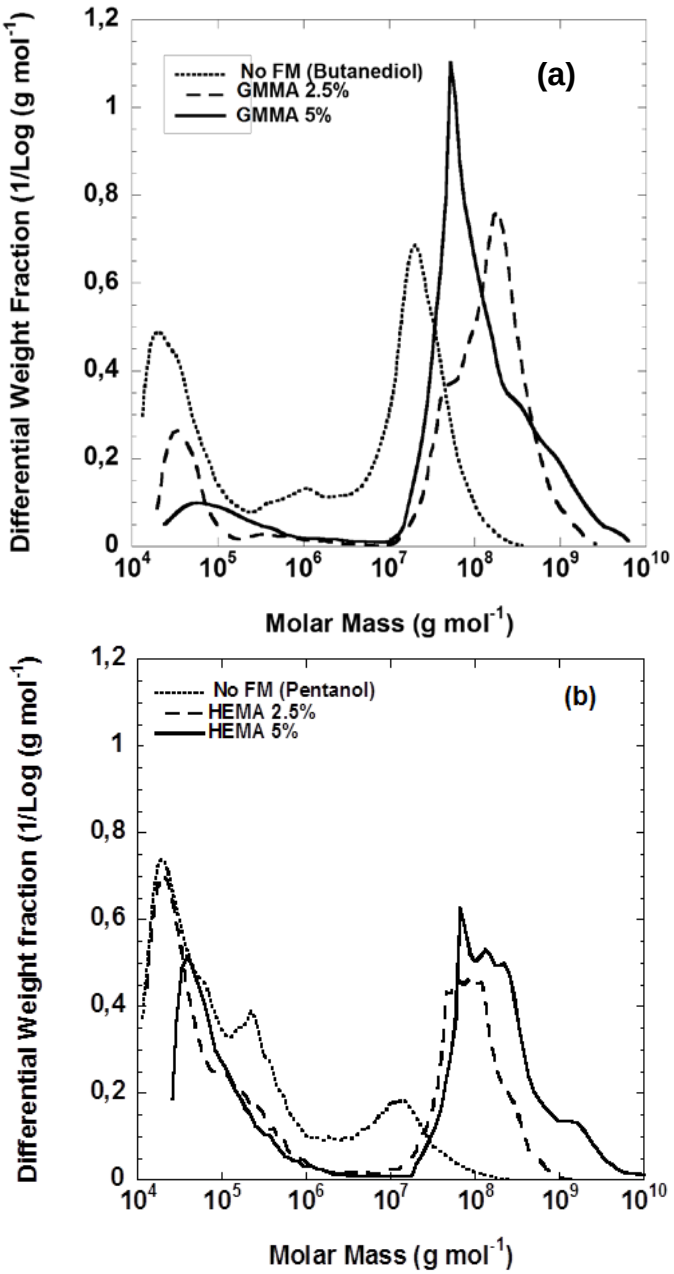

Figure 3.3. Absolute MMD of the non-grafted and grafted PU/(meth)acrylic hybrid dispersion using GMMA (a) and HEMA (b) as FM, obtained by AF4/MALS/RI

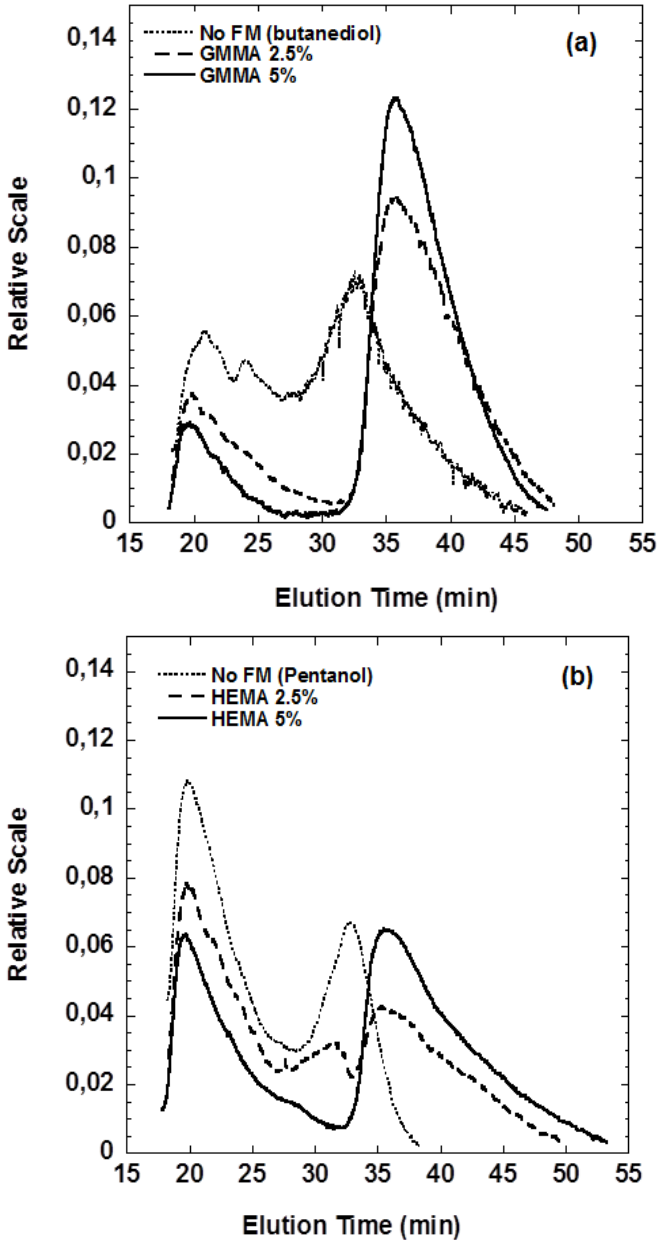

Figure 3.4. RI chromatograms of the non-grafted and grafted PU/(meth)acrylic hybrid dispersion using GMMA (a) and HEMA (b) as FM, obtained by AF4/MALS/RI

Figure 3.3a shows a bimodal MWD for the sample without functional monomer, where the population of high M_ws corresponded to (meth)acrylic polymer and the one with low M_w to PU chains. This assignment is based on the evolution of the MWD during the process carried out in the absence of functional monomer (Figure 3.5). This figure shows that the M_w of the PU increases upon chain extension up to an average M_w of about 10^5 g/mol and that the high M_w polymer only appeared after polymerization of the (meth)acrylic monomers. As there was no grafting, the high M_w polymer should be poly(meth)acrylic.

The very high M_w (10^7 – 10^8 g/mol) observed with butanediol is surprising and suggests the occurrence of some long chain branching in the last stages of the free radical polymerization, when mostly poly(BA) was formed. For pentanol, the MWD was more continuous with quite a few of polymer in the region 10^5 – 10^6 g/mol. Likely, this polymer was poly(MMA-BA). The lower M_w as compared with butanediol might be due to some unreacted pentanol acting as a chain transfer agent.

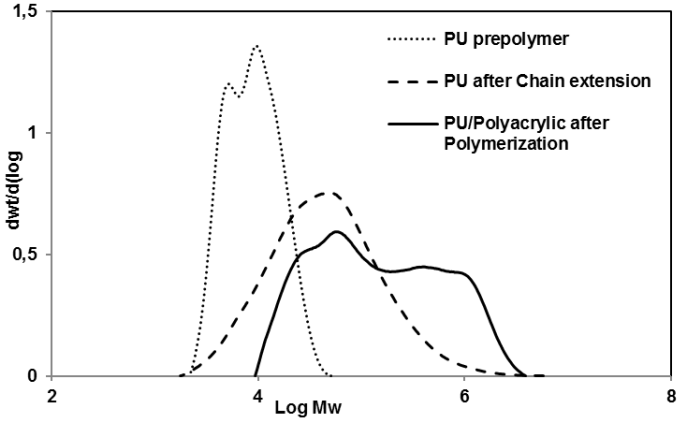

Figure 3.5. Evolution of molar mass distribution during synthesis of PU/(meth)acrylic hybrid (for sample No FM- butanediol)

A substantial increase of the M_ws was observed when functional monomers were used (Figure 3.3). The reason was that due to the double bonds in its structure, the PU behaved as a crosslinker. In addition, insoluble polymer (gel) was formed. The effect was stronger for GMMA. The main reason for this can be directly linked to the nature of the functional monomer that may lead to the obtain PU chains with different length and different position of double bonds. Table 3.3 shows the number average molar mass ($\overline{Mn}$) of PU chains before the free radical polymerization of the (meth)acrylic monomers and the predicted average number of double bonds per PU chain based on the molar mass. With the monofunctional alcohol compounds (HEMA and pentanol), PU with lower M_n was obtained, because the monofunctional alcohols terminate the PU chains. On the other hand, using bifunctional alcohols (GMMA and butanediol), which chain extend the PU, a higher $\overline{Mn}$ was obtained. The difference in molar mass for the same mole fraction of functional monomer means that the average number of double bonds per PU chain is significantly lower in the case of HEMA than GMMA. It should also be noted that the statistical distribution of the functional groups means that some chains will have 2 double bonds and some chains may not have any.

Table 3.3. PU number average molar mass (before polymerization of acrylics) and Number of grafting point per chain

	M_n of PU chains (after chain extension)	**Number of grafting point per chain****
No FM - Butanediol	23 000	0
GMMA - 2.5%*	24 000	1.1
GMMA - 5%*	24 000	2.2
No FM - Pentanol	10 600	0
HEMA - 2.5%*	11 000	0.5
HEMA – 5%*	11 600	1.0

* Mol FM*100/Mol IPDI

**Number of FM per PU chain calculated by $\frac{\text{mol FM in formulation} \times \overline{Mn} \text{ of PU}}{\text{g PU in the formulation}}$

In the grafted hybrids with GMMA (Figure 3.3(a)), the addition of GMMA resulted in a) a decrease of the peak of non-grafted PU and the shift toward higher M_w, and b) an increase of both the fraction and the molar mass of the peak of high molecular weights. The effect became stronger as GMMA content increased. Taking the gel fraction measured by Soxhlet as a reference, the frontier between sol and gel can be placed about 5×10^7 g/mol. Moreover, in the low molar mass region, the MMD shifted to higher values with grafting, especially at higher concentration of GMMA. This is probably due to the propagation of PU chains containing double bond with some acrylics. As was discussed before, despite the high average grafting point per PU chain (2.2 in the case of GMMA 5%, see Table 3.3), not all the PU chains were grafted. Therefore, in addition to the effect of the statistics that may result in PU chains devoid of double bonds, probably some PU chains were incorporated into short acrylic chains and they did not form a network and were therefore not incorporated in the gel fraction.

In the grafted hybrids with HEMA (Figures 3.3(b)), the addition of 2.5% of HEMA did not result in a decrease of the relative size of the PU peak, although the MMA-BA copolymer reached to higher molecular weight. This indicates that only a relatively small fraction of PU was grafted, likely because of the small average number of double bonds per PU chain (0.5). On the other hand, the strong shift of the poly(MMA/BA) chains to higher molar masses indicates that some PU chains acted as crosslinkers (statistical distributions of double bonds may lead to PU chains with two double bonds). When HEMA concentration was increased to 5 %, there was a significant reduction of the PU peak and chains with very high molar masses were observed.

It is worth pointing out some limitations of the AF_4 analysis. On one hand, the limit for M_w is 10^9 g/mol and higher values have been detected. Moreover, the value of dn/dc in the AF_4/MALS/RI analysis was considered to be the average of the value for PU and (meth)acrylic (see Appendix I, section I.2.6). However, the dn/dc value of the low molar mass region (mostly PU) and the high molar mass region (mostly poly(MMA-BA with some grafted PU) are different and this can affect the results obtained.

The two distinct peaks in the RI chromatogram plot (Figures 3.4(a) and 3.4(b)) were integrated and the mass fraction of the peaks are presented in Table 3.4. As the ratio of PU/(meth)acrylic in the formulation is 50/50 wt/wt, the integration of two peak in the absence of functional monomer was close to 50%. However, with grafting, the mass fraction of the first peak decreased and the one of second peak increased confirming the incorporation of grafted chains in the higher molar mass part. It is worth pointing out that the cut-off for defining the gel content in the case of the hybrids with GMMA and butanediol can be considered around 5×10^7 g/mol. However, in the case of the hybrids with HEMA and pentanol, the M_w for the gel cut-off seems to be higher than for GMMA because with the boundary at 5×10^7 g/mol the mass of the second peak is significantly larger than the measured gel.

Table 3.4. Integration of two different peaks in RI chromatogram (in Figure 3.4)

	Gel content (%)	Mass fraction (%)**	
		Peak1 (low molar mass)	Peak2 (high molar mass)
No FM - Butanediol	0	45,1	54,9
GMMA - 2.5%*	67	24,5	75,5
GMMA - 5%*	74	13,8	86,2
No FM - Pentanol	0	55,9	44,1
HEMA - 2.5%*	0	44	56
HEMA – 5%*	48	39	61

* Mol FM*100/Mol IPDI

** Cut-off point sol/gel at 5×10^7 g/mol

3.3.2. Particle and Film Morphology

The TEM micrographs of the PU/acrylic hybrid dispersion (left) and cross-section of the final film (right) are shown in Figures 3.6 and 3.7 for the hybrids with GMMA and HEMA, respectively. As can be seen in Figures 3.6(a)-left and 3.7(a)-left, for the hybrids with no functional monomer a core-shell like particle morphology was observed with the acrylics in the core and PU in the shell as the PU chains contain hydrophilic carboxylic acid groups (DMPA units). With addition of GMMA, PU grafted into acrylics and the particles were more homogeneous with gradual change of the composition. No clear distinction between the individual polymeric phases was noticed for 5% GMMA (Figure 3.6(c)-left). HEMA caused a similar although less strong effect on particle morphology. Using low HEMA content (2.5%), the particles still showed core-shell morphology, but with a less well defined border (Figure 3.7(b)), which supports the finding of lack of efficient grafting of PU into acrylics and no gel formation in this case. However, as the HEMA content increased to 5%, the grafting was more efficient and the particles were more homogeneous.

The TEM of the film cross-section for the hybrid with no functional monomer-butanediol (Figure 3.6(a)-right) showed that the dark spherical domains (acrylics) dispersed within the bright continuous phase (PU). In the case of using GMMA, a more homogeneous distribution of dark (acrylics) and bright (PUs) domains was observed (Figures 3.6(b)-right and 3.6(c)-right) indicating less phase separation due to the grafting. For the maximum amount of GMMA used (5%) no separation was noticed on the nanometric scale (Figure 3.6(c)). The films cast with the HEMA hybrid showed a similar behavior (Figures 3.7(b)-right and 3.7(c)-right).

Although the film containing 5% of HEMA resulted a morphology more homogeneous than that obtained with 2.5% of GMMA.

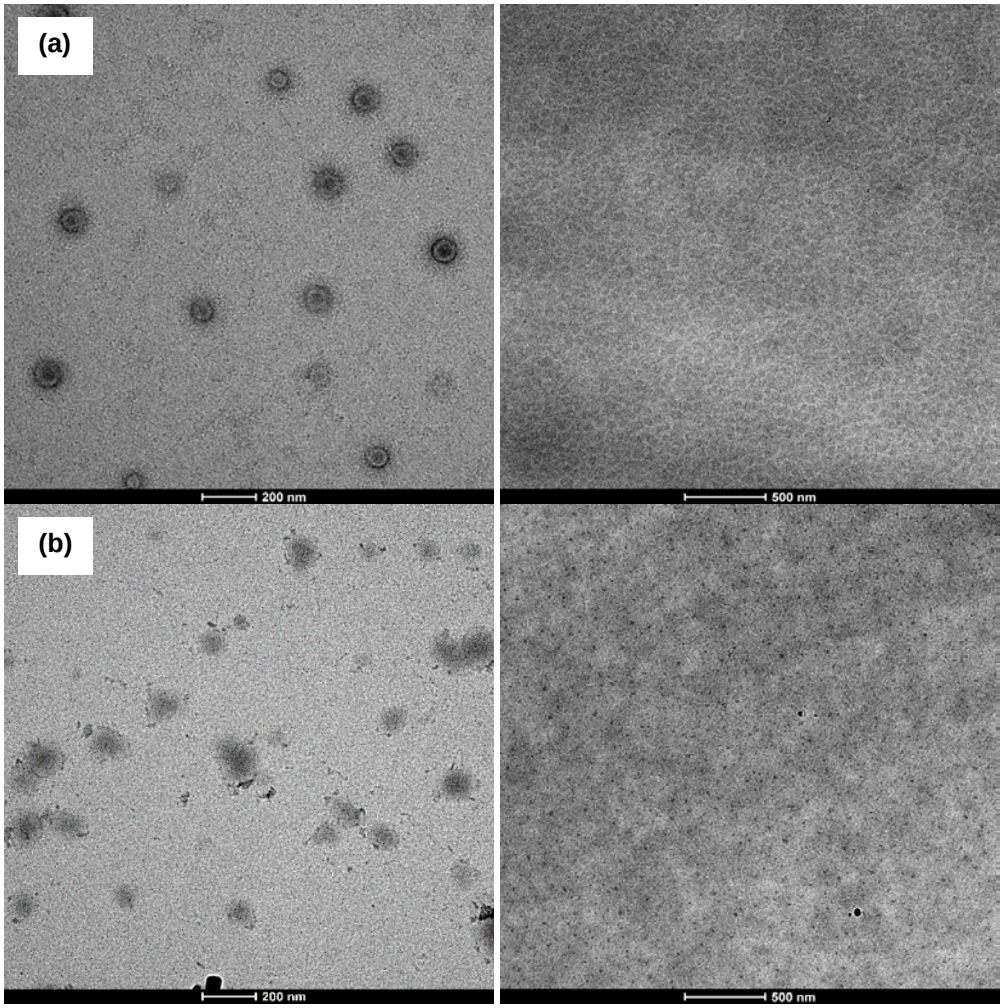

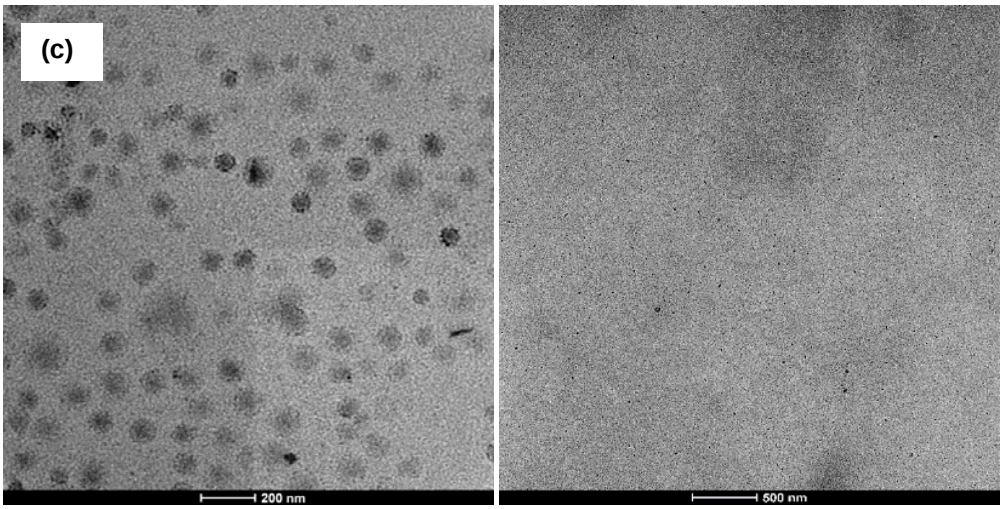

Figure 3.6. Particle morphology (left) and film cross-section surface (right) of PU/(meth)acrylic hybrid: no FM- butanediol (a); GMMA 2.5% (b); and GMMA 5% (c)

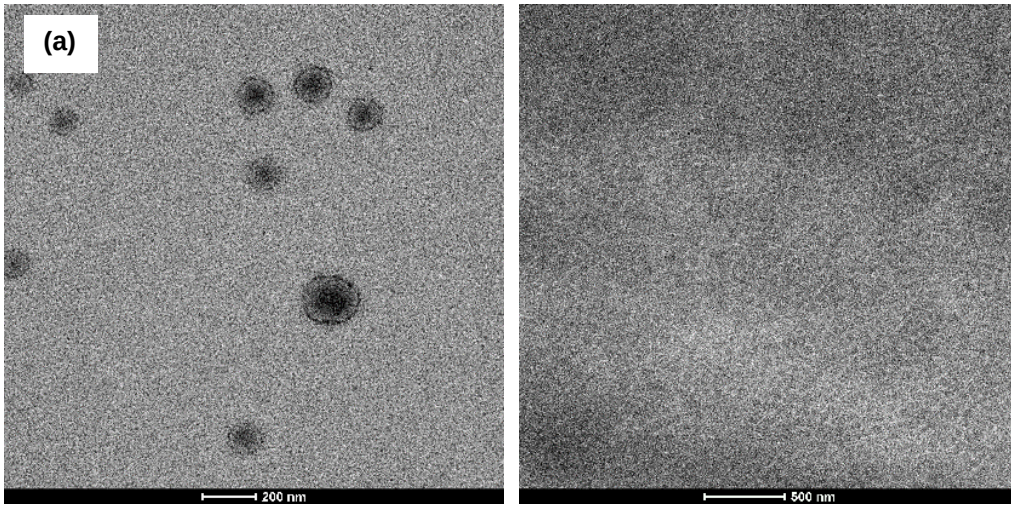

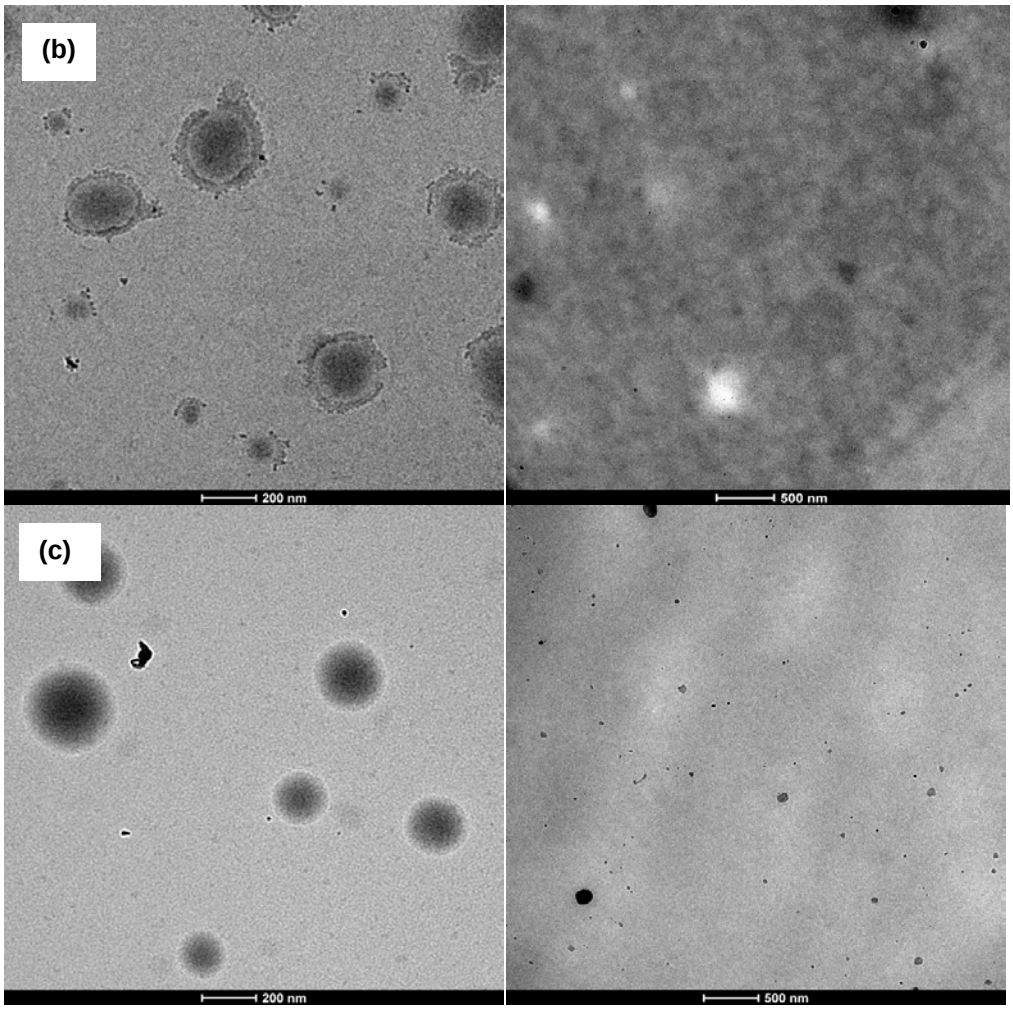

Figure 3.7. Particle morphology (left) and film cross-section surface (right) of PU/(meth)acrylic hybrids: no FM- pentanol (a); HEMA 2.5% (b); and HEMA 5% (c)

3.3.3. Mechanical properties

The stress-strain behavior of non-grafted and grafted PU/(meth)acrylic hybrid films cast at ambient temperature are shown in Figures 3.8(a) and 3.8(b), respectively. The mechanical properties obtained from these experiments are summarized in Table 3.5. It is surprising the

weak effect that grafting and crosslinking had on the mechanical properties for GMMA films in spite of the strong changes in polymer architecture caused by the presence of GMMA (Figure 3.3 and Table 3.2). It is remarkable that even the hybrid synthesized using butanediol instead of GMMA, and therefore devoid of crosslinking points, presented strain-hardening, a characteristic that is typical of crosslinked polymers. This behavior may be due to hydrogen bonding among PU chains that formed a physical network. As the PU was the continuous phase in the polymer film (Figure 3.6(a)-right) it determined the properties of the film. Grafting-crosslinking between PU and poly(MMA-BA) provides additional stiffness to the film, but the increase is modest perhaps due to the loss of some hydrogen bonds among the PU chains that results from the interpenetration with the poly(meth)acrylates. The increase in stiffness results in the increase in Young´s modulus and decrease in the elongation at break.

On the other hand, the effect of HEMA on the tensile test was pronounced and the properties of the polymer evolved from those of an almost liquid-like material to a strain-hardening polymer. The liquid-like behavior is likely due to the short M_w of the PU that is shorter than the critical entanglement length of PUs (11 000 Da in this case) [20]. The effect of the PU molar mass on mechanical properties of the PU/poly(butyl methacrylate) (PBMA) hybrids produced by miniemulsion polymerization has already been reported [20]. It was shown than when the molar mass of PU was too low (below 8000-1200 Da), the PU chains acted as plasticizer and reduced the mechanical property of the PU–PBMA film. In this case, grafting and crosslinking improve the mechanical properties because of the increase in molecular weight and the formation of a network for 5% HEMA that led to a strain-hardening material. The increase of both elongation at break and the stress at break (Figure 3.8(b)) is

an unusual behavior as it is an almost universal observation that structural variations that lead to an increase in elongation at break also lead to a decrease in stress at break and *vice versa.* The observation here can be related to the polymer architecture. As the average number of HEMA units per PU chain is 1 or less then the polymer will have a brush-like structure, in contrast to the case of GMMA, which has the structure of a conventional crosslinked network with relatively few brushes. Brushlike polymers often exhibit unusual rheological behavior and the potential of brush-like polymer to exhibit unique control over mechanical properties of elastomeric materials has recently been demonstrated and highlighted the potential for independent control of parameters that determine material strength [21]. As the quantity of HEMA is increased both the proportion of PU chains containing 2 vinyl groups is increased resulting in a structure with increased crosslink density but a lower content of brushes. Vatankhah-Varnosfaderani *et al.*[21] have shown that in the case of brushlike PDMS elastomers, such an increase in the number of crosslink points with decreasing number of brushes can lead to materials with greater stress at break but without compromise in the maximum strain. In the present case, the network structure is further complicated by the presence of “free” PU chains which are not incorporated into the network but the differences between GMMA and HEMA based PU hybrids can be linked to the molar mass of the PU chains. Yet, even the grafted hybrid with 5% HEMA did not achieve the mechanical properties of the hybrid with no FM and using butanediol, highlighting the importance of the PU properties for the hybrid mechanical properties.

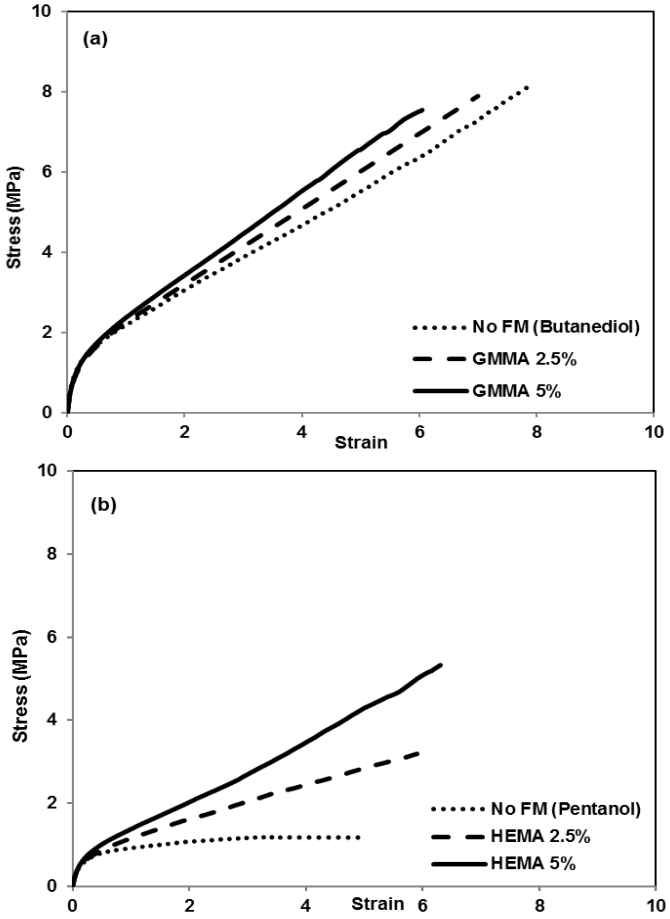

Figure 3.8. The stress-strain behavior of the non-grafted and grafted PU/(meth)acrylic hybrid films using GMMA (a) and HEMA (b) as FM

Table 3.5. Mechanical properties of the PU/Poly(meth)acrylic hybrid films using different FMs

Experiment	Young´s Modulus MPa/100	Yield Stress (MPa)	Elongation at break	Ultimate Strength (MPa)	Toughness (MPa)
No FM-Butanediol	0.08 ± 0.02	1.45 ± 0.08	7.9 ± 0.3	8.2 ± 0.3	36.8 ± 2.1
GMMA 2.5%[a]	0.10 ± 0.01	1.50 ± 0.07	7.0 ± 0.2	7.9 ± 0.3	32.0 ± 1.8
GMMA 5%[a]	0.10 ± 0.01	1.54 ± 0.07	6.1 ± 0.2	7.6 ± 0.4	26.9 ± 1.4
NO FM-Pentanol	0.03 ± 0.01	0.81 ± 0.05	4.9 ± 0.2	1.2 ± 0.3	5.1 ± 1.1
HEMA 2.5%[a]	0.03 ± 0.01	0.84 ± 0.04	5.6 ± 0.4	3. 2 ± 0.2	11.6 ± 1.5
HEMA 5%[a]	0.04 ± 0.01	0.95 ± 0.05	6.3 ± 0.3	5.3 ± 0.2	18.2 ± 1.8

* Mol FM*100/Mol IPDI

3.3.4. Water sensitivity

The water uptake of the polymer films for non-grafted and grafted hybrids with GMMA and HEMA are shown in Figures 3.9(a) and 3.9(b), respectively. The water uptake is rather high, likely due to hydrophilic nature of COOH contained in the PU chains and low T_g of the PU that makes the water swelling easier. The water uptake decreased when grafting was introduced in the system for both GMMA and HEMA and this effect was more pronounced for higher content of functional monomer in the formulation. Moreover, the water uptake showed a tendency to reach a plateau in the case of crosslinked hybrids (GMMA 2.5% and 5% and HEMA 5%). Obviously, the decrease of water uptake is related to the density of crosslinking in the polymer network. The increase in the amount of functional monomer results in higher number of crosslink points, which increased the crosslinked density and decreased the distance between the crosslinked chains. In that way the potential to accommodate water molecules within the structures was significantly decreased. Table 3.6 presents the amount of polymer dissolved in water during the test (as difference in weight before and after water uptake experiments). As can be seen the amount of water soluble species was in the same range (around 2 wt%) for all the films, which can be largely due to the use of hydrophobic chain extender DAD, which led to the smallest production of water soluble oligomers as it was shown in Chapter 2 (see Table 2.11, Chapter 2).

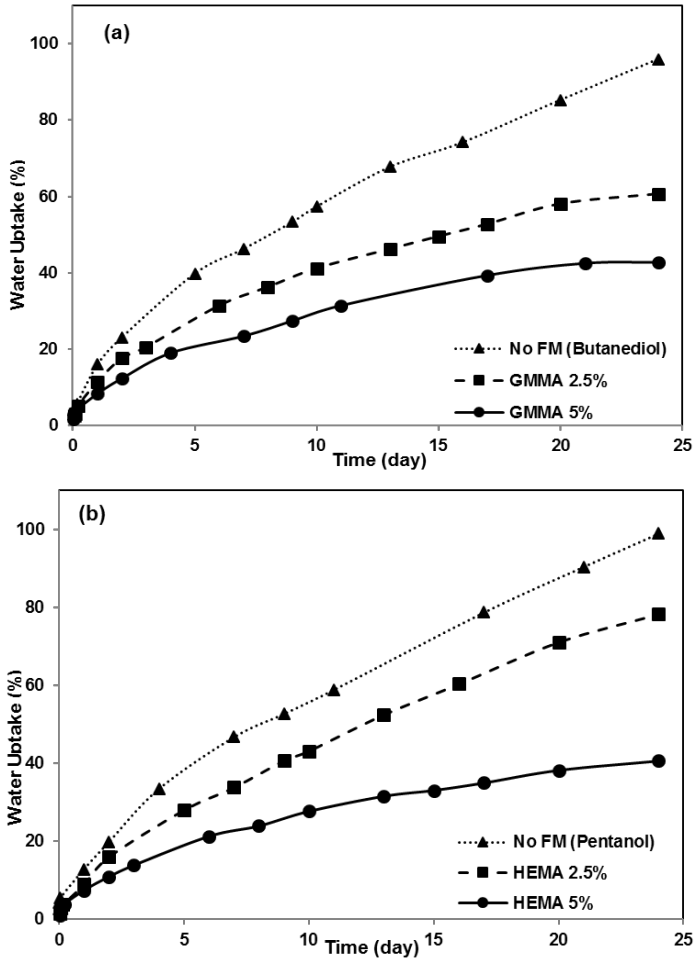

Figure 3.9. The water uptake measurement of the non-grafted and grafted PU/(meth)acrylic hybrid films using GMMA (a) and HEMA (b) as FM

Table 3.6. Amount of polymer dissolved in the water during the water uptake test

	Polymer weight loss after drying (%)
No FM- Butanediol	2.3 ± 0.2
GMMA 2.5%[a]	1.9 ± 0.1
GMMA 5%[a]	2.0 ± 0.2
No FM- Pentanol	2.5 ± 0.3
HEMA 2.5%[a]	2.5 ± 0.2
HEMA 5%[a]	2.1 ± 0.1

3.4. Conclusions

In this chapter, the effect of grafting of the PUs into the poly(meth)acrylics on the characteristic of the hybrid dispersions, polymer microstructure, morphology and performance of the hybrid films was studied. For that aim, solvent-free and emulsifier-free PU/acrylic hybrid dispersions were synthesized using different types and concentrations of functional monomers (glycerol mono-methacrylate (GMMA) and hydroxyethyl methacrylate (HEMA)). For comparison purposes additional reactions were carried out in the absence of the functional monomers using either butanediol or pentanol to replace GMMA and HEMA respectively.

It was observed that the type of the functional monomer influenced the PU microstructure because GMMA is a diol that extends the PU chains, whereas HEMA is monofunctional alcohol that rather terminates the PU chains. Therefore, the PUs synthesized with GMMA had higher molar mass and hence higher number of grafting point per PU chain than those with HEMA. As a result, at low concentration of HEMA (2.5%), no gel was obtained whereas the gel content of the hybrid with 2.5% GMMA was 67% and at higher concentration of functional monomer (5%) the gel content was higher for GMMA than for HEMA, indicating that for the hybrid with HEMA the grafting was less efficient and the polymer network was less crosslinked. The absolute molar mass distribution of the whole polymers (gel+sol) showed mainly two populations of polymer chains, one at lower molar masses that corresponds to the non grafted PU and other at high molar masses which is attributed to the grafted PU/poly(methacrylates). With grafting, the fraction of low molar mass PU decreased and the high molar mass chains shifted to higher values indicating network formation.

The TEM images of grafted PU/(meth)acrylic particles and film cross-section showed more homogeneous particle and film morphologies compared to the non-grafted hybrids indicating less phase separation due to the grafting. However, this effect was less pronounced for HEMA 2.5% as the grafting was not efficient.

Despite the high grafting efficiency and the difference in the polymer microstructure, grafting with GMMA did not show the expected mechanical reinforcement. The hybrid with no GMMA (only butanediol) showed strain-hardening behavior likely due to the hydrogen bonding among the PU chains that act as physical crosslinker. The PU determines the properties of the polymer film as it presents in the continuous phase in the polymer film. Grafting-crosslinking between PU and poly(MMA-BA) provided additional stiffness to the film, but the increase was modest perhaps due to the loss of some hydrogen bonds among the PU chains that resulted from the interpenetration with the poly(meth)acrylates. In the alternative case, with grafting using HEMA the mechanical reinforcement due to grafting was more obvious. In this case, the low molar mass PU chains that were not grafted acted as plasticizer and with grafting, the incorporation of these chains led to an improvement in the mechanical properties. The water sensitivity of the hybrids substantially decreased with grafting likely due to the increased grafting density that reduced the potential of the hybrid films to absorb water. This is an important achievement for coatings application of the hybrids, which due to high content of COOH containing PUs have high water absorption capability.

3.5. References

[1] M. Hirose, F. Kadowaki, J. Zhou, The structure and properties of core-shell type acrylic-polyurethane hybrid aqueous emulsions, Prog. Org. Coatings. 31 (1997) 157–169.

[2] J.I. Amalvy, A kinetic study in emulsion polymerization of polyurethane-acrylate hybrids, Pigment Resin Technol. 31 (2002) 275–283.

[3] A.C. Aznar, O.R. Pardini, J.I. Amalvy, Glossy topcoat exterior paint formulations using water-based polyurethane/acrylic hybrid binders, Prog. Org. Coatings. 55 (2006) 43–49.

[4] M. Li, E.S. Daniels, V. Dimonie, E.D. Sudol, M.S. El-Aasser, Preparation of Polyurethane/Acrylic Hybrid Nanoparticles via a Miniemulsion Polymerization Process, Macromolecules. 38 (2005) 4183–4192.

[5] A. Lopez, Y. Reyes, E. Degrandi-Contraires, E. Canetta, C. Creton, J.L. Keddie, J.M. Asua, Simultaneous free-radical and addition miniemulsion polymerization: Effect of the chain transfer agent on the microstructure of polyurethane-acrylic pressure-sensitive adhesives, Macromol. Mater. Eng. 298 (2013) 53–66.

[6] A. Lopez, E. Degrandi, E. Canetta, J.L. Keddie, C. Creton, J.M. Asua, Simultaneous free radical and addition miniemulsion polymerization: Effect of the diol on the microstructure of polyurethane-acrylic pressure-sensitive adhesives, Polymer (Guildf). 52 (2011) 3021–3030.

[7] E. Degrandi-Contraires, A. Lopez, Y. Reyes, J.M. Asua, C. Creton, High-shear-strength waterborne polyurethane/acrylic soft adhesives, Macromol. Mater. Eng. 298 (2013) 612–623.

[8] R. Udagama, E. Degrandi-Contraires, C. Creton, C. Graillat, T.F.L. McKenna, E. Bourgeat-Lami, Synthesis of acrylic-polyurethane hybrid latexes by miniemulsion polymerization and their pressure-sensitive adhesive applications, Macromolecules. 44 (2011) 2632–2642.

[9] E. Degrandi-Contraires, R. Udagama, E. Bourgeat-Lami, T. McKenna, K. Ouzineb, C. Creton, Mechanical properties of adhesive films obtained from PU-acrylic hybrid particles, Macromolecules. 44 (2011) 2643–2652.

[10] R. Shi, X. Zhang, J. Dai, Synthesis of TDI-Polyurethane/Polyacrylate Composite Emulsion by Solvent-free Method and Performances of the Latex Film, J. Macromol.

Sci. Part A. 50 (2013) 350–357.

[11] L. Zhao, S.N. Sauca, C. Berges, Aqueous polyurethane acrylate hybrid dispersions, EP 3067399 A1, 2016.

[12] R. Ballestero, B.M. Sundaram, H. V. Tippur, M.L. Auad, Sequential graft-interpenetrating polymer networks based on polyurethane and acrylic/ester copolymers, Express Polym. Lett. 10 (2016) 204–215.

[13] H.T. Zhang, R. Guan, Z.H. Yin, L.L. Lin, Soap-free seeded emulsion copolymerization of MMA onto PU-A and their properties, J. Appl. Polym. Sci. 82 (2001) 941–947.

[14] M. Hirose, J. Zhou, K. Nagai, Structure and properties of acrylic-polyurethane hybrid emulsions, Prog. Org. Coatings. 38 (2000) 27–34.

[15] C. Hepburn, Polyurethane Elastomers, Springer Netherlands, Dordrecht, 1992.

[16] S. Mehravar, N. Ballard, A. Agirre, R. Tomovska, J.M. Asua, Relating polymer microstructure to adhesive performance in blends of hybrid polyurethane/acrylic latexes, Eur. Polym. J. 87 (2017) 300–307.

[17] V. Daniloska, P. Carretero, R. Tomovska, J.M. Asua, High performance pressure sensitive adhesives by miniemulsion photopolymerization in a continuous tubular reactor, Polymer (Guildf). 55 (2014) 5050–5056.

[18] V. Daniloska, P. Carretero, R. Tomovska, M. Paulis, J.M. Asua, High-performance adhesives resulting from spontaneous formation of nanogels within miniemulsion particles, ACS Appl. Mater. Interfaces. 6 (2014) 3559–3567.

[19] E. Mehravar, M.A. Gross, A. Agirre, B. Reck, J.R. Leiza, J.M. Asua, Importance of film morphology on the performance of thermo-responsive waterborne pressure sensitive adhesives, Eur. Polym. J. 98 (2018) 63–71.

[20] C. Tian, Q. Zhou, L. Cao, Z. Su, X. Chen, Effect of polyurethane molecular weight on the properties of polyurethane-poly(butyl methacrylate) hybrid latex prepared by miniemulsion polymerization, J. Appl. Polym. Sci. 21 (2011) n/a-n/a.

[21] M. Vatankhah-Varnosfaderani, W.F.M. Daniel, M.H. Everhart, A.A. Pandya, H. Liang, K. Matyjaszewski, A. V. Dobrynin, S.S. Sheiko, Mimicking biological stress–strain behaviour with synthetic elastomers, Nature. 549 (2017) 497–501.

Chapter 4. Modification of polymer microstructure of PU/(meth)acrylic hybrids by altering polyol type

4.1. Introduction

In Chapter 1 it was shown that the composition of PU chains is an important parameter determining final properties of the PU/acrylic hybrids. The PU composition may be varied over a wide range due to the number of different constituents used for the PU synthesis. In Chapter 2 it was demonstrated that the concentration of carboxylic groups and the type of chain extender influence significantly both the colloidal stability and final properties. As the polyol forms the soft segment of the PU chains, the type of polyol may be an important tool for controlling the properties. Polyols or macrodiols are often high molecular weight (typically 1000-2000 g/mol) polyethers, polyesters or polycarbonates. As was discussed in Chapter 1 (Section 1.2.2.2), the influence of the type of polyol and its molar mass on the characteristics of polyurethane dispersions (PUDs) have been studied extensively [1–15] and the polyol type can be chosen depending on the potential application. For example it is know that polyesters convey good mechanical properties [16,17] and polyethers provide flexibility for polymer films [1,4]. Despite the possible strong effect of polyol type on PUDs properties, this effect has not been studied in case of PU/(meth)acrylic hybrid films.

This chapter focuses on the understanding of the effect of the polyol type on the characteristics and properties of the PU/(meth)acrylic hybrids. Different types of polyols (polypropylene glycol (PPG), polytetrahydrofuran (PTHF), polyester and polycarbonate (PCD)) all of them with M_n of about 2000 g/mol were used in PU synthesis, expecting that each of them will convey different properties to the soft segment of the PU/(meth)acrylic hybrids.

Figure 4.1 presents the structure of polyols used in the PU synthesis. As in Chapter 3 it was shown that grafting between the PU and the poly(methacrylates) strongly affect properties, for each polyol, two experiments were performed, one without grafting between the PU and (meth)acrylics and the other promoting grafting by using glycerol mono methacrylate (GMMA). 2.5 mol% GMMA (based on mol of isophorone diisocyanate (IPDI)) was used in the formulation because this amount was enough to obtain an efficient grafting between PU and (meth)acrylics (as shown in Chapter 3).

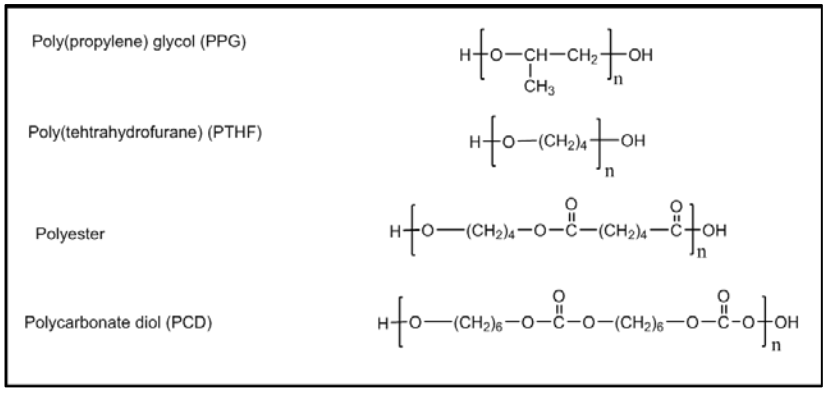

Figure 4.1. Different polyol types used in PU synthesis

4.2. Experimental

4.2.1 Materials

The materials are given in Appendix I.

4.2.2 Synthesis procedures

The synthesis of the PU prepolymer was performed in a 250 mL glass reactor fitted with a reflux condenser, a sampling device (and feeding inlet), a nitrogen inlet, a thermometer and a flat blade turbine stirrer. The temperature of the reaction was controlled by an automatic control system, Camile TG (Biotage). The formulations are presented in Table 4.1. To synthesize the prepolymer, dimethylol propionic acid (DMPA), polyol, isophorone diisocyanate (IPDI, 7.73 g), dibutyltin dilaurate (DBTDL) (0.05 g) and one part of the (meth)acrylic monomers (50 wt% of a mixture of methyl methacrylate (MMA)/ and butyl acrylate (BA), 1/1 by weight) were charged into the reactor. The reaction mixture was brought to 70°C under agitation (250 rpm) and held for 4-5 hours. It is worth mentioning that the technical (meth)acrylic monomers were not purified and therefore the contained inhibitor avoided any radical reaction during the PU synthesis. The free NCO at the end of the reaction was checked with amine-back titration [18]. Then, the mixture of butanediol (BDO) / Glycerol mono methacrylate (GMMA) dissolved in (meth)acrylic monomers (20 wt% of the MMA/BA 1/1 wt/wt) was added to the prepolymer to functionalize the PU chains. BDO was added with the functional monomer as short chain diol in order to keep the NCO/OH similar value and hence to use a fixed amount of chain extender in the case of grafted and non grafted hybrids. After 2 hours, the mixture was cooled to 25°C and additional monomer (15 wt% of the

MMA/BA 1/1 wt/wt) was added to reduce the viscosity. After that, triethylamine (TEA) dissolved in monomers (10 wt% of the MMA/BA 1/1 wt/wt) was added and kept at 25°C for 45 min in order to neutralize the carboxylic groups of DMPA.

Then, the PU/(meth)acrylic solution was dispersed in water. To prepare the aqueous dispersions, the reactor was charged with double deionized water under nitrogen at 25°C and the prepolymer-monomer mixture was added in 15 min under high agitation (750 rpm). After that, the chain extender (diaminododecane, DAD) dissolved in monomers (5 wt% of the MMA/BA 1/1 wt/wt) was added in the reactor and left to react one hour at 70°C. The theoretical molar ratio of NCO/OH (defined as a molar ratio of IPDI and sum of molar ratio of polyol, DMPA, BDO, GMMA and DAD) was 1.8 before chain extension, 1.6 for the functionalized prepolymer and 1.0 after chain extension.

The free radical polymerization of (meth)acrylic monomers was performed at 70°C by adding a shot of potassium persulfate (KPS, 0.5 wt% based on monomer) dissolved in water. The polymerization was performed in batch for 2 hours and a final conversion of (meth)acrylic monomers higher than 95% was achieved in all the cases. The resulting hybrid latexes had a 40% solids content.

Table 4.1. Recipe used to synthesize PU/(meth)acrylic (50/50 wt/wt) hybrids using different polyol type with constant amount of IPDI (7.73 g), DBTDL catalyst (0.05 g), water (71 g) and KPS (0.12 g)

Polyol	Experiment	Polyol	DMPA[a]	BDO	GMMA	TEA[b]	DAD	MMA/*n*BA (1/1 wt/wt) (g/g)
		(mols per 1 mol of IPDI)						
PPG	**No grafting**	0.19	0.37	0.07	0	0.39	0.37	12/12
	Grafted	0.19	0.37	0.045	0.025	0.39	0.37	12/12
PTHF	**No grafting**	0.19	0.37	0.07	0	0.39	0.37	12/12
	Grafted	0.19	0.37	0.045	0.025	0.39	0.37	12/12
Polyester	**No grafting**	0.19	0.37	0.07	0	0.39	0.37	12/12
	Grafted	0.19	0.37	0.045	0.025	0.39	0.37	12/12
PCD	**No grafting**	0.19	0.37	0.07	0	0.39	0.37	12/12
	Grafted	0.19	0.37	0.045	0.025	0.39	0.37	12/12

a) 3.5 wt% based on organic phase
b) 1.05 mol of DMPA

4.2.3. Characterization

Final particle sizes of the latexes were measured by dynamic light scattering (DLS). The unreacted NCO was determined by titration. The conversion of (meth)acrylic monomers was measured gravimetrically. The gel fraction was measured by Soxhlet extraction, using tetrahydrofuran (THF) as the solvent. The molar mass distribution of the soluble fraction of polymers was determined by size exclusion chromatography (SEC/RI/UV). The thermal characterization of the hybrids was carried out by differential scanning calorimetry (DSC). The morphologies of latex particles and films were studied by means of transmission electron microscopy (TEM). The mechanical properties of the films were measured by tensile tests. The water sensitivity of the polymer films was analyzed by contact angle measurement and liquid water uptake test. A detailed description of the characterization methods is provided in Appendix I.

4.3. Results and Discussion

4.3.1. Polymer Microstructure

The characteristics of PU/(meth)acrylic hybrids obtained with PU based on different polyols are presented in Table 4.2. The final particle sizes were in the range of 90-150 nm. The hybrids containing PPG had slightly higher particle size than the others probably due to its lower polarity and higher hydrophobicity. No gel was observed in the absence of GMMA, whereas with GMMA the gel content was between 66% and 72% for all the cases. This demonstrates that the type of polyol does not influence the extent of grafting reaction. Figure 4.2 presents the SEC molar mass distribution of the soluble part. The soluble part of the polymers showed bimodal molar mass distribution for the hybrids with no functional monomer (Figure 4.2). The population of polymer chains at high molar mass mainly corresponded to (meth)acrylics and the one at low molar mass was attributed to the PU chains. On the other hand, the soluble fraction of the grafted hybrids showed a broad distribution with a final tail. The comparison of the grafted and non grafted hybrids shows that the high molar mass (meth)acrylate polymer chains are incorporated into the gel fraction with grafting. This is because when the long (meth)acrylic chains graft into the PU chains, they often form a network whereas in the case of short (meth)acrylics that graft into PUs they may propagate and the networking may not be enough to form a gel (Scheme 4.1).

The DSC analysis showed two glass transition temperatures (T_gs) for all the samples, one at low temperature that corresponds to PU and depend on the polyol type (around -55 °C for PPG and PTHF polyols,-28 °C for polyester polyol, and -36 °C for PCD polyol) and the second T_g at around 25 °C which, corresponds to the MMA/BA copolymer obtained in a batch

system. It is worth pointing out that in batch polymerization due to the difference in the reactivity ratios of MMA and BA, some PMMA rich chains with higher T_g are expected to be formed at the beginning of the process. The two T_gs were slightly shifted toward each other for the grafted samples showing more compatibility and interpenetration of PU and acrylic polymer chains. No evidence of crystallinity was observed, likely due to the low ordering of polyols in the hybrids.

Table 4.2. The characteristics of PU/(meth) hybrids obtained with different polyol type PUs

Polyol	Experiment	Particle Size (nm)	T_g (°C)		Gel Content (%)	Sol $\overline{Mw}$ *(Kg/mol)	
			T_g1 (°C)	T_g2 (°C)		Low M_w	High M_w
PPG	**No grafting**	145	-56	32	0	36	1019
	Grafted	135	-54	27	67 ± 2	30	-
PTHF	**No grafting**	108	-54	26	0	39	1098
	Grafted	129	-53	26	72 ± 3	44	-
Polyester	**No grafting**	90	-28	26	0	36	1188
	Grafted	101	-26	25	66 ± 3	41	-
PCD	**No grafting**	123	-36	25	0	37	1103
	Grafted	109	-32	24	66 ± 2	32	-

* bimodal sol $\overline{Mw}$ contain both low molar mass non grafted PU chains and high molar mass (meth)acrylic chains

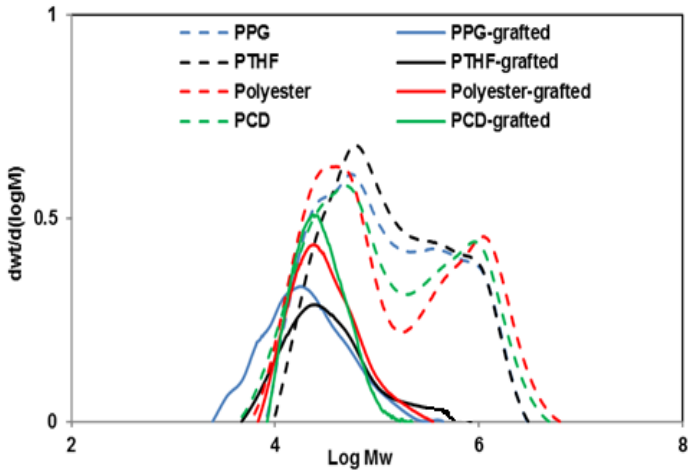

Figure 5.2. Molar mass distribution of soluble fraction in PU/(meth)acrylic hybrids with different with different polyol based PUs obtained by SEC (the curves are normalized based on the soluble fraction)

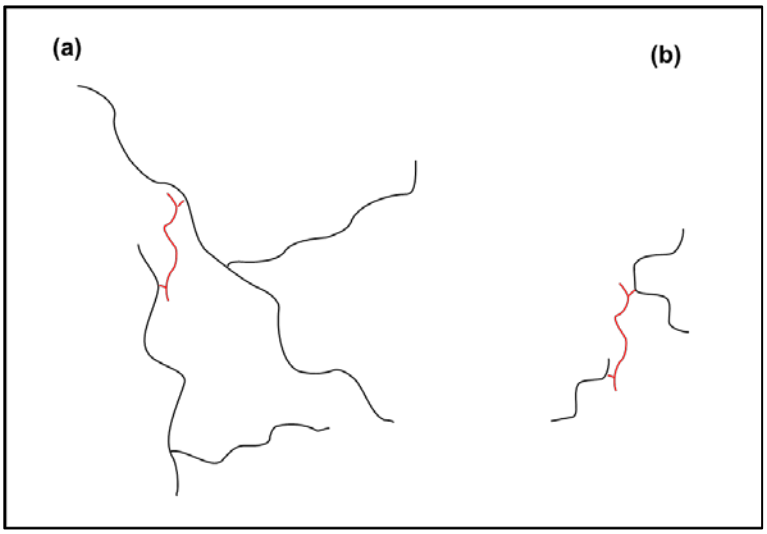

Scheme 4.1. Structure of grafted PU/acrylic hybrid in the long chain (meth)acrylics (a), and in the short chain (meth)acrylics (b) (PUs= red , Acrylics=black)

4.3.2. Particle and Film Morphology

The TEM images of the hybrid latexes and the film cross-sections containing PPG, PTHF, polyester and PCD PUs are shown in Figures 4.3 to 4.6, respectively. The TEM images of the particles with no functional monomer showed a core-shell morphology in all the cases (Figures 4.3(a)-left to 4.6(a)-left) with the acrylics in the core and PU in the shell. With addition of GMMA (Figures 4.3(b)-left to 4.6(b)-left) the particles were more homogeneous with gradual change of color along the radius. It is worth pointing out that in the case of grafted particles, the homogeneity is likely higher than what is suggested by the color change because due to the spherical shape of the particles the thickness of the polymer that the electron beams has to pass through decrease along the radius. The higher homogeneity is likely due to the presence of grafted PU/(meth)acrylic chains that improved the compatibility between PUs and acrylics.

The TEM of the film cross-section for non-grafted hybrids (Figures 4.3(a)-right to 4.6(a)-right) showed that the dark spherical domains (acrylics) were dispersed within the bright continuous phase (PU) in all the cases. On the other hand, smaller and less defined dark domains (acrylics) were observed in the case of grafted hybrids (Figures 4.3(b)-right to 4.6(b)-right) indicating less phase separation due to the grafting.

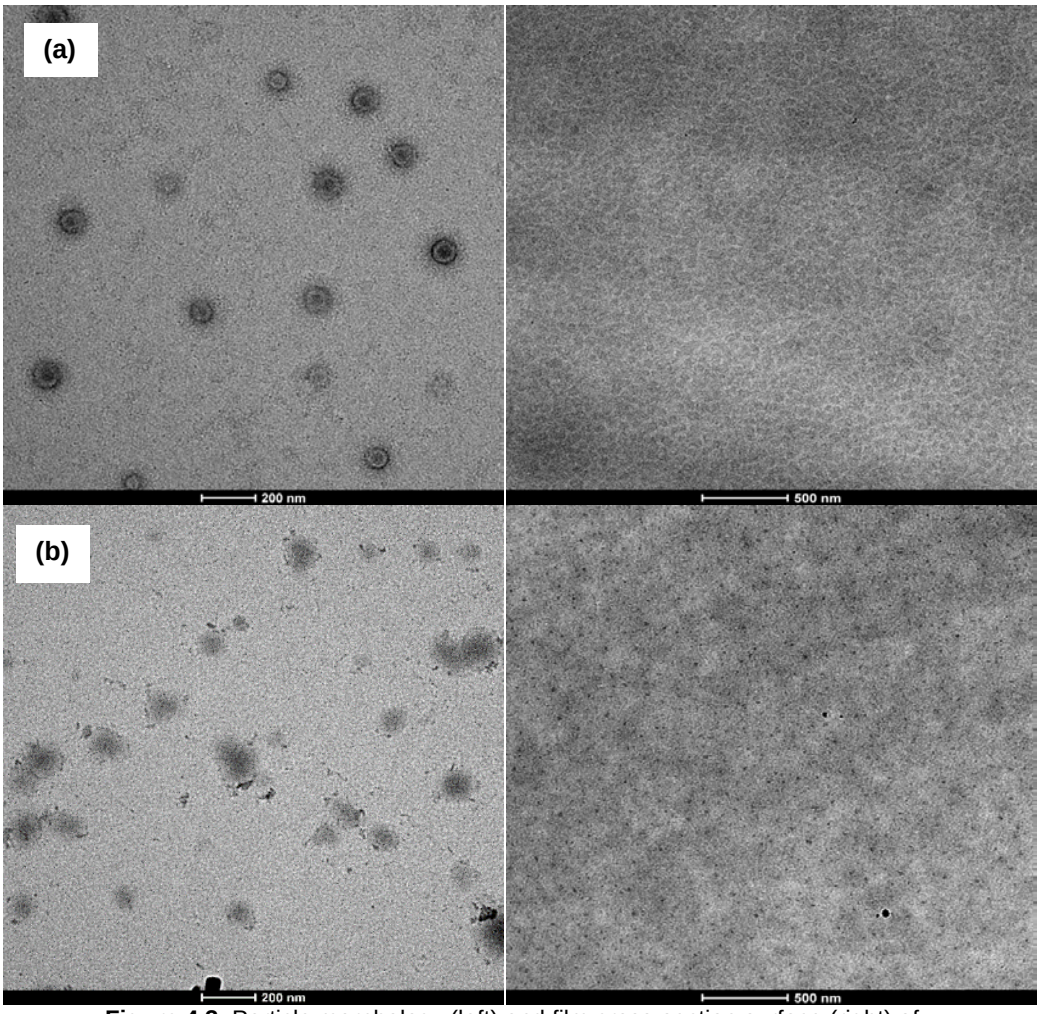

Figure 4.3. Particle morphology (left) and film cross-section surface (right) of PU/(meth)acrylic hybrid obtained with PPG based PUs, No grafting (a), Grafted (b)

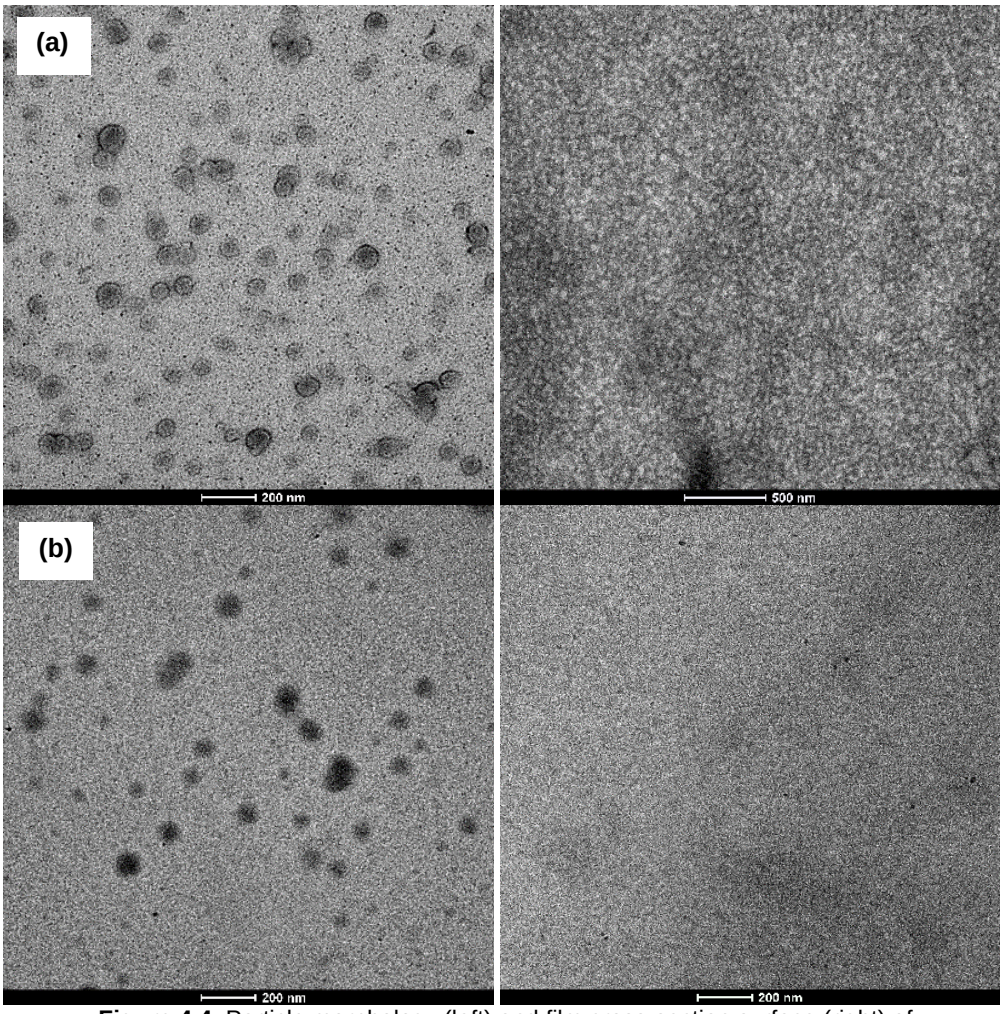

Figure 4.4. Particle morphology (left) and film cross-section surface (right) of PU/(meth)acrylic hybrid obtained with PTHF based PUs, No grafting (a), Grafted (b)

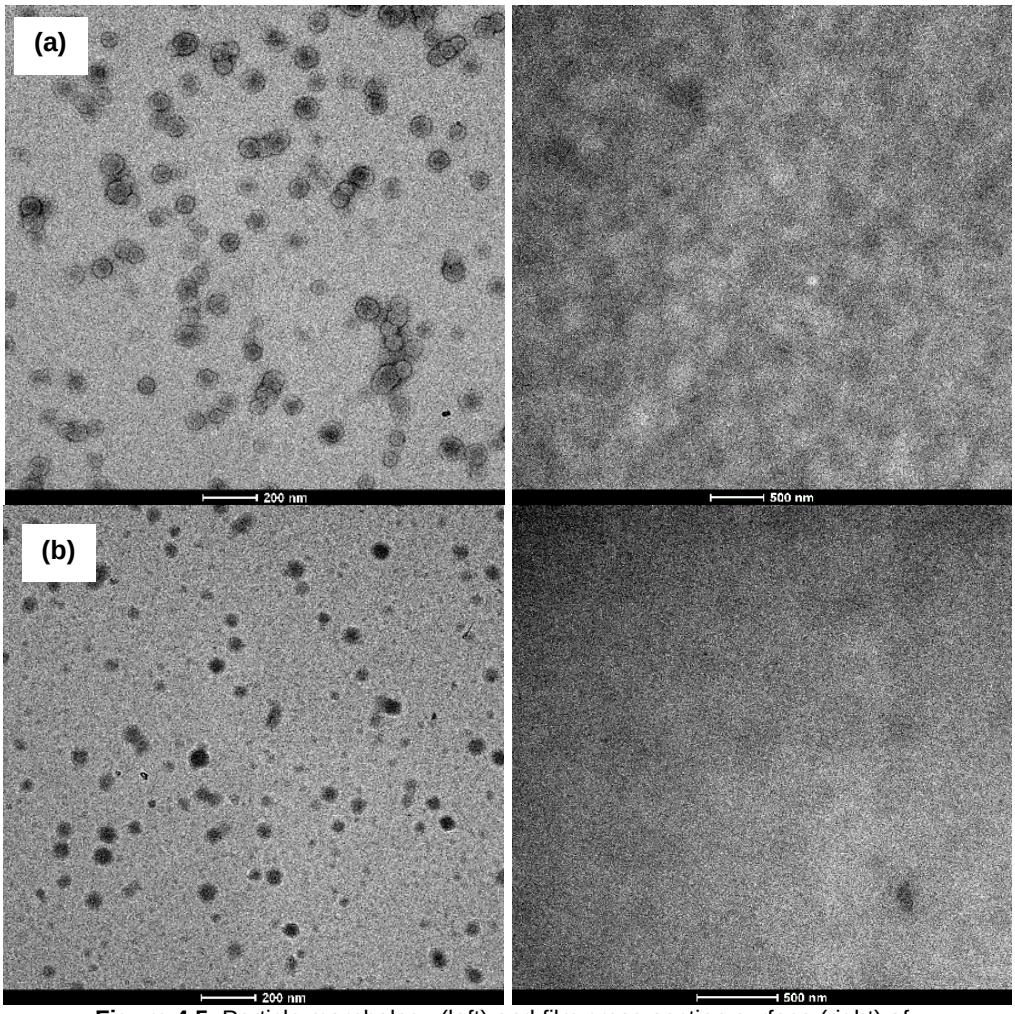

Figure 4.5. Particle morphology (left) and film cross-section surface (right) of PU/(meth)acrylic hybrid obtained with polyester based PUs, No grafting (a), Grafted (b)

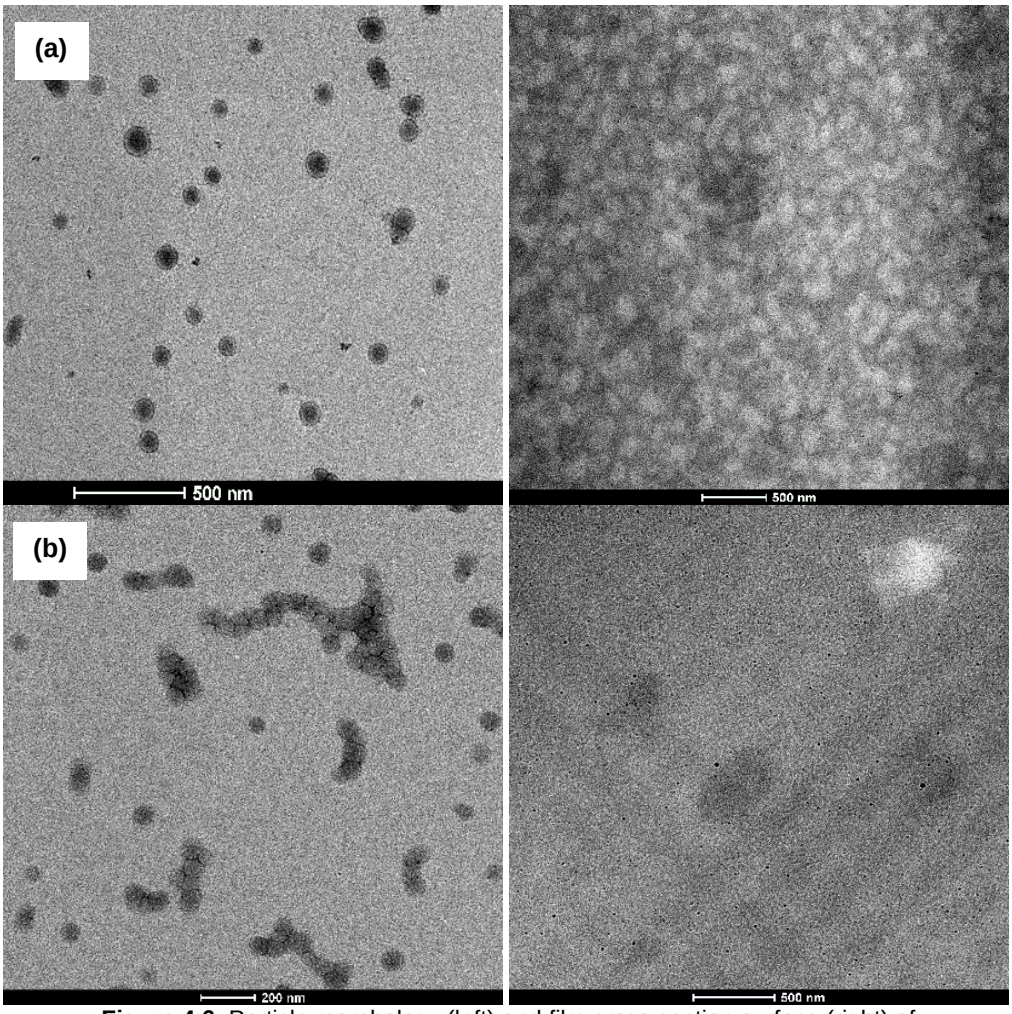

Figure 4.6. Particle morphology (left) and film cross-section surface (right) of PU/(meth)acrylic hybrid obtained with PCD based PUs, No grafting (a), Grafted (b)

4.3.3. Mechanical properties

The stress-strain behavior of the PU/(meth)acrylic polymer films cast at ambient temperature is shown in Figure 4.7. The mechanical properties obtained from these experiments are summarized in Table 4.3. Figure 4.7 indicates that the hybrid polymer

containing PPG based PUs was the softest polymer film with the lowest Young´s modulus and lowest extend of strain hardening. Comparing the hybrid films with PPG and PTHF, the presence of the methyl side groups in PPG hinder the polymer chains aligning for hydrogen-bond formation and therefore the obtained film derived from PTHF had higher Young´s modulus and yield stress and interestingly higher elongation at break compared to the film derived from PPG based PU. This is in agreement with the work of Hourston *et al*. [11] for pure PUs who reported that PTHF-based PUD resulted in a tough material, while maintaining a high degree of elasticity. In the polymer films containing polyester and PCD, the polarity of the ester carbonyl group leads to stronger hydrogen bonds than polyethers [17,16]. Therefore the films derived from polyester and PCD based PUs had higher Young´s modulus and yield stress and a higher extend of strain hardening than the films containing PTHF and PPG. Finally the film containing PCD had even higher Young´s modulus, yield stress and higher extend of strain hardening than those with polyester probably due to the higher hydrogen bonding between hard and soft segment in the PU containing PCD.

The stress-strain behavior of the grafted PPG, polyester and PCD based hybrid films showed a slight improvement in Young´s modulus, yield stress and strain hardening behavior with respect to the non-grafted hybrids and the grafting led to decrease in the elongation at break. This effect was slightly stronger for PTHF based PUs. The weak effect of grafting on the mechanical properties in spite of the observed high gel content (Table 4.2) is surprising. It is remarkable that even the hybrid synthesized using butanediol instead of GMMA, and therefore devoid of crosslinking points, presented strain-hardening, a characteristic that is typical of crosslinked polymers. As it was discussed in Chapter 3, this behavior may be due to hydrogen bonding among PU chains that formed a physical network. As the PU was the

continuous phase in the polymer film (Figures 4.3(a)-right to 4.6(a)-right) it determined the properties of the film. Grafting-crosslinking between PU and poly(MMA-BA) provides additional stiffness to the film, but the increase is modest perhaps due to the loss of some hydrogen bonds among the PU chains that results from the interpenetration with the poly(meth)acrylates. The increase in stiffness results in the increase in Young´s modulus and decrease in the elongation at break.

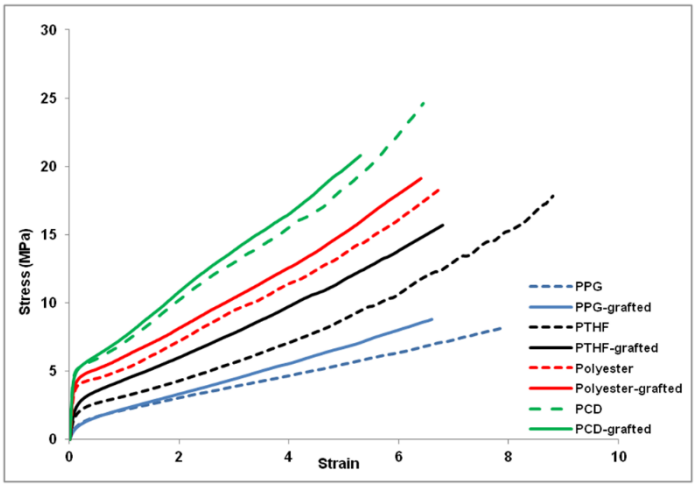

Figure 4.7. Stress-strain behavior of the grafted and non grafted PU/(meth)acrylic polymer films obtained with different polyol based PUs

Table 4.3. Mechanical properties of the PU/acrylic polymer films obtained with different polyol based PUs

Polyol	Experiment	Young´s Modulus MPa/100	Yield Stress (MPa)	Elongation at break	Ultimate Strength (MPa)	Toughness (MPa)
PPG	**No grafting**	0.08 ± 0.02	1.45 ± 0.08	7.9 ± 0.3	8.2 ± 0.3	36.8 ± 2.1
	Grafted	0.10 ± 0.01	1.50 ± 0.07	7.0 ± 0.2	7.9 ± 0.3	32.0 ± 1.8
PTHF	**No grafting**	0.13 ± 0.01	2.28 ± 0.09	8.8 ± 0.5	17.8 ± 0.4	74.3 ± 2.6
	Grafted	0.32 ± 0.02	3.07 ± 0.10	6.8 ± 0.3	15.7 ± 0.3	59.5 ± 2.2
Polyester	**No grafting**	0.57 ± 0.02	4.23 ± 0.05	6.8 ± 0.4	18.5 ± 0.4	70.4 ± 2.5
	Grafted	0.59 ± 0.02	4.57 ± 0.09	6.4 ± 0.2	19.1 ± 0.5	70.6 ± 2.8
PCD	**No grafting**	1.03 ± 0.03	5.34 ± 0.05	6.4 ± 0.2	24.6 ± 0.6	87.9 ± 3.2
	Grafted	1.06 ± 0.04	5.34 ± 0.05	5.3 ± 0.1	20.8 ± 0.5	66.9 ± 2.9

4.3.4. Water sensitivity

The water sensitivity of the polymer films was studied by means of the static contact angle and liquid water uptake test.

Static contact angle measurement

The water static contact angles of the air-film interface before and after rinsing with water are shown in Table 4.4. The static contact angle values were around 70º for all the hybrids containing different polyol type showing that the type of the polyol and also the grafting did not influence the hydrophobicity of the hybrid film interface. Moreover, the contact angle did not change after rinsing with water indicating that there was no significant migration of additional stabilizing chains to the air-film interface as it is the case for conventional surfactants [19] and that some DMPA units were already at the surface and they do not move because they are chemically bonded.

Table 4.4. Static contact angle to air-film interface for the polymer films obtained with different polyol based PUs

Polyol	Experiment	Contact angle (°)	Contact angle of rinsed film (°)
PPG	**No grafting**	71 ± 2	72 ± 3
	Grafted	70 ± 2	72 ± 3
PTHF	**No grafting**	69 ± 3	69 ± 2
	Grafted	70 ± 3	71 ± 3
Polyester	**No grafting**	69 ± 3	69 ± 3
	Grafted	67 ± 2	71 ± 3
PCD	**No grafting**	70 ± 2	72 ± 3
	Grafted	69 ± 3	70 ± 2

Liquid water uptake test

The water uptake of the films obtained with different polyols are shown in Figure 4.8. As can be seen, the hybrids containing PPG and PTHF absorbed the highest amount of water during the test, whereas the ones containing polyester and PCD absorbed lower amount of water. The polymer films of PPG and PTHF became white after 1 day of immersion in water (as an example, the PPG based PUs film is shown in Figure 4.9-right), while the ones with polyester and PCD did not change the aspect and remained transparent until 3 days in water (as an example, the PCD based PUs film is shown in Figure 4.9-left) although whitening started after 3 days. It is worth mentioning that all the cast polymer films were transparent before the water uptake test. This behavior was the same for both grafted and non-grafted samples, indicating that this behavior is related more with the chemical nature of the polyols. The comparison of tensile test result (Figure 4.7) and water uptake measurement (Figure 4.8) clearly shows that the higher mechanical property (especially in terms of hardness) resulted in the lower water uptake. This was due to a slower diffusion of water through the film (mainly determining the initial shape of the curve) as well as to a lower absorption capability (responsible for the plateau). In addition to that, the lower water uptake of the hybrids with PCD and polyester based PU can be related to the stronger hydrogen bonding [20] between the carbonyl group of the polyol (PCD or polyester) in the PU chains and the NH group of urethane that makes the water swelling more difficult. In contrast to these results, Rahman *et al.*[1] for pure PU reported that the water swelling of polyester type PU film was higher than polyether ones. Therefore it seems that in our system, the presence of (meth)acrylics somehow compensated the more hydrophilic characteristics of the ester groups in the hybrids containing polyester and PCD polyols.

Figure 4.8 also shows that with grafting the liquid water uptake decreased and reached a plateau in all the cases, likely due to the crosslinking which inhibits swelling to a certain extent (as it was discussed in Chapter 3). Table 4.5 presents the amount of polymer film dissolved in water during the test (as difference in weight before and after water uptake experiments). As can be seen the amount of water soluble species was in the same range for all the films, however this value was slightly higher for the films containing PPG.

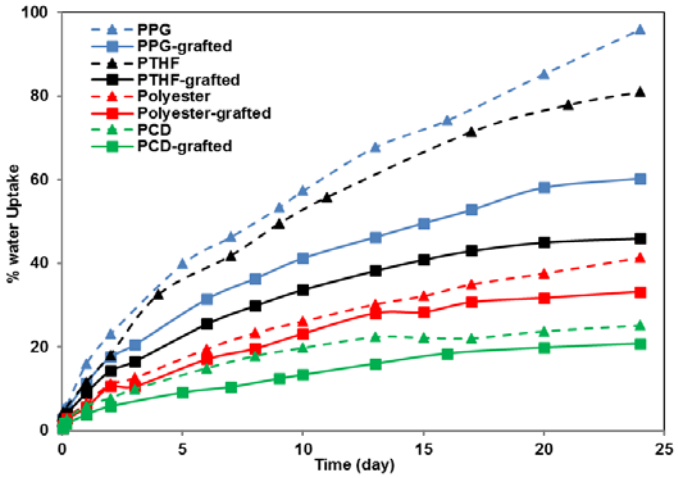

Figure 4.8. The liquid water uptake measurement of the grafted and non grafted PU/(meth)acrylic polymer films with different polyol based PUs

Figure 4.9. Polymer film of non-grafted PCD based (left) and PPG based (right) immersed one day in water

Table 4.5. Amount of polymer dissolved in the water during the water uptake test

polyol	Experiment	Polymer weight loss after drying (%)
PPG	**No grafting**	2.3 ± 0.2
	Grafted	2.3 ± 0.1
PTHF	**No grafting**	2.1 ± 0.2
	Grafted	1.8 ± 0.3
Polyester	**No grafting**	1.6 ± 0.3
	Grafted	1.7 ± 0.2
PCD	**No grafting**	1.6 ± 0.1
	Grafted	1.5 ± 0.2

4.4. Conclusions

The effect of polyol type on the properties of PU/acrylic hybrids was studied in this chapter. Polypropylene glycol (PPG), polytetrahydrofuran (PTHF), polyester and polycarbonate (PCD) with M_n of 2000 g/mol were used in the PU synthesis. Moreover for each polyol type, grafted PU/(meth)acrylic hybrids were synthesized using GMMA.

No gel was observed in the absence of GMMA and around 70% gel was obtained when GMMA was used. The type of polyol did not affect the gel content in the grafted hybrids. For all polyols, the TEM images of grafted PU/(meth)acrylic particles and film cross-section showed more homogeneous particle and film morphologies compared to the non-grafted hybrids indicating less phase separation due to the grafting. The Young´s modulus and yield stress of the hybrid polymer obtained from different polyol type was in the following order: PCD > polyester > PTHF > PPG. This was attributed to the presence of carbonyl groups in PCD and polyester polyols that resulted in higher H-bonding and therefore harder polymer films. In the case of grafted hybrids, only a small improvement in the mechanical properties

was observed. Due to the hydrogen bonding among the PU chains that act as physical crosslinker, the hybrid with no GMMA (only butanediol) showed strain-hardening behavior likely. With grafting between PU and poly(MMA-BA) additional stiffness was provided to the film, but the increase was modest perhaps due to the loss of some hydrogen bonds among the PU chains that resulted from the interpenetration with the poly(meth)acrylates. Moreover, It was observed that the harder polymer films resulted in lower water uptake (higher water resistance) as the water absorption is more difficult in the harder polymer films. Moreover, grafting improved the water sensitivity of the polymer films because of the crosslinking of PU and (meth)acrylics that decreased the extend of swelling. In summary, it can be concluded that the type of the polyol leads toward the development of a range of different hybrids and it is an additional tool for controlling of final properties of the hybrids. Using PCD and polyester polyols, PU/(meth)acrylic polymer film with higher mechanical properties and better water resistance can be obtained. Whereas PPG and PTHF polyols provide softer polymer films with higher elongation.

4.5. References

[1] M.M. Rahman, H.-D. Kim, Characterization of waterborne polyurethane adhesives containing different soft segments, J. Adhes. Sci. Technol. 21 (2007) 81–96.

[2] N. Akram, R.S. Gurney, M. Zuber, M. Ishaq, J.L. Keddie, Influence of Polyol Molecular Weight and Type on the Tack and Peel Properties of Waterborne Polyurethane Pressure-Sensitive Adhesives, Macromol. React. Eng. 7 (2013) 493–503.

[3] F. Mumtaz, M. Zuber, K.M. Zia, T. Jamil, R. Hussain, Synthesis and properties of aqueous polyurethane dispersions: Influence of molecular weight of polyethylene glycol, Korean J. Chem. Eng. 30 (2013) 2259–2263.

[4] G. Gündüz, R.R. Kısakürek, Structure–Property Study of Waterborne Polyurethane

Coatings with Different Hydrophilic Contents and Polyols, J. Dispers. Sci. Technol. 25 (2004) 217–228.

[5] A. Eceiza, M.D. Martin, K. De La Caba, G. Kortaberria, N. Gabilondo, M.A. Corcuera, I. Mondragon, Thermoplastic polyurethane elastomers based on polycarbonate diols with different soft segment molecular weight and chemical structure: Mechanical and thermal properties, Polym. Eng. Sci. 48 (2008) 297–306.

[6] Y.M. Lee, J.C. Lee, B.K. Kim, Effect of soft segment length on the properties of polyurethane anionomer dispersion, Polymer (Guildf). 35 (1994) 1095–1099.

[7] V. García-Pacios, J.A. Jofre-Reche, V. Costa, M. Colera, J.M. Martín-Martínez, Coatings prepared from waterborne polyurethane dispersions obtained with polycarbonates of 1,6-hexanediol of different molecular weights, Prog. Org. Coatings. 76 (2013) 1484–1493.

[8] J. Kloss, M. Munaro, G.P. De Souza, J.V. Gulmine, S.H. Wang, S. Zawadzki, L. Akcelrud, Poly(ester urethane)s with polycaprolactone soft segments: A morphological study, J. Polym. Sci. Part A Polym. Chem. 40 (2002) 4117–4130.

[9] M. Rogulska, A. Kultys, S. Pikus, Studies on thermoplastic polyurethanes based on new diphenylethane-derivative diols. III. The effect of molecular weight and structure of soft segment on some properties of segmented polyurethanes, J. Appl. Polym. Sci. 110 (2008) 1677–1689.

[10] K. Gisselfält, B. Helgee, Effect of soft segment length and chain extender structure on phase separation and morphology in poly(urethane urea)s, Macromol. Mater. Eng. 288 (2003) 265–271.

[11] D.J. Hourston, G. Williams, R. Satguru, J.D. Padget, D. Pears, Structure-property study of polyurethane anionomers based on various polyols and diisocyanates, J. Appl. Polym. Sci. 66 (1997) 2035–2044.

[12] D.-K. Lee, H.-B. Tsai, R.-S. Tsai, Effect of composition on aqueous polyurethane dispersions derived from polycarbonatediols, J. Appl. Polym. Sci. 102 (2006) 4419–4424.

[13] B.K. Kim, J.C. Lee, Polyurethane ionomer dispersions from poly(neopentylene phthalate) glycol and isophorone diisocyanate, Polymer (Guildf). 37 (1996) 469–475.

[14] D. Lee, H. Tsai, W. Yu, R. Tsai, Polyurethane Dispersions Derived from Polycarbonatediols and a Carboxylic Polycaprolactonediol, J. Macromol. Sci. Part A. 42 (2005) 85–93.

[15] S.M. Cakić, M. Spírková, I.S. Ristić, J.K. B-Simendić, M. M-Cincović, R. Poreba, The waterborne polyurethane dispersions based on polycarbonate diol: Effect of ionic content, Mater. Chem. Phys. 138 (2013) 277–285.

[16] B.K. Kim, Aqueous polyurethane dispersions, Colloid Polym. Sci. 274 (1996) 599–611.

[17] C. Prisacariu, Polyurethane Elastomers, Springer Vienna, Vienna, 2011.

[18] C. Hepburn, Polyurethane Elastomers, Springer Netherlands, Dordrecht, 1992.

[19] S. Bilgin, R. Tomovska, J.M. Asua, Effect of ionic monomer concentration on latex and film properties for surfactant-free high solids content polymer dispersions, Eur. Polym. J. 93 (2017) 480–494.

[20] M. Chang, A.S. Myerson, T.K. Kwei, The Effect of Hydrogen Bonding on Vapor Diffusion in Water-Soluble Polymers, J. Appl. Polym. Sci. 66 (1997) 279–291.

Chapter 5. Modification of polymer microstructure of PU/(meth)acrylic hybrids by altering (meth)acrylic chains

5.1. Introduction

As demonstrated in Chapters 2 and 4, the modification of PU part of the PU/(meth)acrylic hybrids affected the properties of the polymer films. In addition to PU, the composition of (meth)acrylic monomers play an important role on the properties of the final hybrid [1,2]. As (meth)acrylics have a wide range of glass transition temperature (T_g) [3], the final polymer film can be very flexible or very stiff depending on the type and proportion of (meth)acrylic monomers. Šebenik *et al.* [1] studied the effect of methyl methacrylate (MMA)/butyl acrylate (BA) proportion on the mechanical properties and Koenig hardness of PU/acrylic hybrid films using N-methyl-2-pyrrolidinone (NMP) as solvent in the PU synthesis. It was observed that with increasing the MMA proportion, the Koenig hardness and the Young´s modulus increased, but the elongation at break decreased. However, only limited range of MMA/BA proportions (from 50/50 to 65/35 wt/wt) was studied. In the solvent-free system using (meth)acrylic monomers as solvent, it was reported that with increasing the of MMA/BA proportion (from 0/100 to 100/0) both the tensile strength (the stress at break) and the pendulum hardness increased [2]. However, no attempt was done in order to understand the effect of grafting in different MMA/BA proportion which is the aim of this chapter.

In the present chapter, the polymer microstructure is modified by altering the (meth)acrylic chains *via* varying the MMA/BA proportion ((0/100), (25/75), (50/50), (75/25) and (100/0) wt/wt) in the formulation and by using glycerol mono methacrylate (GMMA) to graft PU and poly((meth)acrylate) chains. The (meth)acrylic monomers were used as solvent in PU synthesis and once the dispersion formed, they were polymerized by free radical polymerization. In order to expand the range of MMA/BA compositions that form films, the softest polyol (polypropylene glycol (PPG)) was used in the formulation of PU. The characteristics and properties of PU/(meth)acrylic hybrids obtained with different MMA/BA ratios with and without grafting are compared.

5.2. Experimental

5.2.1. Materials

The materials are given in Appendix I.

5.2.2. Synthesis procedures

The synthesis of the PU prepolymer was performed in a 250 mL glass reactor fitted with a reflux condenser, a sampling device (and feeding inlet), a nitrogen inlet, a thermometer and a flat blade turbine stirrer. Reaction temperature was controlled by an automatic control system, Camile TG (Biotage). The formulations of PU/poly(meth)acrylic (50/50 wt/wt) hybrid dispersions are presented in Table 5.1. To synthesize the prepolymer, dimethylol propionic acid (DMPA), PPG, isophorone diisocyanate (IPDI, 7.73 g), dibutyltin dilaurate (DBTDL) (0.05 g) and one part of the (meth)acrylic monomers (50 wt% of the MMA/BA) were charged into

the reactor. The reaction mixture was brought to 70°C under agitation of 250 rpm and held for 4-5 hours. It is worth mentioning that the technical (meth)acrylic monomers were not purified and therefore the contained inhibitor avoided any radical reaction during the PU synthesis. The free NCO was checked with amine-back titration [4]. Later, the mixture of butanediol (BDO)/GMMA dissolved in (meth)acrylic monomers (20 wt% of the MMA/BA) were added to the prepolymer to functionalize the PU chains. BDO was added with the functional monomer as short chain diol in order to keep the NCO/OH value and hence to use a fixed amount of chain extender in the case of grafted and non grafted hybrids. After 2 h, the mixture was cooled to 25°C and additional (meth)acrylic monomers (15 wt% of the MMA/BA) was added to reduce the viscosity. After that, triethylamine (TEA) dissolved in (meth)acrylic monomers (10 wt% of the MMA/BA) was added and kept at 25°C for 45 min in order to neutralize the carboxylic groups of DMPA.

Then, the PU/(meth)acrylic solution was dispersed in water. To prepare the aqueous dispersions, the reactor was charged with double deionized water under nitrogen at 25°C and the prepolymer-monomer mixture was added in 15 min under high agitation (750 rpm). After that, the chain extender (diaminododecane, DAD) dissolved in (meth)acrylic monomers (5 wt% of the MMA/BA) was added into the reactor and left to react one hour at 70°C. The theoretical molar ratio of NCO/OH (defined as a molar ratio of IPDI and sum of molar ratio of PPG, DMPA, BDO, GMMA and DAD) was 1.8 before chain extension, 1.6 for the functionalized prepolymer and 1.0 after chain extension.

The free radical polymerization of (meth)acrylic monomers was performed at 70°C by adding a shot of potassium persulfate (KPS, 0.5 wt% based on monomer) dissolved in water. The polymerization was performed in batch for 2 hours and a final conversion of the

(meth)acrylic monomers higher than 95% was achieved in all the cases. The resulting hybrid latexes had a 40 wt% solids content.

Table 5.1. Recipe used to synthesize PU/(meth)acrylic (50/50 wt/wt) hybrids using different MM/BA proportion with constant amount of IPDI (7.73 g), DBTDL catalyst (0.05 g), water (71 g) and KPS (0.12 g)

(meth)acrylic	Experiment	PPG	DMPA[a]	BDO	GMMA	TEA[b]	DAD	MMA/*n*BA (g/g)
		(mols per 1 mol of IPDI)						
PU/PBA	No grafting	0.19	0.37	0.07	0	0.39	0.37	0/24
	Grafted	0.19	0.37	0.045	0.025	0.39	0.37	0/24
PU/P(MMA/BA) (25/75)	No grafting	0.19	0.37	0.07	0	0.39	0.37	6/18
PU/P(MMA/BA) (50/50)	No grafting	0.19	0.37	0.07	0	0.39	0.37	12/12
	Grafted	0.19	0.37	0.045	0.025	0.39	0.37	12/12
PU/P(MMA/BA) (75/25)	No grafting	0.19	0.37	0.07	0	0.39	0.37	18/6
	Grafted	0.19	0.37	0.045	0.025	0.39	0.37	18/6
PU/PMMA	No grafting	0.19	0.37	0.07	0	0.39	0.37	24/0
	Grafted	0.19	0.37	0.045	0.025	0.39	0.37	24/0

a) 3.5 wt% based on organic phase
b) 1.05 mol of DMPA

5.2.3. Characterization

Final particle sizes of the latexes were measured by dynamic light scattering (DLS). The unreacted NCO was determined by titration. The conversion of (meth)acrylic monomers was measured gravimetrically. The gel fraction was measured by Soxhlet extraction, using tetrahydrofuran (THF) as the solvent. The molar mass distribution of the soluble fraction of polymers was determined by size exclusion chromatography (SEC/RI/UV). The molar mass distribution of the whole polymer was determined by asymmetric-flow field-flow fractionation (AF4) using multi angle light scattering and refractive index detectors (MALS/RI). The thermal

characterization of the hybrids was carried out by differential scanning calorimetry (DSC). The morphologies of latex particles and films were studied by means of transmission electron microscopy (TEM). The mechanical properties of the films were measured by tensile tests. The water sensitivity of the polymer films was analyzed by liquid water uptake test. A detailed description of the characterization methods is provided in Appendix I.

5.3. Results and Discussion

5.3.1. Polymer Microstructure

The polymer microstructure of the hybrid was varied changing the MMA/BA ratio: 0/100, 25/75, 50/50, 75/25 and100/0. For each MMA/BA ratio, experiments with and without GMMA were carried out. The characteristics of the synthesized PU/acrylic hybrids are presented in Table 5.2. The final particle sizes were in the range of 113-150 nm and in general the particle size slightly decreased as the MMA content increased likely due to the higher hydrophilicity of MMA compare to BA. The DSC analysis for PU/P(MMA/BA) (25/75), (50/50), (75/25) and (100/0) showed two T_gs, one at low temperature that corresponds mainly to PU chains, and the second T_g corresponding to the MMA/BA copolymer (or to the PMMA in the case of PU/PMMA) obtained in a batch system and it increased with the MMA content. It is worth pointing out that in batch polymerization due to the difference in the reactivity ratios of MMA and BA, PMMA rich chains with higher T_g are expected to be formed at the beginning of the process. In the case of PU/PBA only one T_g at low temperature was observed due to the absence of MMA in the formulation. This T_g corresponds to both PU and PBA chains. The two T_gs were slightly shifted toward each other for the grafted samples, showing more

compatibility and interpenetration of PU and (meth)acrylic polymer chains. The gel content of the hybrids in the absence of functional monomer was negligible except in the case of PU/PMMA that a substantial amount of gel (69%) was observed, which was unexpected. The probable reason for the observed gel may be the hydrogen abstraction from methylene groups of methacrylate polymer by oxygen centered radical, which produces branches and therefore generates a network structure. The hydrogen abstraction in radical polymerization of methyl methacrylate with oxygen centered radical initiators have been reported in several studies [5–7]. However, gel formation requires termination by combination, that is not prevalent in methacrylates. In addition, it is not clear at all why gel appeared when there was no BA in the formulation, taking into account that BA is prone to suffer hydrogen abstraction [8] and termination by combination [8,9]. In order to check the microstructure of the observed gel, the AF4 technique was used to analyze this sample. The molar mass distribution of the whole sample is shown in Figure 5.1. The large peak at higher molar masses (>$10^{7.5}$ Da) corresponds to the gel. However, its relative size is larger than the gel fraction (69%). A possible reason is that the detection of low molecular weights in the presence of high molecular weight is difficult and the polymer of molar masses about $10^{4.5}$ Da that appeared when the sol polymer was analyzed (Figure 5.2) was not observed in the whole sample. Another surprising point in the PU/PMMA hybrid devoid of GMMA is that the gel fraction (69%) exceeded the fraction of (meth)acrylics (50%). This means that PU is incorporated into the gel. Perhaps the hydrogen abstraction from the methylene group in the PPG led to the incorporation of PU chains to the (meth)acrylics and multiple abstraction in a chain may lead to gel formation. If this is the mechanism responsible for gel formation, then the relative rate of hydrogen abstraction and propagation should be greater for MMA than for BA.

Table 5.2 shows that when GMMA was used, gel content increased with the MMA content on the formulation. This might be attributed to the preferential hydrogen abstraction from the methylene group of the PPG and of the MMA radical as discussed above. In addition, the relative reactivity ratios GMMA/BA and GMMA/MMA may play a role. When BA/MMA is high, the GMMA will react early in the process because $r_{GMMA}>r_{BA}$, and hence there will be no unreacted GMMA for the rest of the process reducing the likelihood of gel formation. At high MMA fractions, the reaction of GMMA groups will occur continuously throughout the reaction and therefore gel will be built during the whole reaction.

Figure 5.2 presents the SEC molar mass distribution of the soluble part. The soluble part of the polymers showed bimodal molar mass distribution for the hybrids with no functional monomer and the grafted hybrids showed a broad distribution with a final tail (Figure 5.2). For the hybrids with no functional monomer, the population of polymer chains at high molar mass mainly corresponds to (meth)acrylics and the one at low molar mass attributed to the PU chains.

Table 5.2. The characteristics of PU/(meth) hybrids with different MMA/BA proportion

(meth)acrylic	Experiment	Final Particle size (nm)	T_g (ºC)		Gel content (%)	Sol $\overline{Mw}$ * (Kg/mol)	
			T_{g1} (ºC)	T_{g2} (ºC)		Low M_w	High M_w
PU/PBA	**No grafting**	150	-52	-	0	32	792
	Grafted	128	-53	-	57 ± 3	45	-
PU/P(MMA/BA) (25/75)	**No grafting**	127	-53	-15	0	27	800
PU/P(MMA/BA) (50/50)	**No grafting**	145	-56	32	0	36	1019
	Grafted	135	-54	27	67 ± 2	30	-
PU/P(MMA/BA) (75/25)	**No grafting**	113	-56	70	0	34	1401
	Grafted	143	-54	65	73 ± 2	36	-
PU/PMMA	**No grafting**	117	-55	118	69 ± 6	39	1634
	Grafted	121	-55	116	83 ± 1	19	-

* The hybrids with no functional monomer had bimodal sol $\overline{Mw}$ contain both low molar mass non grafted PU chains and high molar mass (meth)acrylic chains

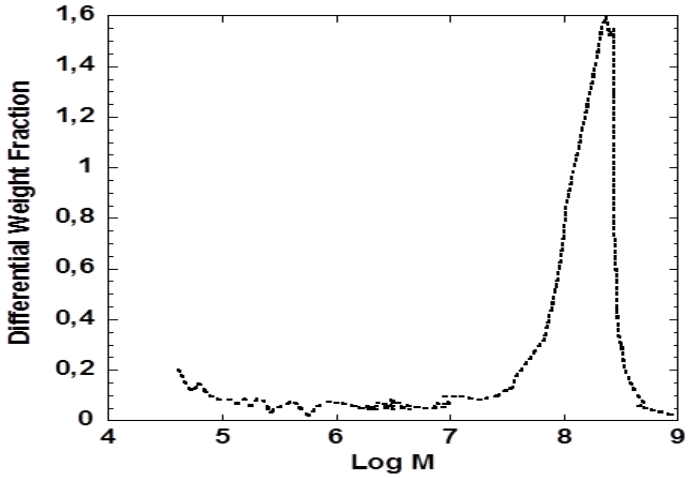

Figure 5.1. Absolute molar mass distribution of the PU/PMMA hybrid without GMMA obtained by AF4/MALS/RI

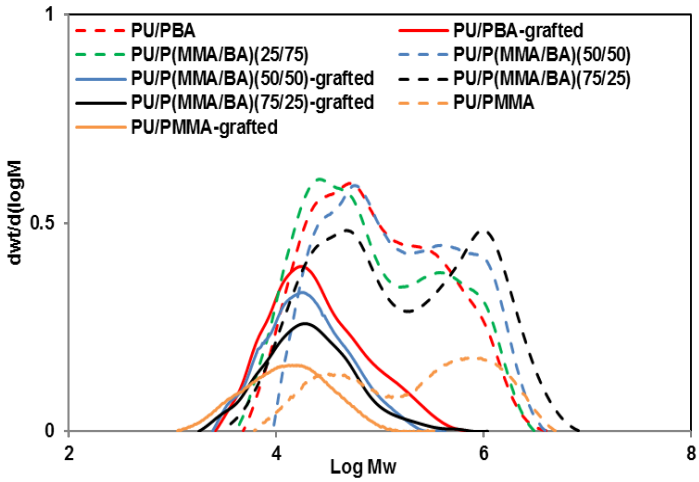

Figure 5.2. Molar mass distribution of soluble fraction in PU/(meth)acrylic hybrids with different MMA/BA proportion obtained by SEC (the curves are normalized based on the soluble fraction)

5.3.2. Particle and Film Morphology

As the PU/PMMA hybrid interestingly formed a film at ambient temperature, the particle and film morphology of PU/PMMA was studied and compared with the PU/P(MMA/BA) (50/50). The TEM of cross-section for the PU/PMMA film is presented in Figure 5.3. It clearly shows a continuous phase composed of the bright domains. The TEM images of the hybrid latexes and the film cross-section of PU/P(MMA/BA) (50/50) and PU/PMMA hybrids are shown in Figures 5.4 and 5.5 respectively. The TEM images of the particles with no GMMA showed core-shell morphologies in both cases (Figures 5.4(a)-left and 5.5(a)-left) with the acrylics in the core and PU in the shell. However, for the PU/PMMA, the acrylic core was much less defined, namely there was no sharp separation between PU and PMMA. This is in agreement with the molar mass distribution obtained for this hybrid that required a substantial

grafting between PU and PMMA. For both P(MMA/BA) and PMMA, the compatibility with PU increased when GMMA was used (Figures 5.4(b)-left and 5.5(b)-left).

Particle morphology translated to the film morphology and the film cross-section of Figures 5.4 and 5.5 clearly show that the films became more homogeneous as grafting increased.

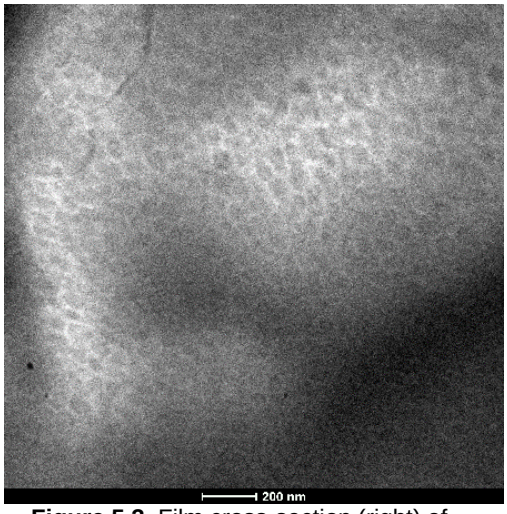

Figure 5.3. Film cross-section (right) of PU/PMMA hybrid with no functional monomer

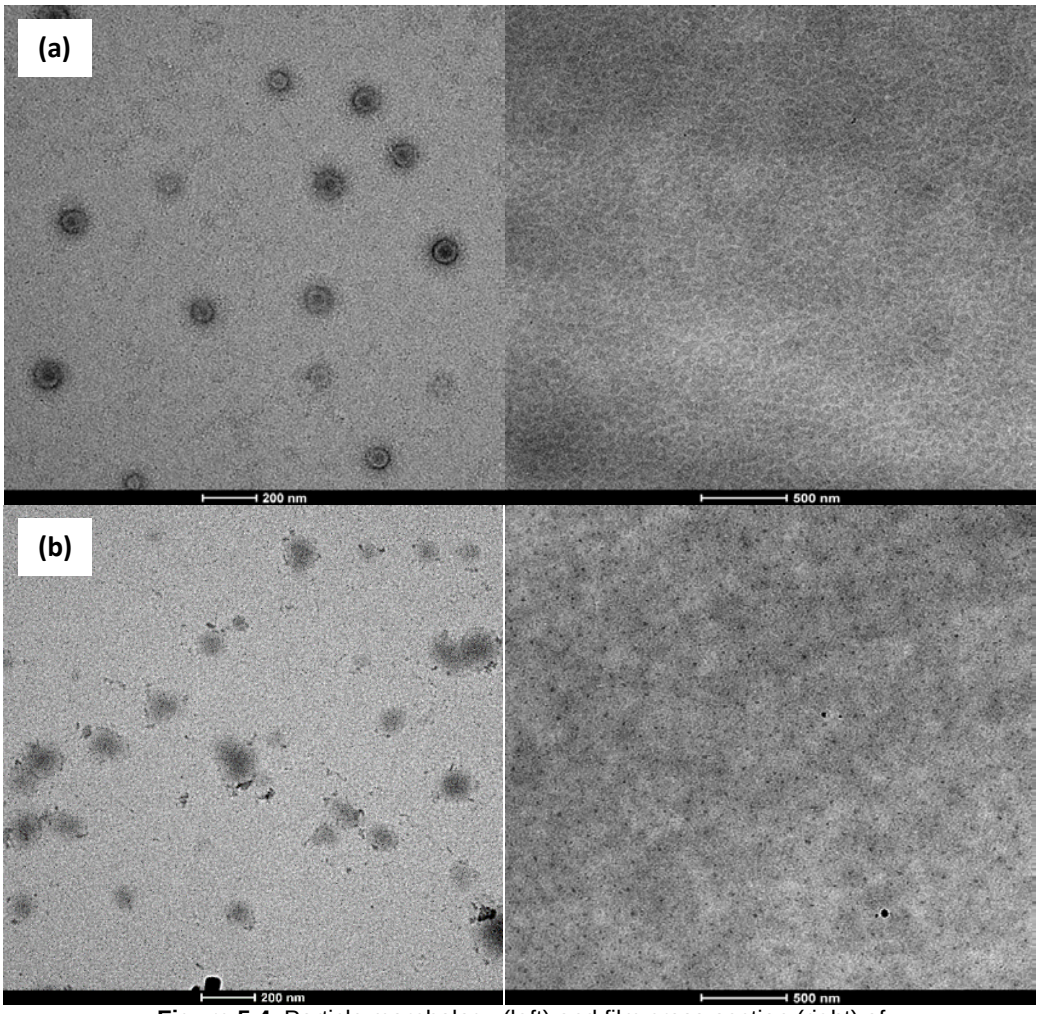

Figure 5.4. Particle morphology (left) and film cross-section (right) of PU/P(MMA/BA)(50/50) hybrid, no functional monomer (a), Grafted (b)

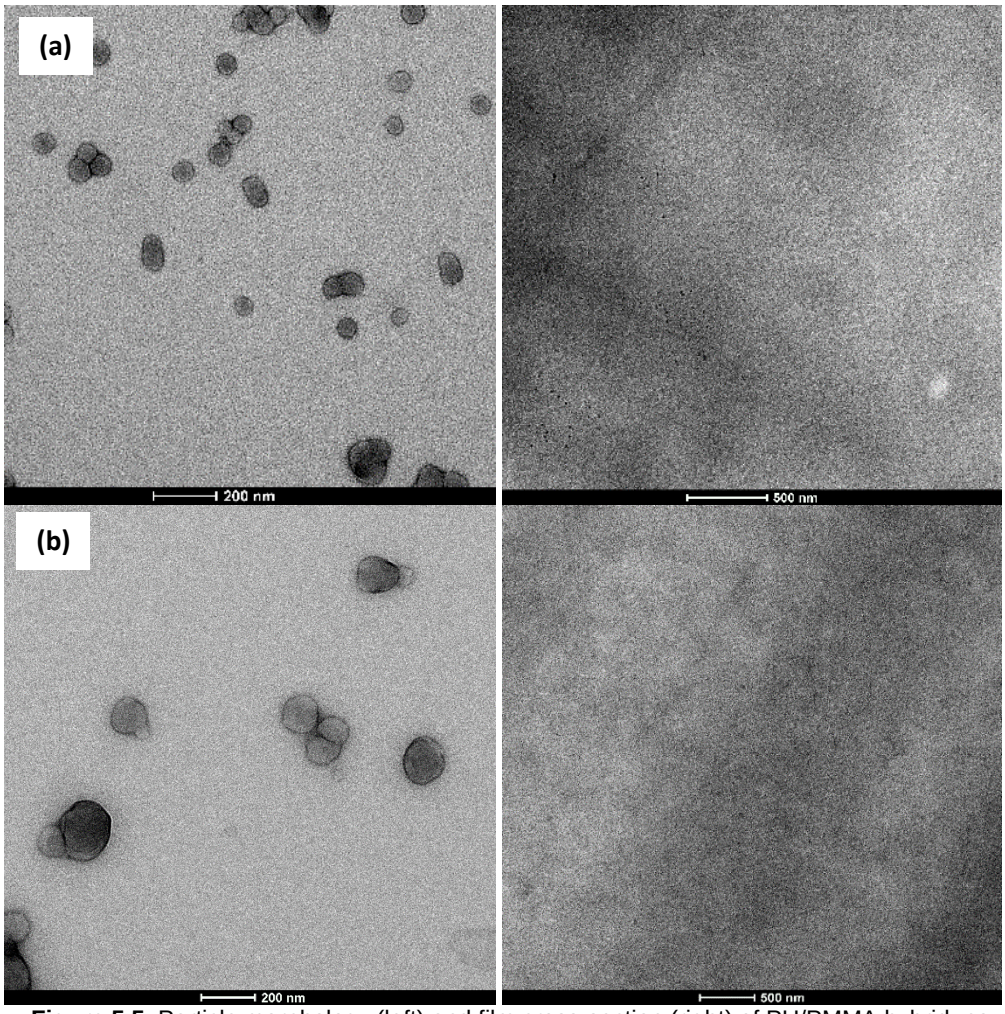

Figure 5.5. Particle morphology (left) and film cross-section (right) of PU/PMMA hybrid, no functional monomer (a), Grafted (b)

5.3.3. Mechanical properties

The stress-strain behavior of the films cast from the hybrid latexes at ambient temperature is shown in Figure 5.6 and the mechanical properties are summarized in Table 5.3. The films of PU/PBA and PU/P(MMA/BA) (25/75) hybrids were very soft and their stress-

strain curves were similar. As the MMA/BA ratio increased Young´s modulus, yield stress, ultimate strength and strain hardening of the polymer film increased dramatically, but the elongation at break decreased. The observed results are in good agreement with literature [1,2] and is related to the high T_g of PMMA that leads to a stiffer hybrid structure. Additionally, grafted hybrids showed higher Young´s modulus, yield stress and strain hardening and lower elongation at break compared to the non-grafted hybrids. Moreover, as the MMA/BA proportion increased, the effect of grafting was more pronounced. The reason for that is likely the combined effect of harder polymer and higher gel content at higher MMA/BA proportion. It is worth mentioning that the grafted PU/PMMA hybrid formed a brittle film at ambient temperature and the tensile test was not performed for this film.

The comparison of these results with the results in the previous chapters (variation in PU composition) revealed that the (meth)acrylic composition has a stronger influence on the mechanical properties of the PU/(meth)acrylic hybrids than PU composition and grafting.

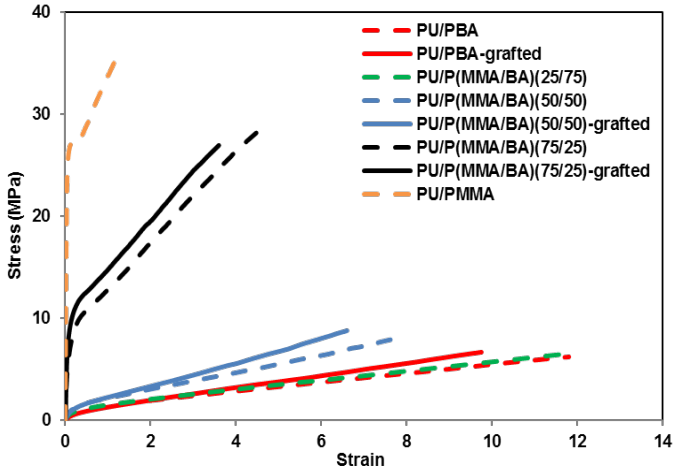

Figure 5.6. The stress-strain behavior of PU/(meth)acrylic hybrid films obtained with different MMA/BA proportion

Table 5.3. Mechanical properties of the PU/(meth)acrylic hybrids films obtained with different MMA/BA proportion

(meth)acrylic	Experiment	Young´s Modulus MPa/100	Yield Stress (MPa)	Elongation at break	Ultimate Strength (MPa)	Toughness (MPa)
PU/PBA	No grafting	0.06 ± 0.01	0.95 ± 0.08	11.8 ± 0.5	6.2 ± 0.3	43.2 ± 2.2
	Grafted	0.06 ± 0.01	0.95 ± 0.05	9.7 ± 0.2	6.7 ± 0.2	36.0 ± 1.2
PU/P(MMA/BA) (25/75)	No grafting	0.06 ± 0.01	1.23 ± 0.12	11.6 ± 0.3	6.5 ± 0.2	44.1± 1.4
PU/P(MMA/BA) (50/50)	No grafting	0.08 ± 0.02	1.45 ± 0.08	7.9 ± 0.3	8.2 ± 0.3	36.8 ± 2.1
	Grafted	0.10 ± 0.01	1.50 ± 0.07	7.0 ± 0.2	7.9 ± 0.3	32.0 ± 1.8
PU/P(MMA/BA) (75/25)	No grafting	0.63 ± 0.05	9.8 ± 1.1	4.6 ± 0.2	28.6 ± 0.4	85.6 ± 5.3
	Grafted	1.77 ± 0.04	11.4 ± 0.8	3.6 ± 0.1	26.95± 0.3	66.5 ± 4.1
PU/PMMA	No grafting	8.20 ± 0.25	27.3 ± 1.3	1.2 ± 0.1	35.1 ± 0.6	33.9 ± 1.5

5.3.4. Water sensitivity

The water sensitivity of the polymer cast at ambient temperature was studied by liquid water uptake measurement and the results is presented in Figure 5.7. It was observed that as MMA/BA proportion in the formulation increased, the water uptake decreased. The water uptake of PU/PMMA film reached a plateau after 5 days and the PU/P(MMA/BA)(75/25) film absorbed higher amount of water and reached a plateau after 10 days. 20 days were needed to reach the plateau for the grafted PU/P(MMA/BA)(50/50). The polymer films of non grafted PU/P(MMA/BA)(50/50), PU/P(MMA/BA)(25/75) and PU/PBA (both grafted and non grafted) kept absorbing water during the test and did not reach a plateau. The comparison of tensile test result (Figure 5.6) and water uptake measurement (Figure 5.7) clearly shows that the stiffer films had lower water uptake, as the absorption of liquid water in harder films is more difficult than in the softer films due to their lower free volume. Moreover they reached a thermodynamic equilibrium (a plateau in the water uptake) and they don't absorb more water.

Similar to what was observed in Chapters 3 and 4, the water uptake of the grafted polymers was lower than that of non-grafted ones in all the cases, likely due to the crosslinking that inhibits swelling to a certain extent. Table 5.4 presents the amount of polymer film dissolved in water during the test (as difference in weight before and after water uptake experiments). As can be seen the amount of water soluble species was in the same range (between 1 wt% to 3 wt%) for all the films suggesting that the fraction of the film that is soluble in water was not affected by the MMA/BA proportion.

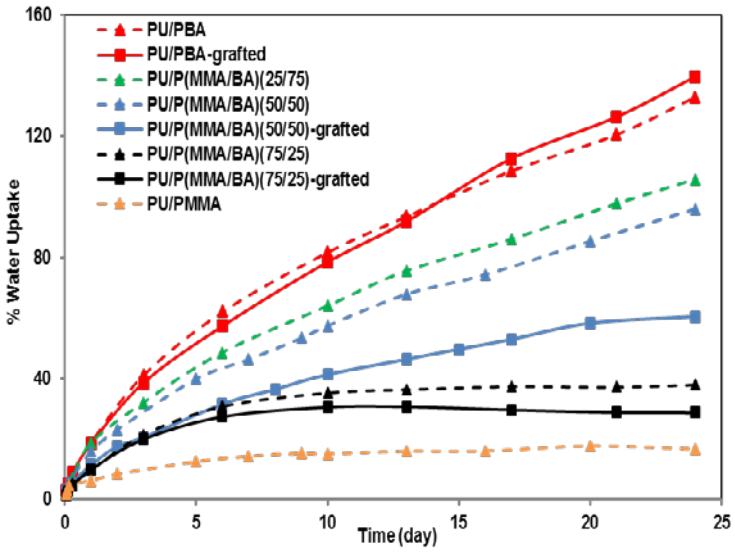

Figure 5.7. Liquid water uptake measurement of the PU/(meth)acrylic polymer films obtained with different MMA/BA proportion

Table 5.4. Amount of polymer dissolved in the water after the water uptake test

(meth)acrylic	Experiment	Polymer weight loss after drying (%)
PU/PBA	**No grafting**	1.2 ± 0.1
	Grafted	1.3 ± 0.2
PU/P(MMA/BA) (25/75)	**No grafting**	1.2 ± 0.1
PU/P(MMA/BA) (50/50)	**No grafting**	2.3 ± 0.2
	Grafted	1.9 ± 0.1
PU/P(MMA/BA) (75/25)	**No grafting**	2.1 ± 0.2
	Grafted	2.5 ± 0.3
PU/PMMA	**No grafting**	2.1 ± 0.2

5.4. Conclusions

The effect of (meth)acrylic monomer on the synthesis and properties of solvent-free, waterborne PU/acrylic hybrids was studied in this chapter. Different proportions of (MMA/BA) ((0/100), (25/75), (50/50), (75/25) and (100/0) wt/wt) were used. The polymerizations were carried out with and without GMMA.

Except in the case of PU/PMMA, no gel content was observed in the absence of GMMA. For PU/PMMA, around 69% gel was observed which shows the incorporation of PUs in the gel. The observed gel was probably as a result of multiple hydrogen abstraction from the methylene group of PPG in PU chains. However the reason for such an observation in the absence of BA is not clear. The gel content of grafted hybrids increased with increasing the MMA proportion due to the combined effect of hydrogen abstraction from the PPG units and the and the higher reactivity of GMMA than BA that led to the fast consumption of GMMA

in the beginning of the reaction and reduced the possibility of gel formation at high BA/MMA proportion.

The TEM images showed that the particles with no GMMA had core-shell morphologies with the acrylics in the core and PU in the shell. And with grafting the compatibility between PU and (meth)acrylics increased and the particles and films became more homogeneous. The stress-strain behavior of the films showed that with increasing the MMA/BA ratio, the Young´s modulus, yield stress and strain hardening of the film increased dramatically, but the elongation at break decreased. For grafted hybrids, the Young´s modulus and yield stress were slightly higher than those of non grafted PU/acrylic hybrids and the elongation at break was lower. This effect was more pronounced as the MMA/BA increased due to the higher gel content and the higher T_g of the (meth)acrylate polymer. Regarding the water sensitivity, as MMA/BA ratio in the formulation increased, the water uptake decreased because the diffusion of water is more difficult in the harder polymer films (higher MMA proportion) and the water uptake reached a plateau and did not absorb more water. In summary, it can be concluded that by using higher proportion of MMA/BA in the formulation, harder polymer films with higher water resistance can be obtained. However, it should be taken into account that by using the softest polyol (PPG) the structure of PU chains was soft. Therefore taking advantage of the soft PU which is the continuous phase in the polymer film, the PU/PMMA dispersion was able to form a film at ambient temperature with good mechanical properties and water sensitivity.

5.5. References:

[1] U. Šebenik, M. Krajnc, Properties of acrylic-polyurethane hybrid emulsions synthesized by the semibatch emulsion copolymerization of acrylates using different polyurethane particles, J. Polym. Sci. Part A Polym. Chem. 43 (2005) 4050–4069.

[2] R. Shi, X. Zhang, J. Dai, Synthesis of TDI-Polyurethane/Polyacrylate Composite Emulsion by Solvent-free Method and Performances of the Latex Film, J. Macromol. Sci. Part A. 50 (2013) 350–357.

[3] R.C. Rodriguez, E.L. Madruga, Glass Transition Temperatures of Butyl Acrylate – Methyl, (1999) 2512–2520.

[4] C. Hepburn, Polyurethane Elastomers, Springer Netherlands, Dordrecht, 1992.

[5] T. Nakamura, W.K. Busfield, I.D. Jenkins, E. Rizzardo, S.H. Thang, S. Suyama, Initiation mechanisms for radical polymerization of methyl methacrylate with tert-butyl peroxypivalate, J. Am. Chem. Soc. 118 (1996) 10824–10828.

[6] T. Nakamura, W.K. Busfield, I.D. Jenkins, E. Rizzardo, S.H. Thang, S. Suyama, Advantage of Using tert -Hexyl Peroxypivalate as an Initiator for the Polymerization of Methyl Methacrylate, Macromolecules. 29 (1996) 8975–8976.

[7] A.L.J. Beckwith, J.S. Poole, Factors affecting the rates of addition of free radicals to alkenes-determination of absolute rate coefficients using the persistent aminoxyl method., J. Am. Chem. Soc. 124 (2002) 9489–97.

[8] I. González, J.M. Asua, J.R. Leiza, The role of methyl methacrylate on branching and gel formation in the emulsion copolymerization of BA/MMA, Polymer (Guildf). 48 (2007) 2542–2547.

[9] N. Ballard, S. Hamzehlou, F. Ruipérez, J.M. Asua, On the Termination Mechanism in the Radical Polymerization of Acrylates, Macromol. Rapid Commun. 37 (2016) 1364–1368.

Chapter 6: Correlating structure and performance of PU/(meth)acrylic hybrids as hardwood floor coating

6.1. Introduction

Polyurethane dispersions (PUDs) have been widely used in the furniture and flooring industry and are often blended with (meth)acrylic polymers in order to achieve the desired coating performance [1–5]. (Meth)acrylics are lower in price than PUDs due to processing and raw material cost. However, many acrylic dispersions contain surfactants, which tend to migrate to the surface of films resulting in reduced gloss. PUDs offer superior abrasion resistance because of intermolecular hydrogen bonding and can be produced in the absence of surfactants, allowing the coatings to reach a high gloss level [6]. Moreover, in contrast to other dispersions the minimum film formation temperature (MFFT) of PUDs is significantly lower than their glass transition temperature (T_g) due to the hydrogen bonding between PU chains and water, which act as plasticizer during film formation. Therefore, owing to the hydrogen bonding of the urethane groups, film properties are not as dependent on T_g as in acrylic latexes [6] and a low MFFT can be achieved without reducing the hardness [7]. However, in a blend of PUD and (meth)acrylic emulsion, problems with compatibility between the two components often result in a lower performance [8–12]. Therefore, PU/acrylic hybrid and grafted hybrid dispersions have been developed that showed superior properties to the

corresponding blends [11–15]. As discussed in Chapter 1 (Section 1.3.2), functional monomers containing both hydroxyl and vinyl groups are often used in order to graft PU and (meth)acrylic polymers [14–20]. Functional monomers containing different types of vinyl groups may act differently as they vary in their reactivity toward the (meth)acrylic monomers. Therefore, the grafting efficiency and hence the polymer microstructure is affected by the nature of the functional monomer. Although the synthesis, characterization and performance of grafted PU/(meth)acrylic dispersion by using methacrylate functional monomers ((hydroxyethyl methacrylate (HEMA) and (glycerol mono methacrylate (GMMA)) has been reported in Chapter 3, there is no available report on the comparison of the grafting efficiency of functional monomers containing different vinyl functionality such as acrylic, allylic and methacrylate on the polymer microstructure and properties.

In the chemically bonded hybrids, the quantification of the degree of grafting gives useful information that allows relating the polymer microstructure to the final properties. Several methods have been implemented in order to quantify the degree of grafting of the PU/acrylic hybrids. One approach is solvent extraction where it is assumed that the grafted polymers can be separated from the non grafted ones using a selective solvent [16,21]. Gooch *et al*. [21] used diethyl ether to separate the free oil-modified PU chains from the grafted PU/acrylics and the degree of grafting was calculated from the amount of the PU that was dissolved in diethyl ether solvent. Zhang *et al.* [16] used a multi-stage solvent extraction with different solvents to separate selectively the linear polymer chains from the crosslinked and grafted ones. In another study [22], the grafting efficiency of PU to polystyrene (PS) was calculated from ^{1}H NMR spectroscopy of the samples before and after extraction with

methanol as polystyrene is not soluble in methanol. However, the solvent method is not particularly accurate as some chains are partially soluble.

Lu *et al.* [23] determined the degree of grafting of the PU/acrylic hybrids by using ^{13}C NMR following the carbon-carbon double bond of the functional monomer (fatty acid). However, it should be taken into account that the consumption of the double bond in the fatty acid does not prove the grafting of PU into the acrylics.

Goikoetxea *el at*. [24] determined the degree of grafting in the alkyd/acrylic hybrid system using the UV signal of Size Exclusion Chromatography (SEC). As the alkyd can be detected by UV and knowing that the non grafted alkyds have low molar masses, the mass fraction of the grafted alkyds that shifted to higher molar masses was measured and the degree of grafting was reported. This technique seems to be more promising and easy to implement and no report is available on the implementation of this technique in the PU/acrylic hybrid system.

In this chapter, a complete study of the effect of the type of functional monomer, polymerization mode of (meth)acrylic monomers (batch and semibatch) on the polymer characteristics, particle and film morphology and final properties of the films as wood floor coatings is presented. Moreover, a SEC technique is used to quantify the degree of grafting obtained with the different functional monomers used in the formulation.

The work of this chapter was carried out at BASF SE, Ludwigshafen, Germany. The formulation of the PU/acrylic hybrids described in this chapter builds on the work of the previous chapters and is modified to take into account industrial constraints. In Chapter 4, it

was demonstrated that using polyester and polycarbonate (PCD) polyols in the PU synthesis, polymer films with good mechanical properties and water resistance were obtained. Therefore, in the designed formulation of PU/(meth)acrylic hybrid dispersions, a polyester Lupraphen® 7600/1 was used as polyol since polyesters are characterized by high toughness and abrasion resistance [25]. Moreover, Lupraphen® 7600/1 contains an aromatic ring in its structure and can absorb light in the UV range. Therefore, the polyols incorporated in the PU chains will generate a signal in the UV response of SEC allowing the measurement of the degree of grafting (the details will be discussed in the next section). Isophorone diamine (IPDA) is used to extend the PU chains as it has an aliphatic ring in its structure and leads to harder structure for the coating. In Chapter 5 the effect of methyl methacrylate (MMA)/butyl acrylate (BA) proportion was studied and it was observed that using high proportion of MMA/BA in the formulation, harder polymer films with higher water resistance were prepared. In this chapter, the ratio of MMA/BA used was 70/30 (wt/wt) to obtain hard films for the wood floor coating. In addition, the polymerization of (meth)acrylic monomers was performed in different modes (batch and semi-batch) in order to compare the polymer properties and final performance. The effect of type of functional monomer was studied in Chapter 3 finding that a mono-alcohol functional monomer (HEMA) blocks the PU chains and it led to decrease in the length of PU and hence the number of grafting per PU chain. Therefore, the obtained polymer microstructure consisted of some short non grafted PU and some grafted PU/acrylic. In the alternative case of the functional monomer with two hydroxyl groups (GMMA), both the length of PU chains and the number of grafting points per chain were higher. Therefore, most of the PU chains were grafted into the acrylic network and formed a gel and the grafting was more efficient in this case. In this chapter, PU/(meth)acrylic hybrids (50/50) (wt/wt) are

synthesized using functional monomers that have two hydroxyl groups but different type of vinyl functionality (Scheme 6.1); allyl ether (in Glycerol mono-allyl ether, GAE), methacrylate (in GMMA) and diacrylate (in Laromer® LR 8765 R). As the reactivity of these vinyl groups in functional monomers are different, it is expected that the degree of grafting, and therefore the final properties, will be different in each case.

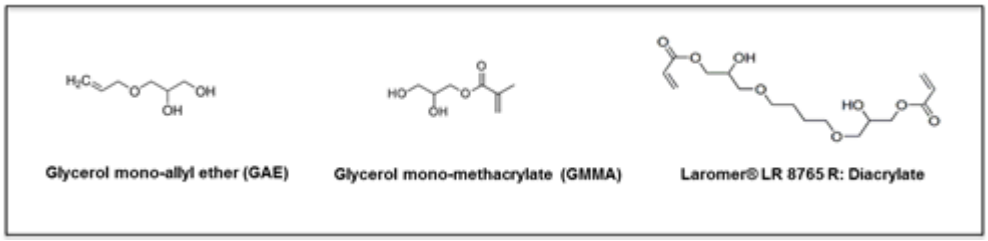

Scheme 6.1. Structure of functional monomers (FM) as grafting point for PU and (meth)acrylics

6.2. Experimental

6.2.1. Materials

The materials are given in Appendix I.

6.2.2. Synthesis procedures

The synthesis was performed in a 1 L glass reactor fitted with a reflux condenser, two feeding inlets (and sampling device), a nitrogen inlet, a thermometer and an anchor stirrer. The temperature was controlled using an oil bath. The formulation is presented in Table 6.1. To synthesize the prepolymer, dimethylol propionic acid (DMPA), Lupraphen 7600/1, butanediol (BDO), and 40 wt% of the (meth)acrylic monomers (MMA/BA, 70/30 wt/wt) were charged into the reactor and the temperature was raised to 70°C under agitation of 100 rpm.

Then the isophorone diisocyanate (IPDI), the Borchi catalyst and 20 wt% of the (meth)acrylic monomers were charged into the reactor with the funnel and the reaction temperature was kept at 80-85°C for 2-3 hours. It is worth mentioning that the technical (meth)acrylic monomers were not purified and therefore the contained inhibitor avoided any radical reaction during the PU synthesis. The free NCO at the end of the reaction was checked with amine-back titration [26]. Then, the mixture of functional monomer and BDO dissolved in 20 wt% of the (meth)acrylic monomers was added to the PU prepolymer. BDO was used in order to maintain the same NCO/OH ratio trying to achieve the same molecular weight of the PUs with and without functional monomer. It is worth pointing out that as Laromer contains 2 vinyl functionalities per molecule, in order to obtain similar vinyl functionality, the number of moles of Laromer used in the formulation was half of those of GMMA and GAE. Therefore in order to control the NCO/OH ratio and hence the chain extender content, higher amount of BDO was used in this case. After 2 hours, the mixture was cooled to 25°C and 10 wt% of the (meth)acrylate monomer mixture was added to reduce the viscosity. Then, triethylamine (TEA) dissolved in 10 wt% of the (meth)acrylate monomers was added to the reactor and kept at 25°C for 45 min in order to neutralize the carboxylic acid groups of DMPA. The ratio of TEA/DMPA was 0.95 in order to avoid the odor of extra TEA in the final product. The syntheses of PU-urea dispersion with no functional monomer and using different functional monomers (GAE, GMMA and Laromer) are shown in Schemes 6.2 to 6.5.

As it was mentioned in Chapter 2, to prepare the dispersion, the PU prepolymer was added to the water. However, in order to follow the industrial constrains a similar procedure in the PUD preparation (adding water to the prepolymer) was used and it resulted in a stable dispersion as the reactor volume was bigger compared to the one used in the synthesis of

the hybrids in the previous chapters and using an anchor stirrer the shear for was higher. Therefore, to prepare the dispersion, distilled water was added dropwise to the mixture of PU prepolymer- (meth)acrylic monomer with the funnel at 25°C in 15 min under high agitation (300 rpm). After that, the chain extender (IPDA) dissolved in water was added into the reactor and left to react for one hour. The theoretical molar ratio of NCO/OH (defined as a molar ratio of IPDI and sum of moles of Lupraphen 7600/1, DMPA, BDO, functional monomer and chain extender) was 1.8 before functionalization, 1.6 after functionalization (before chain extension) and 1.05 after chain extension. The DMPA content in the formulation was 2.9 wt% based on the organic phase.

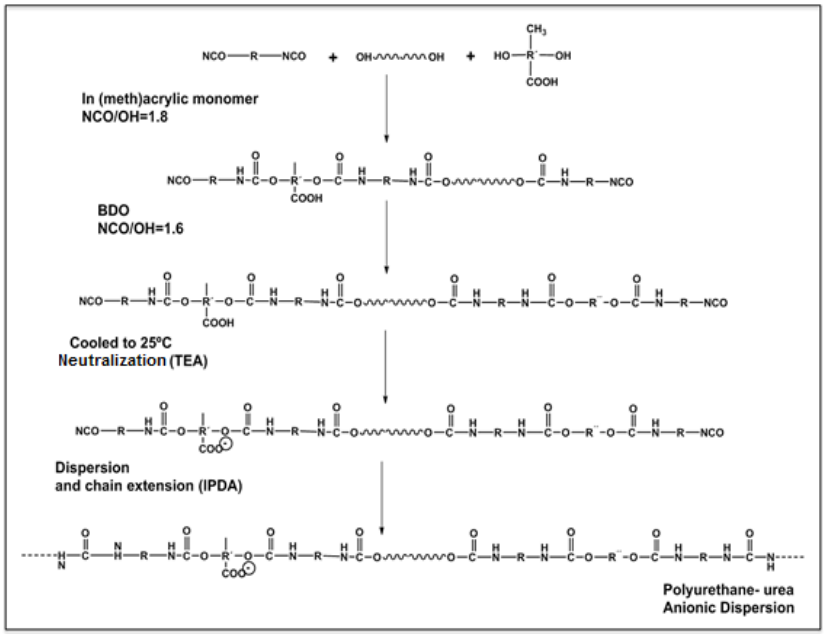

Scheme 6.2. Preparation process for PU-urea dispersion with no functional monomer

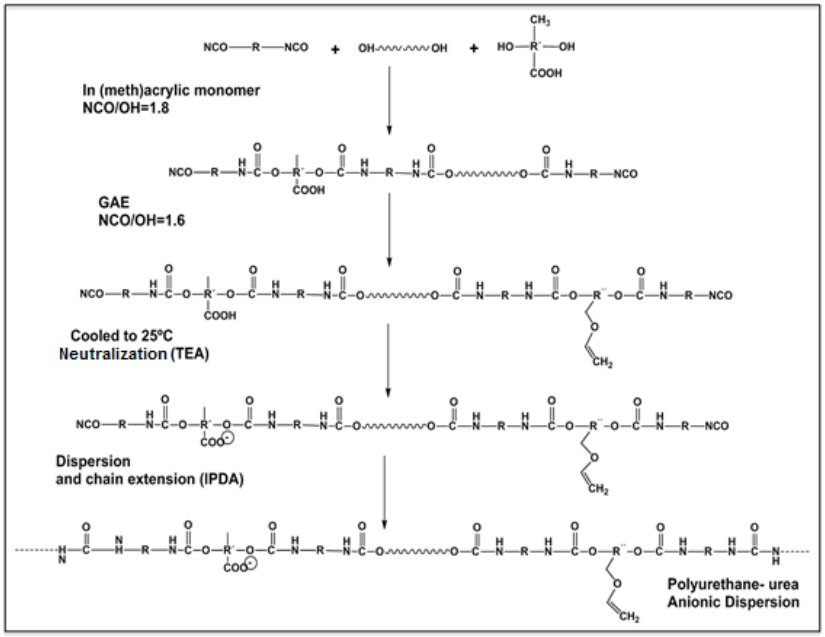

Scheme 6.3. Preparation process for functionalized PU-urea dispersion using GAE

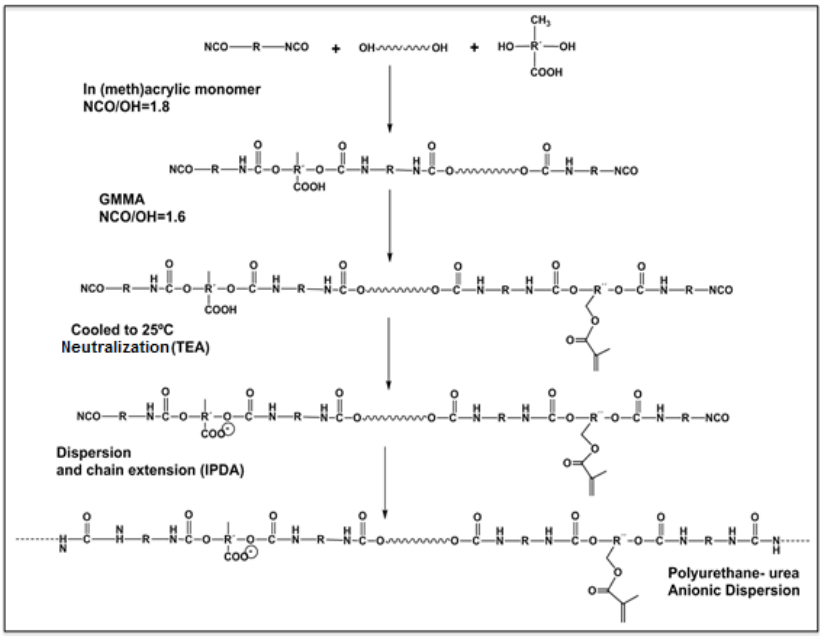

Scheme 6.4. Preparation process for functionalized PU-urea dispersion using GMMA

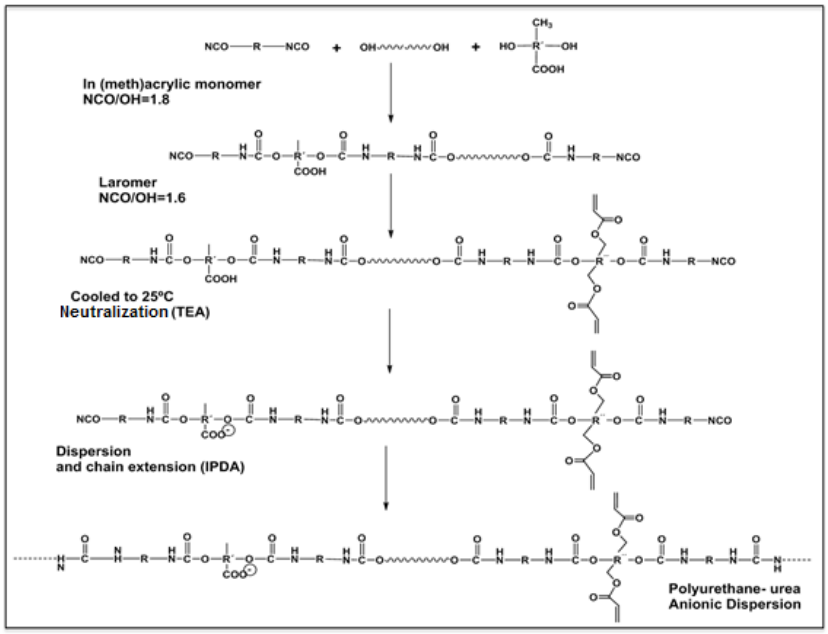

Scheme 6.5. Preparation process for functionalized PU-urea dispersion using Laromer

Table 6.1. Summary of the synthesized PU/(meth)acrylic (50/50 wt/wt) hybrids with constant amount of IPDI (48.4 g) and Borchi catalyst (0.9 g)

Polymerization Mode	Functional Monomer (FM)	Luphrapen 7600/1	BDO	DMPA	FM	BDO add with FM	IPDA	MMA/*n*BA (0.7/0.3)(wt/wt)	KPS[a]
		(mols per 1 mol of IPDI)						(g/g)	(g)
Batch	-	0.18	0.07	0.3	-	0.07	0.33	105/45	0.75
	GAE	0.18	0.07	0.3	0.04	0.03	0.33	105/45	0.75
	GMMA	0.18	0.07	0.3	0.04	0.03	0.33	105/45	0.75
	Laromer	0.18	0.09	0.3	0.02[b]	0.05	0.33	105/45	0.75
Semibatch	-	0.18	0.07	0.3	-	0.07	0.33	105/45[c]	0.75
	GAE	0.18	0.07	0.3	0.04	0.03	0.33	105/45[c]	0.75
	GMMA	0.18	0.07	0.3	0.04	0.03	0.33	105/45[c]	0.75
PU/PMMA-PBA	-	0.18	0.07	0.3	-	0.07	0.33	105/45[d]	0.52/.23[e]

a) 0.5 wt% of (meth)acrylic monomers
b) 1 mole of Laromer contains 2 vinyl functionalities
c) 150 g MEK as solvent in PU synthesis
d) 105 g MMA was used in the synthesis and polymerized in batch, 45 g BA was added later to PU/PMMA
e) KPS was added in two steps to polymerize the MMA and BA fractions

The free radical polymerization of (meth)acrylic monomers was performed at 70°C by adding KPS dissolved in water dropwise in 1 min. The polymerization was performed in batch for 2 hours and the final conversion was higher than 95% in all the cases. The resulting hybrid latexes consist of PU-Urea/Poly(meth)acrylics (50/50 wt/wt) had a 40% solids content.

In a second process, the PU was synthesized in methyl ethyl ketone (MEK) as solvent. After preparation of the polyurethane dispersion, the solvent was evaporated. The (meth)acrylic monomers and initiator (dissolved in water) were fed to the system during two hours and the (meth)acrylic monomers were polymerized in semibatch mode. The reaction was left for another one hour after feeding in order to complete the polymerization of the (meth)acrylic monomers. This series of reactions is referred as semibatch in this chapter. In addition, one reaction was performed by using only the MMA part of the (meth)acrylic monomers as diluent followed by polymerization of MMA in batch system. The BA part was fed to the PU/PMMA seed and polymerized adding a shot of initiator (dissolved in water), so the obtained hybrid is called PU/PMMA-PBA.

6.2.3. Coating preparation

A standard formulation for the preparation of commercial coatings based on PU/(meth)acrylic dispersions was used. Details are given in Appendix II.

A commercially available PU/(meth)acrylic hybrid latex (Joncryl HYB 6340,BASF) was used as reference in order to compare the performance of the synthesized coatings. However, it is worth pointing out that the comparison is not completely fair because the prepared hybrids had lower T_g than the reference (with T_g of 80 ºC) and this difference affects the final hardness of the coating, making direct comparisons difficult in some cases.

6.2.4. Characterization

Final particle sizes of the latexes were measured by dynamic light scattering (DLS). The unreacted NCO was determined by titration. The conversion of (meth)acrylic monomers was measured gravimetrically. The gel fraction and swelling degree were measured by Soxhlet extraction using THF as the solvent. The molar mass distribution of the soluble fraction of polymers and the degree of grafting was determined by size exclusion chromatography (SEC/RI/UV). The molar mass distribution of the whole polymer was determined by asymmetric-flow field-flow fractionation (AF_4/MALS/RI). The thermal characterization of the hybrids was carried out by differential scanning calorimetry (DSC). The morphology of latex particles and coatings were studied by means of transmission electron microscopy (TEM). Atomic force microscopy (AFM) technique was used in order to study the surface morphology of coatings. The performance of the coatings was evaluated in terms of tensile tests, dynamic mechanical thermal analysis (DMTA), gloss, hardness, chemical resistance and abrasion resistance. A detailed description of the characterization methods mentioned above is provided in Appendix I and a detail of coating preparation and the tests for evaluating their performance is given in Appendix II. A special characterization carried out in this chapter is grafting quantification.

The degree of grafting was measured by using the UV signal of the SEC. As Lupraphen 7600/1, the polyol used in the PU prepolymer synthesis, can be detected by the UV signal, grafting can be estimated by comparison of the UV response of the soluble fraction of material with a known amount of PU as reference sample. Knowing that the detected UV signal in the soluble fraction of the polymer belongs to the non grafted PUs, the extent of grafting can be

obtained by comparison of two samples: 1) the known amount of soluble fraction (after Soxhlet extraction) (X grams) that contains Z (unknown) grams of non grafted PU and 2) the same amount of the soluble fraction mixed with a known amount of the PU (Y grams). The PUD synthesized in MEK with no functional monomer was considered as the PU reference sample. Figure 6.1 presents the two analysis for the hybrid with GMMA synthesized in batch polymerization as an example. By comparing the area under the curve of the obtained signals, the degree of grafting of the PU into the acrylics (the fraction of grafted PUs compared to the amount of PU in the formulation) was calculated from the equations 6.1 and 6.2.

$$\frac{\text{Area(PU+sol)}}{\text{Area (neat sol)}} = \frac{Z+Y}{Z} \qquad (6.1)$$

$$\%\ \text{of grafting} = \left(1 - \frac{\text{Z}}{\left(\frac{\text{X}}{\text{ø}_\text{X}}\right)*\text{f}}\right) \qquad (6.2)$$

X: known amount of neat soluble fraction
Y: known amount of PU added as reference
Z: amount of non grafted PU
ϕ_x: sol fraction (from Soxhlet extraction)
f: fraction of PU in the formulation=(0.5)

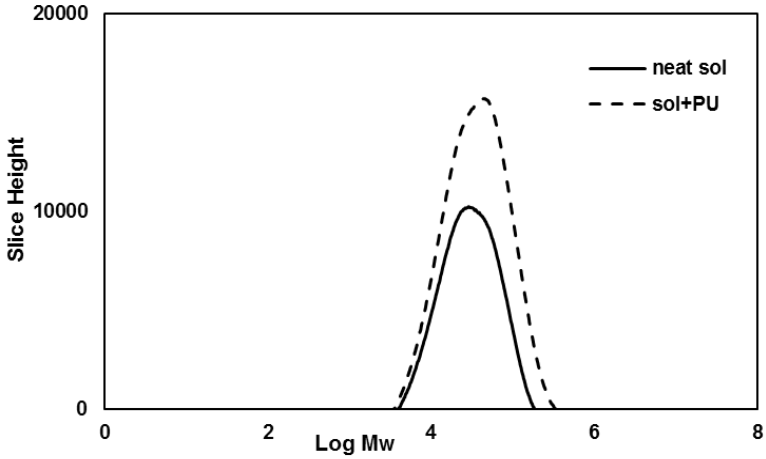

Figure 6.1. UV response of GPC measurement for the hybrid with GMMA synthesized in batch polymerization

6.3. Results and Discussion

6.3.1. Polymer Microstructure

Two series of reactions were performed in which the (meth)acrylic monomers were polymerized in batch and semibatch modes. In the series of batch polymerizations, grafted hybrids were prepared using three different functional monomers (GAE, GMMA and Laromer) and in the series of semibatch polymerization two different functional monomers (GAE, GMMA) were used for grafting. In order to check the effect of grafting, one experiment was performed in the absence of functional monomer in each series. Moreover one experiment was performed with sequential polymerization of first MMA and then BA in order to obtain the PU/PMMA-PBA hybrid. Table 6.2 summarizes the characteristics of the synthesized PU/(meth)acrylic hybrids. The particle sizes were in the range of 88-101 nm for the hybrid dispersions prepared in batch mode and around 145-190 nm for the ones in semibatch mode. It is worth mentioning that the particle size of the PU seed particles synthesized in the solvent

after solvent removal was around 70 nm. The reason for the higher final particle size of the hybrids in semibatch than batch polymerization may be attributed to the particle size of PUD seed after solvent removal which was already in the range of the synthesized hybrids in batch. The addition of (meth)acrylic monomers to the PUD seed and hybridization led to larger particles. Another possible reason can be the higher probability of collision between polymer particles during the polymerization of (meth)acrylics, as the reaction time in semibatch was 3 h (2h feeding+1 h to complete the reaction) whereas for batch it was 2h. The DSC analysis of the films from the hybrids showed two T_gs for all the hybrids, one sharp transition at low temperature (around -16 ºC), which corresponds to the PU chains, and a second T_g corresponding to the MMA/BA (70/30) copolymer. This second T_g was slightly higher for polymers synthesized in batch mode due to the difference in the reactivity ratios of MMA and BA, which leads to the formation of some PMMA rich chains with higher T_g at the beginning of the polymerization. It is worth pointing out that as the MMA/BA proportion in the formulation was 70/30, the T_g of the copolymers of MMA/BA were not very different in batch and semibatch systems. For PU/PMMA-PBA, the first T_g was slightly lower than the other hybrids likely due to the PBA chains and the second T_g around 115 ºC corresponds to the PMMA chains.

Table 6.2. The characteristics of PU/(meth)acrylic hybrids

Polymerization Mode	Functional Monomer (FM)	Particle size (nm)	T_g (°C)		Gel Content (%)	Grafted fraction of PU (%)	Sol M_w* (kg/mol)		Swelling degree
			T_{g1}	T_{g2}			Low M_w	High M_w	
Batch	-	88	-21	49	0	4	55	2180	-
	GAE	86	-21	50	31±2	46	45	1535	26±3
	GMMA	101	-16	52	88±1	89	42	-	4±2
	Laromer	90	-20	53	78±1	77	52	-	8±1
Semibatch	-	145	-16	49	0	11	45	891	-
	GAE	190	-16	46	38±2	51	47	665	21±3
	GMMA	185	-16	46	49±2	64	42	495	12±2
PU/PMMA-PBA	-	116	-23	115	0	7	54	2231	-
Reference		135	-20	80	78±1	-	-	-	4±1

* bimodal sol M_w contain both low molar mass non grafted PU chains and high molar mass (meth)acrylic chains

The molar mass distributions (MMDs) of the soluble fraction are presented in Figure 6.2 and Figure 6.3 shows the whole molar mass distributions obtained by AF_4. Before discussing the results is worth considering the complementary information provided by the gel content and the molar mass distributions (soluble and whole). At first sight, one would say that the whole MMD obtained in the AF_4 is representative of the complete polymer and therefore no additional information would be needed. However, the detection of polymer chains of low molecular weight in the presence of high molecular weight chains is difficult and the AF_4 MMDs usually tends to underestimate the low M_w part of the MMD. On the other hand, this is the part well determined in the MMD of the sol polymer by conventional SEC. The gel fraction provides a semiquantitative indication of the relative weight fraction of the low and moderate M_w polymer with respect to the very high polymer. The word semiquantitative refers to the fact that in terms of the M_ws there is not a clear frontier between soluble and insoluble fractions. The mismatch between the whole and sol MMDs respectively measured by AF_4 and SEC are illustrated in the core of hybrids obtained without functional monomer, where no gel was detected. It can be seen that the strong peak at about 10^5 Da that appeared in the SEC MMD is much smaller in the AF_4, even though no gel was present in this case.

Focusing the discussion on the hybrids prepared with functional monomers, it can be seen that the hybrids with GMMA had the highest gel, and the ones with allyl ether (that is less reactive towards (meth)acrylic monomers) had the lowest gel content. As Laromer has two vinyl functionalities in the structure, the number of moles of Laromer in the formulation was half of those of GMMA and GAE. Considering the number average molecular weight of PU chains before polymerization of (meth)acrylic to be (M_n=25000 g/mol), the number of unit of functional monomer per PU chain was calculated from equation 6.3. The value was around 1.6 for GAE and GMMA and it was 0.8 for Laromer. The statistical distribution of the Laromer units made that a significant fraction of the PU chains did not contain functional monomer. This caused a gel fraction lower than for GMMA.

$$\text{Number of FM per PU chain} = \frac{\text{mol FM in formulation} \times M\text{n of PU}}{\text{g PU in the formulation}} \qquad (6.3)$$

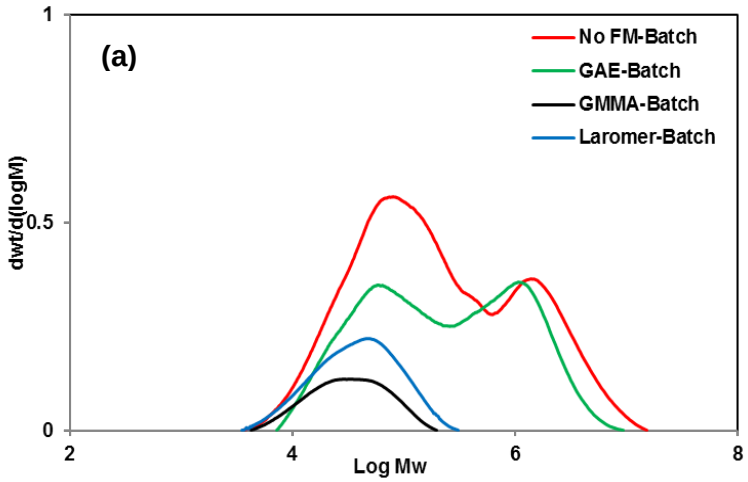

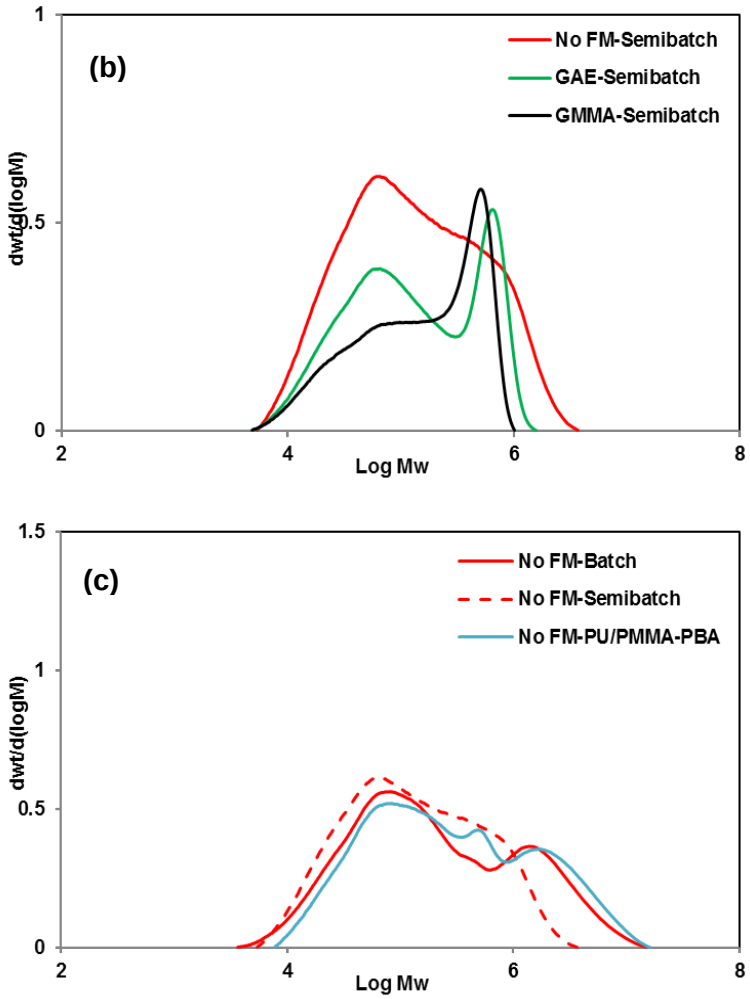

Figure 6.2. Molar mass distribution of the soluble fraction of non-grafted and grafted hybrids of PU/P(MM/BA) synthesized in Batch (a) and semi batch (b) and for PU/PMMA-PBA (c), obtained by SEC (the curves are normalized based on the soluble fraction).

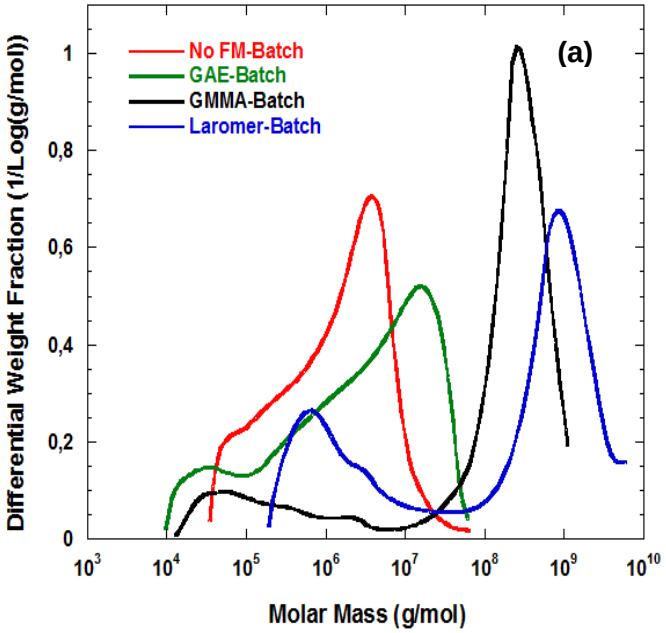
No FM-Batch
GAE-Batch
GMMA-Batch
Laromer-Batch
(a)
Differential Weight Fraction (1/Log(g/mol))
Molar Mass (g/mol)

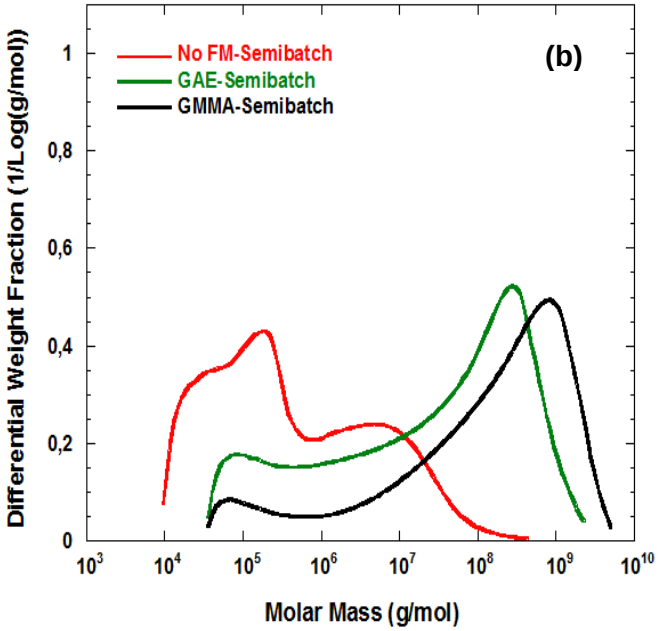
No FM-Semibatch
GAE-Semibatch
GMMA-Semibatch
(b)
Differential Weight Fraction (1/Log(g/mol))
Molar Mass (g/mol)

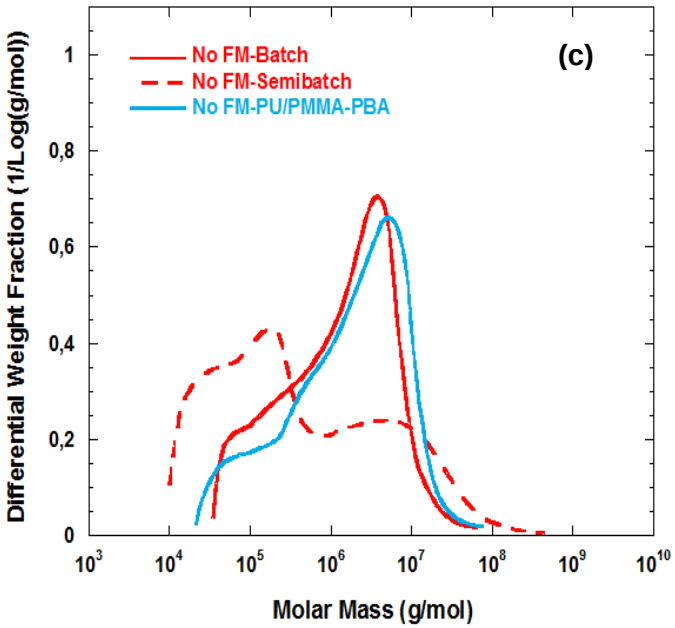

Figure 6.3. Absolute MMD of the non-grafted and grafted hybrids of PU/P(MM/BA) synthesized in Batch (a) and semi batch (b) and for PU/PMMA-PBA (c), obtained by AF4MALS/RI

Interestingly, the gel content obtained in the batch and semibatch modes was different. For example, with GMMA gel content was higher in the batch polymerization than semibatch. This could be due to high reactivity of GMMA that is consumed rapidly, and hence in the semibatch system, there was no functional monomer to react with the (meth)acrylic monomers that were fed to the system at the later part of the feeding time. For GAE, the gel content was higher in the semibatch mode due to its lower reactivity and higher possibility of the reaction of allyl functionality with (meth)acrylic monomers in the semibatch mode. In addition, the presence of higher monomer concentration in the case of batch experiments leads to higher rates of propagation relative to termination and consequently to a higher kinetic chain length of (meth)acrylics as compared to the semibatch system. These larger building blocks contribute to a higher gel content. This idea is supported by the MMDs of the

polymers obtained without functional monomer where no gel was formed. Figure 6.2 shows that a bimodal MMD was obtained and the M_w of the (meth)acrylic peak (that of the higher molar masses) was higher in batch than in the semibatch. The peak of low molar masses corresponds to PU.

The results obtained with GMMA and Laromer in batch are interesting. GMMA gives higher gel (Table 6.2), shorter high M_ws (Figure 6.3) and less swelling. On the other hand, for both functional monomers no (meth)acrylates were evident in the soluble part (Figure 6.2) indicating that most of the (meth)acrylates were incorporated in the high M_w polymer (gel). These differences can be explained as follows. As the number of GMMA units is twice that of Laromer, although the number of double bonds is the same, those of the GMMA are better distributed among the PU chains. The uneven distribution of the Laromer units results in a certain fraction of PU chains without double bonds, that cannot be grafted and appeared as soluble polymer, the statistical distribution of the Laromer units in the PU is calculated in Appendix IV. This calculation estimates that 48% of the PU chains were devoid of double bonds, which assuming that the soluble part mostly consisted of PU and that all of the PU chains containing a double bond were incorporated to the gel yields a gel fraction of 76%, which is in a very good agreement with the measured value (78 %, Table 6.2). A similar calculation for GMMA also provides a good agreement with the experimental data (estimated: 92.5 %; measured: 88%). On the other hand, the calculated value of the PU with double bonds are smaller than those of the grafted fraction of PU estimated from SEC measurement (Table 6.2), which may be overestimated considering that grafting was measured in the absence of functional monomer.

The uneven distribution of units of functional monomer among the PU chains also affect the molecular weight of the (meth)acrylate containing fraction (gel in the batch processes). Although in the case of Laromer, the fraction of PU chains with double bonds is smaller than for GMMA, in those having double bond the number of double bonds per chain is higher than for GMMA. This leads to a higher molecular weight (as compared with GMMA). However, it is surprising that higher swelling (lower crosslinking density) was obtained for Laromer. This may be due to the dangling PU chains that the Laromer gel has as a result of the fact that the two double bounds are in the same monomeric unit (Scheme 6.6).

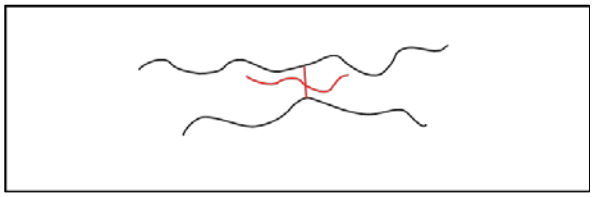

Scheme 6.6. Structure of grafted PU/acrylic hybrid with Laromer (PU containing Laromer= red , Acrylics=black)

In addition to the effect of the gel content discussed above, the type of process (batch vs. semibatch) also influenced the MMD. It can be seen that the molecular weight of the gel fraction is higher for the semibatch process. In the case of GMMA, a possible reason is that the same amount of double bonds was used to form less gel, however this would yield a more crosslinked network, which seems not to be the case because swelling is higher in semibatch.

For GAE, the longer process time of the semibatch process allowed better use if the slowly reactive allyl groups increasing the gel content and slightly increase in the crosslinking density.

6.3.2. Particle and Film Morphology

The TEM micrographs of PU/poly(meth)acrylic hybrid dispersions for the non grafted and grafted hybrids with GMMA synthesized in batch and semibatch modes are shown in Figures 6.5 and 6.6 respectively. As can be seen for the hybrids with no functional monomer (Figures 6.5(a) and 6.6(a)), a core-shell like particle morphology was observed with the acrylics in the core and PU in the shell. For the hybrids with GMMA the particles were more homogeneous and no clear distinction between the individual polymeric areas is noticeable (Figures 6.5(b) and 6.6(b)). It is worth mentioning that the TEM showed smaller particle sizes in the hybrids in semibatch compared the values in Table 6.2 probably due to the higher sensitivity of DLS to big particles [27]. The cross-sections of the films cast from the hybrids (with coating formulation) synthesized in batch and semibatch are shown in Figures 6.7 and 6.8, respectively. For the films with no functional monomer (Figures 6.7(a) and 6.8(a)) it seems that the dark spherical domains (acrylics) dispersed within the bright continuous phase (PU). However, smaller domains and more homogeneous distribution of dark (acrylics) and bright (PUs) domains was observed in the grafted hybrids using GMMA (Figures 6.7(b) and 6.8(b)) indicating less phase separation between PU and (meth)acrylics due to the grafting.

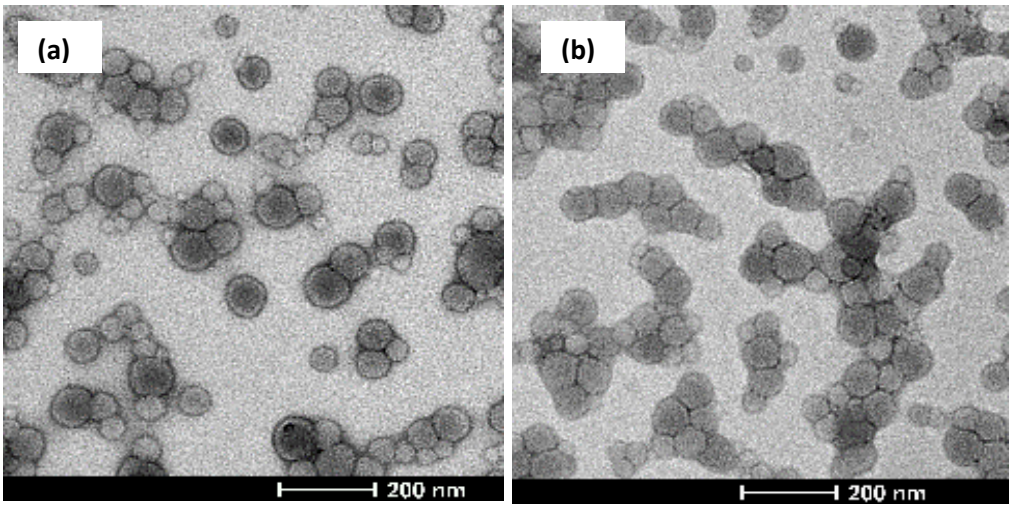

Figure 6.5. The TEM micrographs of PU/poly(meth)acrylic hybrid dispersion with no functional monomer (left-a) and with GMMA (right-b)- For hybrids synthesized in batch mode

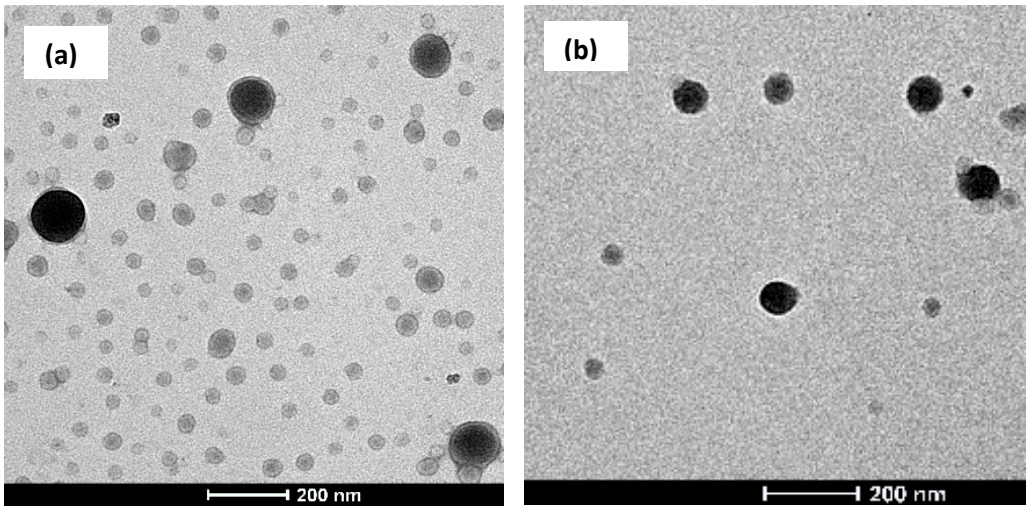

Figure 6.6. The TEM micrographs of PU/poly(meth)acrylic hybrid dispersion with no functional monomer (left-a) and with GMMA (right-b)- For hybrids synthesized in semibatch mode

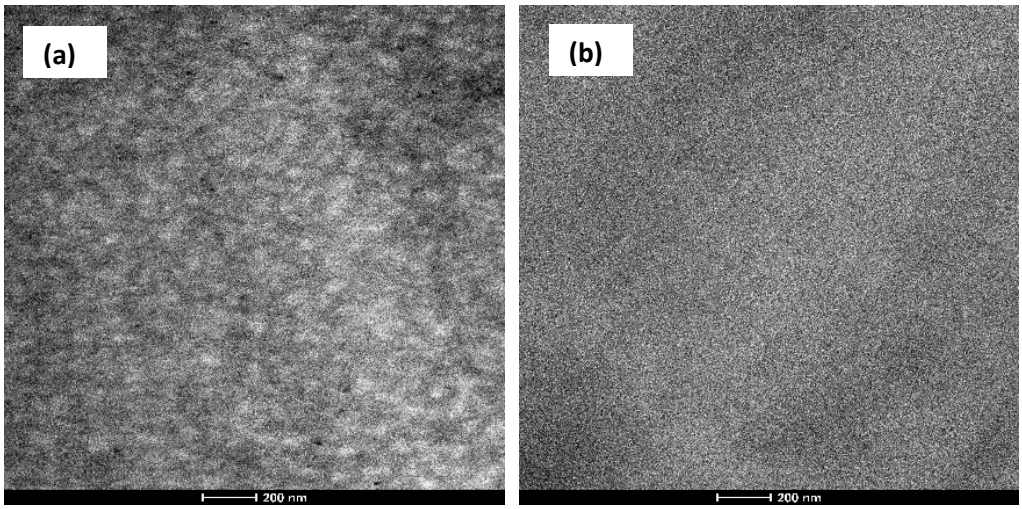

Figure 6.7. The TEM micrographs of the coating cross-section for the PU/poly(meth)acrylic hybrids with no functional monomer (left-a) and with GMMA (right-b)- synthesized in batch mode

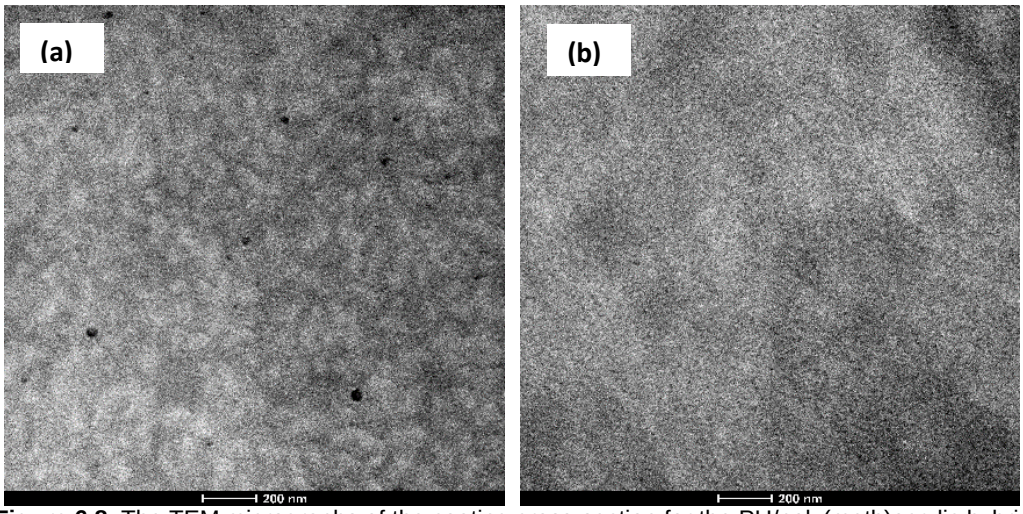

Figure 6.8. The TEM micrographs of the coating cross-section for the PU/poly(meth)acrylic hybrids with no functional monomer (left-a) and with GMMA (right-b)- synthesized in semibatch mode

The AFM height and phase images of the film-air interface for the prepared coating synthesized in batch and semibatch modes are shown in Figures 6.9 and 6.10, respectively.

As can be seen in the height images (left), in all cases, the acrylic domains (bright) are homogeneousely dispersed in PU matrix (dark). The AFM phase images (right) display that the surface of the film cast from grafted hybrids (Figures 6.9(b)right and 6.10(b)right) are smoother than the ones without functional monomer (Figures 6.9(a)right and 6.10(a)right) for both batch and semibatch modes most likely due to the lower phase separation between PU and (meth)acrylic domains for grafted hybrids. On the other hand, the comparison of the hybrid films synthesized in batch and semibatch mode showed smoother surface for the hybrids from batch mode which is most probably due to the narrower particle size distribution (Figure 6.5) and better film formation.

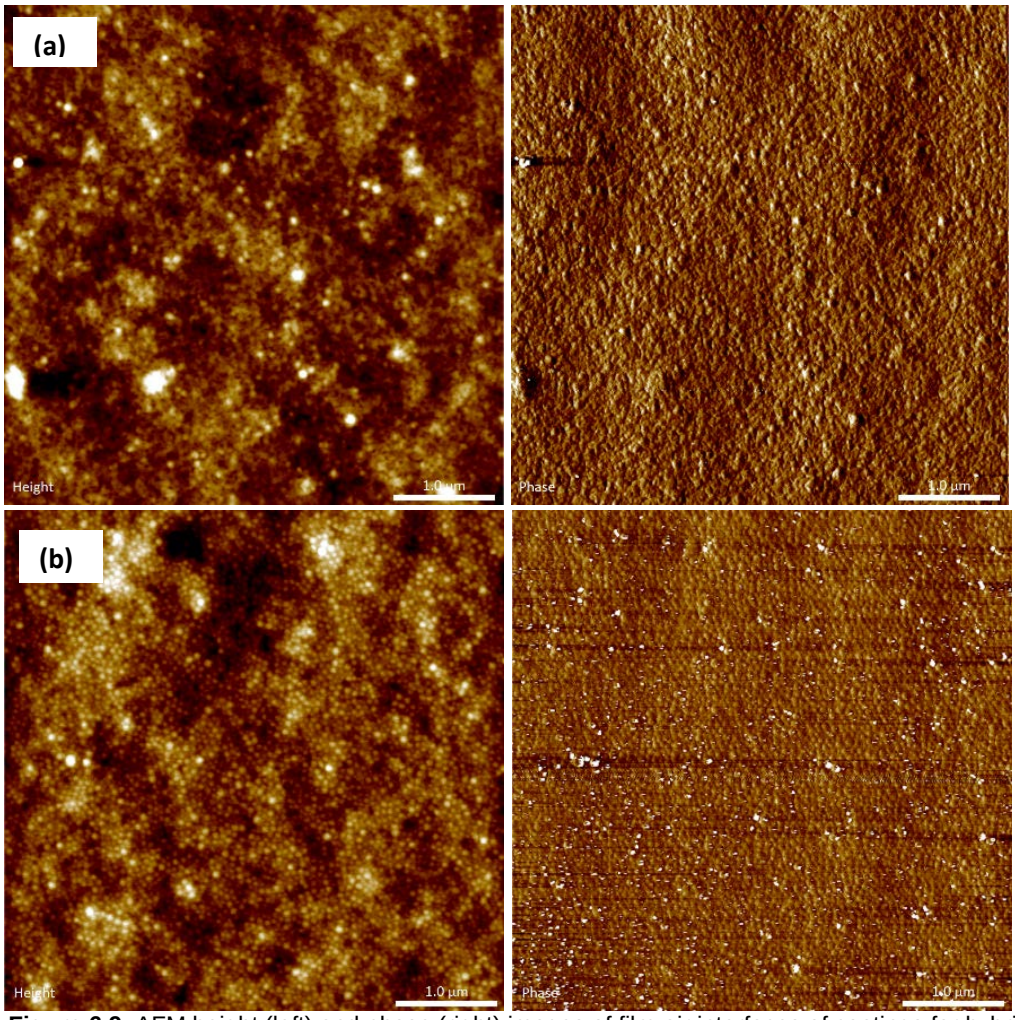

Figure 6.9. AFM height (left) and phase (right) images of film-air interfaces of coatings for hybrids synthesized in batch polymerization prepared by spin coating with no functional monomer (a) and with GMMA (b)

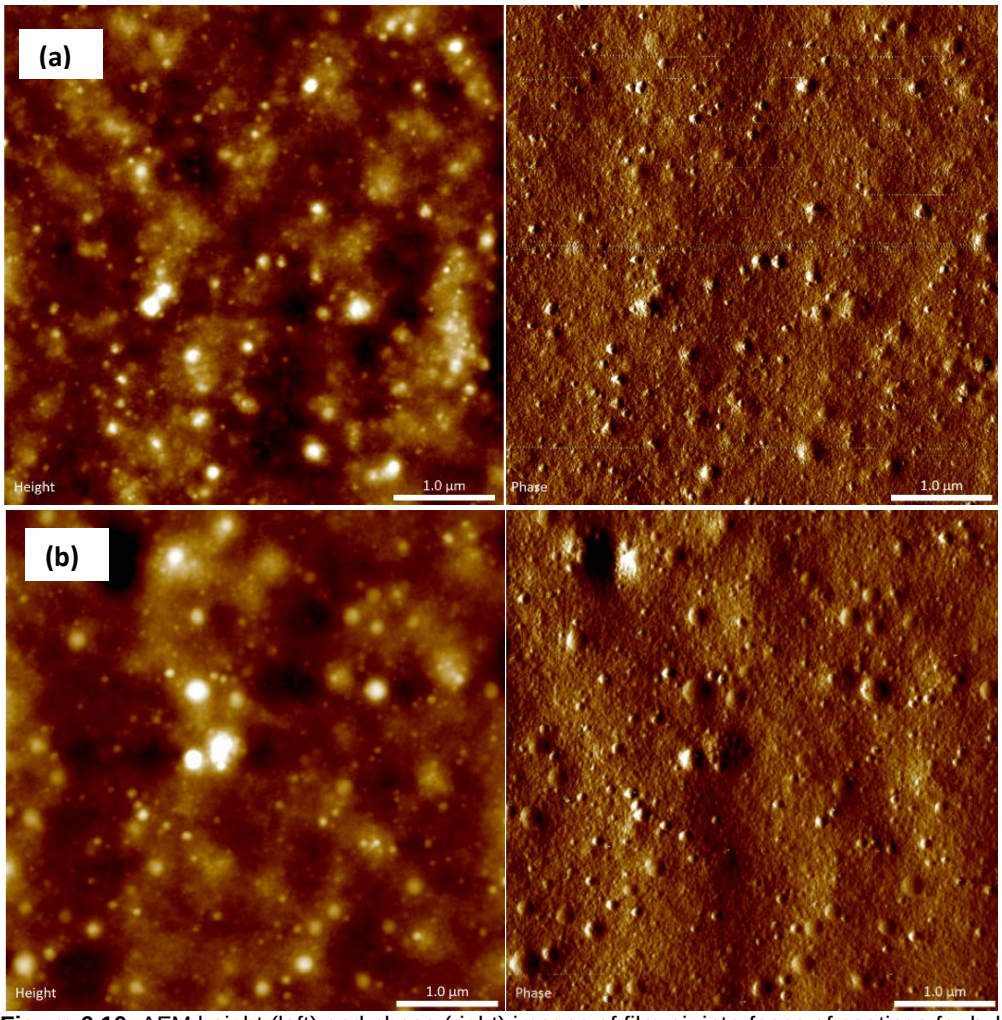

Figure 6.10. AFM height (left) and phase (right) images of film-air interfaces of coatings for hybrids synthesized in semibatch polymerization prepared by spin coating with no functional monomer (a) and with GMMA (b)

6.3.3. Evaluation of the performance of PU/(meth)acrylic hybrid dispersions for wood floor coating application

6.3.3.1. Mechanical properties

The mechanical properties of the formulated coating films cast at ambient temperature were analyzed using dynamic mechanical thermal analysis (DMTA) and tensile measurements.

The DMTA of the formulated coating films from hybrids synthesized in batch and semibatch mode are shown in Figures 6.11(a) and 6.11(b), respectively. Tan δ of all the hybrids showed two transitions, a sharp one around 37 to 42 ºC corresponding to MMA/BA copolymer and a weak transition around -18 ºC corresponding to PU. For the coatings synthesized in batch (Figure 6.11(a)), the storage modulus of the grafted hybrids was higher than the one without functional monomer at room temperature which is in agreement with the tensile test (see below). Moreover, the grafted hybrids with GMMA and Laromer showed a plateau in the rubbery part indicating more crosslinking. For the hybrids synthesized in semibatch mode (Figure 6.11(b)), the storage modulus of all the hybrids were similar, but the grafted hybrids with GMMA showed a plateau in the rubbery region indicating more crosslinking.

The DMTA curve for PU/PMMA-PBA is also shown in Figure 6.11(c). A weak and broad transition between -25 ºC to +40 ºC and a sharp peak around +100 ºC was observed. Moreover, the storage modulus of the PU/PMMA-PBA film was higher than the PU/P(MMA/BA) likely due to the presence of hard PMMA domains. Figure 6.11(d) presents

the DMTA curve for the reference coating with a weak transition at low temperature and two sharp transitions at higher temperatures.

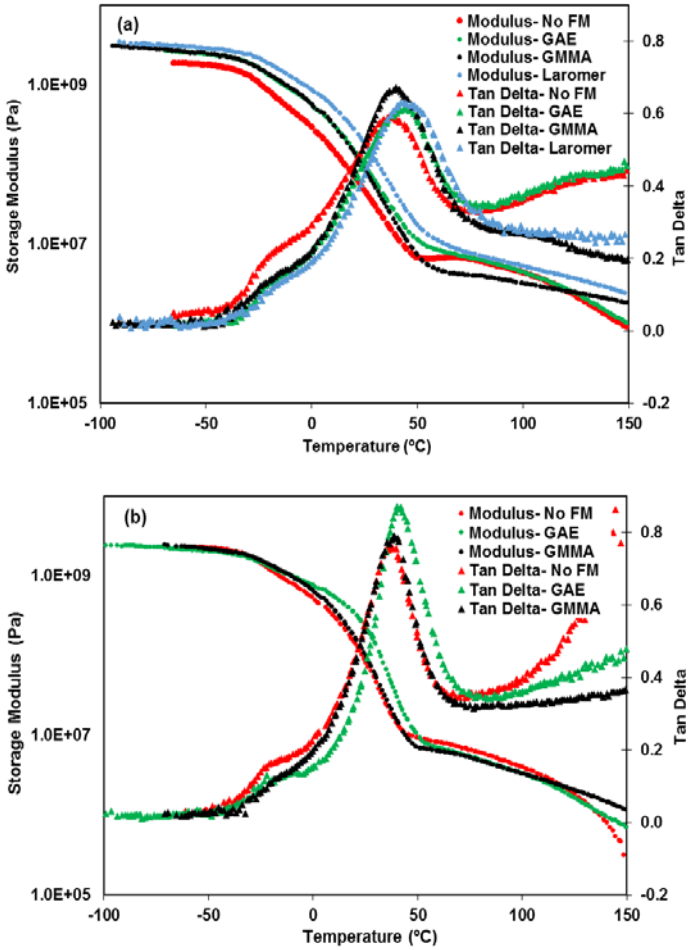

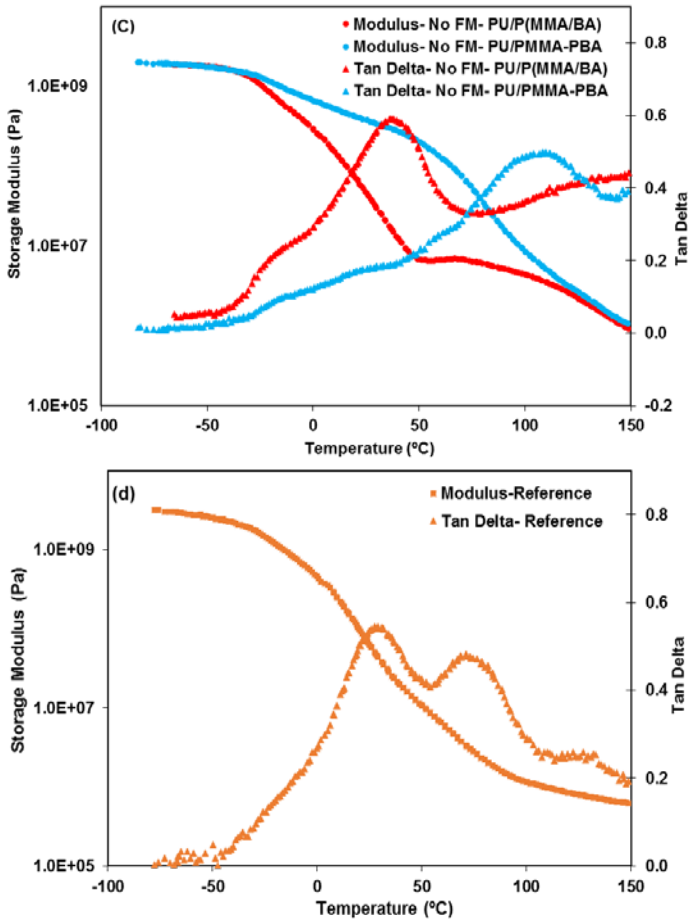

Figure 6.11. Dynamic mechanical analysis of the coatings synthesized in batch mode (a), semibatch mode (b), PU/PMMA-PBA (c) and reference hybrid (d)

The T_g of the coatings obtained from DSC and DMTA analysis are summarized in Table 6.4. Comparing theses value with the T_gs from films directly cast from the hybrids (Table 6.2), the T_gs of the prepared coatings shifted towards lower values for all the coatings as some amount of coalescent and thickener was added to the hybrids in the coating preparation. The differences in the T_g values obtained in DSC and DMTA measurements could be because of the difference in their characterization methods.

Table 6.4. The glass transition temperature (T_g) of the prepared coatings from PU/(meth)acrylic hybrids

Polymerization Mode	Functional Monomer (FM)	T_g (ºC) Obtained from DSC		T_g (ºC) Obtained from DMTA		
		T_{g1} (ºC)	T_{g2} (ºC)	T_{g1} (ºC)	T_{g2} (ºC)	T_{g3} (ºC)
Batch	-	-32	31	-18	38	-
	GAE	-30	27	-18	42	-
	GMMA	-31	25	-18	39	-
	Laromer	-32	29	-18	42	-
Semibatch	-	-32	23	-18	37	-
	GAE	-31	24	-18	40	-
	GMMA	-31	25	-18	38	-
PU/PMMA-PBA	-	-33	83	-18	102	-
Reference		-32	66	-25	28	73

Table 6.5 summarizes the mechanical properties of the coatings from tensile measurement. Figure 6.12(a) shows the stress-strain curves for the coatings from the hybrids synthesized in batch and seeded semibatch using different functional monomers. For the films cast from batch hybrids (solid lines), the Young's modulus (the slope obtained at low strains), yield stress (the stress at beginning of plastic region) and ultimate strength (the stress at break) increased and the elongation at break decreased as grafting increased. This effect was more pronounced in the case of GMMA as it has the highest degree of grafting and gel content. The hybrids synthesized in semibatch mode (dashed lines) followed the same trend with the highest Young's modulus and yield stress for the film with GMMA and the lowest for the film with no functional monomer. The comparison of the hybrids synthesized in batch and semibatch modes shows that for the hybrids with no functional monomer, the film from semibatch mode was a bit softer. This is likely a result of the copolymer containing a fraction of PMMA rich chains in batch polymerization. When GMMA was used, slightly higher Young's modulus was observed in the batch mode likely due to its higher gel content. Alternatively, in

the case of GAE, the hybrid synthesized in semibatch was stiffer as it has higher gel content than the one in batch. The obtained results shows that the difference in the mechanical properties of the coatings formulated from batch and semibatch hybrids is mainly due to the grafting efficiency and gel content. The small changes in the structure of MMA/BA copolymer caused by the process (batch vs. semibatch) were of less importance. It is worth pointing out that the reference sample was stiffer and had higher Young's modulus and yield stress than all the PU/P(MMA/BA) films. This is due to higher T_g of the reference (Table 6.2) which led to stiffer film.

Figure 6.12(b) presents the stress-strain behavior of the coatings from the PU/PMMA-PBA hybrid. The comparison with the PU/P(MMA/BA) films shows that the coating from PU/PMMA-PBA hybrid had much higher Young's modulus and yield stress. As it was discussed in Chapter 5, this is due to the hard PMMA chains that improved the mechanical properties of the polymer films. Moreover the elongation at break was only slightly lower than most of the hybrids. This result shows that the feeding strategy of (meth)acrylic monomers influences the final coating performance more than the grafting. The interesting mechanical properties of the PU/PMMA-PBA comes from the presence of hard PMMA and soft PBA and PU which led to the polymer film with higher Young´s modulus and yield stress as well as similar elongation at break compared to the other hybrids. The comparison of the reference and PU/PMMA-PBA film shows that they have similar Young´s modulus but the yield stress and the elongation of the PU/PMMA-PBA was higher than the reference as it has higher T_g.

It is worth pointing out that the comparison of the observed stress-strain behavior of the films in this chapter and those from the Chapters 3, 4 and 5, shows that the effect of

grafting on the mechanical properties seems to be more pronounced when the two phases (PU/(meth)acrylcis) are harder. In this chapter, the microstructure of the PU was harder using polyester polyol and harder chain extender compared to the other chapters. In addition, in the /(meth)acrylic part, the MMA/BA proportion was 70/30 wt/wt which resulted in hard polymer.

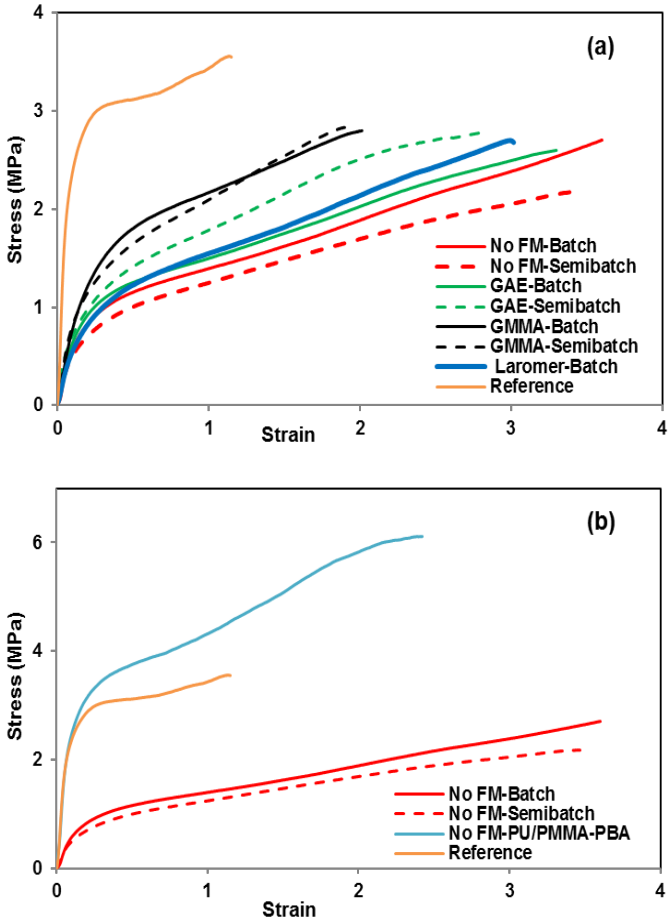

Figure 6.12. Stress-strain behavior of coatings formulated from: (a) PU/P(MMA/BA) synthesized in batch and semi batch mode; (b) PU/PMMA-PBA

Table 6.5. Mechanical properties of the coatings cast at ambient temperature.

Polymerization Mode	Functional Monomer (FM)	Young´s Modulus MPa/100	Yield Stress (MPa)	Elongation at break	Ultimate Strength (MPa)	Toughness (MPa)
Batch	-	0.09 ± 0.01	1.17 ± 0.19	3.59 ± 0.22	2.7 ± 0.1	6.35 ± 1.04
	GAE	0.08 ± 0.01	1.21 ± 0.27	3.30 ± 0.35	2.6 ± 0.2	5.94 ± 1.18
	GMMA	0.09 ± 0.01	1.63 ± 0.35	2.01 ± 0.11	2.8 ± 0.2	4.12 ± 0.78
	Laromer	0.07 ± 0.01	1.19 ± 0.13	3.01 ± 0.34	2.7 ± 0.2	5.37 ± 1.22
Semibatch	-	0.07 ± 0.01	0.99 ± 0.08	3.39 ± 0.25	2.2 ± 0.1	5.28 ± 1.05
	GAE	0.08 ± 0.01	1.28 ± 0.24	2.80 ± 0.15	2.8 ± 0.2	5.59 ± 0.44
	GMMA	0.10 ± 0.01	1.58 ± 0.34	1.90 ± 0.21	2.8 ± 0.1	3.90 ± 0.90
PU/PMM-PBA	-	0.40 ± 0.03	3.32 ± 0.40	2.44± 0.34	6.1 ± 0.4	10.99 ± 1.53
Reference		0.41 ± 0.04	3.12 ± 0.35	1.14 ± 0.13	3.5 ± 0.3	3.44 ± 1.31

6.3.3.2. Gloss

In terms of visual appearance, gloss is one of the key features of hardwood floor coatings. Gloss is related to the ability of a surface to direct reflect light and it is measured at different angles of incidence. More details on the test is given in Appendix II. Table 6.6 presents the gloss values at 20º and 60º for the coatings cast at ambient temperature. As can be seen, the values of gloss were lower in the absence of functional monomer and it was the highest for the grafted hybrids with GMMA. This is likely because of the higher compatibility of polymers in the film that led to smaller domains in the film and therefore less scattering. Moreover, the hybrids synthesized in batch system showed higher gloss than the ones in semibatch. The reason is probably the more homogeneous and narrow particle size distribution in batch mode (Table 6.2) that resulted in smaller domains in the film and therefore less scattering. It is worth mentioning that the grafted coatings in batch had similar gloss value to the reference coating.

Table 6.6. The gloss at 20º and 60º of the coatings cast on leneta substrate at ambient temperature

Polymerization Mode	Functional Monomer (FM)	Gloss after 1 day of drying (GU)	
		20º	60º
Batch	-	8.0	37.0
	GAE	11.8	44.3
	GMMA	17.4	50.9
	Laromer	11.4	43.6
Semibatch	-	4.5	28.1
	GAE	7.0	35.6
	GMMA	9.3	39.9
PU/PMMA-PBA	-	8.6	38.7
Reference		13.1	45.4

6.3.3.3. Chemical resistance

The chemical resistance of the coating is important especially for wood applications, where furniture coatings must be particularly resistant to various types of stains. Polymer films are chemically attacked in three ways [28]. First, there is permeation through the film to attack the interfacial bond between the substrate and the coating. The second attack mechanism is through physical failure, due to the loss of polymer particles or molecules that are carried away. The third attack is by chemical degradation, whereby the polymer is attacked by the chemical to break crosslinks and decrease the molecular weight. Chemicals may also attack the coating by completely different (even unknown) mechanisms. Therefore sometimes it is difficult to define the actual chemicals involved in some chemicals for example mustard or lipstick stains or attack from other household supplies [28].

The chemical resistance of the coatings against some common chemicals was evaluated in this work (details are given in Appendix II). The chemical resistance of the coatings cast on melamine wood substrate is presented in Figure 6.13. The general observation was that the coatings had similar resistance against most of the chemicals and also comparable with the reference coating. Interestingly the resistance against water and red wine for all the hybrids was higher than the reference. As can be seen in Figure 6.14, the surface coated with the reference was damaged after exposure with water and red wine whereas it was not the case for the coatings prepared from hybrids. The acetone resistance was slightly better for the PU/PMMA-PBA, GMMA-batch, GMMA-semibatch and no functional monomer-semibatch. The reason is not very clear as different parameters may affect the chemical resistance. Wegmann [29] reported that the chemical resistance of waterborne epoxy/ amine coatings was influenced by several parameters such as the hydrophilic surfactants, dry-film thickness, drying/curing temperature and film coalescence (microstructure in the film). Moreover it was reported that the crosslinked PUs had better chemical resistance compared to less crosslinked structure [30,31]. The difference in the resistance to acetone for coatings with GMMA perhaps is related to the film coalescence and crosslinking. On the other hand, the ethanol resistance of the GMMA-batch and Laromer-batch was slightly lower than for the other coatings. Therefore it seems that in this case the crosslinking and high gel content did not favor the ethanol resistance. It is worth pointing out that the chemical resistance test is a qualitative test based on the observation of the operator. Therefore it is always subjected to some error.

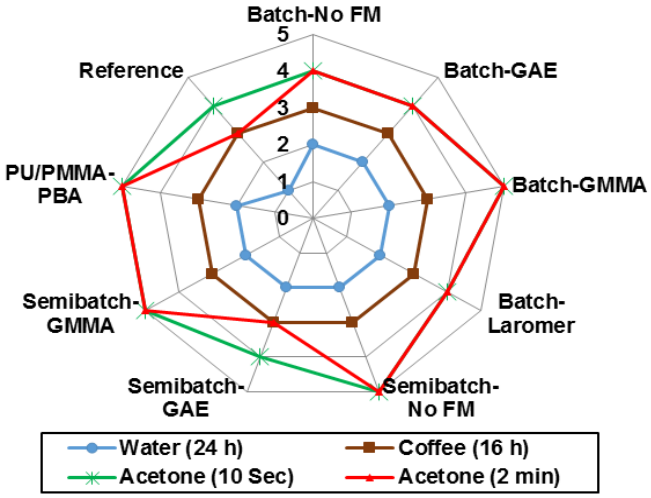

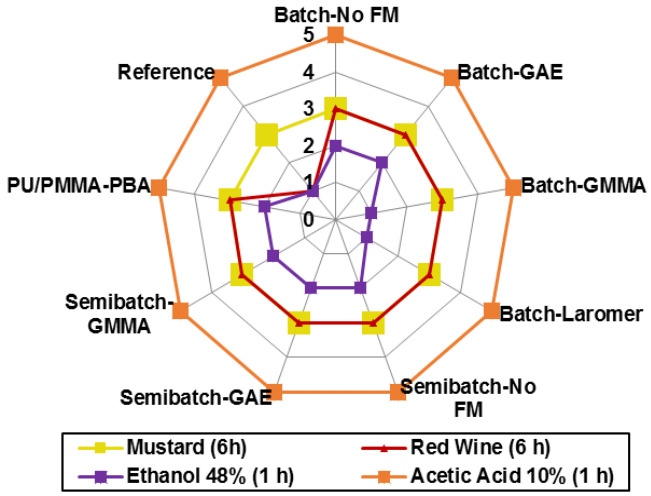

Figure 6.13. Chemical resistance of the prepared coatings cast on melamine wood substrate

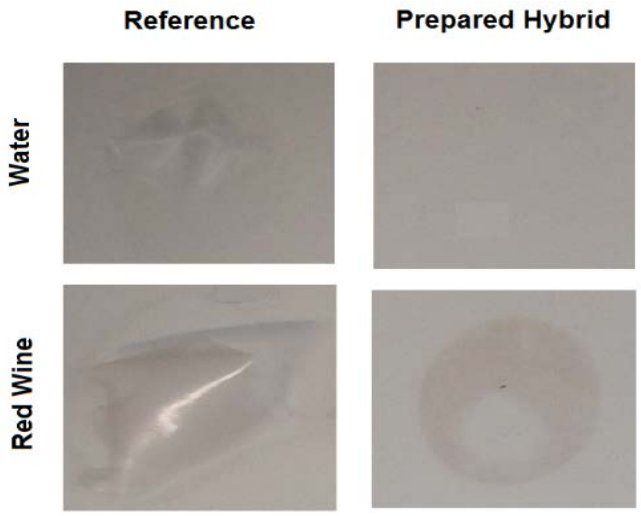

Figure 6.14. The coated melamine substrate with the coatings after chemical resistance test, reference (left), prepared hybrid (right)

6.3.3.4. Hardness

Hardness is described as the property of a coating which is manifested in the resistance of the coating to a mechanical action such as pressure, friction or scratching [32]. Figure 6.15 presents the evolution of pendulum hardness with time for the coatings synthesized in batch (Figure 6.15(a)) and semibatch mode (Figure 6.15(b)). The trend showed the typical increase during drying time for the two polymerization modes (batch and semibatch). The hardness increased with grafting for both batch and semibatch mode, especially in the case of GMMA. The correlation between the mechanical properties and pendulum hardness of the polymer films is well-known [33,34]. It was reported that the film with higher mechanical properties (Young´s modulus) has higher hardness. Therefore, the increase in the pendulum harness with grafting is due to the reinforcing mechanical properties with grafting (Figure 6.12). On

the other hand, the comparison of the coatings synthesized in batch and semibatch system shows that the pendulum hardness was higher for the semibatch system. The reason for that is not clear, but it might be related to the differences in the microstructure of the polymers or in the morphology of the film surface.

The evolution of pendulum hardness for the PU/PMMA-PBA coating is shown in Figure 6.15(c). It can be seen that higher pendulum hardness was observed compared to the PU/P(MMA/BA) coatings in batch and semibatch systems due to its higher mechanical properties. It is worth mentioning that the pendulum hardness of the reference was higher than all the hybrids except the one with GMMA in semibatch, which has a similar value. The reason is not clear as the composition of the reference is not known.

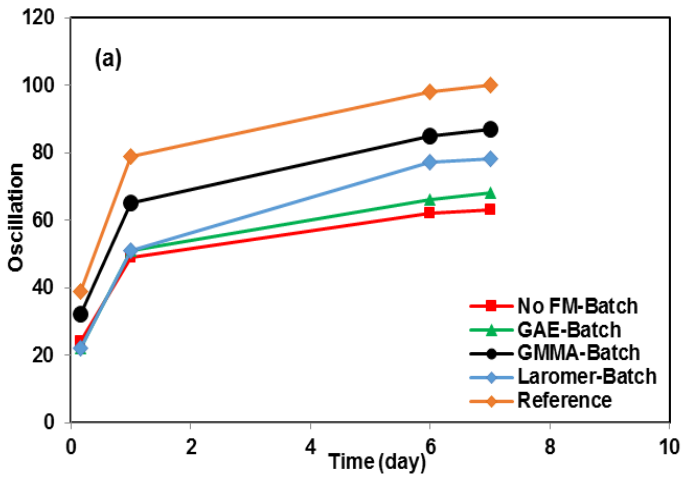

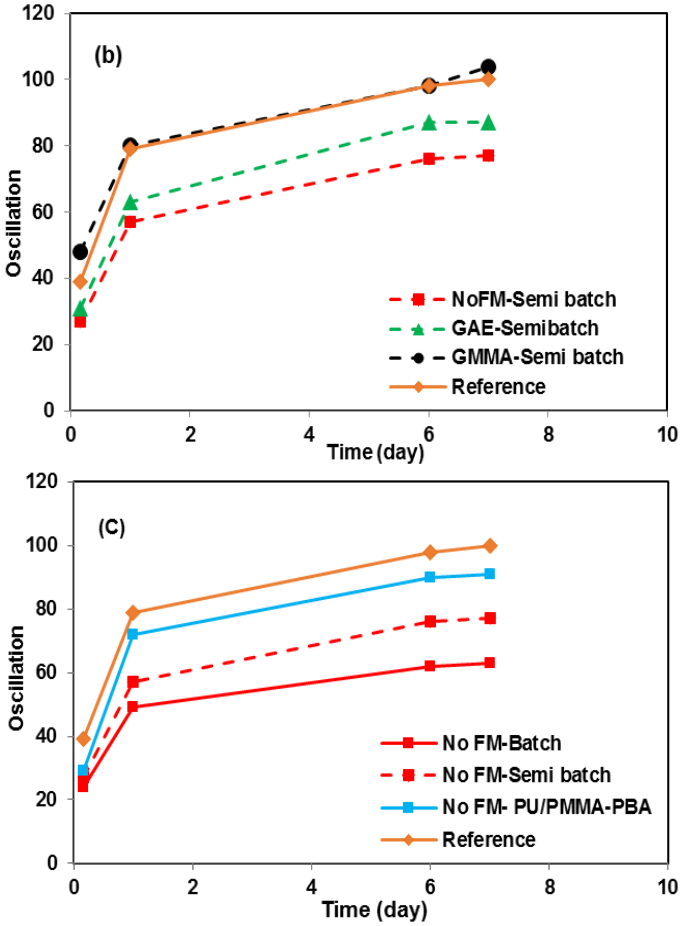

Figure 6.15. Evolution of pendulum hardness for hybrid coatings of PU/P(MM/BA) synthesized in Batch (a) and semi batch (b) – for PU/PMMA-PBA (c)

6.3.3.5. Abrasion resistance

Resistance to abrasion is one of the most significant mechanical properties of any surface. The abrasion resistance of coatings provides information about the ability to withstand abrasive materials such as sand and chippings, as well as scouring brushes. The use of the Taber Abraser is among the most commonly used and best-known methods for testing durability and resistance to wear. The wearing action is caused by two abrasive wheels

with defined applied pressure to the coating. A detailed description of the test is given in Appendix II.

The polymer weight loss during abrasion test is presented in Figures 6.16(a) and 6.16(b) for the hybrids synthesized in batch and semibatch, respectively. For the hybrids prepared in batch there was no correlation between abrasion resistance and polymer characteristics as the best behavior was offered by the hybrid prepared without functional monomer (no gel) but the second best was the one that had the highest gel fraction (GMMA-batch). All batch hybrids were better than the reference. On the other hand, for the semibatch hybrids abrasion resistance decreased with the gel content. However, no similar correlation between abrasion resistance and gel content can be established because the semibatch hybrids had lower gel content and worse abrasion resistance than the batch ones. This illustrates the challenge of linking polymer characteristics and macroscopic properties.

Xiao *et al.* [35] investigated the relationship between mechanical properties (tensile test, compression test and DMTA) and scratch resistance of a variety of PU films synthesized with different soft segment polyols. They reported that in PU films with higher Young´s and compressive modulus and yield stress the start of scratching occurred in higher scratching (abrasion) forces. Moreover, it was observed that when the film was scratched, the amount of sample removal during the test was higher for the films with higher mechanical properties and therefore their abrasion resistance was lower. However, the batch hybrids synthesized in this chapter behave differently as the one with highest modulus and yield stress (GMMA batch) performed better at high number of cycles. However, for GMMA the type of process (batch vs semibatch) did not bring any significant difference in terms of Young´s modulus and

yield stress (Table 6.5) but the abrasion resistance of PU/PMMA-PBA was worse than that of the reference (Figure 6.16(c)), which is aligned with Xiao´s results.

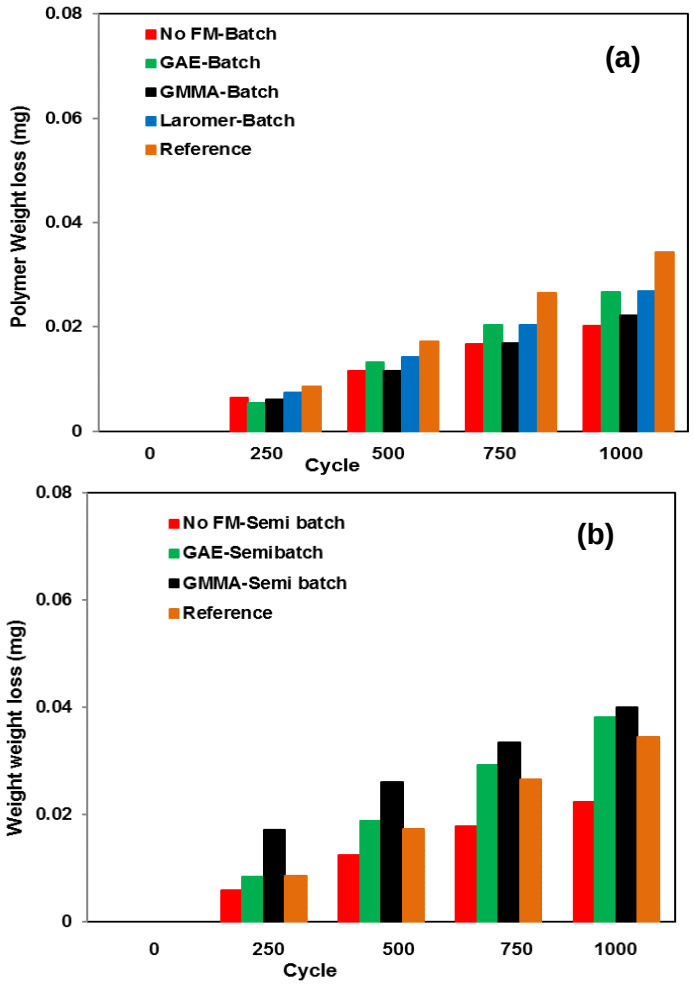

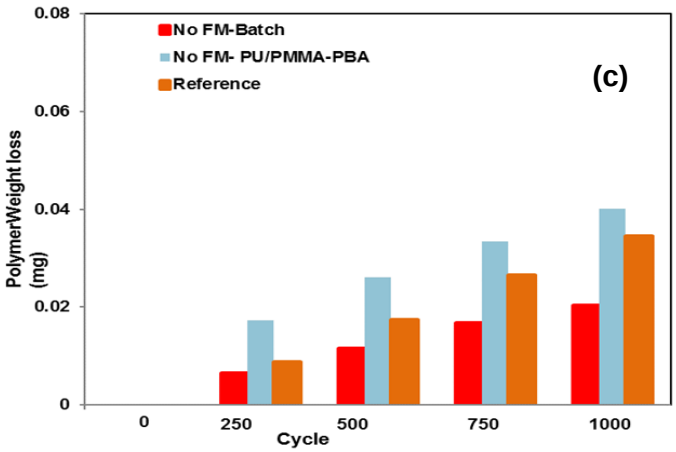

Figure 6.16. Polymer weight loss during Taber abrasion test for hybrid coatings of PU/P(MMA/BA) synthesized in Batch (a) and semi batch (b) -for PU/PMMA-PBA (c)

6.4. Conclusions

PU/(meth)acrylic hybrid dispersions for wood floor coating applications were synthesized using two different methods. In the first method, solvent-free hybrids were synthesized using (meth)acrylic monomers as solvents in the synthesis of the PU and later polymerizing the monomers in batch. In the second one, first the PU dispersion was synthesized using a solvent (MEK) method and then, the (meth)acrylic monomers were fed to the dispersion and polymerized in semibatch mode. In addition, one experiment was done using MMA as solvent to produce a PU and then BA was fed to prepare a PU/PMMA-PBA hybrid.

Three different functional monomers were used in order to graft PU into (meth)acrylics; Glycerol mono-allyl ether (GAE), Glycerol mono methacrylate (GMMA) and Laromer (diacrylate). No gel was formed in the absence of functional monomer. The gel content of the

grafted hybrids using GMMA was the highest, and it was the lowest for those with allyl ether (that is less reactive). In the case of Laromer, as it has two vinyl functionalities in the structure, the number of moles of Laromer in the formulation was half of those of GMMA and GAE and therefore a fraction of the PU chains did not contain any Laromer units and this led to obtain lower gel fraction than GMMA. The molar mass distribution (MMD) of the whole hybrid polymers (gel+sol) analyzed with AF_4 technique showed that the microstructure of the gel fraction from the grafted hybrids with different functional monomers was different. The molar mass of the gel fraction of the hybrid with GAE was lower than those with GMMA and Laromer as a result of less grafting and crosslinking. Comparing the hybrids with GMMA and Laromer, the one with Laromer yielded a gel with higher molar masses than for GMMA (although in the case of Laromer, the fraction of PU chains with double bonds was smaller, in those having double bonds the number of double bonds per chain was higher than for GMMA).

Moreover, the mode of polymerization of (meth)acrylates (batch *vs* semibatch) affected the gel content. In the semibatch polymerization the gel content dropped for the more reactive functional monomer (GMMA) as it was consumed rapidly and did not react with the (meth)acrylic monomers that were fed at later stages of the feeding time. However, for the least reactive one (GAE), the gel content in semibatch mode increased due to the higher possibility of the reaction of the slow allyl group with (meth)acrylic monomers. The degree of grafting was quantified using the UV signal of SEC. The highest value was obtained for GMMA and the lowest value in the case of GAE (less reactive functional monomer).

For both batch and semibatch series, the TEM images of grafted PU/(meth)acrylic particles and film cross-section showed more homogeneous particle and film morphologies compared to non-grafted hybrids indicating less phase separation as a result of grafting.

The performance of the coatings prepared from the hybrids was evaluated in terms of mechanical properties, gloss, hardness, chemical resistance and abrasion resistance and they were compared with a commercially available coating that was taken as reference (however its T_g was higher than the synthesized hybrids). It was observed that with grafting the Young´s modulus and yield stress increased and the elongation at break decreased. This effect was more pronounced in the case of GMMA due to the higher gel content. The PU/PMMA-PBA hybrid gave the highest Young´s modulus and yield stress with the elongation at break similar to the PU/P(MMA/BA) hybrids due to the presence of hard (PMMA) and soft (PBA and PU) domains.

With grafting, the gloss value increased due to higher compatibility of two phases in the films which led to smaller domains and less scattering. The coating from batch system showed higher gloss than the ones in semibatch likely because of the narrower particle size distribution.

All the coatings showed acceptable chemical resistance and better water and red wine resistance than the reference coating. The pendulum hardness of the coatings prepared from the hybrids synthesized in batch increased with grafting due to the increase in the Young´s modulus with grafting. A similar trend was observed for the ones synthesized *via* semibatch, however, they had higher pendulum hardness compared to the ones in batch. The results of the abrasion resistance showed no clear trend with the polymer characteristics. The coatings

with no functional monomer had better abrasion resistance than the grafted ones. Moreover, the abrasion resistance of PU/PMMA-PBA coating was worse than the PU/P(MMA/BA) ones due to the hard PMMA domains that made the polymer film easier to remove upon scratching.

Finally, it can be concluded that solvent-free and emulsifier free PU/(meth)acrylic hybrid dispersions were prepared for wood floor coating applications with comparable final properties to a commercially available reference coating even though their T_g was lower.

6.5. References

[1] T. Gomi, K. Sakata, I. Aoyama, N. Sono, Coating composition, US4622360A, 1986.

[2] C. Irle, W. Kremer, G. Ruf, R. Roschu, Polyurethane dispersions, US6559225B1, 2003.

[3] F.L. Granizo, Polyurethane-acrylic polymer dispersions and uses thereof, WO2011000935 A1, 2011.

[4] M.C. Schrinner, C. Irle, M. Melchiors, G.M. ALMATÓ, E. TEJADA, Use of an aqueous preparation for the coating of wood surfaces to achieve a natural-touch effect, WO2012130764 A1, 2012.

[5] A. Noreen, K.M. Zia, M. Zuber, S. Tabasum, M.J. Saif, Recent trends in environmentally friendly water-borne polyurethane coatings: A review, Korean J. Chem. Eng. 33 (2016) 388–400.

[6] Z.W. Wicks, F.N. Jones, S.P. Pappas, D. a Wicks, Binders Based on Polyisocyanates: Polyurethanes, in: Org. Coatings, John Wiley & Sons, Inc., Hoboken, NJ, USA, 2006: pp. 231–270.

[7] R. Thomas Gray, J. Lee, Method for increasing the open time of aqueous coatings, US6303189 B1, 2001.

[8] L. Wu, B. You, D. Li, Synthesis and characterization of urethane/acrylate composite latex, J. Appl. Polym. Sci. 84 (2002) 1620–1628.

[9] D. Kukanja, J. Golob, A. Zupancic-valant, M. Krajnc, The structure and properties of acrylic-polyurethane hybrid emulsions and comparison with physical blends, J. Appl.

Polym. Sci. 78 (2000) 67–80.

[10] S. Chen, L. Chen, Structure and properties of polyurethane/polyacrylate latex interpenetrating networks hybrid emulsions, Colloid Polym. Sci. 282 (2003) 14–20.

[11] R.A. Brown, R.G. Coogan, D.G. Fortier, M.S. Reeve, J.D. Rega, Comparing and contrasting the properties of urethane/acrylic hybrids with those of corresponding blends of urethane dispersions and acrylic emulsions, Prog. Org. Coatings. 52 (2005) 73–84.

[12] C. Wang, F. Chu, C. Graillat, A. Guyot, C. Gauthier, J.P. Chapel, Hybrid polymer latexes: Acrylics-polyurethane from miniemulsion polymerization: Properties of hybrid latexes versus blends, Polymer (Guildf). 46 (2005) 1113–1124.

[13] M. Hirose, F. Kadowaki, J. Zhou, The structure and properties of core-shell type acrylic-polyurethane hybrid aqueous emulsions, Prog. Org. Coatings. 31 (1997) 157–169.

[14] J.I. Amalvy, A kinetic study in emulsion polymerization of polyurethane-acrylate hybrids, Pigment Resin Technol. 31 (2002) 275–283.

[15] A.C. Aznar, O.R. Pardini, J.I. Amalvy, Glossy topcoat exterior paint formulations using water-based polyurethane/acrylic hybrid binders, Prog. Org. Coatings. 55 (2006) 43–49.

[16] H.T. Zhang, R. Guan, Z.H. Yin, L.L. Lin, Soap-free seeded emulsion copolymerization of MMA onto PU-A and their properties, J. Appl. Polym. Sci. 82 (2001) 941–947.

[17] R. Shi, X. Zhang, J. Dai, Synthesis of TDI-Polyurethane/Polyacrylate Composite Emulsion by Solvent-free Method and Performances of the Latex Film, J. Macromol. Sci. Part A. 50 (2013) 350–357.

[18] L. Zhao, S.N. Sauca, C. Berges, Aqueous polyurethane acrylate hybrid dispersions, EP 3067399 A1, 2016.

[19] T. Yi, G. Ma, C. Hou, S. Li, R. Zhang, J. Wu, X. Hao, H. Zhang, Polyurethane-acrylic hybrid emulsions with high acrylic/polyurethane ratios: Synthesis, characterization, and properties, J. Appl. Polym. Sci. 44488 (2016) 1–9.

[20] R. Ballestero, B.M. Sundaram, H. V. Tippur, M.L. Auad, Sequential graft-interpenetrating polymer networks based on polyurethane and acrylic/ester copolymers, Express Polym. Lett. 10 (2016) 204–215.

[21] J.W. Gooch, H. Dong, F.J. Schork, Waterborne oil-modified polyurethane coatings via hybrid miniemulsion polymerization, J. Appl. Polym. Sci. 76 (2000) 105–114.

[22] H. Wang, M. Wang, X. Ge, Graft copolymers of polyurethane with various vinyl monomers via radiation-induced miniemulsion polymerization: Influential factors to grafting efficiency and particle morphology, Radiat. Phys. Chem. 78 (2009) 112–118.

[23] Y. Lu, R.C. Larock, New hybrid latexes from a soybean oil-based waterborne

polyurethane and acrylics via emulsion polymerization, Biomacromolecules. 8 (2007) 3108–3114.

[24] M. Goikoetxea, R.J. Minari, I. Beristain, M. Paulis, M.J. Barandiaran, J.M. Asua, Polymerization kinetics and microstructure of waterborne acrylic/alkyd nanocomposites synthesized by miniemulsion, J. Polym. Sci. Part A Polym. Chem. 47 (2009) 4871–4885.

[25] Z.W. Wicks, F.N. Jones, S.P. Pappas, D.A. Wicks, Organic Coatings: Science and Technology, 3rd editio, Wiley, Hoboken, NJ, USA, 2007.

[26] C. Hepburn, Polyurethane Elastomers, Springer Netherlands, Dordrecht, 1992.

[27] O. Elizalde, G.P. Leal, J.R. Leiza, Particle Size Distribution Measurements of PolymericDispersions: A Comparative Study, Part. Part. Syst. Charact. 17 (2000) 236–243.

[28] R.D. Athey, Testing coatings for solvent and chemical resistance, Met. Finish. 108 (2010) 359–362.

[29] A. Wegmann, Chemical resistance of waterborne epoxy/amine coatings, Prog. Org. Coatings. 32 (1997) 231–239.

[30] M. Melchiors, M. Sonntag, C. Kobusch, E. Jürgens, Recent developments in aqueous two-component polyurethane (2K-PUR) coatings, Prog. Org. Coatings. 40 (2000) 99–109.

[31] T.S. Velayutham, W.H.A. Majid, A.B. Ahmad, G.Y. Kang, S.N. Gan, Synthesis and characterization of polyurethane coatings derived from polyols synthesized with glycerol, phthalic anhydride and oleic acid, Prog. Org. Coatings. 66 (2009) 367–371.

[32] A. Goldschmidt, H.-J. Streitberger, BASF handbook on Basics of coating technology, Second, Vincentz Network, Hannover, 2007.

[33] K. Sato, The hardness of coating films, Prog. Org. Coatings. 8 (1980) 1–18.

[34] E. Mehravar, J. Leswin, B. Reck, J.R. Leiza, J.M. Asua, Waterborne paints containing nano-sized crystalline domains formed by comb-like polymers, Prog. Org. Coatings. 106 (2017) 11–19.

[35] S. Xiao, M.M. Hossain, P. Liu, H. Wang, F. Hu, H.J. Sue, Scratch behavior of model polyurethane elastomers containing different soft segment types, Mater. Des. 132 (2017) 419–429.

Chapter 7: Conclusions

This PhD thesis aimed at investigating the effect of grafting on particle and film morphology and final properties of solvent-free and emulsifier-free polyurethane (PU)/(meth)acrylic hybrid dispersions. The solvent-free process gives the advantage of avoiding the use of volatile organic compounds (VOC) in the synthesis of PU and hence the solvent removal step is eliminated, which is beneficial in terms of process cost and technical advances. A fundamental study on the effect of the main components of the hybrid on the polymer microstructure and final properties of polymer film was carried out with the aim of understanding the structure-property relationship of the hybrid. The polymer microstructure of PU/(meth)acrylic hybrids was modified through: i) grafting PU chains into the (meth)acrylics *via* incorporation of different functional monomers, ii) altering the PU chains by using different polyol types, and iii) altering the (meth)acrylic chains by using different (meth)acrylic monomer proportion.

The effect of the ionic content (controlled by the dimethylol propionic acid (DMPA) concentration) and the type of chain extenders (highly hydrophilic EDA, less hydrophilic DAO and the hydrophobic DAD) on the particle size and colloidal stability was investigated (Chapter 2). It was found that when using a hydrophilic chain extender, the DMPA content and the average particle size do not have a simple linear relationship as it is the case for the PU synthesized in solvent. The hydrophilic chain extender (EDA) promoted the formation of high amount of water soluble oligomers that are not favorable for particle stabilization as they migrate to the water phase and therefore are not available for particle stabilization. At high

DMPA content, coagulation of the hybrid dispersions occurred after the chain extension step. By increasing the hydrophobicity of the chain extenders (DAO and DAD) the systems became more stable and the DMPA content (and the particle size) could be varied in wider range. The chemical structure of the short chains in the PU prepolymer was analyzed by MALDI-TOF mass spectrometer and it was observed that the short chain in the PU prepolymer chains were not homogeneous in composition. Moreover, Monte Carlo based simulation confirmed the heterogeneity of PU prepolymer composition and it was shown that the heterogeneity mainly resulted from the stoichiometry (high concentration of isocyanate) without any significant effect of the reactivity of PPG and DMPA towards IPDI. The properties of the final films were influenced by the PU structure. The Young´s modulus and yield stress of the polymer films decreased with the length of the chain extender, likely because the hard segment of PU becomes softer for longer chain extenders. Furthermore, the films containing hydrophilic chain extender (EDA) were highly water sensitive and some chains were dissolved in the water during the test. Alternatively, in the case of more hydrophobic chain extenders (DAO and DAD), lower amount of polymer film was dissolved in the water during the test.

The effect of grafting of the PUs into the poly(meth)acrylics on the polymer microstructure, morphology and performance of the final film was studied in Chapter 3. Grafted PU/acrylic hybrid dispersions were synthesized using different types of functional monomers (glycerol mono-methacrylate (GMMA) and hydroxyethyl methacrylate (HEMA)). For the comparison purposes, experiments were carried out in the absence of functional monomer using butanediol in the case of GMMA and pentanol for HEMA. It was observed that the type of the functional monomer influenced the PU microstructure because GMMA is

a diol that extend the PU chains, whereas HEMA is monofunctional alcohol that rather terminates the PU chains. Therefore, the PUs synthesized with GMMA had higher molar mass and hence higher number of grafting point per PU chain than those with HEMA, indicating that for the hybrid with HEMA the grafting was less efficient and the polymer network was less crosslinked. The TEM images of grafted PU/(meth)acrylic particles and film cross-section showed more homogeneous particle and film morphologies compared to the non-grafted hybrids indicating less phase separation as a result of grafting. Despite the high grafting efficiency and the difference in the polymer microstructure, grafting with GMMA did not show the expected mechanical reinforcement. The hybrid with no GMMA (only butanediol) showed strain-hardening behavior likely due to the hydrogen bonding among the PU chains that act as physical crosslinker. The PU determined the properties of the polymer film as it was the continuous phase in the polymer film. Grafting-crosslinking between PU and poly(MMA-BA) provided additional stiffness to the film, but the increase was modest perhaps due to the loss of some hydrogen bonds among the PU chains that resulted from the interpenetration with the poly(meth)acrylates. In the alternative case with grafting using HEMA, the mechanical reinforcement due to grafting was more obvious. In this case, the short and low molar mass PU chains acted as plasticizer and with grafting the incorporation of these chains led to an improvement in the mechanical properties. The water sensitivity of the hybrids substantially decreased with grafting likely due to the increased grafting density that reduced the potential of the hybrid films to absorb water.

The nature of PU chains was varied by using different polyol types (polypropylene glycol (PPG), polytetrahydrofuran (PTHF), polyester and polycarbonate (PCD) in the PU

synthesis (Chapter 4). The effect of polyol type and grafting on the particle and film morphology and final film properties of the hybrids was investigated. It was observed that in the grafted hybrids, the type of polyol did not affect the observed gel content. The Young´s modulus and yield stress of the final film obtained from PCD and polyester polyols was higher than those with PTHF and PPG polyols due to the presence of carbonyl groups in the structure of PCD and polyester polyols. The films with higher Young´s modulus (the ones containing PCD and polyester polyols) had lower water uptake (higher water resistance) as the water absorption is more difficult in the harder polymer films. The particle and film morphology of the grafted hybrids were more homogeneous compared to the non grafted ones.

The (meth)acrylic chains were altered by using different proportion of (MMA/BA) ((0/100), (25/75), (50/50), (75/25) and (100/0) wt/wt) in the formulation, for grafted and non grafted hybrids (Chapter 5). The gel content of grafted hybrids increased with increasing the MMA proportion due to the combined effect of hydrogen abstraction from the PPG units and the fast consumption of GMMA in the beginning of the reaction where higher BA/MMA ratios were used, thus reducing the possibility of gel formation later in the reaction. Regarding the mechanical properties of the final films, it was found that with increasing the MMA/BA ratio, the Young´s modulus, yield stress and strain hardening of the film increased dramatically, but the elongation at break decreased. For grafted hybrids, the Young´s modulus and yield stress were slightly higher than those of non grafted PU/acrylic hybrids and the elongation at break was lower. This effect was more pronounced as the MMA/BA ratio increased due to the higher gel content and the higher T_g of the (meth)acrylate polymer. The particle and film morphology of the grafted hybrids was more homogeneous indicating less phase separation between PU

and (meth)acrylics. Regarding the water sensitivity, as the MMA/BA ratio in the formulation increased, the water uptake decreased because the diffusion of water is more difficult in the harder polymer films (higher MMA proportion) and the water uptake reached a plateau.

PU/(meth)acrylic hybrid dispersions were synthesized for wood floor coating applications (Chapter 6). Three functional monomers (containing two hydroxyl groups but different vinyl functionality) were used in order to graft PU into (meth)acrylics; Glycerol mono-allyl ether (GAE), Glycerol mono methacrylate (GMMA) and Laromer (diacrylate). The degree of grafting was quantified using the UV signal of size exclusion chromatography (SEC). The highest value was obtained for GMMA and the lowest value in the case of GAE (less reactive functional monomer). The polymer microstructure of the grafted hybrids with different functional monomers was different. The molar mass of the gel fraction of the hybrid with GAE was lower than those with GMMA and Laromer as a result of less grafting and crosslinking. Comparing the hybrids with GMMA and Laromer, the gel content of the hybrid with GMMA was higher but the hybrid with Laromer yielded a gel with higher molar masses than for GMMA due to the presence of double vinyl functionality in Laromer (diacrylate).

The performance of PU/(meth)acrylic hybrid dispersions in wood floor coating applications was evaluated and compared with a commercially available PU/(meth)acrylic hybrid (provided by BASF though its T_g was higher than the synthesized hybrids). It was shown that with grafting, the Young´s modulus and yield stress increased and the elongation at break decreased. This effect was more pronounced in case of GMMA due to the higher gel content. The gloss value increased with grafting due to higher compatibility of two phases in the films which led to smaller domains and less scattering. Moreover, the pendulum hardness

of the coatings increased with grafting because of the increase in the Young´s modulus and the abrasion resistance decreased due to the lower elasticity with grafting. The prepared coatings showed comparable final properties to the commercially available reference coating even though their T_g was lower.

Resumen y Conclusiones

El objetivo de este trabajo es investigar el efecto del injerto de las estructuras de poliuretano (PU) en las cadenas (met)acrílicas sobre la morfología y propiedades de las partículas y de las películas, y sobre las propiedades finales de los híbridos. El proceso de la síntesis de los híbridos poliuretano(PU)/(met)acrílico es libre de disolventes y libre de emulsionantes. El proceso sin uso de disolventes ofrece la ventaja de disminuir el uso de compuestos orgánicos volátiles (VOC) en la síntesis de PU y, por lo tanto, se elimina la etapa de destilación del disolvente, lo que es beneficioso en términos de costes de proceso y avances técnicos.

En este trabajo se estudió el efecto de los componentes de síntesis del híbrido sobre la microestructura del polímero y las propiedades finales de las películas de polímero con el objetivo de comprender la relación estructura-propiedades del híbrido. La microestructura de los híbridos PU/(met)acrílico se modificó mediante: i) injerto de cadenas de PU en los (met)acrílicos a través del uso de diferentes monómeros funcionales; ii) alteración de las cadenas de PU mediante el uso de diferentes tipos de polioles; y iii) alteración de las cadenas (met)acrílicas usando diferentes proporciones de monómeros (met)acrílicos.

En el Capitulo 1 de este trabajo se estudió el estado de arte en detalle,tanto para la síntesis del PU, como para para los síntesis de los híbridos de PU/(met)acrílicos. Se concluyó que este tema es importante para la industria y el progreso está en mayoría en los patentes.

En la literatura abierta, el progreso se refiere en mayoría a la síntesis de los PU en disolventes y muy pocos estudios se han hecho respecto a la síntesis de PUs sin uso de los disolventes. En estos estudios se ha investigado el efecto de la relación de PU y acrílicos o la relación entre los (met)acrílicos en las propiedades mecánicas y la sensibilidad al agua de los films híbridos. No se ha investigado el efecto de la composición de los PUs y tampoco el efecto del injerto sobre las propiedades coloidales, la morfología de las partículas y de los films y los propiedades finales de los híbridos.

El PU se sintetizó en disolución de monómeros metacrilato de metilo (MMA) y acrilato de butilo (BA) en relación 50/50. Para la síntesis de PU se usó ácido dimetilol propiónico (DMPA) para introducir grupos carboxilos en las cadenas de PU, que tienen el rol de estabilizantes coloidales en la preparación de dispersiones acuosas de las mezclas de PU y monómeros MMA/BA. Se investigó el efecto del contenido iónico (controlado por la concentración de DMPA) y el tipo de extendedores de las cadenas de PU (completamente hidrófilo ethylene diamine (EDA), menos hidrófilo 1,8-Diaminooctane (DAO) y el hidrófobo 1,12-Diaminododecane (DAD)) en el tamaño del partículas y la estabilidad coloidal (Capítulo 2). Se descubrió que cuando se usa un extendedor de cadenas hidrófilo, para obtener dispersiones acuosas estables el contenido de DMPA se puede cambiar en rangos muy limitados, porque el extensor de las cadenas hidrófilo (EDA) promovió la formación de una gran cantidad de oligómeros solubles en agua, que no son favorables para la estabilización de partículas. Con un alto contenido de DMPA, las dispersiones híbridas se coagularon después del proceso de la extensión de las cadenas. Al aumentar la hidrofobicidad de los extensores de las cadenas, usando DAO y DAD, los sistemas son más estables y el

contenido de DMPA (y el tamaño de partícula) se podría variar en un rango más amplio. La estructura química de las cadenas de prepolímero de PU se analizó con espectrómetro de masas MALDI-TOF y se observó que estas cadenas no eran homogéneas en su composición. Además, la simulación de Monte Carlo confirmó la heterogeneidad de composición en las cadenas del prepolímero de PU y se demostró que la heterogeneidad resultaba principalmente de la estequiometria (alta concentración de isocianato), sin efecto significativo de la reactividad de otros reactivos en las síntesis de PU (el macrodiol poly(propylene glycol) (PPG) y el diol ionico DMPA hacia el isoforon diisocyanato (IPDI)). La estructura del PU ha tenido influencia en las propiedades de las películas finales. El módulo de Young y el límite elástico de las películas de polímero disminuyeron con la longitud del extensor de las cadenas, probablemente porque el segmento duro del PU se vuelve más blando para los extensores de cadena más largos. Además, las películas que contenían EDA eran muy sensibles al agua y algunas cadenas se disolvieron en el agua durante la prueba, después de alcanzarse un valor constante en la absorción de agua. Alternativamente, en el caso de extensores de cadena más hidrofóbicos (DAO y DAD), se disolvió una cantidad menor de la película de polímero en el agua durante la prueba, aunque la absorción del agua aumentó gradualmente.

El efecto del injerto de las PU en los (met)acrílatos sobre la microestructura del polímero, la morfología y los propiedades de los films se estudió en el Capítulo 3. Las dispersiones híbridas de PU/(met)acrílico injertado se sintetizaron utilizando diferentes tipos de monómeros funcionales (glicerol mono- metacrilato (GMMA) y metacrilato de hidroxietilo (HEMA)). Para comparación, los experimentos se llevaron a cabo en ausencia de monómero

funcional usando butanodiol en el caso de GMMA y pentanol para el HEMA, para no cambiar el numero de OH en las mezclas. Se observó que el tipo de monómero funcional influye en la microestructura del PU porque el GMMA es un diol que extiende las cadenas del PU, mientras que el HEMA es un alcohol monofuncional que termina las cadenas del PU. Por lo tanto, los PUs sintetizados con el GMMA tenían mayor peso molecular y mayor número de puntos de injerto por cadena que aquellas sintetizadas con el HEMA, lo que indica que para el híbrido con el HEMA el injerto era menos eficiente y la red del polímero estaba menos reticulada. Las imágenes TEM de partículas y películas de PU/(met)acrílicos injertadas mostraron morfologías de partículas y películas más homogéneas en comparación con los híbridos no injertados que indican un menor separación de las fases como resultado del injerto. Aunque la eficiencia de injerto era alta y la microestructura de los polímeros era diferente, el injerto con el GMMA no mostró el refuerzo mecánico esperado. El híbrido sin el GMMA (solo butanodiol) mostró un comportamiento de endurecimiento de la deformación (strain-hardening) probablemente debido a los enlaces de hidrógeno entre las cadenas del PU que actúan como reticulante físico. La composición del PU determinó las propiedades del film hibrido ya que era la fase continua en el film. El injerto reticulado entre PU y poli(MMA/BA) proporcionó rigidez adicional al film, pero el aumento fue modesto, tal vez debido a la pérdida de algunos enlaces de hidrógeno entre las cadenas de PU que resultaron de la interpenetración con los poli(met)acrilatos. En el caso del injerto con el HEMA, el refuerzo mecánico debido al injerto fue más obvio. En este caso, las cadenas de PU de peso molecular corto actuaron como plastificante y con el injerto la incorporación de estas cadenas condujo a una mejora importante en las propiedades mecánicas. La sensibilidad al agua de los

híbridos disminuyó con el injerto, probablemente debido a que en los films con la mayor densidad del injerto el potencial de las películas híbridas para absorber el agua disminuye.

En Capitulo 4 se investigó el efecto de la composición del PU sobre la propiedades de los films PU/(met)acrilato híbridos. La composición del PU se modificó utilizando diferentes tipos de polioles (polipropilenglicol (PPG), politetrahidrofurano (PTHF), poliéster y policarbonato (PCD)) en la síntesis de PU. Se investigó el efecto del tipo de poliol y el injerto en la morfología de los films híbridos y sus propiedades finales. Se observó que en los híbridos injertados, el tipo de poliol no afectaba el contenido de gel observado. Los films de los híbridos que contienen PCD y poliéster tenían el módulo de Young y la tensión elástica más altos que aquellos con PTHF y PPG polioles, debido a la presencia de grupos carbonilo en la estructura de PCD y poliéster. Además, los films con mayor módulo de Young (las que contienen PCD y poliéster) tenían menor absorción de agua (mayor resistencia al absorción del agua), ya que la absorción del agua es más difícil en las películas de polímero más duras. Las partículas y los films híbridos injertados tenían la morfología más homogénea con menos separación de las fases en comparación con los films no injertadas.

Las cadenas (met)acrílicas en los PU/(met)acrilatos híbridos se modificaron usando una proporción diferente de (MMA/BA) ((0/100), (25/75), (50/50), (75/25) y (100/0) wt/wt) en la formulación, para híbridos injertados y no injertados (Capítulo 5). El contenido del gel de los híbridos injertados aumentó al aumentar la proporción del MMA debido al efecto combinado de la abstracción del hidrógeno de las unidades de PPG y el consumo rápido de GMMA en el inicio de la reacción donde se usaron relaciones de BA/MMA más altas, reduciendo así la posibilidad de formación del gel más tarde en la reacción. Con respecto a

las propiedades mecánicas de los film híbridos, se encontró que al aumentar la relación MMA/BA, el módulo de Young y la tensión elástica aumentaba drásticamente, pero el alargamiento a la rotura disminuyó. Para los híbridos injertados, el módulo de Young y la tensión elástica fueron más altos que los de los híbridos no injertados y alargamiento a la rotura disminuyó. Este efecto fue más pronunciado en caso de la relación MMA/BA alta debido al mayor contenido del gel y la mayor T_g del MMA. La morfología de las partículas y los films híbridos injertados fue más homogénea, indicando una menor separación de las fases entre PU y (met)acrílicos. Con el respecto a la sensibilidad al agua de los films, a medida que aumentó la relación MMA/BA en la formulación, la absorción del agua disminuyó porque la difusión del agua es más difícil en los polímeros más duros (mayor proporción de MMA).

En el Capítulo 6 se sintetizaron PU/(met)acrílico híbridos para aplicaciones de revestimiento de madera. Se usaron tres monómeros funcionales (que contienen dos grupos hidroxilo pero con funcionalidad de vinilo diferente) para injertar el PU en los (met)acrílicos: glicerol mono-alil éter (GAE), glicerol mono metacrilato (GMMA) y Laromer (diacrilato). El grado de injerto se cuantificó utilizando la señal UV de cromatografía de exclusión por tamaño (SEC). El valor más alto de la injerto se obtuvo para el GMMA y el valor más bajo en el caso del GAE (el monómero funcional menos reactivo de los usados). Los polímeros híbridos injertados con diferentes monómeros funcionales presentaron diferente microestructura. El peso molecular de la fracción del gel del híbrido con GAE fue menor que con GMMA y Laromer, como resultado de menor número de injertos. Comparando los híbridos con el GMMA y el Laromer, el contenido del gel con el GMMA fue más alto, pero el híbrido con

Laromer produjo un gel con el peso molecular más alto que para el GMMA debido a la presencia de la funcionalidad de doble vinilo en Laromer (diacrilato).

Se evaluó el rendimiento de las dispersiones híbridas de PU/(met)acrílico en aplicaciones de revestimiento de madera y se comparó con un híbrido PU/(met)acrílico disponible comercialmente (proporcionado por BASF, con el T_g más alta que los híbridos sintetizados en este trabajo). Se demostró que con el injerto, el módulo de Young y la tensión elástica aumentaba y el alargamiento a la rotura disminuía. Este efecto fue más pronunciado en el caso del GMMA debido al mayor contenido de gel. El valor del brillo aumentó con el injerto debido a la mayor compatibilidad de las dos fases en las películas, lo que condujo a dominios más pequeños y menos dispersos. Además, la dureza del péndulo de los recubrimientos aumentó con el injerto, probablemente debido al aumento en el módulo de Young y la resistencia a la abrasión disminuyó debido a la menor elasticidad con el injerto. Los revestimientos preparados mostraron propiedades finales comparables al revestimiento de referencia disponible comercialmente, aunque su T_g era más baja.

Appendix I. Materials and characterization methods

I.1. Materials

Isophorone diisocyanate (IPDI, Aldrich; 98%), 2,2-bis(hydroxymethyl) propionic acid (DMPA, Aldrich; 98%), dibutyltin dilaurate (DBTDL, Aldrich; 95%), borchi® Kat 315 (BASF), poly(propylene glycol) (PPG, Aldrich) (M_n=2000 g/mol), polytetrahydrofuran (PTHF, Aldrich) (M_n=2000 g/mol), polyester diol (Polyester, BASF) (M_n:2000 g/mol), polycarbonate diol (PCD, ETERNACOLL® UH 200, UBE) (M_n=2000 g/mol), Lupraphen® 7600/1 (polyester polyol, M_n=2000, BASF), 1,4-butanediol (BDO, Aldrich; 99%), glycerol mono methacrylate (GMMA, Fluorochem; 96%), 2-hydroxyethyl methacrylate (HEMA, Aldrich; 98%), 1-pentanol (Aldrich; ≥99%), Glycerol α-monoallyl ether (GAE, Aldrich), 1,4-Butanediylbis[oxy(2-hydroxy-3,1-propanediyl)] diacrylate commercially known as Laromer® LR 8765 R (Laromer, BASF), triethylamine (TEA, Aldrich; ≥99.5%), Ethylene diamine (EDA, Aldrich; ≥99.5%), 1,6-Diaminohexane (DAH, Aldrich; 98%), 1,8-Diaminooctane (DAO, Aldrich; 98%) 1,12-Diaminododecane (DAD, Aldrich; 98%), Isophorone diamine (IPDA, TCI America; ≥99%) were used as received for the synthesis of Polyurethane. The structure of the chemicals for PU synthesis are shown in Figure I.1.

Potassium persulfate (KPS, Aldrich; ≥99%) and methyl ethyl ketone (MEK, Aldrich; ≥99.5%) were used as received. Technical grade monomers, methyl methacrylate (MMA, Quimidroga; 99.9%, 45-55 ppm MEHQ) and *n*-butyl acrylate (BA, Quimidroga; 99.5%, 10-20 ppm MEHQ) were used without further purification.

1 N Hydrochloric acid (HCl, Panreac) aqueous solution, toluene (Aldrich; 99.8%), ethanol (Scharlab; 99.9%), di-butylamine (DBA, Aldrich; ≥99.5%) and bromophenol (Aldrich) were used in the titration of free NCO. Trans-2-[3-(4-tert-Butylphenyl)-2-methyl-2-propenylidene] malonitrile (DCTB, Fluka) was used as matrix for MALDI-TOF analysis. Deuterium oxide (D_2O, Deutero; 99.9%) and Deuterochloroform ($CDCl_3$, Deutero; 99.8%) were used as solvent for the NMR analysis. Tetrahydrofuran (THF, Scharlau; 99.9%) was used as solvent for was used as solvent for Size Exclusion Chromatography (SEC) and Soxhlet extraction. Double deionized (DDI) water was used as polymerization media throughout the work.

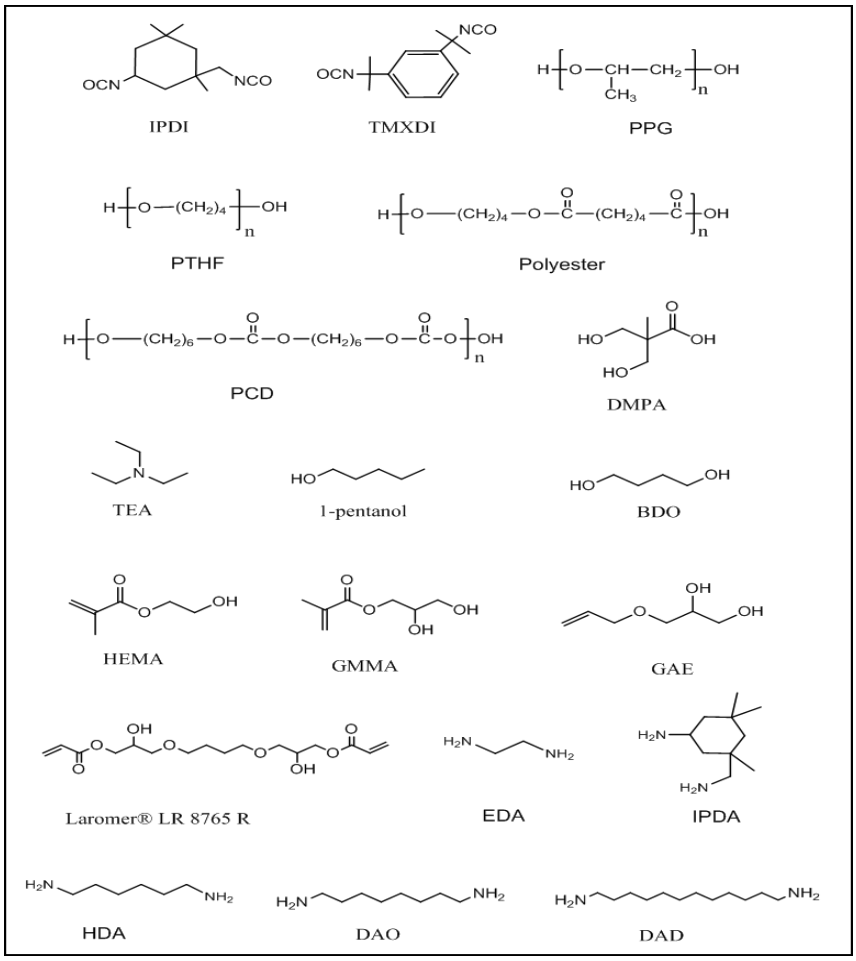

Figure I.1. Structure of the chemicals used in PU synthesis

I.2. Characterization methods

I.2.1. Quantification of the unreacted NCO groups

The unreacted NCO was determined by titration. The procedure is as follows: 1 g of sample was placed into the conical flask and 6.67 ml (5.77 g) toluene was added to dissolve the sample. 6.67 ml (5.47 g) of 2 molar di-n-butylamine solution (in toluene) was added and

it was left for 20 min to react. Then, 33 ml (25.33 g) ethanol was added, followed by addition of bromophenol blue as a titration indicator. The solution was titrated with 1 molar HCl solution. The end point was a color change from blue to pale yellow. The blank titer was done similar but without sample. The free NCO was calculated as follow:

$$Free\ NCO\ (mol) = \frac{B-A}{1000} \quad \text{(I.1)}$$

$$Free\ NCO\ (mol\%) = \frac{Free\ NCO\ (mol)}{mol\ NCO\ in\ fomulation} \quad \text{(I.2)}$$

Where B is blank titer and A is sample titer.

I.2.2. Conversion of (meth)acrylic monomers

The conversion of the (meth)acrylic monomers was determined gravimetrically and it was calculated with respect to the monomer, i.e. the PU was not taken into account.

I.2.3. Particle size measurement

The particle sizes were measured by dynamic light scattering (DLS) in a Zetasizer Nano Z (Malvern Instruments). The equipment determines the particle size by measuring the rate of fluctuations in laser light intensity scattered by particles as they diffuse through a fluid. The samples were prepared by dilution of the latex in double deionized water. The analyses were carried out at 25 ºC and a run consisted in 1 minutes of temperature equilibration followed by 3 size measurements of 120 seconds each. The values given from the DLS are z-average values obtained through cumulate analysis.

I.2.4. Fourier transform infrared spectroscopy (FTIR)

Fourier transform infrared spectroscopy (FTIR) was used in order to follow the consumption of isocyanate groups during synthesis of polyurethane. The IR spectra was obtained using Alpha FT-IR spectrometer Platinum ATR operated with OPUS software.

I.2.5. Gel content and swelling capability

The gel content is defined as the fraction of polymer that is not soluble in a good solvent (tetrahydrofuran, THF, in this case) and the swelling degree is inversely related with the crosslinking density of the gel. The gel fraction and swelling degree were measured by Soxhlet extraction (Figure I.2), using THF as the solvent. A glass fiber square pad was used as backing. A few (10-15) drops of latex were deposited on the pad and dried overnight. The dried polymer were weighed (weight=W_p) before performing a continuous extraction with THF under reflux in the Soxhlet for 24 hours. After this period, the gel remained in the glass fiber and it was weighed in wet conditions (w_s) and after drying in the oven at 60ºC (w_g), whereas the sol polymer was recovered from the THF solution. The fraction of gel and swelling degree were calculated as follows:

$$\text{gel}(\%) = \frac{w_g}{w_P} \times 100 \qquad \text{(I.3)}$$

$$\text{Sweeling degree} = \frac{w_s}{w_g} \qquad \text{(I.4)}$$

where w_g is the weight of insoluble fraction of sample (dried sample), w_s is the weight of the swollen gel after 24 hours extraction and w_P is the weight of whole polymer sample.

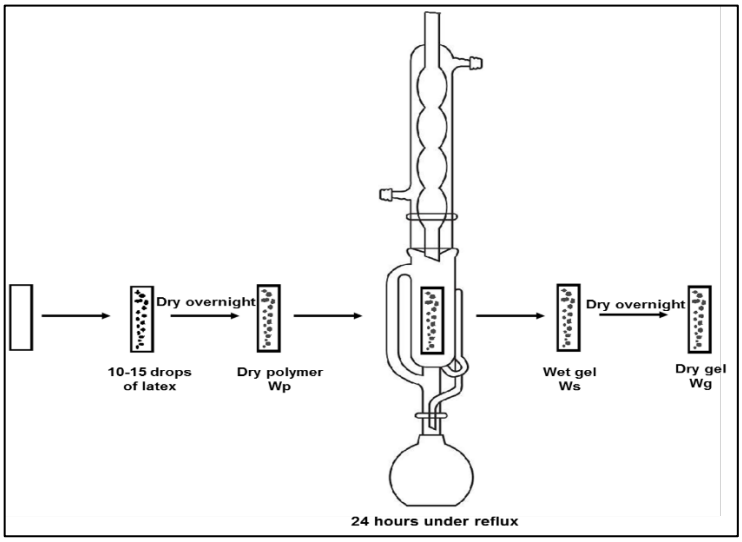

Figure I.2. Schematic of Soxhlet extraction method for gel content and swelling capability measurements

I.2.6. Molecular weight and molecular weight distribution

The molecular weight of the sol (obtained by Soxhlet extraction) was determined by **Size Exclusion Chromatography/Gel Permeation Chromatography (SEC/GPC)**. The soluble samples obtained from the Soxhlet were first dried, redissolved in THF to achieve a concentration of about 0.1% (g/ml) and filtered ((polyamide filter, pore size = 0.45 μm, Scharlab) before injection into the SEC instrument. The set up consisted of a pump (LC-20A, Shimadzu), an autosampler (Waters 717), a differential refractometer (Waters 2410), a dual λ absorbance detector (Waters 2487) and three columns in series (Styragel HR2, HR4 and HR6, with pore sizes ranging from 102 to 106 Å). Chromatograms were obtained at 35 ºC using a THF flow rate of 1 ml/min. The equipment was calibrated using polystyrene standards (5th order universal calibration) and therefore the molecular weight was referred to polystyrene.

The Molar mass distribution of the whole polymer was determined by **asymmetric-flow field-flow fractionation (AF_4/MALS/RI, Wyatt Eclipse 3)** using THF as solvent at 25 ºC. The set up consisted of a pump (LC-20, Shimadzu) coupled to a DAWN Heleos Multi Angle (18 angles ranging from 10º to 160º) Light Scattering laser photometer (MALS, Wyatt) equipped with a He-Ne laser (k = 658 nm) and an Optilab Rex differential refractometer (k = 658 nm) (RI, Wyatt). In this method, the separation is based on the interplay between the flows of the carrier and the Brownian motion of the macromolecules occurring in an open channel [1]. First the sample is injected into a channel and dissolved or dispersed macromolecules are driven by the cross-flow towards the bottom of the channel (see Figure I.3). the diffusion, associated with the Brownian motion, creates a counteracting motion and balance between the two transparent processes form a cloud of macromolecules having an equilibrium concentration distribution. The laminar flow of the carrier creates a parabolic flow profile within the channel. The smaller molecules, with higher diffusion coefficients, move closer to the channel center,where the axial flow is faster, and elute before the larger ones. The main advantage of AF_4 is that due to the lack of stationary phase very large macromolecules can be analyzed. The MALS value in combination with RI signal at each elution time allows obtaining the MWD of the whole polymer. The data collection and treatment were carried out by ASTRA 6 software (Wyatt technology). The molar mass was calculated from the RI/MALS data using the Debye plot (with second-order Berry formalism) using the average dn/dc value for PU/(meth)acrylic 50/50 wt/wt. The dn/dc values for PU, MMA and BA were considered to be 0.1469 ml/g [2], 0.084 ml/g [1] and 0.064 ml/g [1] respectively. Therefore the dn/dc value of (meth)acrylic part was the average of MMA/BA 50/50 (0.074 ml/g) and for the hybrid was the average of PU/(meth)acrylic 50/50 (0.1105 ml/g).

The samples were prepared by dissolving directly the latex in THF at a concentration of 7 mg/ml to avoid coagulation of the latex particles. The dispersion stirred for 24 hours at room temperature in THF to ensure a good dispersion of the insoluble part (swollen gels).

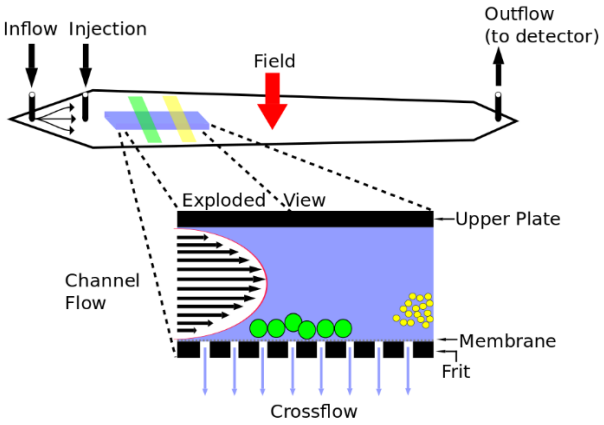

Figure I.3. Schematic of asymmetric-flow field-flow fractionation (AF_4/MALS/RI)

I.2.7. Differential scanning calorimetry (DSC)

The glass transition temperature (T_g) was determined by Differential scanning calorimetry (DSC, Q1000, TA Instruments). The films were cast at 23 °C from the final latexes. The scanning cycles consisted of first cooling to -80 °C at 10 °C/min, then heating from -80 to 130 °C (or 100 ºC depending on the sample) at 10 °C/min, cooling again from 130 (or 100) to -80 °C at 10 °C/min, and then heating to 130 °C(or 100ºC) at a rate of 10 °C/min.

I.2.8. ^{1}H NMR

The ^{1}H NMR measurements were performed on a Bruker AVANCE 400 MHz spectrometers with D_2O as solvent and using the WATERGATE pulse sequence for

suppression of the signal from water [3]. In order to prepare the sample, 300 µl of serum part of the hybrid was mixed with 300 µl D_2O and 10 µl DMF as external standard.

I.2.9. Matrix Assisted Laser Desorption/Ionization-Time of Flight Mass Spectrometry (MALDI-TOF-MS)

Matrix-assisted laser desorption/ionization (MALDI) is an ionization technique that uses a laser energy absorbing matrix to create ions from large molecules with minimal fragmentation. MALDI methodology is a three-step process [4]. First, the sample is mixed with a suitable matrix material and applied to a metal plate. Second, a pulsed laser irradiates the sample, triggering ablation and desorption of the sample and matrix material. Finally, the molecules are ionized by being protonated or deprotonated in the hot plume of ablated gases, and can then be accelerated into time of fight mass spectrometer (TOF-MS) to be analyzed. In the TOF-MS a potential difference V_0 between the sample slide and ground attracts the ions in the direction shown in Figure I.4. The velocity of the attracted ions V is determined by the law of conservation of energy. As the potential difference V_0 is constant with respect to all ions, ions with smaller m/z value (lighter ions) and more highly charged ions move faster through the drift space until they reach the detector. Consequently, the time of ion flight differs according to the mass-to-charge ratio (m/z) value of the ion.

The MALDI-TOF-MS measurements were performed on a Bruker Autoflex Speed instrument (Bruker, Germany) equipped with a 355 nm Nd:YAG laser. The spectra were acquired in the positive-ion reflector mode and linear mode (accelerating voltage 20 kV, pressure 5 x 10^{-6} mbar). DCTB (trans-2-[3-(4-tert-Butylphenyl)-2-methyl-2-propenylidene] malonitrile) was used as a matrix. The matrix was dissolved in THF at a concentration of 20

mg/ml. The polymer sample was dissolved in THF (4 mg/ml). In the case of PU prepolymer, after dissolving the prepolymer in THF, 3-4 drops of DBA was added in order to react with the free NCO groups and to avoid the side reaction with water during the test. The matrix and polymer solutions were premixed at a 3:1 ratio, respectively. Approximately 0.5 µL of the obtained mixture were spotted by hand on the ground steel target plate. For each spectrum 10000 laser shots were accumulated.

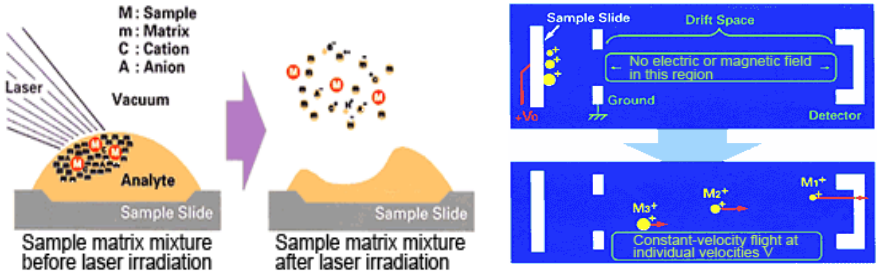

Figure I.4. Schematic of MALDI (left) and TOF-MS (right)

I.2.10. Transmission electron microscopy (TEM)

The morphology of latex particles and film cross-sections was studied by means of transmission electron microscopy (TEM). TEM analysis was carried out with a TecnaiTM G2 20 Twin device at 200 kV (FEI Electron Microscopes). The latexes were diluted with deionized water (0.05 wt%) dropped on copper grids covered with Formvar R and dried at ambient temperature. The coatings were cryosectioned with a Leica EMUC6 cryoultramicrotome at 30 °C below the Tg of the sample, with a Diatome 45° diamond knife, and the observations were made in the microscope.

I.2.11. Atomic force microscopy (AFM)

The morphology of the coating surfaces was analyzed by Atomic force microscopy (AFM) using Dimension ICON AFM with a Nanoscope V controller (Bruker) operating in tapping mode. An integrated silicon tip/cantilever with a resonance frequency of around 300 kHz was used, performing measurements at a scan rate of 1 Hz/sec with 512 scan lines.

I.2.12. Surface tension

The liquid surface tension was measured using a tensiometer (KSV, Sigma 700, KSV Instruments Ltd.) with platinum ring. The test was performed under atmospheric pressure and by Du Nouy ring method. The platinum ring was thoroughly cleaned and flame-dried before each measurement.

I.2.13. Static water contact angle measurements

In order to measure the static contact angle (CA), a thin film of 120 µm (wet thickness) was cast on the glass under controlled environment (23°C and 55% humidity) for three days. The measurements were performed by the sessile drop method with distilled water, using a goniometer OCA 20 with a high performance image processing system (Data Physics Instruments GmbH), in air under controlled environment (23°C and 55% humidity). The data presented are the average of 20-30 readings. For the measurement of the contact angle after rinsing the surface, the films casted on the glasses were immersed in distilled water for 15 min and then dried for one week at ambient temperature.

I.2.14. Water uptake measurements

For water uptake test, rectangular samples of dimensions 1 cmx4 cm and 0.2 cm thickness were prepared in Teflon molds and dried at 23 °C and 55% relative humidity for 10 days. The films were kept at 60ºC for one day to complete the drying process. the films were weighted (m_0) and each film was left in 100 ml deionized water at room temperature. At some intervals, the films were taken out of the vials, smoothly blotted with paper and weighed (m_t) and put back again in distilled water. The water uptake was calculated in relation to the initial dry weight of the sample (equation I.5).

$$\text{Water uptake}(\%) = \frac{m_t - m_0}{m_0} \times 100 \qquad \text{(I.5)}$$

After water uptake test, the samples were taken, dried at 60 °C for one week. The samples were reweighed to calculate the weight loss compared to the initial weight of the sample before the test. The reported data for each film is the average of 3 samples.

I.2.15. Tensile test

The Mechanical properties of the synthesized latexes were determined by tensile test measurements according to ASTM D882 standard test method. The films with the thickness of 500-700 µm were prepared by drying in Teflon molds at 23 °C and 55% of humidity for one week and dogbone shaped specimens were punched out of the films. The measurements were carried out in a Stable Micro System TA HD Plus Texture Analyzer under controlled conditions (23 °C and 55% of humidity), with a constant strain velocity of 0.42 $mm.sec^{-1}$. The results reported were the average of 3-5 repeated measurements.

I.2.16. Dynamic-Mechanical Thermal Analysis (DMTA)

The DMTA measurement was carried out using a dynamic mechanical thermal analyzer (DMTA) (Triton 2000DMA, Triton Technology, Ltd). The films were casted from coatings at standard condition (23 ºC and 55% RH) with the dimension of 7*10*0.7 mm^3. A single cantilever tension geometry was used. The real (storage modulus, E´) and imaginary (loss modulus, E") components of the complex shear modulus E* = E´+ i E" and the internal fraction coefficient tan (δ)= E"/E´ (mechanical loss) were measured over the temperature range -70 °C to 150°C in constant frequency of 1 Hz. The heating rate was 4 °C/min. During the experiment, a sinusoidal strain is applied and the response of the sample is registered, that is to say, the stress necessary to maintain the deformation. The results reported were the average of 2-3 repeated measurements.

I.3. References

[1] S. Podzimek, Light Scattering, Size Exclusion Chromatography and Asymmetric Flow Field Flow Fractionation: Powerful Tools for the Characterization of Polymers, Proteins and Nanoparticles, Wiley, 2011.

[2] http://www.ampolymer.com/dndc.html

[3] M. Piotto, V. Saudek, V. Sklenar, Gradient-tailored excitation for single quantum NMR spectroscopy of aqueous solutions, J.Biomol.NMR. 2 (1992) 661–666.

[4] F. Hillenkamp, M. Karas, R.C. Beavis, B.T. Chait, Matrix-assisted laser desorption/ionization mass spectrometry of biopolymers, Anal. Chem. 63 (1991) 1193A–1203A.

Appendix II. Preparation of coatings and their performance

II.1. Coating preparation

The waterborne coatings were prepared by using a standard procedure of coating preparation for Joncryl HYB 6340 (a commercially available PU/(meth)acrylic hybrid dispersion) in several steps according to the formulation in Table II.1. First, one part of the hybrid dispersion was mixed with the wetting agent (Hydropalat® WE 3120, BASF), the defoamer (FoamStar® SI 2293, BASF) and matting agent (ACEMATT® TS 100, ACEMATT) and stirred at 600 rpm using a high speed disperser blade (DISPERMAT). Then some amount of tap water was added to the mixer followed by addition of thickener (Rheovis® PU 125, BASF). The mixture let to stir at 1200 rpm for about 10 min. After that, the second part of the dispersion, the open time prolonger (Propylene glycol, Aldrich) and two different coalescent (Dipropylene glycol n-butyl ether and Butyl glycol, both Aldirch) were added followed by adding more defoamer and thickener. Then the mixture stirred for 10 min at 2000 rpm. Finally more water was added to the mixture and the final PH reached to 8.2 – 8.5 using ammonia solution and the resulting coating was stirred for 5 min at 1000 rpm to have a homogenous mixture.

Table II.1. Coating formulation

Ingredient	Trade name	Weight (g)
Hybrid dispersion	-	30
Wetting agent	Hydropalat® WE 3120	0.3
Defoamer	FoamStar® SI 2293	0.3
Matting agent	ACEMATT® TS 100	0.7
Water	-	2.0
Thickener	Rheovis® PU 1250	0.1
Hybrid dispersion	-	50
Open time prolonger	Propylene glycol	1.5
Coalescent	Dipropylene glycol n-butyl ether (DPnB)	4.0
Coalescent	Butyl glycol (BG)	4.0
Defoamer	FoamStar® SI 2293	0.2
Thickener	Rheovis® PU 1250	0.2
Water	-	6.6
Ammonia solution	Ammonia 10% solution	Variable[a]

a) To reach PH around 8.2 - 8.5

II.2.Gloss

The gloss measurement was performed with a BYK Micro-TRI-Gloss Meter to determine specular gloss of the coating films with luminous flux at defined angles according to DIN EN ISO 2813. The gloss measurement can be performed with different angles depending on the type of the surface; 20º (high gloss surfaces), 60º (medium gloss surfaces) and 85º (low gloss surfaces) (Figure II.1). Here the gloss measurement was performed at angles of 20º and 60º which are used to measure high gloss and semi-gloss surfaces [52]. Gloss might vary from polymer film to coating film due to the incorporation of additives that affect particle stability and increase heterogeneity. A 120 µm film from the coatings was prepared on the leneta substrate and the gloss was measured after 1 day of drying. The reported value is the average of three measurements from different parts of the coating.

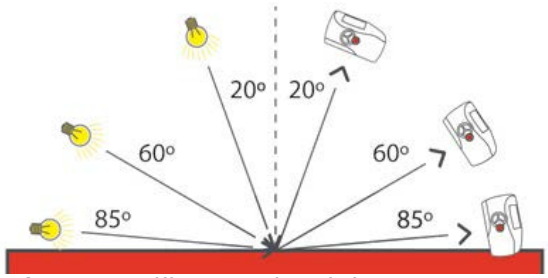

Figure II.1. Different angles of gloss measurement

II.3.Chemical Resistance

The resistance of the coatings against different materials was tested according to DIN EN ISO 68861-1. A 120 µm film was prepared on the melamine wood substrate and after 4 h drying, another layer of 120 µm was casted. The coatings were tested after 6 days drying at ambient temperature. The corresponding chemical was prepared and deposited on the coatings and after a given time it was swept off and the damage in the substrate was evaluated one day after the chemical removal. Table II.2 gives the description of the tested chemicals. The resistance of the coatings against different chemicals is shown with numbers from 1 to 5 as follow:

5 = no visible changes at all possible angles

4 = just noticeable changes in brightness and color at minimum one angle of view

3 = slight change in gloss and color; the structure of the test surface is not changed

2 = strong marks visible; the structure of the surface is largely intact

1 = strong marks visible; the structure of the surface is changed

Table II.2. Description of the tested media for the chemical resistance

Tested Media	Description
Acetic Acid	10% aqueous solution
Ethanol	Non denatured, 48% aqueous solution(volume fraction)
Red Wine	From Southern Europe; Alcohol content =>13% (volume fraction)
Coffee	40 g of instant coffee, freeze dried, in 1 L of boiled water
Water	Deionized or distilled water, with PH value 7.0±0.5
Acetone	-
Mustard	Medium hot

II.4.Hardness

In order to examine the surface properties of coatings, the pendulum hardness of the coating films were measured by method according to DIN EN ISO 1522. The pendulum hardness evaluates the hardness by measuring the damping time of an oscillation pendulum. The measurements provide information about the coating film resistance to dampen vibrations. The pendulum hardness of the coating films was tested by an Erichsen Pendulum Damping Tester (reference glass). The device itself consists of a pendulum, to the support of which two agate balls are attached (Figure II.2). The coating films were casted on the glass substrate (wet thickness = 120 µm) and dried at standard condition (23 ºC and 55% humidity) for 6 days. The pendulum hardness of the films was measured during time for 6 days, after that the substrates were place in the oven for one night to reach the final Hardness.

Figure II.2. Pendulum hardness tester

II.5.Taber abrasion Test

Resistance to abrasion is one of the most significant mechanical properties of any surface. The use of the taber abraser is counted among the most commonly used and best-known methods for testing durability and resistance to wear. The wearing action is caused by two abrasive wheels which are applied at a defined pressure to the material sample which has been mounted on a rotating specimen holder (Figure II.3). A 120 μm film was prepared on the glass substrate and after 1 day of drying, another layer of 120 μm was casted. The third layer of 120 μm was casted 4 h after drying the second layer and the substrates were left at 40ºC for 4 days to accelerate the drying process. The test was performed on Dual-abrasion test instrument TABER® ABRASER 352 H (Type 5155) using 500 g weight wheel and CS10 type taber. The weight loss of the substrate coated with the coating was measured in each 250 round. Two measurements were done for each sample and the average weight loss was reported. The lower the weight loss, the higher the abrasion resistance.

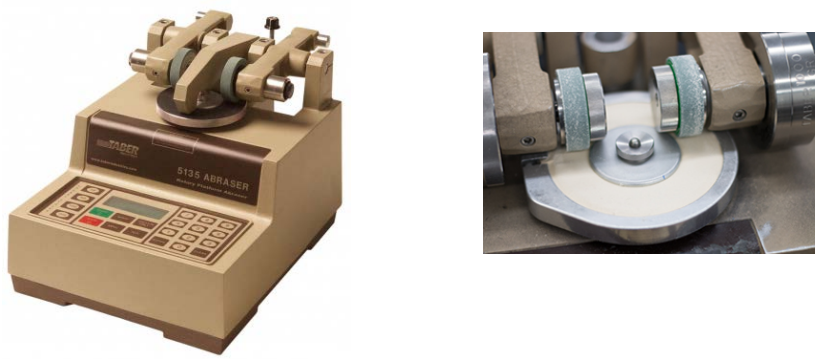

Figure II.3. Taber abraser equipment

Appendix III. Supporting Information for Chapter 2

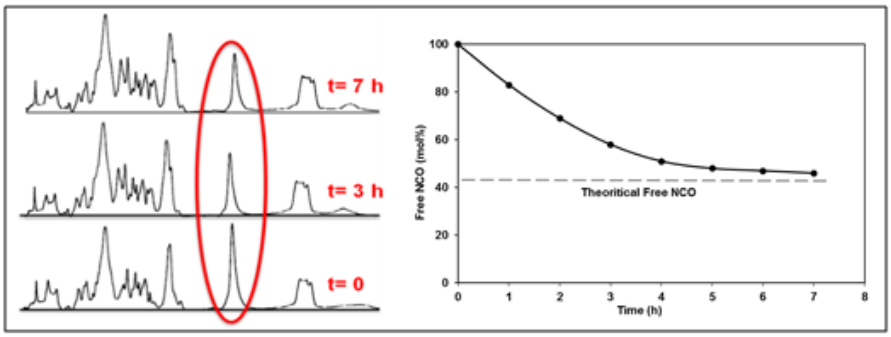

Figure III.1. Free NCO monitored with FTIR technique during prepolymer synthesis (NCO/OH=1.8)

^{1}H NMR analysis

10 µl of Dimethylformamide (DMF) was added to the sample as external reference corresponding to the peak at 7.92 ppm. The amount of IPDI in the sample can be estimated from the integral of the peaks at 0.75-1 ppm, which correspond to the 9 methyl hydrogen atoms from IPDI as shown in Figure 2.1, based on the known concentration of DMF.

$$[IPDI] = [DMF]\frac{I_{0.75-1}}{I_{7.9}*9} \qquad \text{(III.1)}$$

From this value the concentration of IPDI in the aqueous phase of the latex, $[IPDI]_{aq}$ can be calculated. Similarly, the concentration of PPG in the aqueous phase can be calculated from the intensity of the signal at 1.1 ppm arising from the methyl hydrogens the propylene glycol repeat unit and knowing the average degree of polymerization of the polypropylene glycol, DP_{PPG}.

$$[PPG] = [DMF]\frac{I_{1.1}}{I_{7.9}*3*DP_{PPG}} \qquad \text{(III.2)}$$

MALDI-TOF analysis

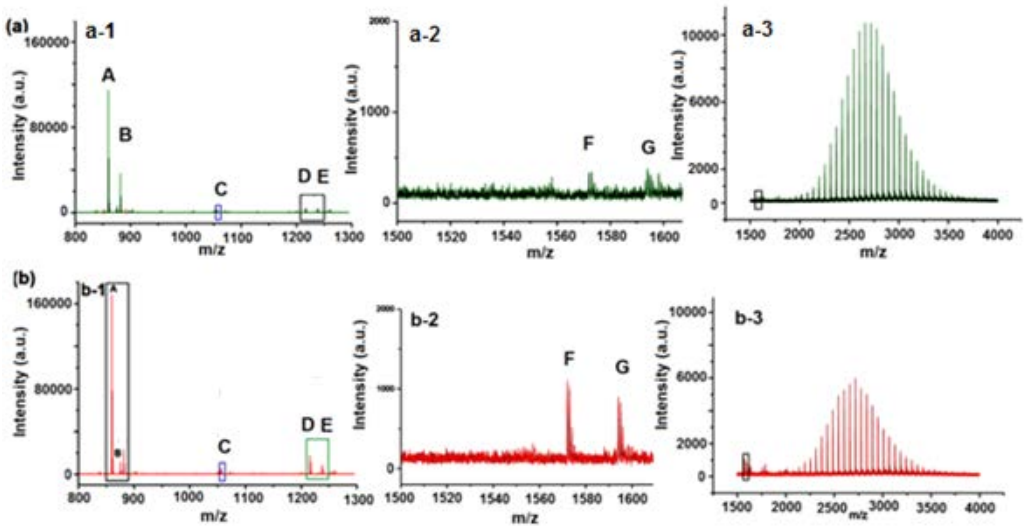

Figure III.2. MALDI-TOF mass spectra of PU prepolymer with (a) 2.9 wt% DMPA and (b) 5 wt% DMPA

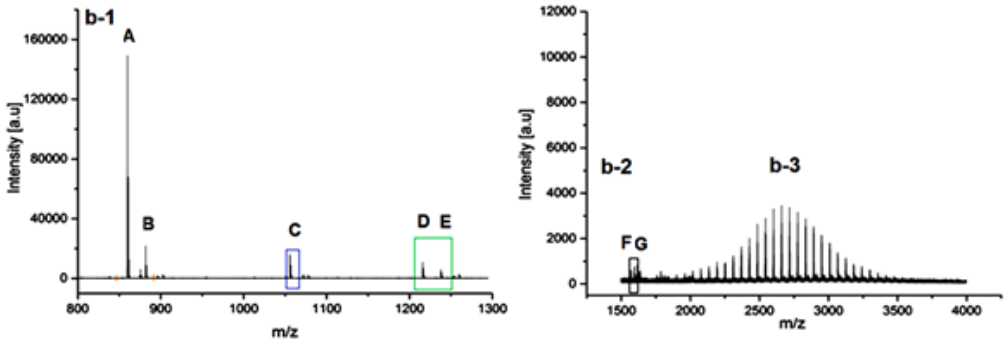

Figure III.3. MALDI-TOF mass spectra of PU prepolymer with 5 wt% DMPA synthesized in MEK as solvent

Monte Carlo simulation model

The kinetic Monte Carlo (KMC) algorithm proposed by Gillespie [1] was used as the basis of the model. A control volume, *V*, was defined at time zero that contains the reactant molecules consisting of two different polyols and a diisocyanate with two groups of different reactivity. It is assumed that the system is perfectly mixed. The stochastic rate constants, C^{MC}, are obtained by the transformation of the experimental rate constants, k_{exp} by the following:

$$C^{MC} = \frac{k_{exp}}{V \times N_A} \qquad \text{(III.3)}$$

Where N_A is the Avogadro constant. The stochastic rate, R_v, of a given reaction, *v*, is defined as:

$$R_v = C_v^{MC} h_v \qquad \text{(III.4)}$$

Where C_v^{MC} is the stochastic rate constant of reaction *v* and h_v is the number of possible combinations between reactants involved in reaction *v*. The probability of a given reaction occurring, P_v, is given by:

$$P_v = \frac{R_v}{\int_{v=1}^{N} R_v} \qquad \text{(III.5)}$$

Where *N* is the total number of reactions considered in the polymerization scheme. At each point in the simulation a given reaction is chosen based on the above probabilities using a random number, r_1:

$$\sum_{v=1}^{\mu-1} P_v < r_1 < \sum_{v=1}^{\mu} P_v$$

Where μ is the number of the selected reaction. A time interval, τ, is selected on the basis of a second randomly generated number, r_2, such that:

$$\tau = \frac{1}{\sum_{v=1}^{N} R_v} ln \frac{1}{r_2} \qquad \text{(III.6)}$$

The KMC algorithm was applied to the reactions shown in Scheme 2.3.

The implementation of the KMC simulation is shown as a flowchart in Scheme III.1, based on the work of Johnson and O'Driscoll [2]. Starting from a given reaction volume, the number of molecules is calculated based on the reaction formulation. Typically a volume is chosen so that the final prepolymer contains > 10^4 chains. This allows a reasonable simulation time on a standard computer whilst giving enough information for accurate information on chain statistics. Each molecule and each functional group is numbered. The direction (left or right) of the functional group within each molecule was also defined so that every molecule has well defined end groups. At each step in the reaction a distinct chemical reaction with reaction time was chosen according to the number of functional groups in the system using the KMC method detailed above. The particular functional groups that take part in a given reaction are then chosen randomly. This process identifies the two reacting molecules which are condensed into one and the polymer sequence and the chain ends are stored. All molecules and functional groups are subsequently renumbered as necessary. This proceeded until the complete disappearance of the hydroxyl groups in the system. Following the simulation, the simulation yields the full sequence a series of polymer chains, which can then be used to gain statistical information of the distribution of chain lengths and compositional heterogeneity.

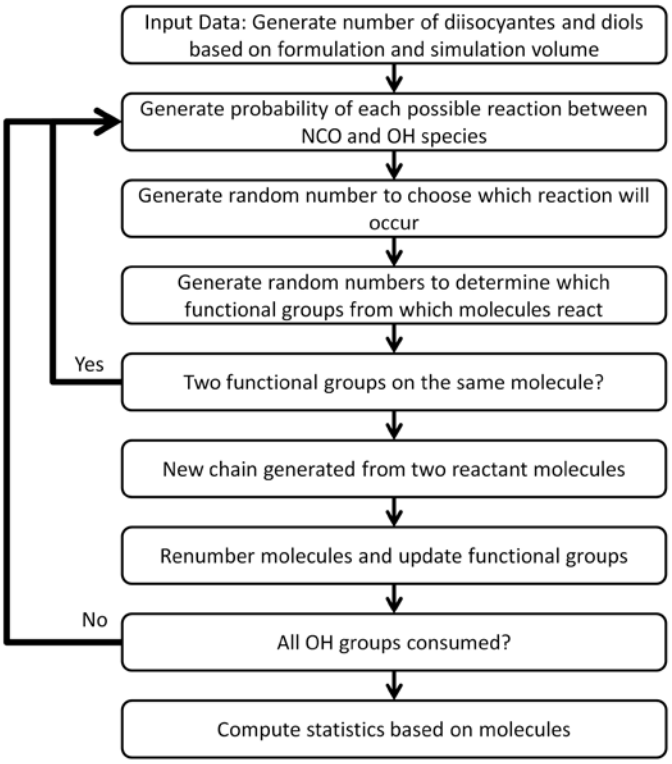

Scheme III.1. Flow chart for implementation of kinetic Monte Carlo simulations

The influence of the rate coefficients on polymer microstructure was checked to ensure that the results are not excessively sensitive to the exact values and that the results obtained can be assumed to be of reasonable accuracy. This is particularly important as the implication is that regardless of the type of diol and diisocyanate the structure of the PU prepolymer remains relatively unaffected, being mainly influenced by the stoichiometry of the various components of the reaction rather than their inherent reactivity (Figure III.4 and Table III.1).

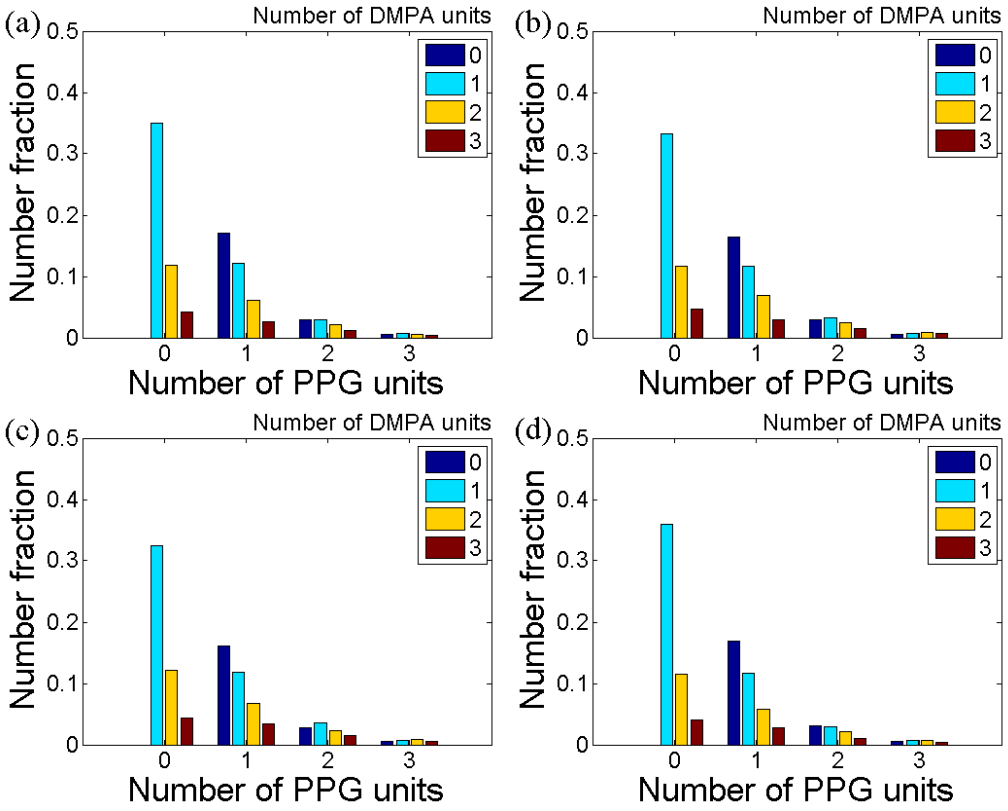

Figure III.4. Prepolymer compositional distribution for various assumed reactivity between IPDI, PPG and DMPA in the case of 3.5 wt% DMPA;(a) Rate coefficients shown in Table S1 considering both enhanced reactivity of the secondary NCO group of IPDI and of the primary alcohol group of PPG, (b) Rates between all NCO groups and OH groups assumed equal ($k_{1a1} = k_{1a2} = k_{2a1} = k_{2a2} = k_{1b} = k_{2b} = 0.001\ M^{-1}s^{-1}$), (c) Rate coefficient of reaction between DMPA hydroxyl groups and NCO groups assumed to be twice the rate coefficient of reaction between PPG hydroxyl groups and NCO groups ($k_{1a1} = k_{1a2} = k_{2a1} = k_{2a2} = 0.001\ M^{-1}s^{-1},\ k_{1b} = k_{2b} = 0.002\ M^{-1}s^{-1}$), (d) Rate coefficients shown in Table S1 considering enhanced reactivity of secondary NCO groups of IPDI but assuming equal reactivity between chain ends of PPG ($k_{1a1} = k_{1a2} = k_{1b} = 0.0025\ M^{-1}s^{-1},\ k_{2a1} = k_{2a2} = k_{2b} = 0.001\ M^{-1}s^{-1}$).

Table III.1. Simulated effect of rate coefficient on microstructure of PU prepolymer

Rate coefficient × 10^3 ($M^{-1}s^{-1}$)						M_n (g/mol)	Đ	F_{noDMPA}[a]	F_{noPPG}[b]	$F_{IPDI\ unreacted}$[c]
k_{1a1}	k_{1a2}	k_{1b}	k_{2a1}	k_{2a2}	k_{2b}					
2.5	0.83	2.5	1	0.3	1	2200	1.73	0.19	0.50	0.17
1	1	1	1	1	1	2400	1.75	0.18	0.47	0.20
1	1	2	1	1	2	2400	1.75	0.18	0.47	0.20
2.5	2.5	2.5	1	1	1	2200	1.77	0.19	0.50	0.17

[a] Number fraction of chains that contain no DMPA
[b] Number fraction of chains that contain no PPG
[c] Fraction of initial IPDI that remains unreacted after consumption of all hydroxyl groups

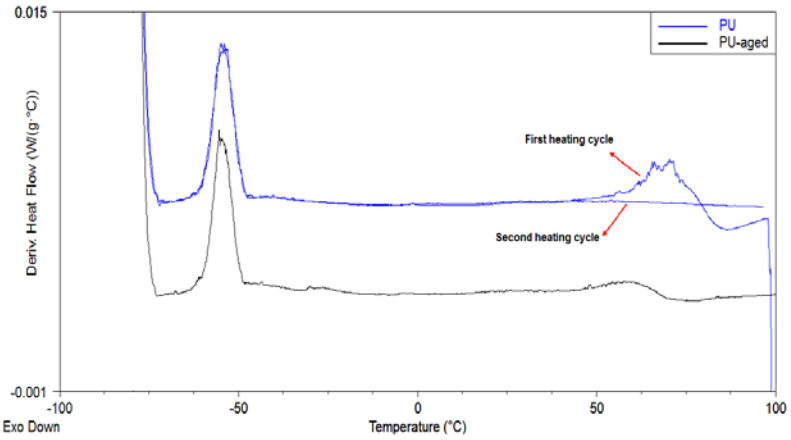

Figure III.5. DSC derivative curves of PU film and repeating after 2 days aging

References

[1] D.T. Gillespie, Exact stochastic simulation of coupled chemical reactions, J. Phys. Chem. 81 (1977) 2340–2361.

[2] A.F. Johnson, K.F. O'Driscoll, Monte Carlo simulation of sequence distributions in step growth copolymerization, Eur. Polym. J. 20 (1984) 979–983.

[3] S.R. Liao, Y. Wei, S.L. An, Research on the Reaction of IPDI and PPG with Organo-Tin Mixed Catalyst, in: Front. Adv. Mater. Eng. Technol., Trans Tech Publications, 2012: pp. 399–403.

[4] H.-K. Ono, F.N. Jones, S.P. Pappas, Relative reactivity of isocyanate groups of

isophorone diisocyanate. Unexpected high reactivity of the secondary isocyanate group, J. Polym. Sci. Polym. Lett. Ed. 23 (1985) 509–515.

[5] K. Hatada, K. Ute, K.-I. Oka, S.P. Pappas, Unambiguous 13C-NMR assignments for isocyanate carbons of isophorone diisocyanate and reactivity of isocyanate groups in Z - and E-stereoisomers, J. Polym. Sci. Part A Polym. Chem. 28 (1990) 3019–3027.

[6] S. Wang, X. Yang, Q. Bai, T. Li, In Situ Monitoring of Selective Catalysts on Urethane Formation by FT-IR Spectroscopy, Int. J. Polym. Anal. Charact. 18 (2013) 146–153.

Appendix IV. Supporting Information for Chapter 6

Let us distribute the Laromer units. In the distribution the probability that a PU chain receive a unit is X. therefore, the probability of receiving 2 units is X2,3 us X3 and son on.

The average number of Laromer units per chain is

$0.8 = X + 2X^2 + 3X^3 + 4X^4 + \ldots.$

$= (X + X^2 + X^3 + \ldots.) + (X^2 + X^3 + X^4 + \ldots) + (X^3 + X^4 + \ldots) + (X^4 + \ldots) + \ldots$

As each of the terms is a geometric progression

$$0.8 = \frac{X}{1-X} + \frac{X^2}{1-X} + \frac{X^3}{1-X} = \frac{X}{(1-X)^2}$$

Therefore X = 0.344

Consequently the fraction of chains without Laromer is

$$1 - \left(\frac{X}{1-X}\right) = \frac{1-2X}{1-X} = 0.48$$

Founding that PU chains without double bonds cannot be incorporated to the gel, and that all of the (meth)acrylate is in the gel (Figure 6.2), the predicted gel will be (1-0.48/2)*100=76%, which is very close to the measured value (Table 6.2).

A similar calculation for GMMA gives a measured gel of 92.5%, which is in a reasonable agreement with the experimental value 88% (table 6.2).

Abbreviations and Acronyms

AF_4	asymmetric-flow field-flow fractionation
AFM	atomic force microscopy
BA	butyl acrylate
BDO	butanediol
CTA	chain transfer agent
DAD	diaminododecane
DAH	diaminohexane
DAO	diaminooctane
DBA	di-butylamine
DBTDL	dibutyltin dilaurate
DDI	double deionized
DLS	dynamic light scattering
DMPA	dimethylol propionic acid
DSC	differential scanning calorimetry
DMTA	dynamic mechanical thermal analysis
EDA	ethylene diamine
FTIR	fourier transform infrared spectroscopy
GMMA	glycerol mom methacrylate
GAE	glycerol α-monoallyl ether
GPC	gel permission chromatography
HDI	hexamethylene diisocyanate

HEA hydroxyethyl acrylate

HEMA hydroxyethyl methacrylate

HMDI dicyclohexyl methane diisocianate

HPA hydroxypropyl acrylate

HS hard segment

HTPB hydroxyl-terminated polybutadiene

HCl hydrochloric acid

IPDA isophorone diamine

IPDI isophorone diisocyanate

KPS potassium persulfate

MALDI matrix assisted laser desorption/ionization

MDI diphenylmethane diisocyanate

MEK methyl ethyl ketone

MMA methyl methacrylate

MMD molar mass distribution

M_n number average molecular weight

M_w weight average molecular weight

MWD molecular weight distribution

NIPU non isocyanate polyurethanes

NMP n-methyl pyrolidone

NMR nuclear magnetic resonance

PBA poly butyl acrylate

PCD polycarbonate diol

PCL polycaprolactone diol

PDMS poly(dimethylsiloxane) diols

PEG polyethylene glycol

PMMA poly methyl methacrylate

PPG polypropylene glycol

PS polystyrene

PSA pressure sensitive adhesive

PTHF polytetrahydrofuran

PTMG polytetramethylene glycol

PU polyurethane

PUD polyurethane dispersion

SAFT shear adhesion failure temperature

SEC size exclusion chromatography

SS soft segment

TDI toluene diisocyanate

TEA triethylamine

TEM transmission electron microscopy

TOF-MS time of fight mass spectrometer

THF tetrahydrofuran

T_g glass transition temperature

TXMDI tetramethylxylylene diisocyanate

VOC volatile organic compounds